# Characterising the Activity of Peroxidasin in the Extracellular Matrix

Boushra Bathish

A thesis submitted for the degree of
Doctor of Philosophy

Department of Pathology and Biomedical Science
University of Otago
New Zealand

December 2019

*Life is nothing but an electron looking for a place to rest.*

Albert Szent-György

# Abstract

Peroxidasin is a rising star in the field of redox biology. It is a peculiar heme peroxidase that uniquely contains non-catalytic domains in addition to the peroxidase domain. Peroxidasin catalyses the formation of an unusual sulfilimine bond between methionine and hydroxylysine in the non-collagenous domain of collagen IV in the extracellular matrix (ECM). The mechanism is proposed to involve the generation of hypobromous acid (HOBr) in a rare example of an anabolic function of this powerful oxidant and destructive bactericide. Peroxidasin is implicated in many pathologies, including cardiovascular diseases, fibrosis and cancer. A lot is unknown about the exact mechanism of collagen IV cross-linking, the substrate specificity and selectivity of peroxidasin, and regulation of its activity. One of the main questions that surrounded peroxidasin since its discovery is whether it causes collateral oxidative modifications of biomolecules.

In this thesis, I investigated the selectivity and modulation of the activity of peroxidasin in the ECM. I optimised an *in situ* model system and confirmed the activity of peroxidasin embedded in the ECM. The results demonstrate that peroxidasin is highly efficient in cross-linking collagen IV using low concentrations of bromide and hydrogen peroxide. Peroxidasin catalyses the oxidation of exogenous NADH to bromohydrin, providing direct evidence that it generates free HOBr in the decellularised ECM. I investigated the modulation of collagen IV cross-linking by peroxidase substrates and scavengers of HOBr. Physiological levels of thiocyanate and urate modulate collagen IV cross-linking. Overall, peroxidasin shows preference for bromide over other physiological substrates, although the basis of this specificity is not yet known. Scavengers of HOBr, like methionine and glutathione are inefficient in inhibiting the sulfilimine bond in collagen IV. These observations demonstrate selectivity of the reactions of HOBr produced by peroxidasin for collagen IV cross-linking.

I investigated whether HOBr produced by peroxidasin in the ECM undergoes reactions beyond cross-linking collagen IV. I developed mass spectrometry

methods to measure markers of oxidative modifications of proteins. The results show that peroxidasin indeed catalyses the formation of 3-bromotyrosine, a specific marker of the reaction of HOBr with tyrosine. The levels of 3-bromotyrosine on proteins are significantly lower when peroxidasin is inhibited or knocked out. Formation of 3-bromotyrosine is more susceptible to inhibition by thiocyanate, urate and nitrite than the cross-linking of collagen IV. These results suggest selectivity of HOBr reactions towards the deliberate sulfilimine bond formation over the presumably collateral reactions with other amino acid residues on proteins.

Taken together, the evidence I present here demonstrates that the reactions of peroxidasin in the ECM are highly specific for, but not limited to, the cross-linking of collagen IV. It strengthens the hypothesis that HOBr generated by peroxidasin is targeted towards collagen IV, though likely to diffuse a short distance in the ECM. The novel finding that peroxidasin contributes to the formation of 3-bromoytrosine on proteins brings it to the fore as an enzymatic source of oxidative modifications of proteins. It also raises more questions about the extent and effect of peroxidasin-catalysed oxidative modifications of proteins in physiology and pathology.

# Acknowledgements

First, I would like to express my deep gratitude for my supervisors Professor Christine Winterbourn and Professor Tony Kettle for your unwavering support and guidance throughout this project. With your wisdom and patience, you helped me develop the skills and confidence to navigate the highs and lows of this academic journey. I am truly grateful to Christine for your continuous valuable input, thorough feedback and exceptional scientific rigor. Thank you Tony for sharing your knowledge and passion for science and communication.

I would like to thank my advisor Dr. Martina Paumann-Page for helping me with many aspects of my PhD. I am particularly thankful for your insightful advice, scientific expertise and contagious enthusiasm. I also would like to thank Dr. Rufus Turner and Dr. Louise Paton for developing some of the mass spectrometry methods and helping me to learn and troubleshoot. Thank you to Assistant Professor Gautam Bhave from Vanderbilt University for the peroxidasin-knockout cell line, which has been a valuable model in my research project. Thank you to Professor Miklós Geiszt from Semmelweis University for the anti-peroxidasin antibody and peptide.

Thank you to the members of the Centre for Free Radical Research. I was fortunate to conduct my research in such a positive and nourishing environment. I am especially thankful to Louisa, Andrew, Nina and Nick for your moral and academic support. Thank you to my PhD convenor, Associate Professor Margaret Currie for ensuring that my academic progress is on track. Thank you to the Administration team at the Department of Pathology and Biomedical Science for all your assistance. I am thankful for the University of Otago Doctoral Scholarship for funding my study.

Finally, special thanks to my dear family and friends around the world. This journey would have been impossibly hard without your love, support and encouragement.

# Publications arising from this thesis

**Bathish B**, Turner R, Paumann-Page M, Kettle AJ, Winterbourn CC. Characterisation of peroxidasin activity in isolated extracellular matrix and direct detection of hypobromous acid formation. Arch Biochem Biophys. 2018;646:120-7.

**Bathish B**, Paton L, Turner R, Paumann-Page M, Kettle AJ, Winterbourn CC. Detection of 3-bromotyrosine formation by peroxidasin in the extracellular matrix. *In preparation*.

**Bathish B**, Paumann-Page M, Kettle AJ, Winterbourn CC. Peroxidasin; structure and function, review. *In preparation*.

**Conference proceedings**

**Bathish B**, Turner R, Kettle AJ, Winterbourn CC (2016). Peroxidasin-catalysed oxidative modifications of proteins in the extracellular matrix. Free Radical Biology & Medicine, 100(Suppl.), (pp. S19-S20).

# Table of Contents

# List of Tables

# List of Figures

# List of Abbreviations

| | |
|---|---|
| (v/v) | Volume per volume |
| (w/v) | Weight per volume |
| ABAH | 4-aminobenzoic acid hydrazide |
| ANOVA | Analysis of variance |
| APS | Ammonium persulfate |
| BB | Backbone amide |
| BM | Basement membrane |
| BSA | Bovine serum albumin |
| Br-Tyr/ BY | Bromotyrosine |
| Cat | Catalase |
| CPS | Counts per second |
| CYP | Cytochrome P450 |
| $dH_2O$ | Double deionised water |
| DTT | Dithiothreitol |
| Duox | Dual oxidase |
| ECM | Extracellular matrix |
| EDTA | Ethylenediaminetetraacetic acid |
| EPO | Eosinophil peroxidase |
| FA | Formic acid |
| FBS | Fetal bovine serum |
| FOX | Ferrous oxidation of xylenol orange |
| GPx | Glutathione peroxidase |
| GSH | Glutathione |
| HPLC | High performance liquid chromatography |
| HRP | Horseradish peroxidase |
| hsPxd01-con4 | Recombinant human peroxidasin 1, construct 4 |
| IAM | Iodoacetamide |
| $IC_{50}$ | The half maximal inhibitory concentration |
| ICE | Intracellular extract |
| IECM | Interstitial extracellular matrix |
| Ig | Immunoglobulin |

| | |
|---|---|
| KO | Knock out |
| LC-MS | Liquid chromatography mass spectrometry |
| LPO | Lactoperoxidase |
| LRR | leucine-rich repeats |
| MEF | Mouse embryonic fibroblasts |
| Met-O | Methionine sulfoxide |
| MG50 | melanoma gene |
| MPO | Myeloperoxidase |
| MS | Mass spectrometry |
| MSA | Methane sulfonic acid |
| NADPH | Nicotinamide adenine dinucleotide phosphate |
| NC1/NCD | Non-collagenous domain |
| NOX | NADPH-oxidase |
| Nrf2 | Nuclear factor erythroid-2-related factor 2 |
| $NO_2$-Tyr/NY | Nitrotyrosine |
| PAGE | Polyacrylamide gel electrophoresis |
| PBS | Phosphate buffered saline |
| PHG | Phloroglucinol |
| PRG2 | p53-responsive gene 2 |
| PVDF | Polyvinylidene fluoride |
| PXDN | Peroxidasin |
| PXDNL | peroxidasin-like protein |
| RNS | Reactive nitrogen species |
| ROS | Reactive oxygen species |
| RT-PCR | Reverse transcription polymerase chain reaction |
| SDS | Sodium dodecyl sulfate |
| SEM | Standard error of mean |
| SOD | Superoxide dismutase |
| SPE | Solid phase extraction |
| S-S | Disulfide |
| TBS | Tris buffered saline |
| TBST | Tris buffered saline Tween |
| TDPA | thiodipropionic acid |

| | |
|---|---|
| TEMED | Tetramethylethylenediamine |
| TFA | Trifluoracetic acid |
| TNB | 5-Thio-2-nitrobenzoic acid |
| TPO | Thyroid peroxidase |
| TX1 | 3-isobutyl-2-thioxo-7H-purin-6-one |
| UV | Ultraviolet |
| VPO | Vascular peroxidase |
| VWC | Von Willebrand factor type C |
| WT | Wilde type |

# List of Chemical Formulae

| | |
|---|---|
| $^{\bullet}OH$ | Hydroxyl radical |
| $Br^{-}$ | Bromide |
| $Cl^{-}$ | Chloride |
| $Fe^{2+}$ / Fe(II) | Ferrous iron |
| $Fe^{3+}$/ Fe(III) | Ferric iron |
| $H^{+}$ | Hydrogen ion |
| $H_2O$ | Water |
| $H_2O_2$ | Hydrogen peroxide |
| HCl | Hydrochloric acid |
| HOBr | Hypobromous acid |
| HOCl | Hypochlorous acid |
| HOSCN | Hypothiocyanous acid |
| HOX | Hypohalous acid |
| $I^{-}$ | Iodide |
| MeOH | Methanol |
| NaBr | Sodium bromide |
| NaCl | Sodium chloride |
| NaP | Sodium phosphate |
| $NO^{\bullet}$ | Nitric oxide |
| $NO_2^{-}$ | Nitrite |
| $NO_2^{\bullet}$ | Nitrogen dioxide |
| $O_2$ | Molecular oxygen |
| $O_2^{-\bullet}$ | Superoxide |
| $^{-}OBr$ | Hypobromite |
| $^{-}OCl$ | Hypochlorite |
| $ONOO^{-}$ | Peroxynitrite |
| $RNH_2$ | Amine |
| RNHX | Halamine |
| $RNX_2$ | Dihalamine |
| $SCN^{-}$ | Thiocyanate |

# Chapter 1 Introduction

Peroxidasin rose to fame as the enzyme that catalyses an unusual sulfur-nitrogen cross link in collagen IV. It attracted attention as a peculiar new member of the exclusive mammalian heme peroxidases. In addition to the catalytic domain, which displays high sequence homology in all peroxidases, peroxidasin uniquely contains additional domains that facilitate its interaction with other proteins. The main known physiological function of peroxidasin is to catalyse the formation of an essential sulfilimine bond in collagen IV. This intermolecular bond is crucial for the functionality and integrity of the basement membrane, a specialised form of the extracellular matrix (ECM). Though it has not been directly demonstrated, the mechanism is thought to involve the oxidation of bromide to hypobromous acid, which then promotes the cross link between methionine and hydroxylysine residues joining two protomers of collagen IV. Recently, peroxidasin has been shown to be involved in various pathological processes, including kidney fibrosis, developmental glaucoma and many types of cancer.

There are many questions surrounding the mechanism of sulfilimine cross link formation and the enzymology of peroxidasin. Does peroxidasin undergo a concerted reaction with collagen IV or release HOBr into its surroundings? Does HOBr react with other components of the ECM? What are the effects of other physiological peroxidase substrates on the activity of peroxidasin? This research project addresses some of the questions regarding the enzymology of peroxidasin and the specificity of the oxidation reactions.

In this chapter, I review the literature on mammalian heme peroxidases, focusing on the current knowledge on peroxidasin structure, function, reaction mechanism and role in diseases. I summarise the relevant literature on the production of

oxidants and oxidative modifications of biomolecules. I also review what is known about the physiology and pathology of the ECM and collagen IV.

## 1.1. Mammalian heme peroxidases

The mammalian heme peroxidases are a group of enzymes that contain a conserved catalytic peroxidase domain. They activate hydrogen peroxide to oxidise organic substrates and halides (1). It is a distinct group from other peroxidases (plant, fungal, bacterial) and they have evolved convergently (2-4). Peroxidases contain a heme group with Fe(III) bound to the four pyrrole nitrogens (**Figure 1**). The fifth coordination position (proximal) is bound to the imidazole nitrogen on a histidine residue, while the sixth coordination position (distal) remains vacant in the native enzyme and forms a Fe(IV)=O linkage when oxidised by hydrogen peroxide (1).

The mammalian heme peroxidases include myeloperoxidase (MPO), lactoperoxidase (LPO), eosinophil peroxidase (EPO), thyroid peroxidase (TPO), and peroxidasin (PXDN). Sequence alignment of the five human heme peroxidases reveals that the key catalytic residues (Gln, His, Arg, Asn) as well as the residues involved in the two covalent links with the prosthetic group (Asp and Glu) are all conserved. The calcium binding sequence (LTS-XX-DAS) is also conserved (2).

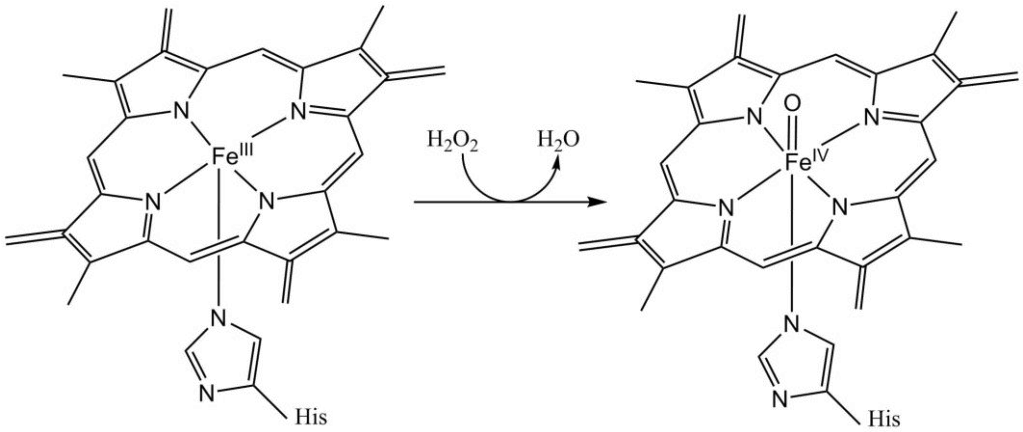


**Figure 1. The heme structure of the active site of peroxidases**. The reaction of the Fe(III) with hydrogen peroxide lead to the formation of Fe(IV)=O in compound I.

The catalytic function of mammalian heme peroxidases involves the oxidation of a substrate using hydrogen peroxide ($H_2O_2$) as a co-substrate. Peroxidases can catalyse two types of reactions: peroxidation and halogenation (**Figure 2**). The catalytic cycle starts when $H_2O_2$ reacts with the native enzyme (ferric), to generate compound I (oxy-ferryl). Compound I can then enter the halogenase cycle in which it catalyses two-electron oxidation of halides (chloride, bromide and iodide), and the pseudohalide thiocyanate, which regenerates the native enzyme. Compound I can also enter the peroxidase cycle in which it catalyses two sequential one-electron oxidation steps of organic substrates producing radicals (2, 5, 6).

Mammalian heme peroxidases oxidise a variety of physiological substrates for diverse biological functions. MPO mainly oxidises chloride producing the bactericidal hypochlorous acid inside the phagosomes of stimulated neutrophils (7). LPO oxidises thiocyanate to produce hypothiocyanous acids in saliva (8, 9). EPO produces hypobromous acid when eosinophil granulocytes are stimulated (10). TPO produces hypoiodous acid for the biosynthesis of thyroid hormones (11). Plasma concentrations of some physiological substrates and the rate constants for their reactions with peroxidases are summarised in **Table 1**. In addition to their beneficial physiological roles, peroxidases can also cause harm. The highly reactive hypohalous acids produced by peroxidases react with many biomolecules and can damage the invading pathogens as well as the host tissues, especially during inflammation (5, 12).

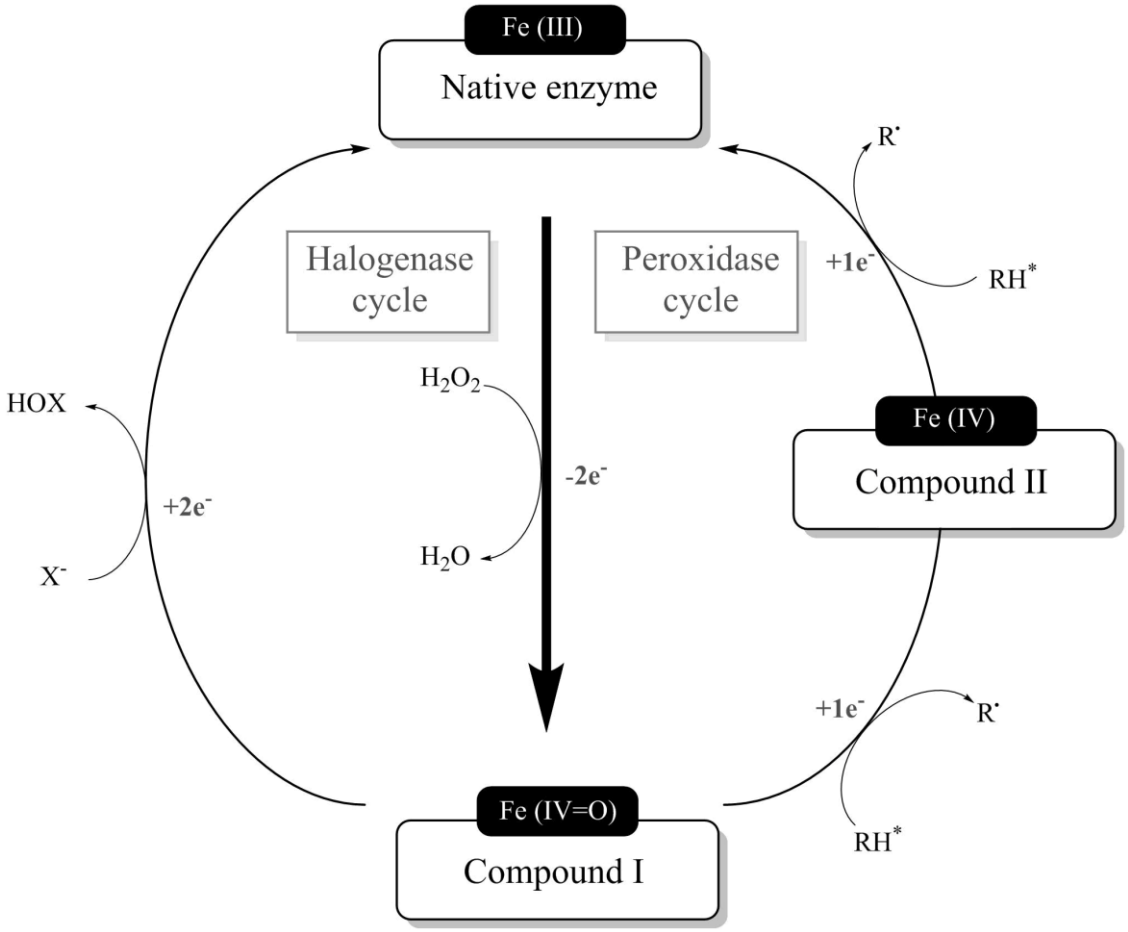


**Figure 2. The catalytic cycles of animal heme peroxidases**. The native enzyme is oxidised by hydrogen peroxide to Compound I, which can then undergo two-electron reduction (halogenase cycle), or two consecutive one-electron reduction (peroxidase cycle), and return back to the native enzyme. $RH^*$= organic substrate, $R^\bullet$= organic radical, $X^-$= halide, HOX= hypohalous acids.

**Table 1. Peroxidases and their substrates**. Plasma concentrations of some of the physiological peroxidase substrates and the rate constants for their reactions with peroxidases (13, 14).

| | Plasma concentrations | hsPxd01-con4* | MPO | EPO | LPO |
|---|---|---|---|---|---|
| Chloride | 140 mM | 0 | $2.5 \times 10^4$ | $0.31 \times 10^4$ | 0 |
| Bromide | 20-100 μM | $5.6 \times 10^6$ | $1.1 \times 10^6$ | $1.9 \times 10^7$ | $4.1 \times 10^4$ |
| Iodide | 100-500 nM | $1.68 \times 10^7$ | $7.2 \times 10^6$ | $9.3 \times 10^7$ | $1.2 \times 10^8$ |
| Thiocyanate | 20-120 μM | $1.83 \times 10^7$ | $9.6 \times 10^6$ | $10 \times 10^7$ | $2 \times 10^8$ |

* hsPxd01-con4 = a truncated recombinant human peroxidasin that contains peroxidase and Ig domains.

## 1.2. Peroxidasin

### *1.2.1 History*

Peroxidasin was first discovered in 1994, when Nelson *et al.* isolated and characterised the protein from *Drosophila* cells in culture (15). Peroxidasin was found in the hemocytes; migratory cells in the hemolymph which are involved in ECM deposition and destruction of apoptotic cells. Based on analysis of its structure and spatio-temporal expression, peroxidasin was hypothesised to be involved in the consolidation of the ECM, pathogenic defense and phagocytosis (15). Five years later, a homolog of *Drosophila* peroxidasin gene was found to be upregulated in p53-dependent apoptotic cells in a human colorectal cancer cell line (16). This gene, named p53-responsive gene 2 (PRG2), was not well characterised but hypothesised to have a role in apoptosis induced by reactive oxygen species. The PRG2 mRNA is expressed in most normal human tissues, with the highest expression in the heart, placenta, spleen, ovary and intestines (16). Shortly after, the melanoma gene (MG50) was reported in a human squamous lung carcinoma cell line (17). The sequence of the MG50 product has 75% homology to the *Drosophila* peroxidasin. Based on homology with other genes, MG50 was hypothesised to code for the IL-1 receptor antagonist protein, a pro-inflammatory cytokine (17). Eight years later, two other homologs of *Drosophila* peroxidasin were found in humans by a sequence homology search (18). These two proteins were termed vascular peroxidases (VPO1 and VPO2) because they were thought to be mostly expressed in the vascular system. The peroxidase domain of human and mouse VPO1 is highly homologous to that in other heme peroxidases (MPO, EPO, LPO and TPO). RT-PCR showed that VPO1 mRNA is expressed in many embryonic and adult tissues. However, the protein was only found in the heart tissues and vascular wall as measured by western blotting (18). In this study, Cheng *et al.* also reported detection of high levels of VPO1 (~1 μM) circulating in normal human plasma. A later study reported that plasma VPO1 is enzymatically active (19). VPO2, alternatively named peroxidasin 2, or peroxidasin-like protein (PXDNL) is catalytically inactive. It is only expressed in the human heart and elevated in the failing heart (20). A third human

peroxidasin, which is nearly identical to peroxidasin 2 is thought to be a splicing variant (21).

It is worth noting that the naming of VPO1 is controversial and seems redundant. The protein itself is not different from the one discovered by Nelson *et al* in 1994 (15), which most of the published literature refers to as peroxidasin. In this thesis, I use peroxidasin (PXDN) to refer to peroxidasin 1, the catalytically active enzyme.

Peroxidasin was confirmed to be produced by human primary cells, such as fibroblasts (22). Immunofluorescence labelling revealed that peroxidasin co-localises intracellularly with the endoplasmic reticulum, as well as extracellularly in fibril-like structures. A homolog of *Drosophila* peroxidasin was reported in *Xenopus tropicalis*, with high expression in the neural tube and pronephros during development, and later in adult kidney (23). These reports in invertebrates and vertebrates all pointed to a novel evolutionarily conserved heme peroxidase. The following sections outline the current knowledge on the structure, function and reaction mechanism of peroxidasin, as well as its role in disease.

### *1.2.2 Structure*

Peroxidasin is a large protein with several domains and linking regions (15). Arrangement and model structures of peroxidasin domains are shown in **Figure 3** and **Figure 4**. The hydrophobic signal peptide at the N-terminal is for secretion of the protein to the extracellular space (15, 21, 24). The next domain contains five leucine-rich repeats (LRRs), which is a common feature in proteins that function in protein-protein interactions, cell adhesion and signalling (15, 21). A flanking region connects the LRRs to four immunoglobulin-loop (Ig) motifs, which are ubiquitous and play a variety of roles, mainly in cell adhesion. The enzymatically active peroxidase domain is highly homologous to the catalytic domains of other mammalian heme peroxidases (~40 % identical and >20 % similar amino acid sequence to other mammalian peroxidases), with the highest similarity to lactoperoxidase (15). The peroxidase domain forms α-helical structures, with a heme group in the centre. The sequence contains ten conserved cysteine residues

involved in disulfide bridges (21, 25). A multiple sequence alignment shows that the key catalytic and metal binding residues are conserved, including the distal His, Gln, and Arg and the proximal His and Asn (**Figure 5**). Flanking the peroxidase domain on the C-terminus is the von Willebrand factor type C domain (VWC), which features in a large number of ECM proteins. This domain was thought to be involved in the trimerisation of peroxidasin. However, a recent study showed the alpha-helical linker region located between the peroxidase and the VWC domains is actually the crucial sequence for trimerisation (26).

The peroxidasin monomer has a molecular weight of ~ 165 kDa. Three monomers are linked by disulfide bonds to form a homotrimer that has a size of ~500 kDa (**Figure 6**) (15, 24). Oligomerisation of peroxidasin into a trimer occurs intracellularly (26). Trimerisation is not necessary for catalytic activity, as monomeric peroxidasin is equally active. However trimerisation is essential for the incorporation in the ECM and optimal cross-linking of collagen IV (24). The native trimeric peroxidasin was found in the endoplasmic reticulum and on the cell surface. When a cysteine residue was mutated to stop it from trimerising, the monomeric construct was not detected on the cell surface, indicating that oligomerisation is necessary for the attachment of secreted peroxidasin to the cell surface.

Peroxidasin is post-translationally modified by *N*-glycosylation at eleven sites (25) and cleavage by proprotein convertases close to its C-terminus. Truncation of the VWC domain enhances its enzymatic activity and provides a regulatory mechanism for its function (27). The multiple domains and overall structure of peroxidasin make it the most structurally complex mammalian heme peroxidase. Interestingly, peroxidasin is proposed to be the ancestral enzyme of the animal heme peroxidase family, with the loss of the non-catalytic domains giving rise to TPO, LPO, EPO, and MPO (**Figure 7**) (28).


**Figure 3. Domain arrangement of peroxidasin**. Schematic presentation of the linear arrangement of peroxidasin domains, including the secretory signal (S), leucine rich repeats (LRR), immunoglobulin domains (Ig), peroxidase domain and von Willebrand factor C domain (VWC).

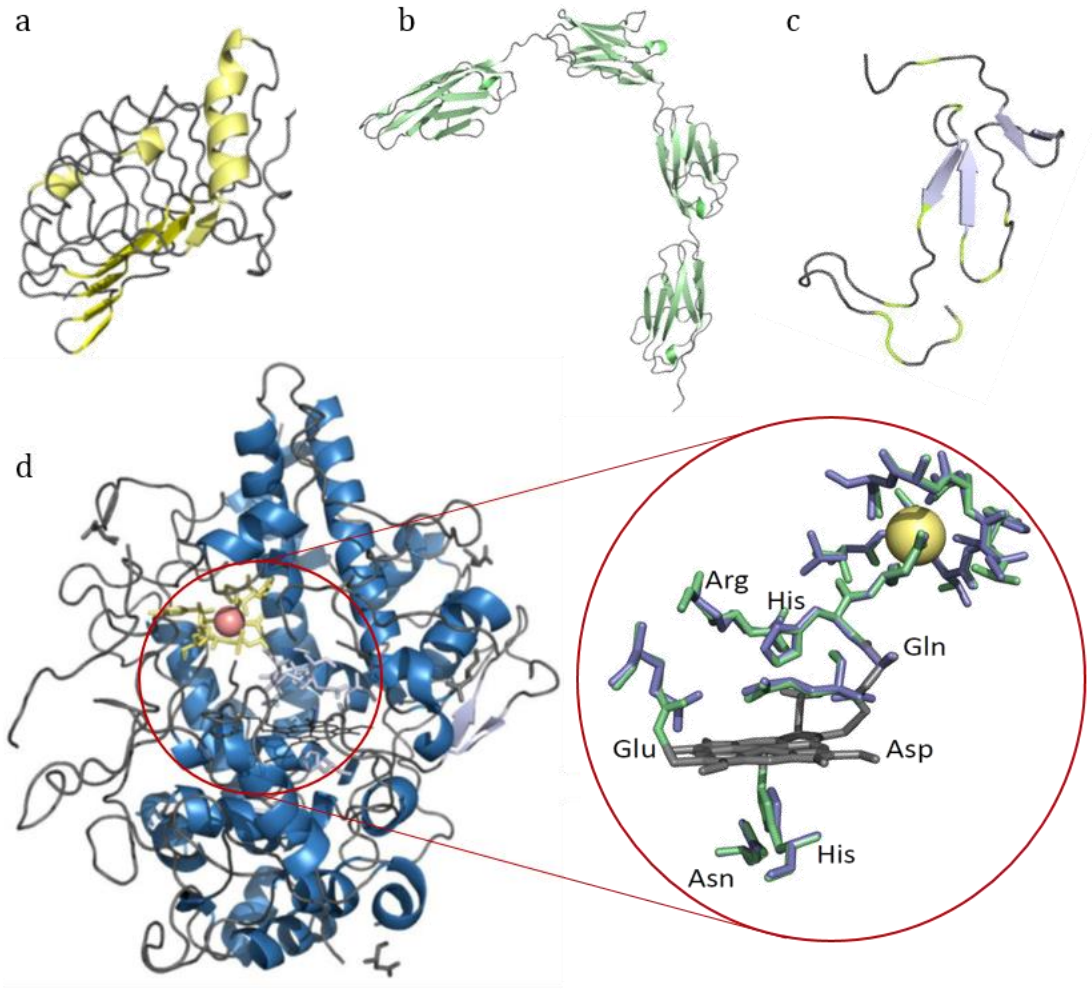


**Figure 4. Model structures of peroxidasin domains**. Models for (a) LRR domain, (b) four Ig domains, (c) VWC domain and (d) peroxidase domain. Inset shows the active site of peroxidasin with the heme- and calcium-binding amino acid residues. The peroxidase model is constructed using homologous goat LPO as a template. The crystal structure of peroxidasin has not been solved yet. Adapted from (25, 29).


**Figure 5. Amino acid sequence of the peroxidase domain of peroxidasin**. Residues conserved across human PXDN, MPO, LPO, TPO and EPO are enclosed in an open box. Catalytic residues are highlighted in red. Residues that bind prosthetic group are highlighted in grey. Residues that bind to calcium are highlighted in yellow. Cysteine residues involved in disulfide bridges are connected. The two cysteine residues responsible for trimer formation are boxed in red. The free cysteines are underlined. Sequences were obtained from Uniprot. Multiple sequence alignment was performed using Cobalt Constraint-based Multiple Alignment Tool (NCBI) (25, 26).

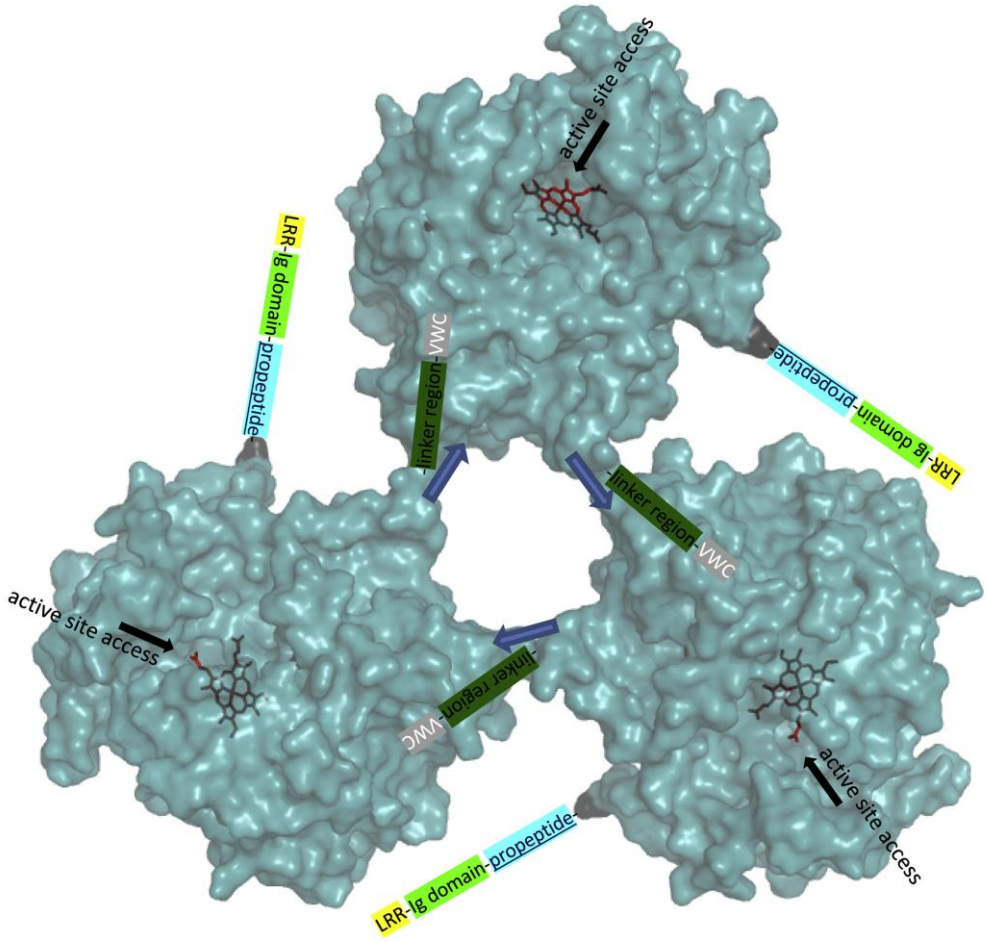


**Figure 6. Model of the trimeric peroxidase domain of peroxidasin**. The model of the peroxidase domain of peroxidasin was constructed with SWISS model using the structure of goat lactoperoxidase (PDB code 2R5L) as a template. It comprises the amino acids Ala718-Asp1314 of peroxidasin with addition of Cys1315 at the C-terminus. The heme is shown in the active site. Blue arrows mark the disulfide bonds between monomers, black arrows mark the access to the active site (26).

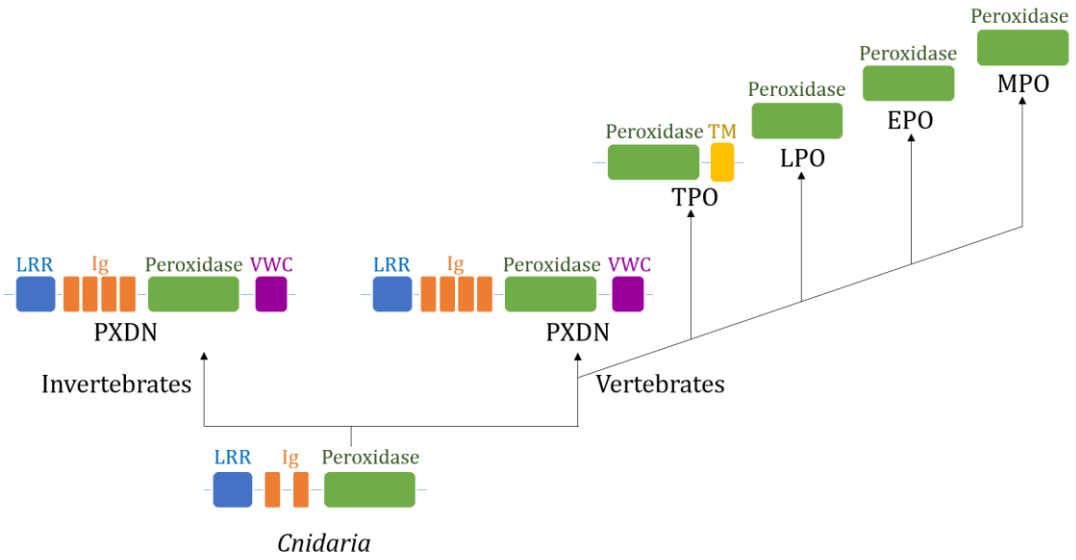


**Figure 7. Evolution of animal peroxidases**. Peroxidasin is proposed to be the ancestral animal heme peroxidase in *Cnidaria*, which extended into invertebrates and vertebrates with addition of Ig and VWC domains. TPO arose from peroxidasin as a result of gene duplication, deletion of non-catalytic domains and fusion with a transmembrane (TM) domain. Loss of TM domain and successive gene duplications gave rise to LPO, EPO and MPO (28).

### *1.2.3 Function*

Since its discovery in *Drosophila*, peroxidasin was thought to have extracellular and intracellular functions. The uncommon combination of the non-catalytic domains with the active peroxidase domain, and the constitutive secretion of peroxidasin led to the hypothesis that peroxidasin is involved in cross-linking of the extracellular matrix (15). In addition, peroxidasin was proposed to act intracellularly in the phagocytic breakdown of apoptotic cells. The mechanism of activity was unclear, but Nelson and colleagues postulated that it might be similar to the cross-linking of tyrosine residues by other peroxidases (**Figure 8**), such as ovoperoxidase in sea urchin which forms dityrosine bridges to stabilise the ECM (30). Peroxidasin purified from *Drosophila* exhibited peroxidase activity, with oxidative iodination of proteins and formation of dityrosine (15). The heme poison azide inhibited the enzymatic activity of peroxidasin, providing further evidence that this protein is indeed a heme peroxidase. A lysate of peroxidasin-transfected cells was also found to oxidise Amplex red to the fluorescent resorufin, strengthening the evidence that peroxidasin has peroxidase activity (22).

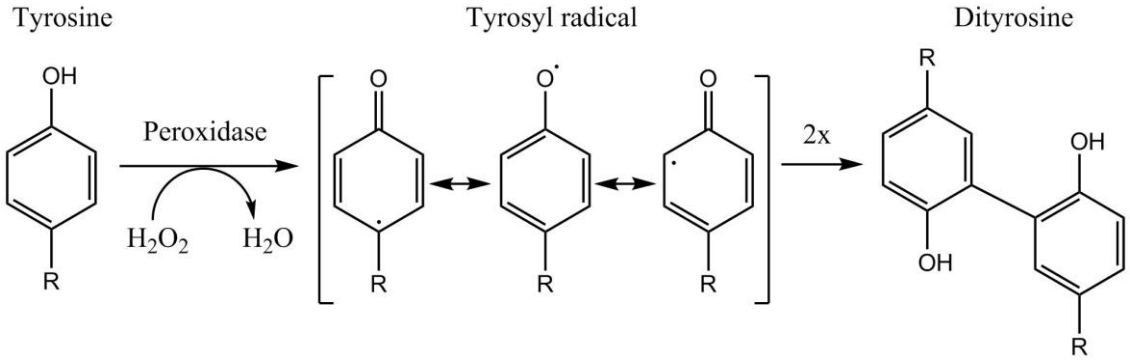


**Figure 8. Formation of dityrosine by peroxidases**. Peroxidases can oxidise tyrosine in two sequential one-electron oxidation steps to form radicals that dimerise into dityrosine.

Gotenstein *et al.* reported an essential biological function of peroxidasin 2 in *C. elegans* embryonic morphogenesis (31). They showed that peroxidasin 2 promotes elongation and muscle attachment at specific embryonic developmental stages, as well as axon regrowth following injury in adult worms. Mutations in the *pxn-2* gene caused abnormal epidermal morphology, some of which were lethal. A later study showed that peroxidasin 1 was also involved in the structural integrity of ECM and neuronal guidance during *C. elegans* development (32). The knockout of peroxidasin gene in mouse embryonic fibroblasts and *Drosophila* resulted in a disorganised network of collagen IV, which further supported the hypothesised biological function of peroxidasin in cross-linking ECM (24, 33). Peroxidasin was found in the epithelial layers of the cornea and lens. Evidence from human case studies suggested that peroxidasin is essential for the normal development of the eyes, and plays a role in supporting the structure of the cornea and lens, and potentially protecting the eye against oxidative damage (34). All of this data is consistent with the proposed role of peroxidasin in the biogenesis and maintenance of the ECM.

Our understanding of the physiological function of peroxidasin in mammals gained a leap forward when Bhave *et al.* provided the first *in vitro* evidence that peroxidasin catalyses the formation of the sulfilimine bond to cross link collagen IV in ECM isolated from a mouse epithelial cell line (33). They showed that peroxidasin was involved in the cross-linking through the production of hypohalous acids (**Figure 9**). Interestingly, myeloperoxidase and lactoperoxidase were inefficient in catalysing the sulfilimine bond formation in collagen IV when overlaid on top of isolated uncross-linked ECM (33). Collagen IV isolated from peroxidasin knockout mice lacks sulfilimine cross links which are present the wild type (24). Bromide was shown to be essential for the peroxidasin-catalysed cross-linking of collagen IV. Dietary bromide deficiency resulted in a significant loss of the sulfilimine bond and increased lethality in *Drosophila* (35).

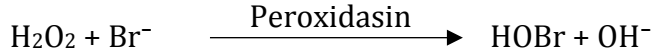


**Figure 9. Proposed reaction for the generation of HOBr by peroxidasin**.

The physiological function of peroxidasin as a generator of a powerful oxidant in the ECM may not be limited to cross-linking of collagen IV. A study has shown that the expression of peroxidasin was upregulated after bacterial infection in the gut of mosquito (36). Some studies also suggested an antibacterial activity of peroxidasin (37, 38) and a role in redox signalling by interacting with the antioxidant response transcription factor Nrf2 (39). Peroxidasin is also suggested to play a role in wound repair through cross-linking tyrosine (40). More recently, peroxidasin was shown to function in angiogenesis by promoting phosphorylation of different kinases and inducing the proangiogenic downstream genes (41).

### *1.2.4 Reaction mechanism*

Progress in elucidating the enzymology of peroxidasin is limited by technical challenges to purify or express the native full-length trimeric enzyme, with heme incorporation and enzymatic activity. Researchers in Obinger's laboratory in Vienna have successfully produced an active truncated monomeric variant of peroxidasin containing only the peroxidase and the four Ig domains with the heme prosthetic group covalently attached. Kinetic studies using this construct (hsPxd01-con4) provided very useful insights into peroxidasin substrate specificity and mechanism of catalysis (13, 25).

The spectral features of this monomeric construct (hsPxd01-con4) are very similar to those of lactoperoxidase (**Figure 10**), which reflects the similarity in amino acid sequence and active site environment. Spectroelectrochemical analysis of hsPxd01-con4 gave a standard reduction $E'^{\circ}$ [Fe(III)/Fe(II)] of -128 mV, second to myeloperoxidase in oxidising power (**Table 2**).

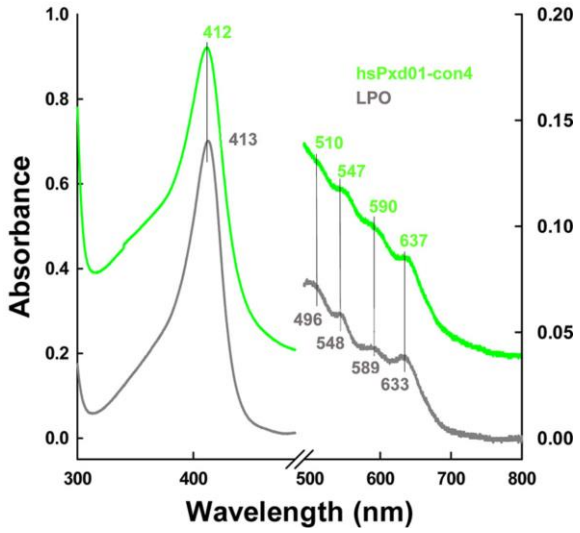


**Figure 10. Spectral features of peroxidasin**. UV-visible spectra of hsPxd01-con4 (green) and lactoperoxidase (grey) in 100 mM phosphate buffer, pH 7.4. Figure from (13).

**Table 2. Reduction potentials for mammalian peroxidases**. Fe(III)/Fe(II) reduction potential for hsPxd01-con4 (in 100 mM phosphate buffer, pH 7.4), for MPO, EPO and LPO (in 10 mM phosphate buffer, pH 7.0).

| | MPO | hsPxd01-con4 | EPO | LPO |
|---|---|---|---|---|
| Fe(III)/Fe(II) | +5 (42) | -128 (13) | -176 (43) | -183 (43) |

These studies demonstrated that hydrogen peroxide efficiently oxidises the native peroxidasin (ferric) to the redox active compound I (oxyiron(IV)). The catalytic cycle of peroxidasin starts when the native enzyme in the ferric state reacts with hydrogen peroxide to form compound I with the oxoiron(IV) state, which increases its oxidising power:

$$\text{Ferric enzyme [Fe(III)]} + H_2O_2 \rightarrow \text{Compound I } [^{\bullet+}\text{Fe(IV=O)}] + H_2O$$

Reaction 1

The apparent rate constant ($k_{app}$) for this bimolecular reaction is within the same range as other mammalian heme peroxidases ($1.1 - 5.6 \times 10^7$ $M^{-1}$ $s^{-1}$). The conserved distal His and Arg aid with the heterolytic cleavage of hydrogen peroxide (44).

Similar to other mammalian heme peroxidases, a high molar excess of hydrogen peroxide converts compound II to the inactive compound III (13), (reaction 2):

Compound II [Fe(IV=O)] + $H_2O_2$ → Compound III [Fe(II)-$O_2$] ↔ [Fe(III)-$O_2^{\bullet-}$] + $H_2O$

Reaction 2

Compound I can enter the peroxidation cycle (**Figure 2**), which involves two consequential one-electron oxidation steps of an organic substrate (AH), producing radicals ($^{\bullet}$AH) (Reactions 3 and 4):

Compound I [$^{\bullet+}$Fe(IV=O)]+ AH → Compound II [Fe(IV=O)] + $^{\bullet}$AH

Reaction 3

Compound II [Fe(IV=O)] + AH → Ferric enzyme [Fe(III)] + $^{\bullet}$AH + $H_2O$

Reaction 4

Compound I can also enter the halogenation cycle, which involves one-step two electron oxidation of a halide ($X^-$) producing a hypohalous acid (HOX) (Reaction 5):

Compound I [$^{\bullet+}$Fe(IV=O)] + $X^-$ + $H^+$ → Ferric enzyme [Fe(III)] + HOX

Reaction 5

Bromide reacts with compound I and converts it back to the ferric state (rate $5.6\times10^6$ $M^{-1}$ $s^{-1}$ at pH 7.4). It therefore outperforms MPO and LPO but not EPO (**Table 1**) (13). Thiocyanate and iodide are also highly efficient in converting compound I of peroxidasin to the ferric state (rates 1.83 and $1.68\times10^7$ $M^{-1}$ $s^{-1}$ at pH 7.4). Interestingly, high concentrations of iodide (10 mM) inhibited the sulfilimine bond formation in collagen IV, possibly due to acting as a competitive substrate (33).

Peroxidasin was initially reported to moderately oxidise chloride as well (33, 45). Until then, this was thought to be an exceptional ability of MPO, due to the unique sulfonium linkage between the heme and Met residue in its active site. The pre-steady state kinetic study using the recombinant monomeric construct (hsPxd01-con4) showed that chloride cannot reduce compound I of peroxidasin (13). The oxidation activity that was observed in the earlier studies was probably due to residual bromide contamination in chloride (33, 35, 45). Furthermore, the production of hypohalous acids by peroxidasin was determined by tetramethylbenzidine (TMB) assay (33). This assay detects HOCl and HOBr by converting them to the respective chloramine and bromamine. It distinguishes the derived species by the addition of iodide (46), but does not provide a definitive chemical identification of the oxidant produced.

Recent work from the Obinger group shows that peroxidasin can react with endogenous peroxidase substrates (urate, ascorbate, nitrite, serotonin and tyrosine) by one-electron oxidations to generate their respective radicals. These substrates reduced compound I to compound II (rates range between $10^4$ – $10^5$ $M^{-1}$ $s^{-1}$). Reduction of compound II to the resting enzyme by these substrates is approximately 100 fold slower (47).

One of the puzzling questions regarding peroxidasin activity, is the source of hydrogen peroxide, the necessary co-substrate to initiate the catalytic cycle. In the case of other peroxidases, NADPH-oxidases (Nox or Duox enzymes) are the sources of $H_2O_2$ (48). However, a recent study found that Nox knockout and hypoxia had no effect on peroxidasin-catalysed cross-linking of collagen IV (49). One possibility is that intracellular $H_2O_2$ diffuses to the ECM where peroxidasin can use it (50), as mitochondria are often located at the basolateral side of epithelial cells close to the basement membrane, but that hypothesis is yet to be tested.

### *1.2.5 Role in disease*

An increasing amount of evidence implicates peroxidasin in a number of pathologies. Loss of function of peroxidasin is detrimental to *Drosophila and C. elegans* because of compromised integrity of the basement membrane (15, 31-33, 51). Peroxidasin mutation is not lethal in mice or humans, but causes disruption to the basement membrane, especially in the eye lens and cornea (52). Mutations in peroxidasin lead to inherited eye disorders, including microphthalmia (small eye), anterior segment dysgenesis, congenital cataract and developmental glaucoma in humans (34, 52-54). A missense mutation was found in patients with recessively inherited congenital cataract-microcornea with corneal opacity. In this mutation, a conserved arginine in the peroxidase domain is changed to a cysteine residue, altering the structure and function of peroxidasin and leading to the pathology (34).

Peroxidasin (termed VPO1 in these studies) was found to promote oxidative stress in the cardiovascular system and contribute to the oxidation of low density lipoprotein and endothelial dysfunction (55-62). Other studies proposed the involvement of peroxidasin in mediating oxidative injury following ischemia-reperfusion (63), and showed that its inhibition alleviates cardiac dysfunction and ischemia-reperfusion induced apoptosis (64, 65). Expression of peroxidasin was upregulated in a rat model of hypertension, suggesting its involvement in the regulation of vascular smooth muscle cell proliferation and possible contribution to vascular remodelling in hypertension (66, 67).

Peroxidasin is also implicated in renal and pulmonary pathologies. It contributes to renal inflammation and fibrosis in a mouse model of chronic kidney disease (22, 68). Inhibitory anti-peroxidasin antibodies were found in the sera of patients with pulmonary-renal syndromes, in samples taken before and during active disease, suggesting a role in the pathogenesis (69).

Increasing evidence in recent years shows altered expression of peroxidasin in various types of cancer including melanoma, acute myeloid leukemia, metastatic glioblastoma, breast, renal, colon and ovarian cancers (70-76). Upregulation of

peroxidasin expression in prostate cancer promotes disease progression by altering the redox environment and decreasing cell apoptosis (77). Peroxidasin is involved in epithelial-mesenchymal transition, a process in which cancers acquire an invasive phenotype (78). Gene expression profiling in fourteen types of cancer demonstrates that the peroxidasin gene plays a key role in the heme-oxygenase-1-dependent cell adhesion and invasion in neoplastic cells (79). Silencing the peroxidasin gene abolished the adhesion-promoting effect of heme oxygenase-1 in two melanoma cell lines. The human homolog of peroxidasin found in colorectal cancer (PRG2) was proposed to have an intracellular role in producing reactive oxidants that induce apoptosis by inactivating the p53 tumour suppressor protein (16).

In summary, peroxidasin plays a role in a multitude of diseases by different mechanisms that include altering the redox homeostasis, changing ECM properties and promoting fibrosis, angiogenesis and cancer metastasis.

## 1.3. Biological oxidants

Oxidants are a wide class of molecules that remove one or two electrons from other molecules to become reduced. They include radical and non-radical reactive oxygen species (ROS), reactive nitrogen species (RNS), and halogenated species (**Figure 11**). Biological oxidants are produced constantly as part of normal physiological processes such as respiration (80). There are endogenous sources of ROS (e.g. mitochondria, NADPH oxidases) and exogenous sources (e.g. radiation, xenobiotics) (81).

Regulated production of ROS plays essential roles in signalling pathways, cellular differentiation, immune response and responding to growth hormones (82, 83) (**Figure 12**). Dysregulated ROS production can distort the redox balance, leading to oxidative stress, which can have deleterious effects especially in chronic inflammatory conditions (83).

Alongside oxidants, there are complex protective mechanisms that include antioxidant enzymes (e.g. catalase, superoxide dismutase, peroxiredoxins), and low molecular weight antioxidant compounds (e.g. glutathione, ascorbate, tocopherols) (84, 85). These antioxidant systems counteract the oxidative burden and maintain steady-state redox homeostasis. Oxidative stress occurs when antioxidant systems are overwhelmed by oxidants.

Oxidants are not made equal in their oxidative power (86). Similarly, antioxidants differ in their reactivities with oxidants. Appropriate attention should be given to each individual case of oxidant and antioxidant to assess their contribution to physiological and pathological processes. For relevance to the research topic, I will focus here on reactive halogen species and their biological reactions.

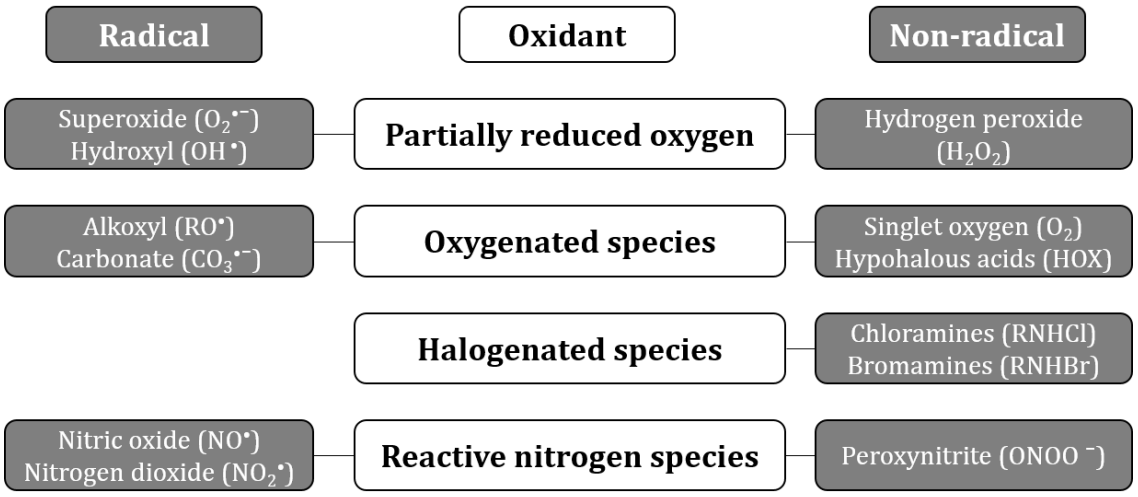


**Figure 11. Major types of biological oxidants and some examples**. (81).

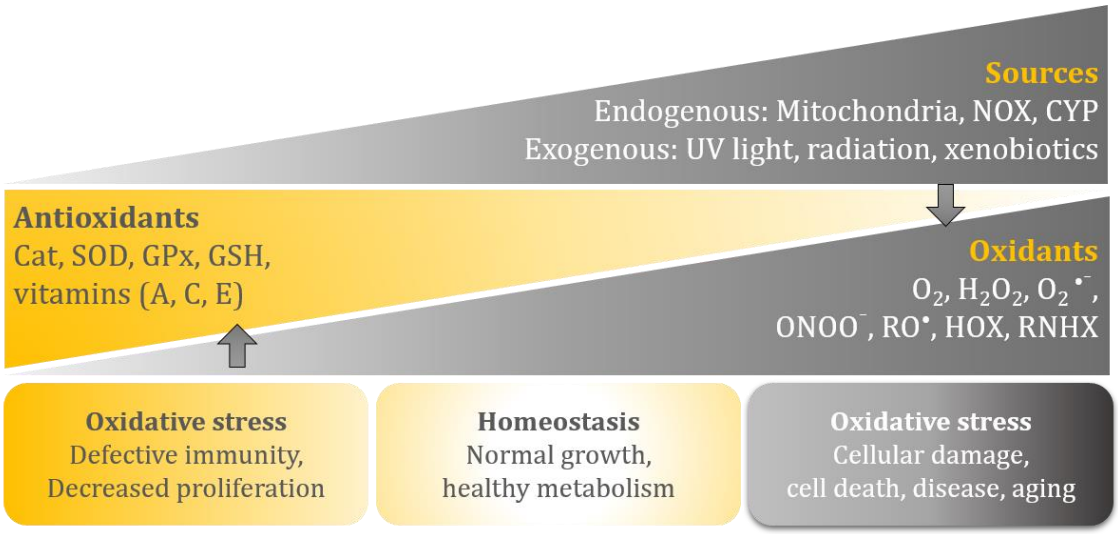


**Figure 12. Sources and physiological functions of biological oxidants**. There are endogenous and exogenous sources of ROS. Redox homeostasis is important for normal physiological processes, which can be impaired under oxidative stress. NOX, NADPH oxidases, CYP, cytochrome P450, Cat, catalase, SOD, superoxide dismutases, GPx, glutathione peroxidase, GSH, glutathione (84).

### *1.3.1 Reactive halogen species*

Cytotoxic (pseudo)hypohalous acids are produced by the reactions of hydrogen peroxide with halide ions ($Cl^-$, $Br^-$ and $I^-$) and the pseudohalide $SCN^-$, which are catalysed by mammalian heme peroxidases (87). Reactive halogen species have diverse biological functions like antimicrobial defence, hormone biosynthesis and consolidation of ECM. They can also cause extensive damage to host tissues, which contributes to the aetiology and progression of inflammatory diseases (12, 88).

Hypohalous acids differ in their oxidising power (HOCl > HOBr > HOSCN) and rates of reactions with different biological targets (14). They are highly reactive with sulfur-containing compounds (e.g. methionine, cysteine and glutathione), and less so with amines (e.g., N-terminus and the side chains of lysine and arginine), aromatic compounds (e.g., tyrosine and tryptophan), double bonds (e.g., fatty acids and cholesterol) and water-soluble antioxidants (e.g., urate and ascorbate) (5, 89-92). It is essential to keep in mind that the rates of reactions of HOCl and HOBr can vary substantially (**Figure 13**). The rates of reactions of HOCl with Met and Cys are 10-fold faster than those for HOBr. Conversely, HOBr reacts with amines and double bonds faster than HOCl (93). Halohydrins form on phospholipids at lower concentrations of HOBr than HOCl (94, 95). With the exception of ascorbate, antioxidants react faster with HOBr than with HOCl. HOCl is a stronger two-electron oxidant (**Table 3**) (96), but HOBr is a more powerful electrophile and hence a better halogenating agent (97). These are important considerations when studying the hypohalous acid-mediated oxidative modifications and their roles in different pathologies.

The reactions of HOCl and HOBr with primary amines form the respective mono- and dichloramines and bromamines (Equations 1 and 2) (98, 99). They retain some of the oxidising power and selectivity of the original oxidants. They can be highly abundant, and therefore key mediators of oxidative modifications (83).

$RNH_2 + HOX \rightarrow RNHX + H_2O$ (X=Cl, Br) Equation 1

$RNHX + HOX \rightarrow RNX_2 + H_2O$ Equation 2

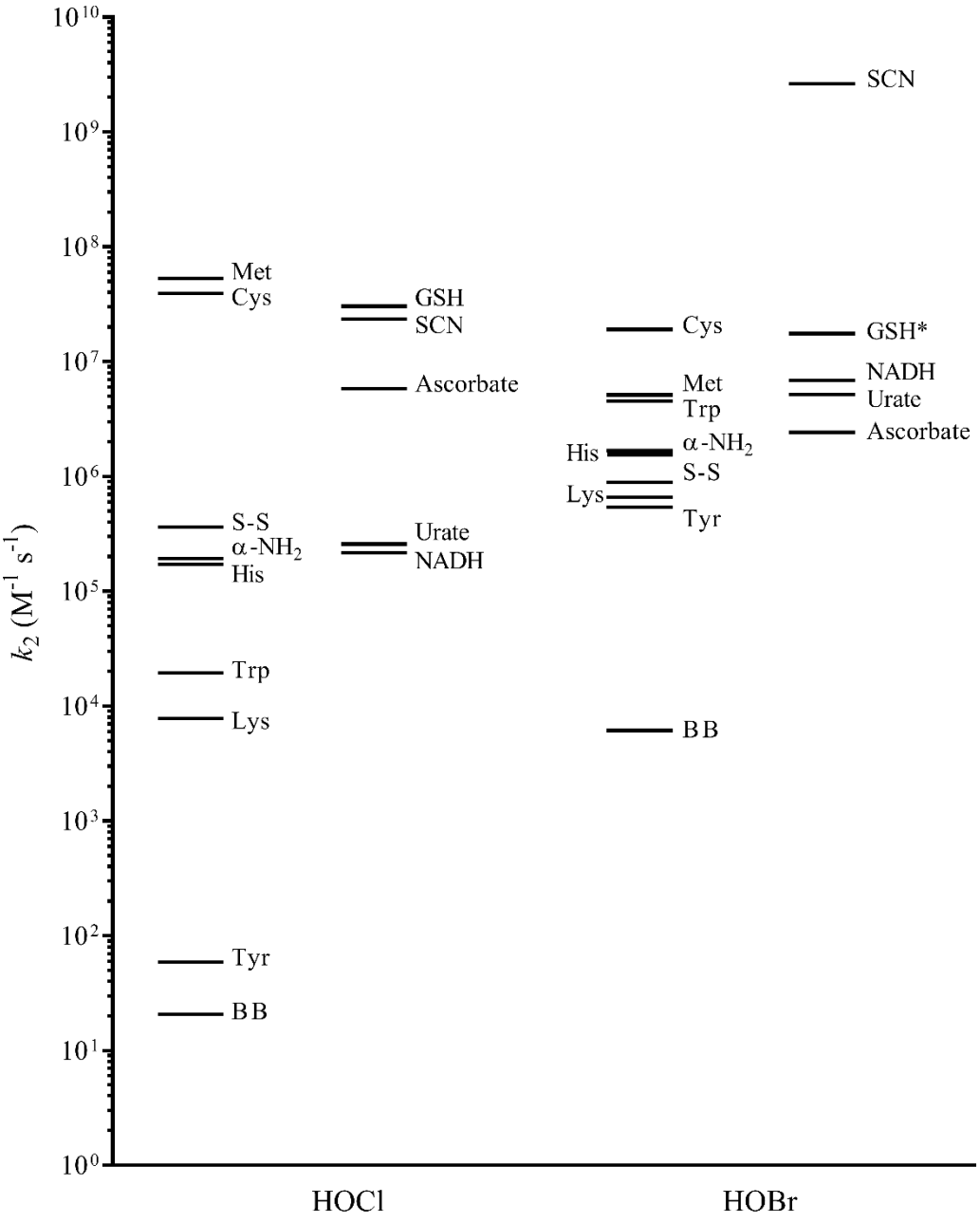


**Figure 13. Reactions of HOCl and HOBr**. Summary of second-order rate constants for the reactions of HOCl and HOBr with different amino acids, antioxidants and scavengers on a log scale. Most of the rate constants were measured at physiological pH at 22°C. S-S, disulfide bond, α-$NH_2$, terminal amine, BB, backbone amides. The rate constant for the reaction of HOBr with GSH* is shown as that measured for *N*-acetylcysteine. (5, 81, 87, 92, 93, 96, 100, 101).

At physiological pH (7.4), hypohalous acids exist in equilibrium with their anions (HOCl/$^{-}$OCl, HOBr/$^{-}$OBr, HOSCN/$^{-}$OSCN). Their pKa values vary substantially and consequently the major active species will be different for each of them at physiological pH (**Table 3**) (14). The properties and reactivity of hypohalous acids can be significantly altered by slight variations in pH, especially cell permeability as they become more membrane permeable when they are protonated (14). Therefore, special attention should be given to reaction conditions in kinetic studies.

**Table 3. Properties of HOCl, HOBr, and HOSCN**. Reduction potentials and pKa values for hypochlorous acid (HOCl), hypobromous acid (HOBr) and hypothiocyanous acid (HOSCN) (14, 96, 102, 103).

| | HOCl | HOBr | HOSCN |
|---|---|---|---|
| E° (V) | 1.28 | 1.13 | 0.56 |
| pKa | 7.59 | 8.7 | 5.3 |

## 1.4. Protein oxidation

Biomolecules are constantly exposed to oxidants produced as part of normal physiological processes. Proteins are major targets for oxidants, because of their abundance and the high reaction rates of oxidants with amino acid side chains. Protein oxidation can be reversible, like disulfide bond formation and *S*-nitrosylation, or irreversible, like oxidation of aromatic amino acid side chains. Oxidative modifications of proteins are often regarded as collateral damage. While this is true in a lot of the cases, protein oxidation can be deliberate and serve a particular function, such as redox-regulated intracellular and intercellular signalling. For example, oxidation and reduction of thiol groups to activate peroxiredoxins and caspases (104). Another example of a deliberate oxidative modification is the cross-linking of collagen IV, which is explained in more detail in Section 1.5.2.

Nonetheless, oxidative damage occurs, despite multiple antioxidant systems and prevention and repair mechanisms. This is especially the case in chronic inflammation, deterioration in enzyme efficiency and accumulation of damage with aging (84). Oxidative damage can affect DNA, proteins, carbohydrates and lipids (104). Protein oxidative damage can impair the structure and function of enzymes, and interfere with the function of receptors, transport proteins and antibodies (104). For example, oxidative damage to DNA polymerase can compromise the fidelity in DNA replication (104). Oxidised proteins can be immunogenic causing autoimmune diseases, such as rheumatoid arthritis (12, 105). Accumulation of oxidatively damaged proteins in brain tissues is one of the hallmarks of Alzheimer's diseases (106-108). Oxidative damage to fibronectin causes cross-linking of the protein, increases its susceptibility to proteolysis and impairs its functions (109, 110). Hypohalous acids mediated cross-linking of membrane proteins leads to lysis of red blood cells (111). These examples highlight how oxidative damage is involved, as a cause or a consequence, in a raft of diseases.

In the following section, I will focus on two amino acids that are major targets of oxidants and are used as biomarkers for oxidative modifications.

### *1.4.1 Methionine*

The sulfur of methionine is easily oxidised by one- or two-electron oxidants. Oxidation of methionine produces methionine sulfoxide (Met-O), sulfone and dehydromethionine (**Figure 14**) (108, 112-114). Methionine sulfoxide is more hydrophilic than methionine, which can alter protein structure and lead to loss or gain of function (104). The high reactivity of methionine makes it a good endogenous anti-oxidant because of its ability to scavenge oxidants and protect other key amino acids (115). Methionine sulfoxide can be repaired by methionine sulfoxide reductases (116). This reversibility can be used as a switch to activate and inactivate proteins (104). However, oxidised methionine can accumulate with aging and in inflammatory diseases, especially in collagens of long-lived tissues, such as the skin and eye (117, 118).

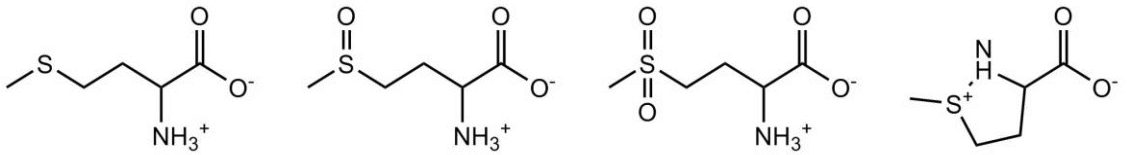


**Figure 14. Chemical structures of methionine and its oxidation products**.

### *1.4.2 Tyrosine*

The aromatic ring of tyrosine is a target for oxidative modifications by different pathways (**Figure 15**). Halogenated tyrosines are minor products but used widely as specific, quantifiable biomarkers of hypohalous acid mediated damage to proteins (119). Chlorotyrosine and bromotyrosine are products of the reactions between tyrosine and HOCl and HOBr, respectively. It is important to bear in mind that the rates of tyrosine bromination by HOBr is 5000-fold faster than chlorination by HOCl (**Figure 13**) (93, 120). This is a potential pitfall if chlorotyrosine and bromotyrosine are used as biomarkers, as it might cause over- or underestimation of the oxidative damage by the respective oxidants.

Tyrosine is also a substrate for peroxidases and can be oxidised directly, producing reactive phenoxyl radicals, which can cross-link to form dityrosine (**Figure 8**) (90, 121). Nitrotyrosine is another product of tyrosine oxidation (122). Peroxidases can oxidise nitrite to nitrogen dioxide ($NO_2^{\bullet}$), which undergoes reactions with the phenol of tyrosine forming nitrotyrosine (123, 124). Nitrotyrosine is elevated in bronchoalveolar lavage of asthmatic patients (125) and in human atherosclerotic lesions (126), due to the activities of human peroxidases. Nitrotyrosine can also arise from oxidation by nitrating species such as peroxynitrite (127).

Tyrosine residues play key roles in signaling and enzymatic catalysis. Oxidation of tyrosine can lead to substantial changes in protein structure and function, such as signalling with tyrosine kinase or phosphatase (128). Oxidation products of tyrosine can be useful biomarkers for oxidative damage, especially in pathological situations. Chlorotyrosine is significantly elevated in human atherosclerotic lesions (129, 130). High levels of chlorotyrosine are also found in the sputum and bronchoalveolar lavage fluid of patients with cystic fibrosis (131) and in brain tissues of patients with Alzheimer's disease (107). Bromotyrosine is a specific biomarker for protein modifications by eosinophil peroxidase in asthmatic patients (89, 132). Products of hypohalous acid oxidation are elevated in a multitude of diseases such as cystic fibrosis, asthma, cardiovascular diseases and rheumatoid arthritis (14, 132-140).

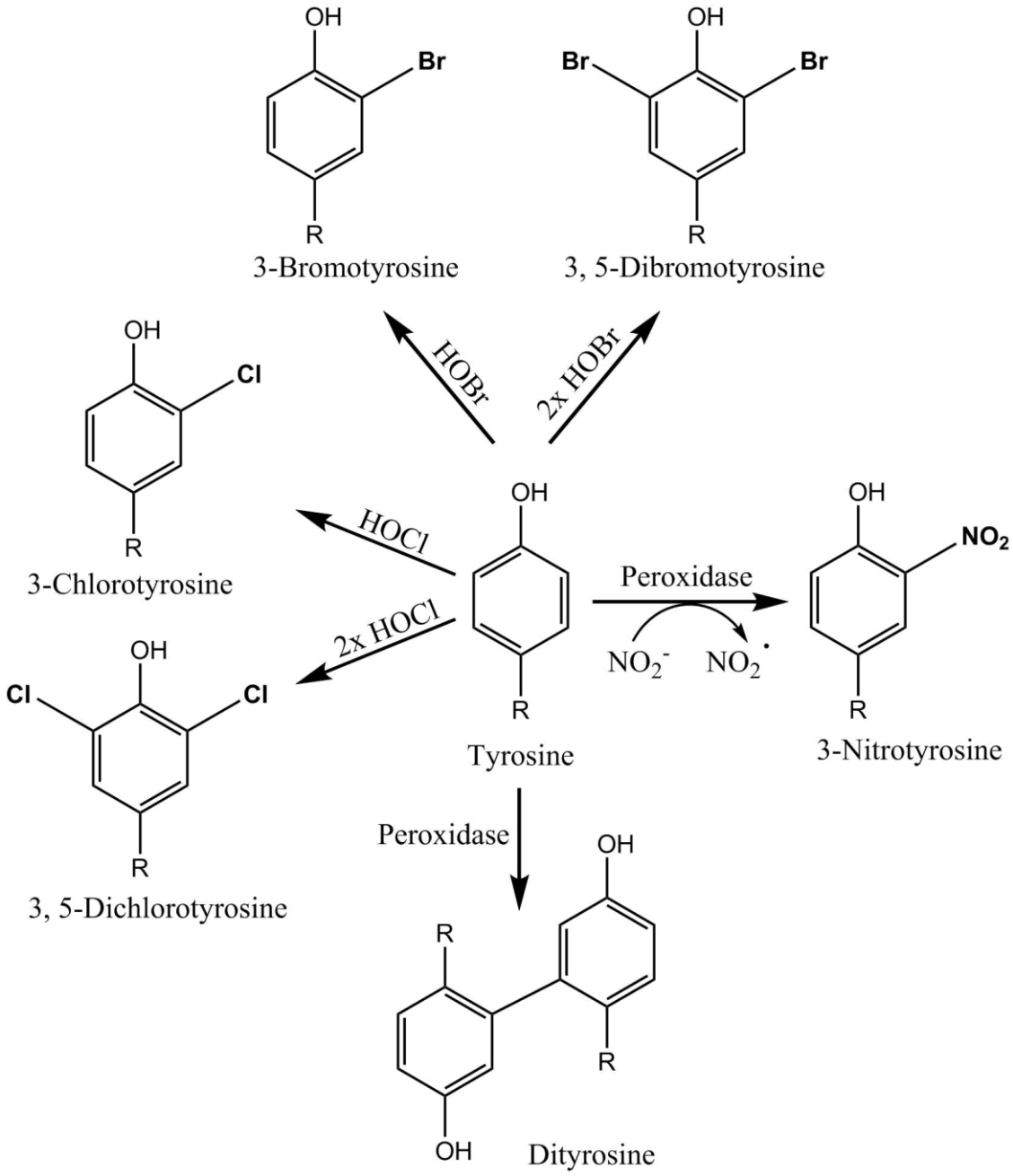


**Figure 15. Tyrosine and some of its oxidation products**. The reaction of HOBr with tyrosine generates 3-bromotyrosine and 3, 5-dibromotyrosine. HOCl reacts with tyrosine to produced 3-chlorotyrosine and 3, 5-dichlorotyrosine. Peroxidases can oxidise tyrosine directly to produce tyrosyl radicals that can dimerise into dityrosine. Peroxidases can also oxidise nitrite ($NO_2^-$) to generate nitrogen dioxide radical ($NO_2^{\bullet}$) which reacts with tyrosyl radical to form 3-nitrotyrosine (119, 141, 142). R= amino acid backbone.

## 1.5. The extracellular matrix and collagen IV

The extracellular matrix is a complex multi-component network of highly cross-linked insoluble material. The major classes of ECM constituents are fibrous proteins (e.g. collagens and elastin) and glycoproteins (e.g. fibronectin, laminin and proteoglycans) (143). The evolution of ECM was a crucial event for the development of multicellular life. ECM provides the structural platform for cells to adhere to, polarise, proliferate, communicate and migrate (144, 145). It also regulates hydration and the pH of the microenvironment and the response to growth factors. Because of its essential and diverse functions, ECM abnormalities can cause dysregulated cell behavior and lead to the progression of many diseases, such as tissue fibrosis and cancers (146-148).

Basement membrane (BM) is a specialised form of ECM that lies between epithelial cell layers and a variety of tissues (**Figure 16**) (149). For most epithelial cells, the BM is the only physical contact with the rest of the body. For example, epithelial cells in the lungs and kidneys are only in contact with the BM, and air and urine, respectively. BM also surrounds endothelial cells of blood vessels, the outer layer of organs, muscle fibers, fat cells and nerve cells. All types of BM consist of laminin, nidogen, perlecan, agrin and collagen IV (**Figure 17**). In addition to the ECM functions above, BM maintains the structural integrity and homeostasis for cells, filters macromolecules and compartmentalises tissues (143).

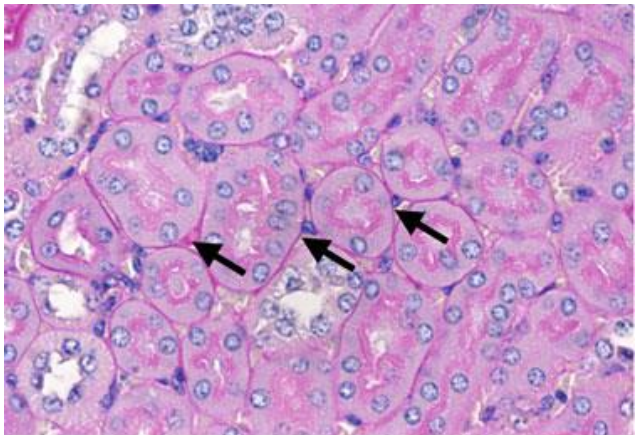

**Figure 16. Histological identification of basement membrane**. Arrows point to basement membrane around tubules of a mouse kidney paraffin section stained with Periodic acid-Schiff. Figure from (143).

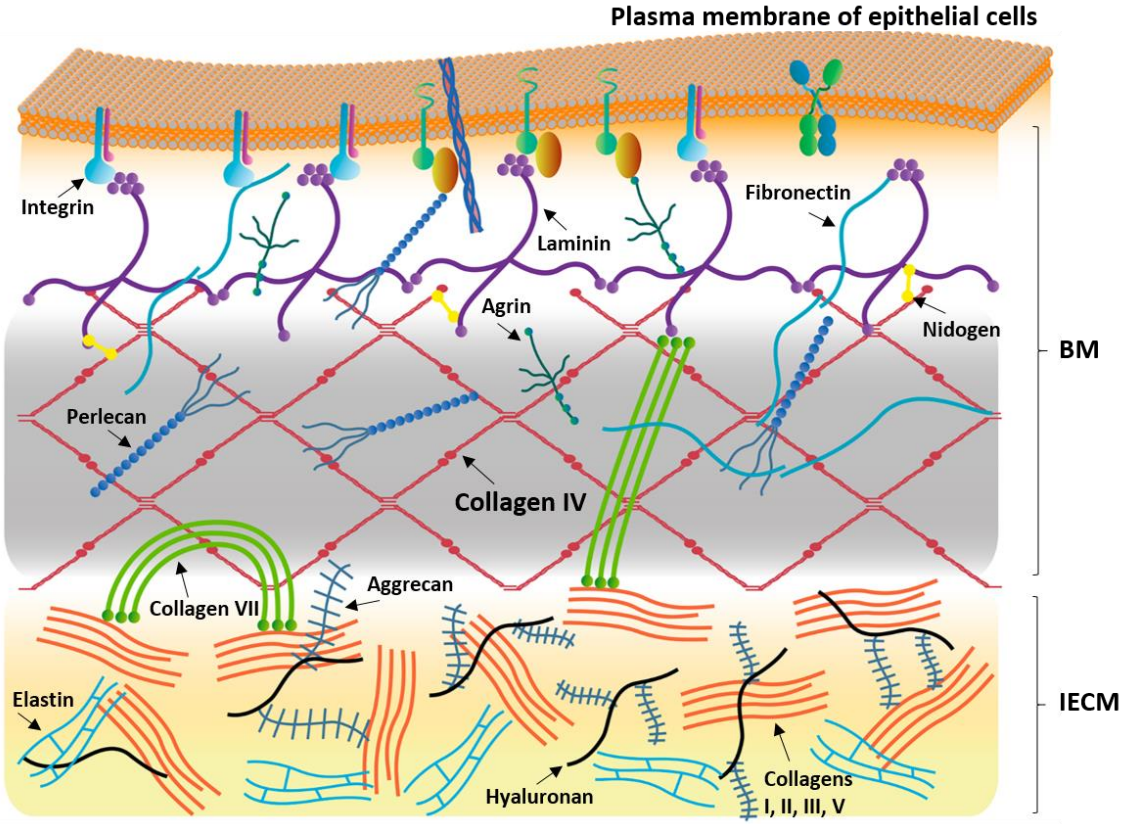


**Figure 17. Schematic model of the basement membrane**. The BM lies between the epithelial cells and interstitial extracellular matrix (IECM). It consists of two layers of laminin and collagen IV which are interconnected by perlecan and nidogen. Figure from (150) with modifications.

### *1.5.1 Collagen IV*

Collagen IV is a major constituent of the basement membrane (accounts for ~50 % of its structural components), and is common to all metazoans, from sponges to primates (151). Collagen IV networks provide tensile mechanical strength and act as scaffolds for the interaction of BM components. These interactions are essential for tissue genesis, cell differentiation, morphogenesis, adhesion, migration, proliferation, homeostasis and signalling (149). Collagen IV is the binding partner for various types of cells including keratinocytes (152), hepatocytes (153), and pancreatic cells (154).

The collagen IV molecule contains three domains; a short domain at the amino terminal (7S), a major collagenous domain that contains Gly-Xaa-Yaa triplet repeats (X, Y= any amino acid), and a non-collagenous domain (NC1 or NCD) at the carboxy terminal (**Figure 18**) (155, 156). There are six homologous but genetically distinct chains (α1- α6) that are differentially expressed in various tissues and developmental stages. Of the several possible combinations, only three heterotrimers occur; α1α1α2, α3α4α5, and α5α5α6. (149). Collagen IV is subject to post-translational modifications, such as oligomerisation, glycosylation of lysine residues, hydroxylation of lysine and proline residues and formation of interchain disulfide bonds between cysteine residues (149, 157). Proteolytic release of the NCD of collagen IV (and other types of collagen) modulates cell migration, proliferation and survival (158). These modifications are vital for proper folding and functioning of collagen IV.

Oligomerisation of collagen IV is a complex process with intracellular and extracellular steps (**Figure 18**). Inside the cell, three chains assemble into a 400-nm-long triple helical protomer. With the help of chaperone proteins, collagen IV heterotrimers are secreted into the ECM where they assemble into a supramolecular polygonal chicken-wire like network (159). The higher chloride concentration outside the cell activates the assembly of two protomers at the NCD with intermolecular electrostatic interaction (160). These interactions are

enzymatically stabilised by sulfur-nitrogen cross links at the NCD (33), and aldehyde cross links at the 7S domain (161).

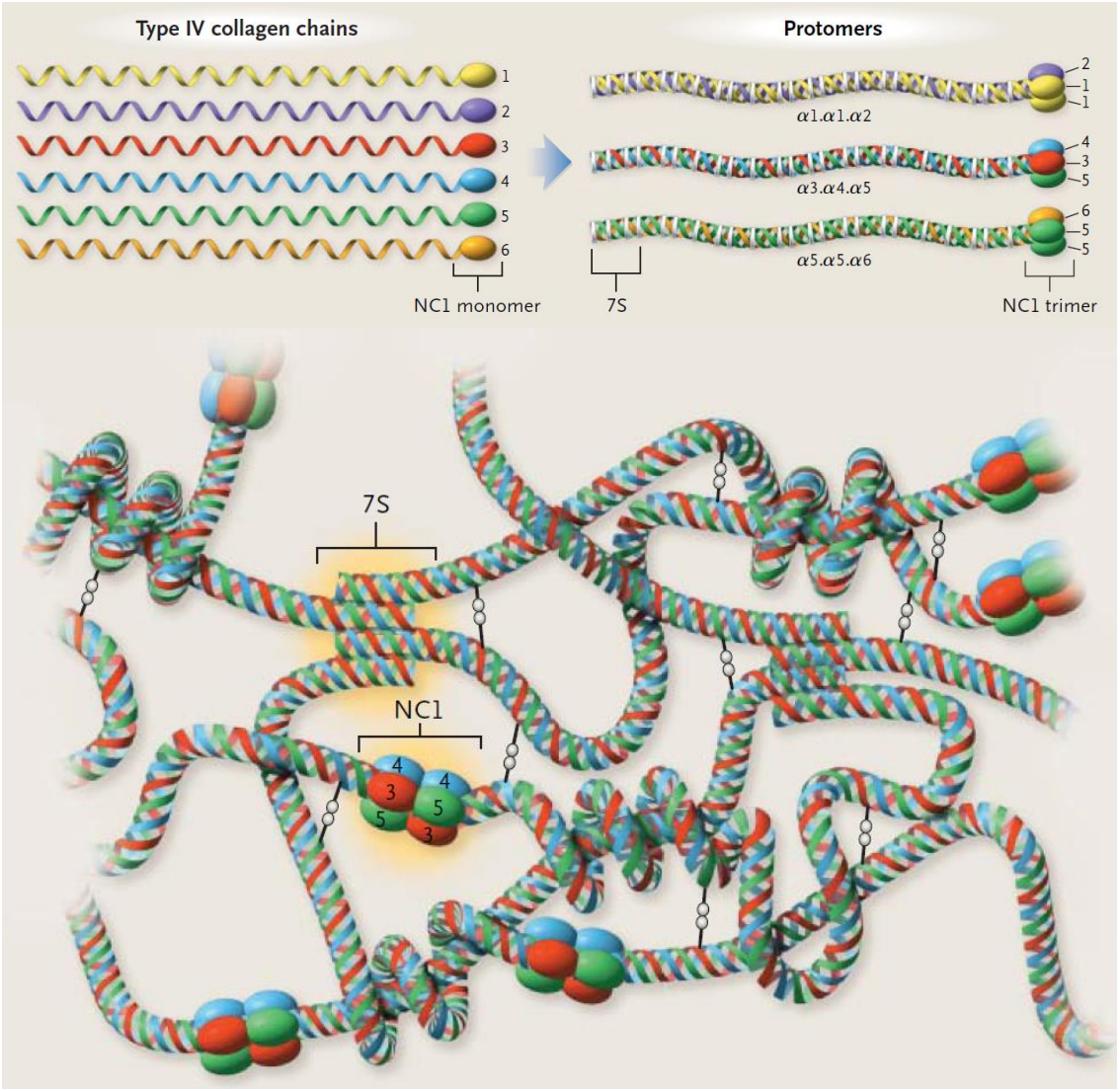


**Figure 18. Collagen IV structure and assembly**. The different types of collagen IV monomers (a1-6) with 7S domain, central collagen domain (~1400 AAs long) and the NCD (~230 AAs). Intracellularly, three monomers assemble into heterotrimers by intermolecular disulfide bonds at the central collagen domain. Extracellularly, two trimers join at the NCD forming an interface hexamer at the C-terminus, and four triple helical 7S domains at the N-terminus forming supramolecular structures. Figure from (162).

### *1.5.2 The sulfilimine bond*

The chemical nature of the cross link at the NCD intersection was a subject of controversy. The bond was hypothesised to be a disulfide bridge (163, 164) or covalent sulfur-nitrogen bond between methionine and lysine (165, 166). Subsequent mass spectrometric evidence led to speculation that the nature of the bond was an *S*-hydroxylysyl-methionine cross link (167). Finally, this sulfur-centered bond was characterised by mass spectrometry and nuclear magnetic resonance as a sulfilimine link, a covalent double bond between the sulfur of $Met^{93}$ and the amine of the juxtaposed $Hyl^{211}$ located at the NCD interfaces of two protomers (168). One or two sulfilimine bonds can form between two NCD molecules, with a maximum of six cross links at the trimer-trimer interface of the hexamer (35). The presence of the sulfilimine cross link modulates mechanical resilience and stiffness of the basement membrane (169).

This peculiar cross link occurred over 500 million years ago, and is conserved throughout the Eumetazoa subkingdom (170). The occurrence of nitrogen-sulfur bonds in biology is rare. The sulfilimine bond is even rarer, with collagen IV being the only known biomolecule to contain this unusual bond (171). Sulfilimine bonds were reported to form intra- and intermolecular cross links in peptides treated with hypohalous acids *in vitro* (172). The sulfur-nitrogen bond in the sulfilimine bond is similar to that in dehydromethionine (**Figure 14**), one of the products of the reaction between methionine and hypobromous acid (114).

The chemical mechanism of sulfilimine bond formation is still not clear. It is proposed to proceed through bromide transfer from HOBr to $Met^{93}$ forming a bromosulfonium cation intermediate, followed by a nucleophilic attack by the amine of $Hyl^{211}$ forming the intermolecular sulfur-nitrogen double bond (**Figure 19**). Reagent HOBr efficiently generated the sulfilimine cross link in isolated NCD of collagen IV, but HOCl was inefficient (35). When HOCl was reacted with the NCD, formation of methionine sulfoxide increased as identified by mass spectrometry. Pre-treatment of NCD with reagent HOCl inhibited the formation of the cross link by HOBr, indicating that methionine sulfoxide is a dead-end intermediate which

does not react with hydroxylysine to form the sulfilimine bond. This explains the selectivity for bromide in generating this bond.

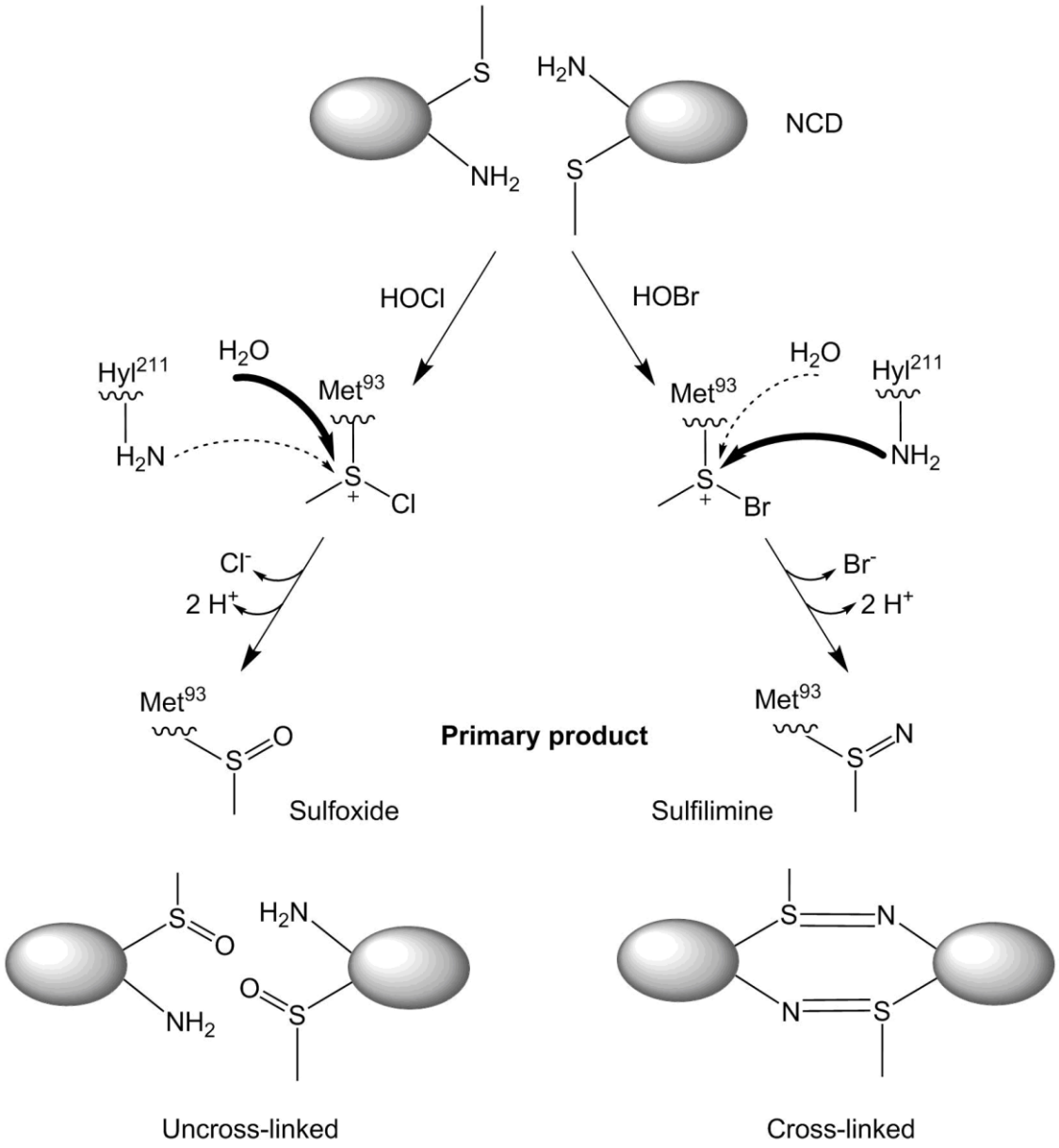


**Figure 19. Chemical mechanism for the formation of the sulfilimine cross link in collagen IV.** The proposed mechanism of sulfilimine bond formation by HOBr involves a bromosulfonium ion intermediate on Met that reacts with the amine of Hyl yielding a sulfilimine link as the primary product. The chlorosulfonium ion thermodynamically favours the reaction with water which yields sulfoxide as the primary product (35, 172). Bold arrows indicate major reactions.

### *1.5.3 Pathologies of collagen IV and the ECM*

Collagen IV malfunction is implicated in several genetic and acquired diseases. Abnormalities in collagen IV destabilise the basement membranes of many organs and impair tissue function, particularly the kidney, due to the key role of basement membrane in glomerulus structure and function (149, 162, 173). Some mutations in collagen IV genes are embryonically lethal, while others lead to human diseases varying in severity, like Alport's syndrome, Goodpasture autoimmune disease, diabetic nephropathy and angiopathy (174).

Alport's syndrome is a genetic disease that causes inflammation of renal glomeruli and is associated with deafness. Mutation in any of the collagen IV (a3, a4 or a5) genes leads to formation of abnormal collagen IV chains, and subsequently formation of defective glomerular basement membranes (175). Symptoms such as blood in urine begin in childhood and renal failure develops by adolescence (176). Goodpasture syndrome is an autoimmune disease characterised by glomerulonephritis and lung haemorrhage that can be detrimental if not treated early (162). The disease is caused by pathogenic circulating antibodies to a3(IV)NCD, which are predominant in the kidney glomerular BM and the lung alveolar BM (177). The sulfilimine cross link provides protection against the collagen IV antigen of Goodpasture disease (173).

Collagen IV also plays a role in tumour pathogenesis and malignancy, possibly through regulating angiogenesis (148). It is the binding substrate for many cancer cells, including melanoma (178), breast (179) and prostate (180), and it accumulates in the tumour interstitium (148).

The extracellular matrix is ubiquitous and has essential and diverse functions that affect cells, tissues and organs. Therefore, ECM abnormality can cause dysregulated cell-matrix interactions and lead to progression of many diseases, such as tissue fibrosis, muscular dystrophy and cancers (146-148, 181).

Fibrosis is a heterogeneous disorder that affects connective tissues in all organs, especially the heart, liver and kidney (182). It usually results from a defective wound healing process. Fibroblasts normally respond to injury signals and differentiate into myofibroblasts, which synthesise matrix material to repair the damaged ECM. When this processes is disrupted, fibrotic tissues can develop and lead to disorganised, stiff and dysfunctional ECM, which sets off a cascade of downstream effects and causes a multitude of diseases in the affected organs (183). For example, fibrosis of the heart leads to diastolic heart failure (184).

Damage to ECM can be mediated by oxidants. In contrast to inside the cell, the extracellular space is deficient in antioxidant defense mechanisms (121). Moreover, ECM components turn over slowly with limited mechanisms for repair or removal of damaged proteins. Oxidative modification of ECM can alter protein structure and function, leading to changes in solubility and aggregation, rigidity, permeability, signaling and ligand binding. Oxidative damage to the ECM is associated with many pathologies, including cardiovascular, lung and kidney diseases (12). A significant number of studies point to the role of myeloperoxidase as the source of oxidants at inflammatory sites (6, 131, 185, 186). Hypohalous acids increase post-translational modifications of renal tissues and ECM proteins, particularly collagen IV in experimental diabetic nephropathy (187). More recently peroxidasin has emerged as a contributor to the damage in pulmonary and renal inflammation, and fibrosis (22, 68, 69), as reviewed earlier in Section 1.2.5. The proposed mechanisms of promoting these pathologies are related to oxidative modification of tissues and destabilisation of the ECM.

## 1.6. Summary and aims

Peroxidasin is a rising star in the field of human peroxidases. It is an unusual peroxidase in its structure as it contains non-catalytic domains in addition to the catalytic peroxidase domain. It catalyses the formation of an unusual sulfilimine cross link that is only found in collagen IV, in a rare example of an anabolic function of hypobromous acid, a powerful oxidant and destructive bactericide. This physiological function of peroxidasin was unravelled in 2012, eighteen years after the discovery of the protein. Other functions have been suggested or demonstrated, such as activation of angiogenic signalling pathways (41). There has been increasing interest in studying peroxidasin and elucidating its enzymology (**Figure 20**). However, there are more questions than answers about its activity and roles in physiology and pathology. The inherent physical and chemical properties of peroxidasin make it difficult to purify or express in an active form that would allow studying it in an isolated system. There is increasing evidence that implicates peroxidasin in a number of diseases, which suggests it has physiological and pathological functions beyond cross-linking collagen IV. It also opens up many questions about the regulation of peroxidasin activity as a generator of a powerful oxidant in the ECM.

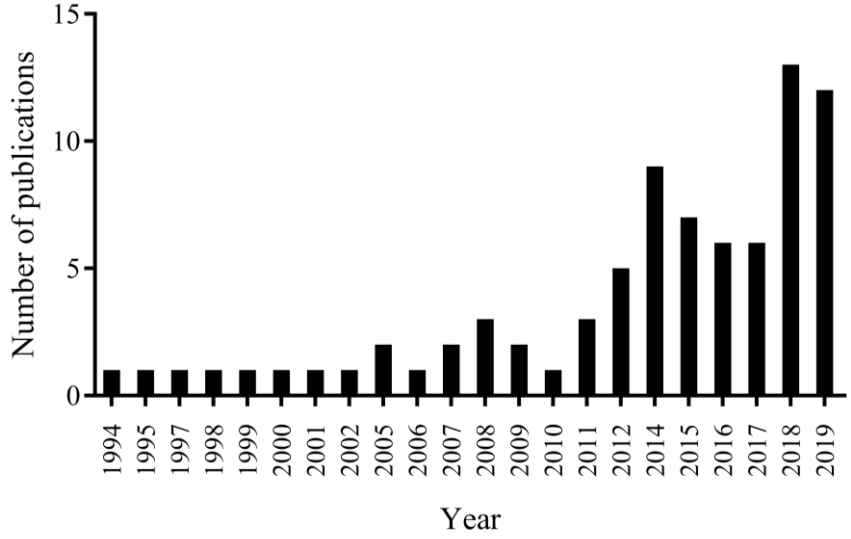


**Figure 20. The number of publications on peroxidasin since its discovery in 1994**. Web of science (10 Dec 2019).

In this research project, I aim to explore some of the questions surrounding the enzymology of peroxidasin. In particular, my goals in this thesis are to:

- Establish a model system to study the activity of peroxidasin in the ECM.
- Investigate peroxidasin substrate requirement for cross-linking collagen IV.
- Investigate the production of HOBr by peroxidasin in the ECM.
- Study the effects of substrates and inhibitors of other peroxidases on the activity of peroxidasin.
- Develop methods to measure biomarkers of protein oxidation, namely methionine sulfoxide, 3-bromotyrosine and 3-nitrotyrosine with application to ECM.
- Explore reactions of HOBr beyond catalysing the formation of the sulfilimine bond in collagen IV.

# Chapter 2 Materials and Methods

## 2.1 Materials

### *2.1.1 Chemicals*

All chemicals used in this project were of analytical purity grade. The chemicals used and manufacturers are listed in **Table 4**.

**Table 4. List of chemicals used in this thesis.**

| Item | Manufacturer/Supplier |
|---|---|
| $^{13}C_6$ Tyrosine | Isotec |
| 3-isobutyl-2-thioxo-7H-purin-6-one (TX1) | Gift from AstraZeneca |
| 4-aminobenzoic acid hydrazide (ABAH) | Fluka |
| Acetaminophen | Sigma-Aldrich |
| Acetic acid | Univar Solutions |
| Acetonitrile | Scharlau |
| Acrylamide:bis solution 37.5:1 | Bio-Rad |
| Ammonium ferrous sulfate | Baker |
| Ammonium Persulfate (APS) | Sigma-Aldrich |
| Amplex™ UltraRed Reagent | Invitrogen |
| Bovine serum albumin (BSA) | Gibco Life Technologies |
| Catalase | Sigma-Aldrich |
| Collagenase | Worthington Biochemical |
| Complete™ Protease inhibitor cocktail | Roche |
| Coomassie Brilliant Blue R-250 | ThermoFisher |
| Diethylaminoethyl (DEAE) Sepahrose | GE Life Sciences |
| Dithiothreitol (DTT) | Sigma-Aldrich |
| Ethanol | Merck |
| Ethylenediaminetetraacetic acid (EDTA) | Sigma-Aldrich |
| Formic acid | Merck |
| Glutathione (GSH) | Sigma-Aldrich |
| Glycerol | Merck |

| | |
|---|---|
| Glycine | Sigma-Aldrich |
| Hybond-P™ polyvinylidene fluoride (PVDF) membrane | Amersham Biosciences |
| Hydrochloric acid (HCl) | Fisher Chemicals |
| Hydrogen peroxide 30 % analytical grade | Lab Serv. |
| Iodoacetamide (IAM) | Sigma |
| L-methionine | Sigma-Aldrich |
| Methane sulfonic acid (MSA) | Sigma-Aldrich |
| Methionine | Sigma-Aldrich |
| NADH | Sigma-Aldrich |
| Phloroglucinol | Sigma-Aldrich |
| Pierce ECL™ Plus Western Blotting Substrate #32132 | Thermo Scientific |
| Potassium bromide | BDH Laboratories |
| Precision Plus Protein™ Dual Color Standards | Bio-Rad |
| Pronase from Streptomyces griseus | Sigma-Aldrich |
| R19-S | FutureChem Co. |
| Sodium ascorbate | Sigma-Aldrich |
| Sodium azide | Sigma-Aldrich |
| Sodium chloride | Labserv |
| Sodium deoxycholate | Sigma-Aldrich |
| Sodium dodecyl sulfate (SDS) | BDH |
| Sodium hypochlorite (Janola) | Pental Products |
| Sodium nitrite | Fisons |
| Sodium thiocyanate | Sigma-Aldrich |
| Sorbitol | Sigma-Aldrich |
| Sulfuric acid | Merck |
| Taurine | Sigma-Aldrich |
| Tetramethylethylenediamine (TEMED) | Sigma-Aldrich |
| Thiodipropionic acid | Sigma-Aldrich |
| Tris Base | Roche |
| Tris(hydroxymethyl)aminomethane (Tris base) | Roche |
| Trypsin | Promega |
| Tween®20 | Sigma-Aldrich |
| Tyrosine | Sigma-Aldrich |
| Uric acid | Sigma-Aldrich |
| Xylenol Orange | Sigma-Aldrich |

### *2.1.2 Cell culture media*

Cell culture media, fetal bovine serum (FBS), antibiotics (Penicillin-Streptomycin) and TrypLE® Express are all from Gibco Life Technologies.

### *2.1.3 Antibodies*

Antibodies used for western blotting are listed in **Table 5**.

**Table 5. Antibodies and manufacturers.**

| **Antibodies** | |
|---|---|
| Rabbit polyclonal anti-catalase. | Abcam |
| Rabbit polyclonal anti-peroxidasin. | Gift from Miklos Geizst, Budapest, Hungary |
| Goat anti-rabbit HRP. | Sigma |

### *2.1.4 Equipment and Software*

Equipment and software used in this project are listed in **Table 6**.

**Table 6. Equipment and software used in this project**.

| **Equipment** | |
|---|---|
| Direct Detect® Infrared Spectrometer | Merck Millipore |
| Heracell™ 150i $CO_2$ incubation | Thermo Scientific |
| NanoDrop™ Lite Spectrophotometer | Thermo Scientific |
| NanoPhotometer® Spectrophotometer | IMPLEN |
| SpectraMax 190 Microplate Reader | Molecular Devices |
| Spectrophotometer 8453 | Agilent |
| Spectrophotometric plate Reader Varioskan Flash | Thermo Scientific |
| Ultrasonic homogeniser Sonic Ruptor 400 | OMNI-INC |
| UVITEC Cambridge Gel documentation system | UVITEC Cambridge |

| Software | |
|---|---|
| ChemDraw Prime V17.0.0.206 (121) | PerkinElmer Informatics, Inc |
| Excel MS Office 2010 | Microsoft Corporation |
| GraphPad Prism V 7.04 | GraphPad Software, Inc. |
| Skan It RE for Varioskan Flash 2.4.3 (Research Edition) | Thermo Scientific |
| SoftMax Pro 5.3 | Molecular Devices |
| UVITEC Alliance 4.7 | UVITEC Cambridge |

### *2.1.5 General buffers and solutions*

The general buffers and solutions and their compositions are listed in **Table 7**.

**Table 7. Compositions of general buffers and solutions.**

| Buffers | |
|---|---|
| Phosphate buffered saline (PBS) | 140 mM NaCl, 13 mM KCl in 10 mM sodium phosphate buffer, pH 7.4. |
| Tris buffered saline (TBS) | 20 mM Tris-HCl, 140 mM NaCl, pH 7.6. |
| Sample buffer | 300 mM Tris-base pH 6.8, 25 % glycerol, 10 % (w/v) SDS, 0.05 % (w/v) bromophenol blue. |
| Electrophoresis running buffer (10x top tank) | 25 mM Tris, 192 mM glycine, 0.1 % (w/v) SDS. |
| Electrophoresis running buffer (lower tank) | 83 mM Tris |
| Transfer buffer | 25 mM Tris, 192 mM glycine, 15 % (v/v) methanol, pH 8.3 |
| Coomassie staining solution | 0.25 % (w/v) Coomassie Blue R-250, 45 % (v/v) ethanol, 10 % (v/v) acetic acid |
| Destaining solution | 45 % (v/v) ethanol, 10 % (v/v) acetic acid) |

## 2.1 Methods

### *2.2.1 Cell culture*

All cell lines used were available in the cell culture stocks within the Centre for Free Radical Research, and were originally obtained from the American Tissue Culture Collection (ATCC). Cell types, media and culture properties are shown in **Table 8**.

Cell handling was carried out using sterile techniques. All cells were incubated at 37°C in a humidified environment containing 5 % $CO_2$. Adherent cells were passaged when confluent (every four days) using TrypLE®Express to detach cells and seeded in new flasks with fresh medium at 1 x $10^6$ cells/ml. Cells were routinely tested and found to be mycoplasma free.

**Table 8. Cell lines used in this research project.**

| Cell line | Type | Medium | Properties |
|---|---|---|---|
| MEF | Mouse embryonic fibroblasts (ATCC® SCRC-1040™) | DMEM + 10 % FBS + 1 % pen/strep antibiotics + 5 % L-Asn. | Adherent |
| PFHR9 WT | Mouse epithelial cells (ATCC® CRL-2423™) | DMEM, 10 % FBS, 1 % pen/strep antibiotics. | Adherent |
| PFHR9 KO | Peroxidasin-knockout mouse epithelial cells obtained as a gift from Gautam Bhave laboratory, Vanderbilt University, Nashville, Tennesse, USA. CRISPR-mediated Knock-out method is described in (27). | DMEM, 10 % FBS, 1 % pen/strep antibiotics. | Adherent |

### *2.2.2 Isolation of the extracellular matrix*

A cell model was used to study peroxidasin in the ECM. Mouse epithelial-like cells (PFHR9) deposit appreciable amounts of ECM. The procedure was followed as described by Bhave *et al.* (33). PFHR9 cells were seeded at confluent density in 6-well, 10 cm or 15 cm plates, and kept in culture with a daily change of medium (DMEM + 10 % fetal bovine serum + 1 % penicillin/streptomycin antibiotics) and the indicated treatment for 6-8 days. For harvesting, the media was removed and the cells were washed twice with 1x PBS. Cells were incubated for 2 minutes in ice cold Lysis Buffer (10 mM Tris pH8, 1 mM EDTA, 1 % Sodium deoxycholate, 1x Complete® Protease Inhibitor), then scraped with a cell scraper and transferred to an Eppendorf tube. The lysate was sonicated with a fine tip probe three to four times, ten seconds each until lysate was homogeneous. The lysate was spun at 20,000 g for 20 min at 4°C, and the supernatant was separated from the pellet. The pellet was washed twice in Wash Buffer (1M NaCl, 10 mM Tris pH7.5) with spinning at 20,000 g for 10 minutes at 4°C. The ECM pellet was resuspended in PBS with brief sonication. Protein concentration was measured using Direct Detect® Infrared Spectrometer. The yield of ECM proteins from a 15 cm culture plate after 6-8 days was approximately 5 mg.

### *2.2.3 Isolation of the non-collagenous domain*

To separate the non-collagenous domain, ECM was first digested with collagenase. The isolated ECM was resuspended in digestion buffer (2mg/ml bacterial collagenase in 50 mM sodium phosphate pH 7.4) and left overnight at 37°C (188). The NCD was purified by anion-exchange chromatography using DEAE resin (189). The digest was spun down at 20,000 g for 2 minutes, and the supernatant was mixed with an equal volume of DEAE resin (equilibrated in 50 mM Tris pH 7.4) with shaking for 1 hour at 4°C. The slurry was spun down at 10,000 g for 2 minutes, and the soluble unbound NCD was taken in the supernatant for analysis. The procedure is outlined in **Figure 21**.

### *2.2.4 Cross-linking of collagen IV in the decellularised ECM*

Epithelial cells were grown for 6-8 days in the presence of 50 μM phloroglucinol (PHG) to inhibit peroxidasin (15). Cells were lysed and ECM was isolated as described above. Decellularised ECM was resuspended in PBS with sonication. The cross-linking reaction was initiated by adding $Br^-$ and $H_2O_2$, reagent HOBr or taurine bromamine (concentrations 50-100 μM, unless stated otherwise) to the isolated ECM (**Figure 21**). Other substrates and inhibitors were added at the concentrations stated in each figure. The standard incubation time was 60 minutes at 37°C unless stated otherwise. The reaction was stopped by adding a peroxidase inhibitor (sodium azide), or an appropriate oxidant scavenger (catalase or methionine), then the ECM was spun down and the supernatant was discarded. ECM was washed again to remove any residual oxidants before analysis.

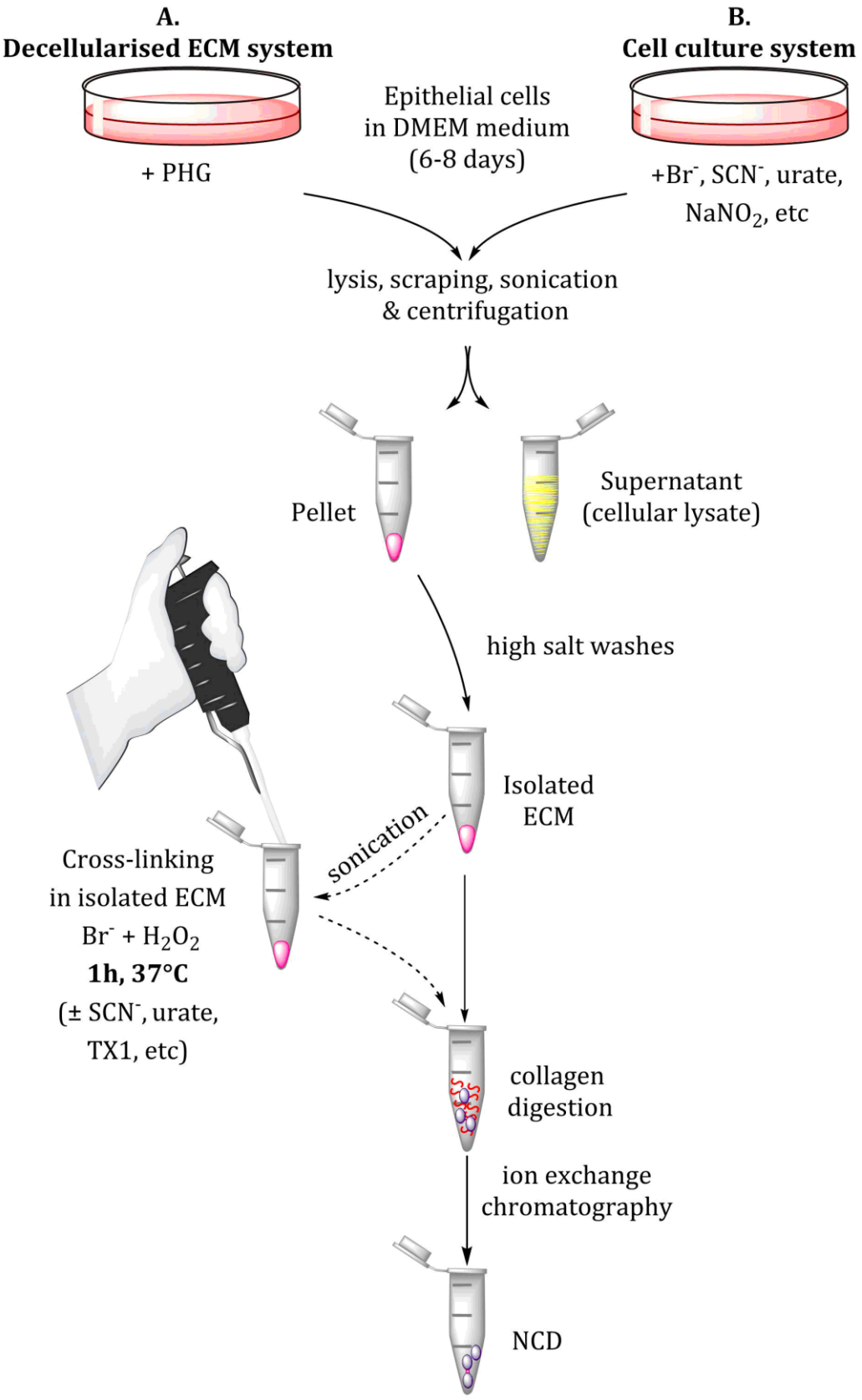


**Figure 21. Schematic diagram for isolation of ECM and NCD from two systems, decellularised ECM or cell culture.**

*Preparation of oxidants*

- *Hydrogen peroxide ($H_2O_2$)*

A stock solution (30 %) was diluted 1:1000 in deionised $H_2O$ while vortexing. Concentration was determined by measuring its absorbance at 240 nm, (Extinction coefficient 43.6 $M^{-1}$ $cm^{-1}$). The concentration was calculated using Beer-Lambert Law: $c = A/\varepsilon l$ (c= concentration, A= absorbance, ε= extinction coefficient, *l*= length of the light path in cm).

- *Hypochlorous acid (HOCl)*

A stock solution of commercial chlorine bleach (Janola) was diluted 1:20 in PBS with vortexing. To determine the concentration, the working solution was diluted 1:10 in 200 mM potassium hydroxide. The absorbance was measured at 292 nm (extinction coefficient 350 $M^{-1}$ $cm^{-1}$). Subsequent dilutions from this stock were made in PBS and kept on ice in the dark.

- Hypobromous acid (HOBr)

Fresh HOBr was prepared by mixing equal volumes of freshly prepared 19 mM HOCl and 20 mM potassium bromide and incubating in the dark for 15 minutes at room temperature. To determine the concentration, the solution was diluted 1:10 in 200 mM potassium hydroxide. The absorbance was measured at 329 nm (extinction coefficient 335 $M^{-1}$ $cm^{-1}$). Subsequent dilutions from this stock were made in PBS and used for experiments within 30 minutes.

- *Taurine bromamine*

HOBr was gradually added to ten-fold excess of taurine. The mixture was kept on ice and used within 30 minutes.

### *2.2.6 Determination of protein concentration*

Direct Detect® Infrared Spectrometer was used to measure protein concentration. The Direct Detect method uses Mid-Infrared (MIR) spectroscopy, which is based on the absorption of radiation in the range 4000-400 $cm^{-1}$. Biomolecules (Carbohydrates, lipids, proteins, etc.) have distinct IR spectra and can be analysed concurrently. Measuring proteins utilises the distinct vibration of amides in the infrared region to calculate protein concentration. It requires spotting 2 µl of the sample or blank on a hydrophilic polytetrafluoroethylene (PTFE) membrane Assay Free® card and leaving it to dry then performing the reading with the Direct Detect® instrument.

### *2.2.7 Gel electrophoresis*

Discontinuous mini gels were used to separate proteins by SDS-PAGE (190). For the analysis of dimer formation in the non-collagenous domain of collagen IV, 10-well 12 % acrylamide gels were prepared (**Table 9**). For analysis of other samples, BIO-RAD Mini-PROTEAN® TGX™ precast gels (4-15 %) were used. Protein loading was ~ 5 µg of NCD samples for dimer analysis, and 25 µg of lysate for western blot analysis.

Samples were mixed 5:1 with 5 x non-reducing sample buffer (**Table 7**). Samples were heated at 95°C for 3 minutes, spun down then loaded into the wells of the gel. Gels were run in Running Buffers (**Table 7**) at constant current (200 V) until the dye front ran off the gel (45-50 minutes).

**Table 9. Compositions of acrylamide gels.**

| Gel type | Stock solution | Volume |
|---|---|---|
| 4 % stacking | 0.5 M Tris pH 6.8 | 1.25 |
| | 40 % (w/v) acrylamide | 0.5 ml |
| | $dH_2O$ | 3 ml |
| | 20 w (w/v) SDS | 25 µl |
| | 10 % (w/v) APS | 25 ul |
| | TEMED | 8 µl |
| 12 % resolving | 2 M Tris pH 8 | 2 ml |
| | 40 % (w/v) acrylamide | 3 ml |
| | $dH_2O$ | 4.9 ml |
| | 20 % (w/v) SDS | 50 µl |
| | 10 % (w/v) APS | 50 ul |
| | TEMED | 15 µl |

### *2.2.8 Coomassie staining*

Commassie Brilliant Blue R-250 is a dye that interacts noncovalently with amino acids and is used to visualise protein bands on the gel (191). Gels were incubated in Coomassie R250 staining solution (**Table 7**) for 1 hour with shaking, then destained in multiple washes with Destain solution (**Table 7**) for 2 hours, then soaked in deionised $H_2O$ for a minimum of one hour.

### *2.2.9 Densitometry analysis*

Gel imaging was performed using Alliance Uvitec Cambridge imager. Densitometry analysis was performed using Alliance software Uviband-max.

### *2.2.10 Western blotting*

Proteins separated by SDS-PAGE were blotted on a polyvinylidene fluoride (PVDF) membrane by wet transfer (192). The PVDF membrane was activated by methanol, then equilibrated with the Transfer Buffer (**Table 7**). The polyacrylamide gel and PVDF membrane were assembled into a sandwich with filter paper and pads on each side then inserted into a BIO-RAD® tank with the Transfer Buffer. An icepack and a magnetic stirrer were also added to the tank. Proteins were transferred from the gel to the membrane at 100 V in 60 minutes. For larger proteins (e.g. peroxidasin), transfer took 18 hours at 33 mA at 4°C. After the transfer, the

membrane was blocked with 5 % (w/v) non-fat milk or 3 % (w/v) BSA in TBST for one hour at room temperature on a rocker. The membrane was then incubated with the primary antibody in TBST for 18 hours at 4°C on a rocker (**Table 10**). The membrane was washed three times in TBST, 10 minutes each on a rocker. The secondary antibody was added in TBST with 5 % (w/v) milk or 3 % (w/v) BSA for one hour at room temperature on a rocker. Washing steps were repeated and the blot was developed using chemiluminescence and analysed by UVITEC Cambridge Gel imager.

**Table 10. Primary and secondary antibodies and dilutions.**

| Primary antibody | Dilution | Secondary antibody | Dilution |
|---|---|---|---|
| Rabbit polyclonal anti-peroxidasin | 1:500 | Goat anti-rabbit HRP | 1:20,000 |
| Rabbit polyclonal anti-catalase | 1:2000 | Goat anti-rabbit HRP | 1:20,000 |

### *2.2.11 Proteomic identification of Peroxidasin*

To confirm the presence of peroxidasin in extracts from cells used as a model to study peroxidasin, a proteomic mass spectrometry method was developed by Dr. Louise Paton. The protocol for tryptic digestion of samples was followed as described in (193). Protein samples from intracellular lysate or ECM (400 µg) were dried in a SpeedVac then reconstituted in 50 µl of 100 mM ammonium bicarbonate buffer with vortexing. Samples were then mixed with 50 µl of the gel-aided sample preparation (GASP) buffer (40 % (w/v) acrylamide, 5 µl TEMED and 5 µl 10 % (w/v) APS) and allowed to polymerise for 10 minutes. The polymerised gel was then sliced into 1×1 mm pieces and fixed with 500 µl Fix solution (50 % methanol, 40 % HAc, 10 % $dH_2O$) for ten minutes with vortexing. The Fix solution was removed then samples were incubated with 500 µl acetonitrile for 10 minutes, spun down and the supernatant was discarded. Samples were submerged in reducing buffer (10 mM DTT in 100 mM ammonium bicarbonate) for 30 minutes at 56°C and washed again with 500 µl acetonitrile. Samples were submerged with alkylation buffer (55 mM iodoacetamide in 100 mM ammonium bicarbonate) for 20 minutes in the dark and washed again with 500 µl acetonitrile. Samples were submerged in protease buffer (10 mM ammonium bicarbonate, 10 % acetonitrile, protease 20 µg in 1.5 ml) and incubated at 4°C for 2 hours and topped up with protease buffer if necessary. Samples were left to digest at 37°C overnight. To extract peptides, 2 volumes of extraction buffer relative to digest were added to sample and incubated for 15 minutes at 37°C with shaking. Supernatant was transferred to speed-vacuum Eppendorf tubes and dried in the SpeedVac. Peptides were reconstituted in 20 µl of 0.1 % (v/v) formic acid, vortexed, and centrifuged for analysis by HPLC/MS.

Semi-quantitative data was acquired with a QTRAP 6500 (SCIEX, Framingham, MA) coupled to an HPLC model 1290 (Agilent, Santa Clara, CA). Instrument control, data acquisition, and analysis were performed using Analyst 1.6.3 and PeakView 2.2. Samples were kept at 4°C in the autosampler prior to injection. Chromatographic separation was achieved on a Phenomenex Jupiter Proteo 90Å C12 (2.0 mm × 150 mm, 4 µm) column with the column temperature set to 40°C. The mobile phase consisted of: solvent A, 0.1 % formic acid in water, and solvent B, 0.1 % formic acid

in acetonitrile. The mobile phases were eluted at 250 uL/min. The gradient was as follows: 2 % B for 5 min, increased to 30 % B over 20 min, increased further to 98 % B at 26 min, held for 5 min and then decreased to 2 % B at 32 min, followed by 5 min equilibration. The QTRAP 6500 mass spectrometer was operated with the following parameters: Spray voltage: 5500 V, Temperature: 400 °C, Ion source gas 1: 35, Ion source gas 2: 35, Declustering potential: 90, Entrance potential: 10, Collision cell exit potential: 14. The eluted peptides were analysed using multiple reaction monitoring. The doubly charged Y3 fragment of $^{675}$AGEIFER$^{681}$ was monitored as a 411.4/451.3 transition (CE:23) and the Y5 fragment of $^{1101}$AFFSPFR$^{1107}$ was monitored as a 436.2/653.3 transition (CE:24). The area under the curve was used for quantitation.

### *2.2.12 Peroxidase activity assay*

Amplex Red undergoes peroxidase-catalysed oxidation by $H_2O_2$ in a 1:1 stoichiometry to produce resorufin, a red fluorescent compound (**Figure 22**). To measure peroxidase activity, 50 µM of Amplex red was added to the isolated ECM (~200-250 µg per sample resuspended and sonicated in 120 µl PBS) with 50 µM $H_2O_2$, incubated in the dark for 0-20 minutes and stopped by adding 1 mM azide. The ECM was spun down and 100 µl of supernatant was transferred to a 96-well plate to measure resorufin fluorescence (ex 544 nm, em 590 nm).

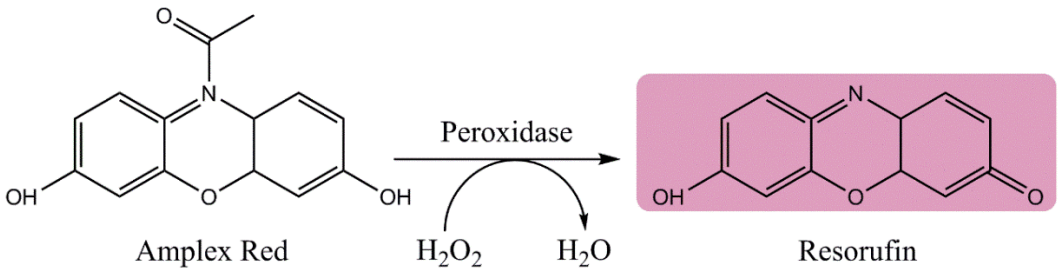


**Figure 22. Reaction scheme of Amplex red with hydrogen peroxide and peroxidase to produce fluorescent resorufin**.

### *2.2.13 Consumption of hydrogen peroxide in the isolated ECM*

The consumption of $H_2O_2$ in the isolated ECM was measured by the spectrophotometric FOX assay (ferrous ion oxidation of xylenol orange) (194). Hydrogen peroxide oxidises ferrous to ferric ion selectively (Eq. 1). The ferric sensitive dye xylenol orange (XO) binds to ferric ions to produce a blue-purple complex (Eq. 2), which is an indirect way to measure the concentration of hydrogen peroxide.

$$Fe^{2+} + H_2O_2 \rightarrow Fe^{3+} + RO^{\bullet} + OH^{-} \qquad \text{Equation 1}$$

$$Fe^{3+} + XO \rightarrow \text{colored complex} \qquad \text{Equation 2}$$

To make the FOX reagent, 25 mM sulfuric acid was added to 100 µM xylenol orange, 250 µM ferrous ammonium sulfate and 100 mM sorbitol. It is essential to add the acid first before adding $dH_2O$. The solution was used within 1 day of preparation. The isolated ECM (150-200 µg total protein in 120 µl final volume) was treated with 50 µM $H_2O_2$ ± 100 µM $Br^-$, 50 µM PHG or 1 mM sodium azide. After various incubation times (2-60 min), the ECM was spun down, and 50 µl of the supernatant was mixed with 950 µl of FOX reagent with vortexing. Absorbance was measured after at least 40 minutes at 560 nm and related to a $H_2O_2$ standard curve (**Figure 23**).

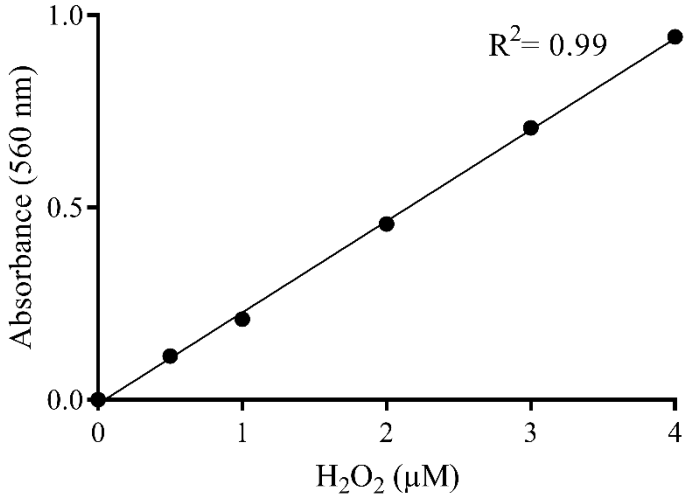


**Figure 23. Standard calibration curve for the concentration of $H_2O_2$.**

### *2.2.14 Measuring NADH bromohydrin by LC/MS*

Hypobromous acid reacts rapidly with NADH, adding across a C=C bond to form a bromohydrin (Apparent rate constant $4\times10^6$ $M^{-1}$ $s^{-1}$) (102) (**Figure 24**). This product was used to measure the production of HOBr by peroxidasin in the ECM. Decellularised ECM (~200 µg of ECM proteins) was incubated with 200 µM NADH, various concentrations of $Br^-$ and 50 or 100 µM $H_2O_2$ in 50 µl final volume of PBS for 2-25 minutes. The supernatant was separated and analysed for NADH and its bromohydrin products by LC-MS. A standard curve was generated by reacting 200 µM NADH with reagent HOBr (5-500 nM) (shown later in Chapter 3). Samples were separated on a PS C18 (150x2.1 mm, Phenomenex, Framingham, USA) using a gradient of methanol (2-50 % over 10 min) in 10 mM ammonium acetate (pH 6.9) with a flow rate of 250 µl/min using an Ultimate 3000 pump (Thermo, San Jose, USA). The samples were delivered into a Velos Pro Ion Trap mass spectrometer (Thermo). Samples were detected using the selected reaction monitoring in the negative ion mode. The ion spray was set to -3.5kV and the interface heater to 300 $^0$C and the capillary was 275 $^0$C. NADH was measured using the transition m/z 664.2 to 408.1, and the bromohydrins by m/z 760.2 and 762.2 both going to m/z 680.2. The collision gas was nitrogen and the collision energy was 30 % in each of the cases. Area of peaks were calculated using XCaliber Software (Thermo). Dr. Rufus Turner developed the LC/MS method.

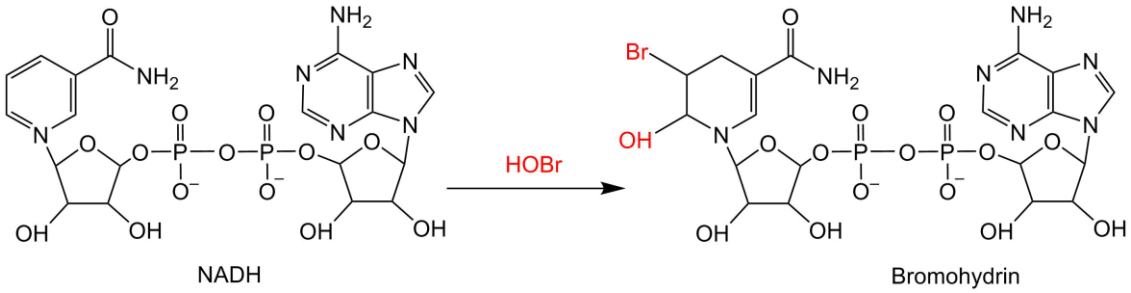


**Figure 24. Reaction scheme for bromination of NADH by HOBr.**

### *2.2.15 Detection of hypobromous acid using the probe R19-S*

The fluorescent probe R19-S reacts with hypochlorous and hypobromous acids to produce the fluorescent product R19 (**Figure 25**) (195, 196).

A 1 mM stock solution was prepared fresh weekly by dissolving R19S in acetonitrile and heating it at 50°C in the dark for 1 hour. To determine the concentration, the stock was diluted 1:200 in acetonitrile and its absorbance was measured at 308 nm (extinction coefficient 14100 $M^{-1}$ $cm^{-1}$) (195). Subsequent dilutions were made in sodium phosphate buffer.

To detect the production of HOBr, decellularised ECM was homogenised by sonication in PBS and then incubated with 100 µM bromide, 50 µM hydrogen peroxide and 50 µM R19S probe and incubated for 60 minutes at 37°C. The reaction supernatant was removed and fluorescence was measured (ex 515 nm, em 550 nm). As a positive control, 5 µM reagent HOBr was added to the probe alone, or to the ECM and the probe.

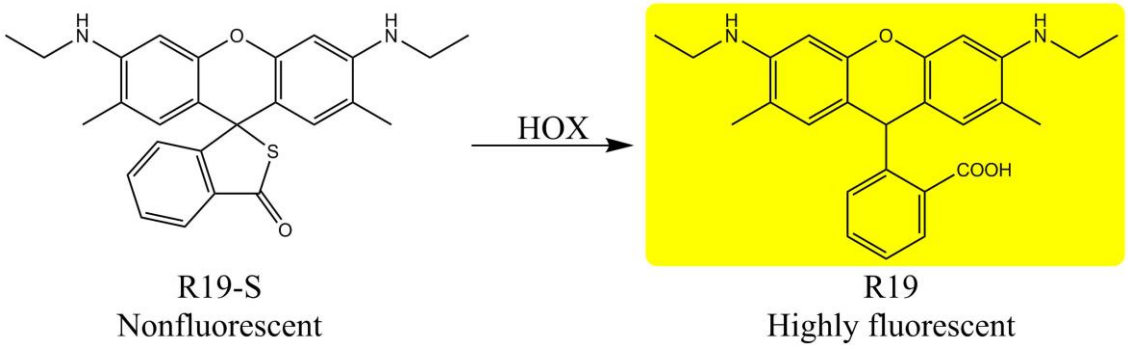


**Figure 25. Reaction scheme of the probe R19-S with hypohalous acidsto yield a fluorescent probe R19**.

### *2.2.16 Measuring methionine sulfoxide*

A stable isotope dilution LC/MS/MS method was used for the detection and quantification of methionine and methionine sulfoxide. Isotopically-labelled standards ($^{13}C_5$ $^{15}N$ methionine and $^{13}C_5$ $^{15}N$ methionine sulfoxide) were used to control for experimental variations, such as recovery, matrix effect and ionisation. The elution times of isotopically-labelled internal standards are the same as the unlabelled counterparts, but they differ in masses (**Figure 26**).

To make isotopically-labelled methionine sulfoxide internal standards, $^{13}C_5{}^{15}N$ methionine was treated with a large excess of hydrogen peroxide (900 µl of 110 mM $H_2O_2$ to 100 µl of 10 mM methionine) and incubated at room temperature for 2 hours. To remove excess $H_2O_2$ after the reaction, 0.25 µg/ml catalase was added to the mixture and incubated until air bubbles stopped forming. The FOX assay was used to test for any remaining $H_2O_2$. Reactants were analysed by LC-MS to ensure complete oxidation of methionine to methionine sulfoxide (**Figure 27**).

To measure methionine sulfoxide in proteins, intracellular lysate or ECM samples were first digested to individual amino acids by pronase. Samples (50 µg) were placed in speed-vacuum Eppendorf tubes with internal standards (100 pmol $^{13}C_5$ $^{15}N$ Met and Met-O) and dried in a vacuum concentrator (SpeedVac). Pronase was added to protein samples in 1:10 ratio (w/w protein) in digestion buffer (5 µg pronase, 100 mM Tris buffer pH 7.5, 10mM $CaCl_2$, 0.1 % (w/v) SDS). Samples were digested for 48 hours at 37°C. After digestion, samples were dried down in the SpeedVac and reconstituted in 22 µl of 10 mM ammonium formate pH 3.8 for analysis by LC-MS.

Samples were separated on a Hypercarb™ Porous Graphitic Carbon column (250x2.1 mm) using an Agilent 1290 Binary Pump at a flow rate of 200 µl/ minute. The mobile phase gradient started with 100 % 10 mM ammonium formate that gradually decreased over seven minutes to 65 % and 35 % acetonitrile. The column was washed with 100 % organic solvent for five minutes then equilibrated with the starting eluent (**Table 11**). The analytes were delivered into a Qtrap® 6500 mass

spectrometer (Sciex) and detected in multiple reaction monitoring mode using the positive ionisation mode. The ion spray was set to -3.5kV and the interface heater to 300 $^{0}$C and the capillary was 275 $^{0}$C. The collision gas was nitrogen and the collision energy was 30 %. Area of peaks were calculated using XCaliber Software (Thermo). Mass spectra and fragmentation patterns for methionine and methionine sulfoxide are shown in **Figure 28**, **Figure 29** and **Table 12**. Standard calibration curves for methionine and methionine sulfoxide are shown in **Figure 30**.

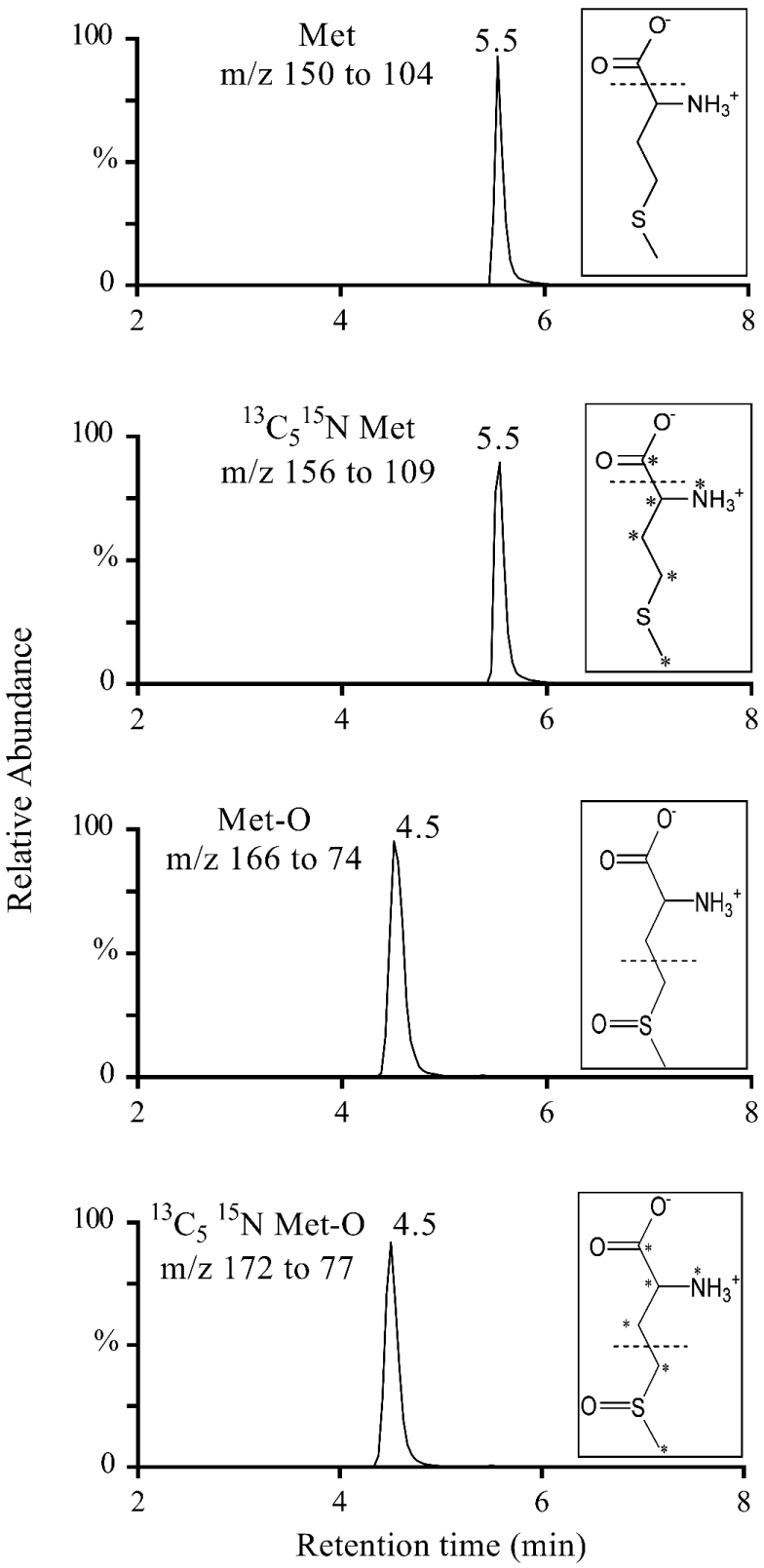


**Figure 26. Typical LC/MS/MS chromatograms for the analysis of Met**, isotopically-labelled $^{13}C_5{}^{15}N$ methionine, methionine sulfoxide and isotopically-labelled $^{13}C_5{}^{15}N$ methionine sulfoxide. Structures of methionine and methionine sulfoxide with their isotopically-labelled atoms (*) are shown in the insets.

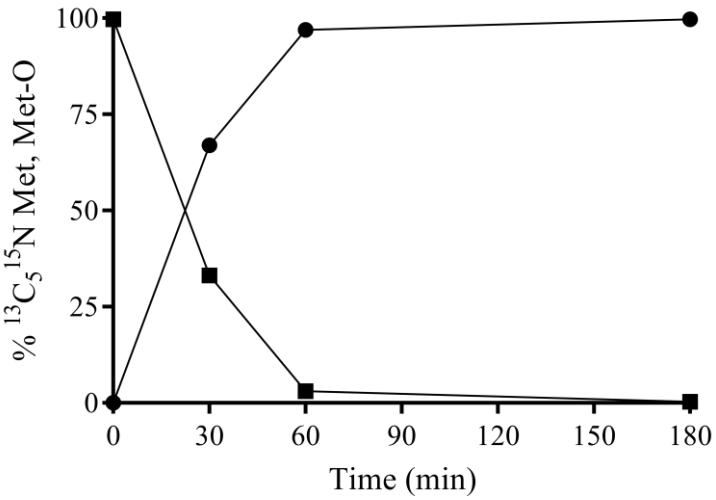


**Figure 27. Generation of labelled Met-O**. The loss of $^{13}C_5{}^{15}N$ Met (■) and formation of $^{13}C_5{}^{15}N$ Met-O (●) are monitored by LC/MS/MS analysis over time of incubation with $H_2O_2$.

**Table 11. Composition of the mobile phase for elution of Met and Met-O**. Buffers: A: 10 mM ammonium formate, pH 3.8 (made fresh weekly. pH adjusted with formic acid), B: Acetonitrile.

| Time (min) | % A | % B |
|---|---|---|
| 0 | 100 | 0 |
| 7 | 65 | 35 |
| 7.1 | 0 | 100 |
| 12 | 0 | 100 |
| 12.1 | 100 | 0 |
| 17 | 100 | 0 |

**Table 12. Analysis of Met and Met-O by MS**. Analytes, mass-to-charge ratios and fragments monitored in the multiple reaction monitoring positive ionisation mode. Q, transition used for quantitation; C, transition used for the confirmation of the presence of the analyte.

| Analyte | Q1 mass (Da) | Q3 mass (Da) | Q/C |
|---|---|---|---|
| Met | 150 | 61 | C |
| | 150 | 56 | C |
| | 150 | 104 | Q |
| | 150 | 133 | C |
| Met-O | 166 | 102 | C |
| | 166 | 149 | C |
| | 166 | 74 | Q |
| | 166 | 56 | C |
| $^{13}C_5$ $^{15}N$ Met | 156 | 138 | C |
| | 156 | 109 | Q |
| | 156 | 63 | C |
| | 156 | 107 | C |
| $^{13}C_5$ $^{15}N$ Met-O | 172 | 77 | Q |
| | 172 | 107 | C |
| | 172 | 125 | C |
| | 172 | 154 | C |

a

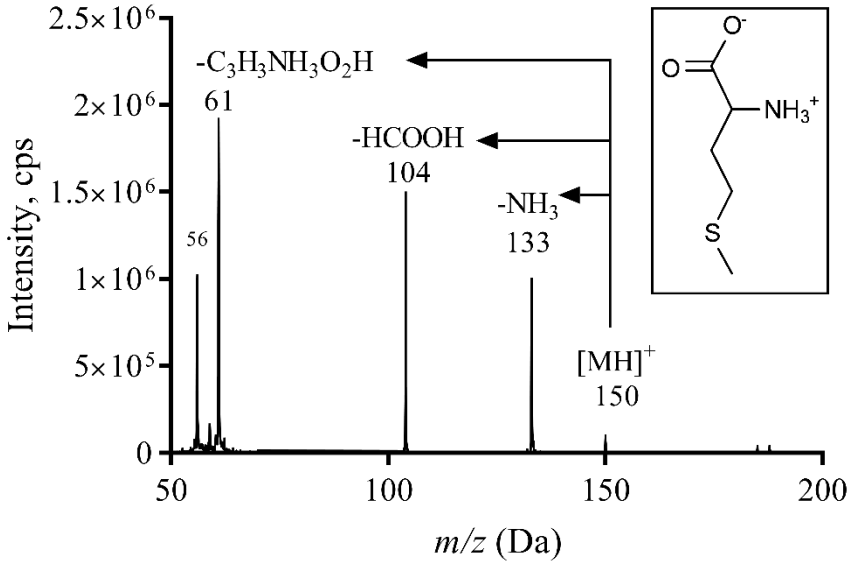


b

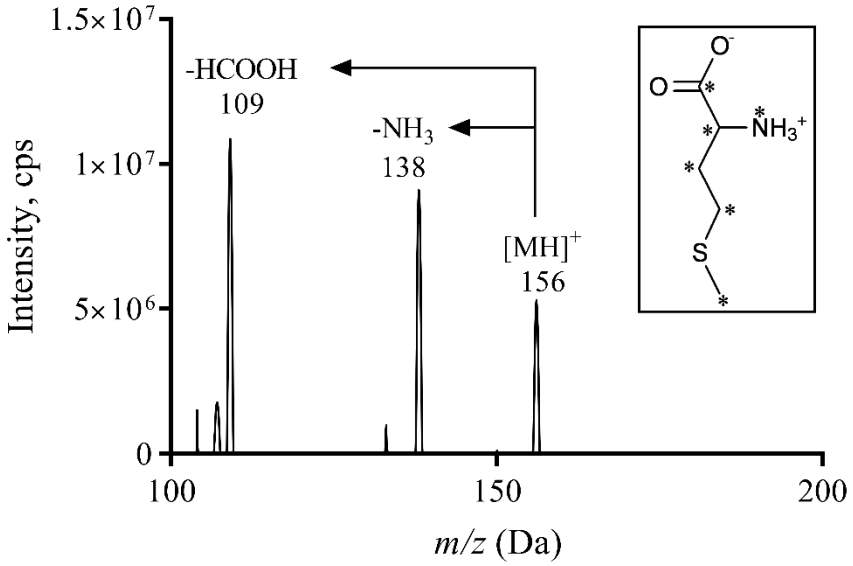


**Figure 28. The mass spectra and fragmentation patterns of Met.** (a) Methionine (m/z 150) and (b) isotopically-labelled $^{13}C_5{}^{15}N$ methionine (m/z 156). In addition to parent ions $(MH]^+$, fragments and functional groups lost are shown. Structure of methionine and labelled heavy isotope atoms (*) are shown in the insets.

a

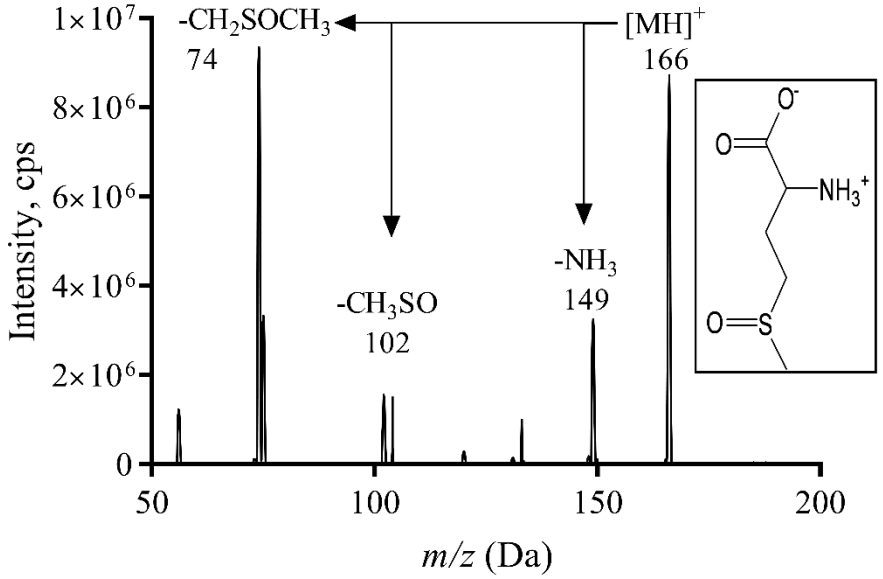


b

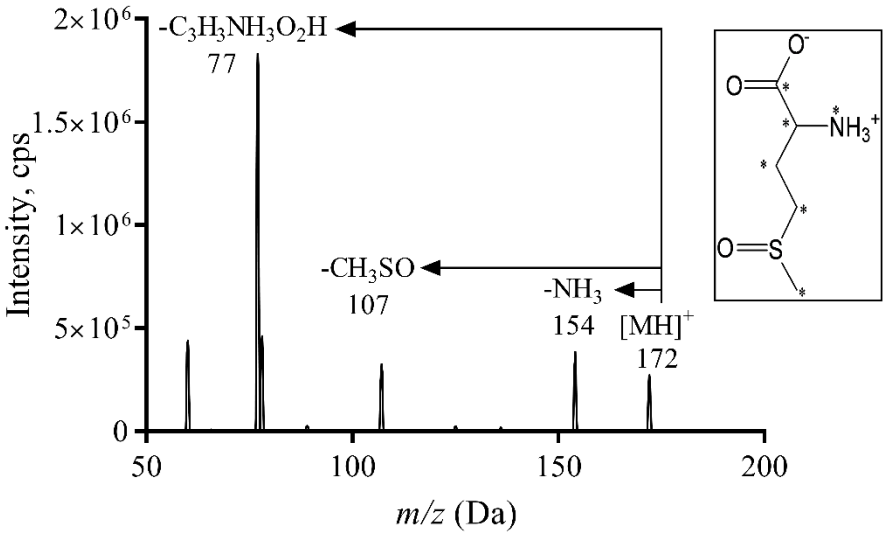


**Figure 29. The mass spectra and fragmentation patterns of Met-O**. (a) methionine sulfoxide (m/z 166) and (b) isotopically-labelled $^{13}C_5{}^{15}N$ methionine sulfoxide (m/z 172). In addition to parent ions $[MH]^+$, fragments and functional groups lost are shown. Structure of methionine sulfoxide and labelled heavy isotope atoms (*) are shown in the insets.

a

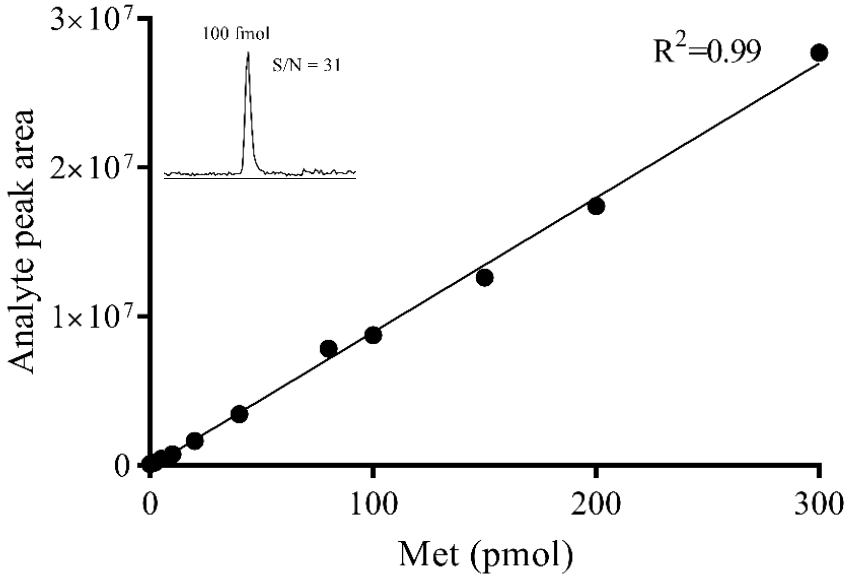


b

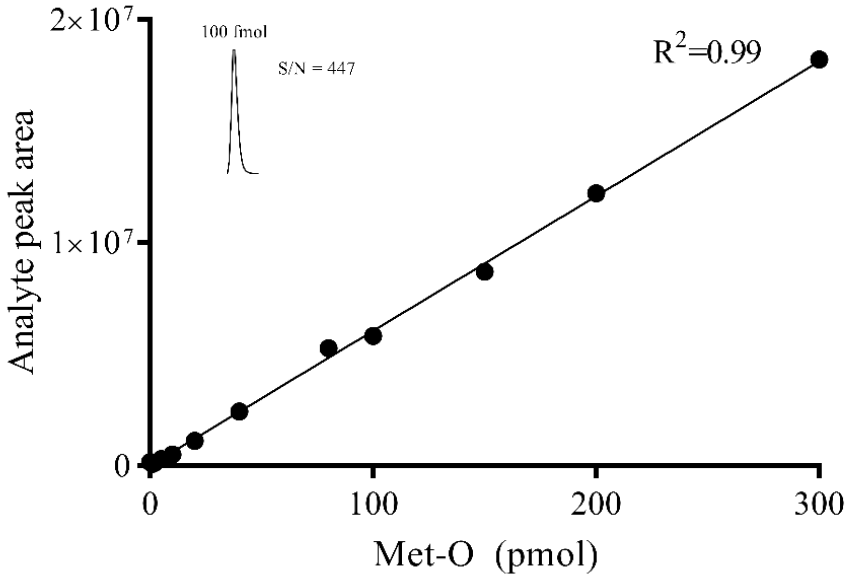


**Figure 30. Standard calibration curves for (a) Met and (b) Met-O** Range 0.1-300 pmol. Insets show signal-to-noise ratios for 100 fmol.

### *2.2.17 Measuring 3-bromotyrosine*

A stable isotope dilution LC/MS/MS method was used for the detection and quantification of 3-bromotyrosine levels in proteins (89, 197). Isotopically-labelled standards ($^{13}C_6$ tyrosine and $^{13}C_9$ 3-bromotyrosine) were used to control for experimental variations, such as recovery, matrix effect and ionisation. The elution times of isotopically-labelled internal standards are the same as the unlabelled counterparts, but they differ in mass (**Figure 31** and **Table 13**). Artefactual bromination was monitored by measuring any conversion of $^{13}C_6$ tyrosine to $^{13}C_6$ 3-bromotyrosine.

Protein samples were first hydrolysed to individual amino acids. Intracellular lysate, ECM and NCD (50 µg) were placed in Kimble tubes with internal standards (6 nmol $^{13}C_6$ Tyr and 6 pmol $^{13}C_9$ 3-Br-Tyr) and dried in the SpeedVac. Then, 100 µl of 4 M methane sulfonic acid, supplemented with 1 % (w/v) phenol, was added to each tube and vortexed. The Kimble tubes were then placed into a capped vial, flushed with nitrogen four times and sealed under positive pressure. The vial was then placed in an oven inside a fume cupboard, and left at 110°C for 18 hours.

After hydrolysis, samples were left to cool down at room temperature before opening the vial. Kimble tubes were removed from the vial, and their content was diluted with 500 µl $dH_2O$ with 0.1 % (v/v) trifluoroacetic acid (TFA) and vortexed. The hydrolysate was processed by solid phase extraction (SPE) to remove the acid. C-18 cartridges were first conditioned with 3 ml methanol, followed by 2 ml $dH_2O$ with 0.1 % (v/v) TFA, without allowing cartridges to dry. Samples were then loaded onto cartridges, washed with 2 ml $dH_2O$ with 0.1 % (v/v) TFA. To elute the analytes, 1.1 ml 80 % (v/v) methanol was added to cartridges and collected in speed-vacuum Eppendorf tubes. Samples were dried in the SpeedVac and reconstituted in 22 µl $dH_2O$ with 0.1 % (v/v) formic acid for analysis by HPLC-MS/MS.

Samples were separated on a Kinetex® 2.6 µm C18 100Å column (150x2.1 mm), using an Agilent 1290 Binary Pump at a flow rate of 200 µl/ minute in a mobile phase outlined in **Table 14**. The gradient started with 2 % organic solvent

(acetonitrile with 0.1 % (v/v) formic acid) for four minutes, followed by a gradual increase of organic solvent concentration to 80 % for three minutes. The column was washed with 80 % organic solvent for three minutes then equilibrated with the starting eluent.

The analytes were delivered into a Qtrap® 6500 mass spectrometer (Sciex) and detected in multiple reaction monitoring mode using positive ion mode. The ion spray was set to -3.5kV and the interface heater to 300 $^{O}$C and the capillary was 275$^{O}$C. The collision gas was nitrogen and the collision energy was 30 %. The areas of peaks were calculated using XCaliber Software (Thermo). Examples of mass spectra and fragmentation patterns for tyrosine and 3-bromotyrosine are shown in **Figure 32**. Standard calibration curves for tyrosine and 3-bromotyrosine are shown in **Figure 33**.

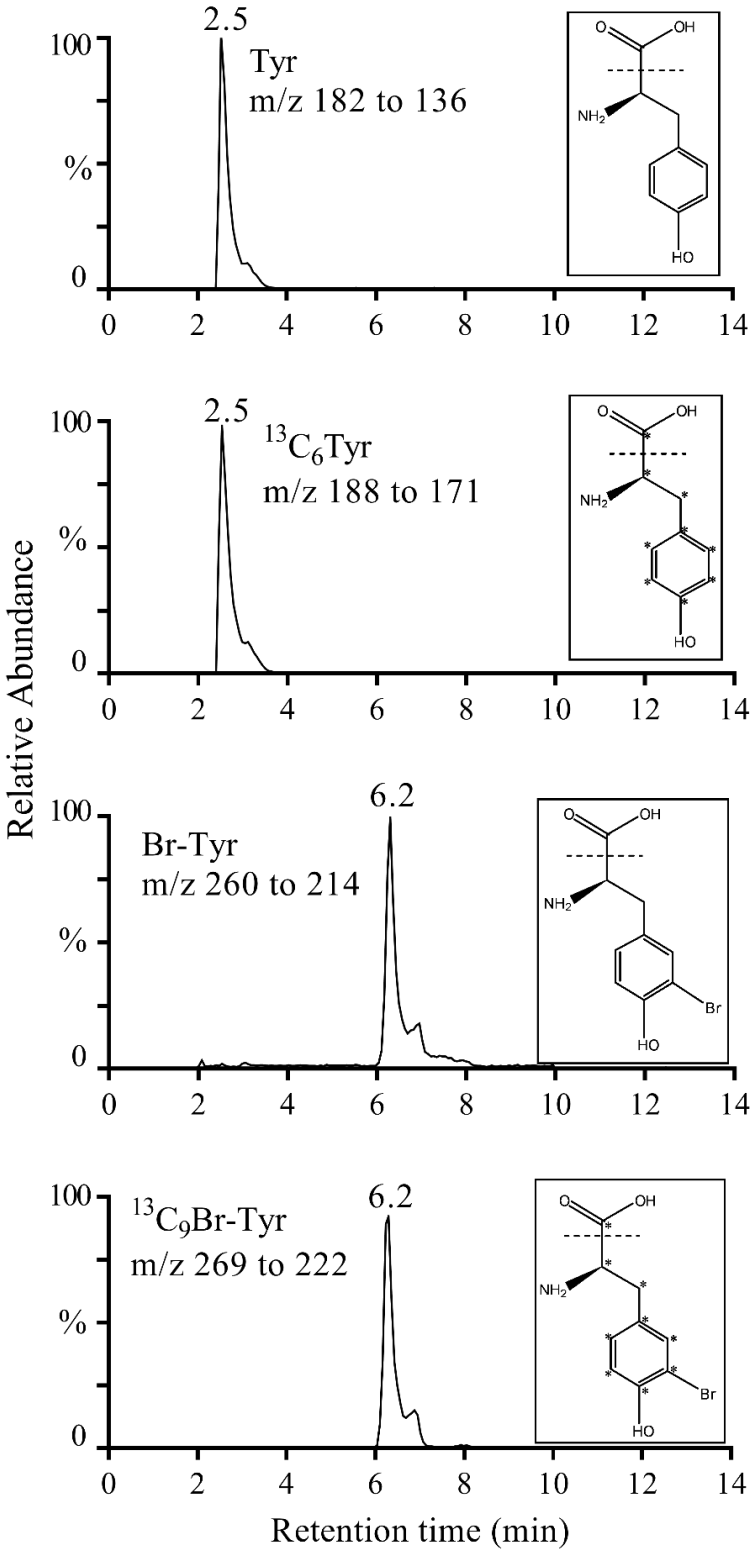


**Figure 31. Typical LC/MS/MS chromatograms for analysis of Tyr, isotopically-labelled $^{13}C_6$ Tyr, 3-Br-Tyr and isotopically-labelled $^{13}C_9$ 3-Br-Tyr**. Structures of tyrosine and 3-bromotyrosine with their isotopically-labelled atoms (*) are shown in the insets.

**Table 13. Analysis of Tyr and 3-Br-Tyr by MS**. Analytes, mass-to-charge ratios and fragments monitored in the multiple reaction monitoring positive ionisation mode.

| Analyte | | Precursor ion (m/z) | Product ions (m/z) |
|---|---|---|---|
| $^{12}C$ Tyr | Sample | 182 | 136, 165 |
| $^{13}C_6$ Tyr | Internal standard | 188 | 171 |
| $^{12}C$ 3-$Br^{79}$-Tyr | Sample | 260 | 214 |
| $^{12}C$ 3-$Br^{81}$-Tyr | Sample | 262 | 216 |
| $^{13}C_6$ 3-$Br^{79}$-Tyr | Artefact bromination | 266 | 220 |
| $^{13}C_6$ 3-$Br^{81}$-Tyr | Artefact bromination | 268 | 222 |
| $^{13}C_9$ 3-$Br^{79}$-Tyr | Internal standard | 269 | 222 |
| $^{13}C_9$ 3-$Br^{81}$-Tyr | Internal standard | 271 | 224 |

**Table 14. Composition of the mobile phase for elution of Tyr and 3-Br-Tyr**. Buffers A: $dH_2O$ with 0.1 % (v/v) formic acid, and B: acetonitrile with 0.1 % (v/v) formic acid.

| Time (min) | % A | % B |
|---|---|---|
| 0 | 98 | 2 |
| 4 | 98 | 2 |
| 7.1 | 20 | 80 |
| 10 | 20 | 80 |
| 10.1 | 98 | 2 |
| 15 | 98 | 2 |

a

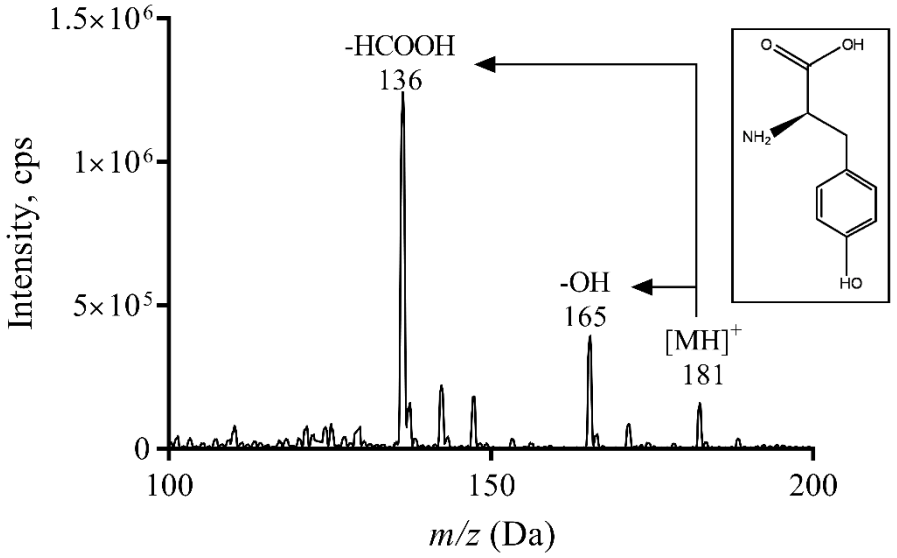


b

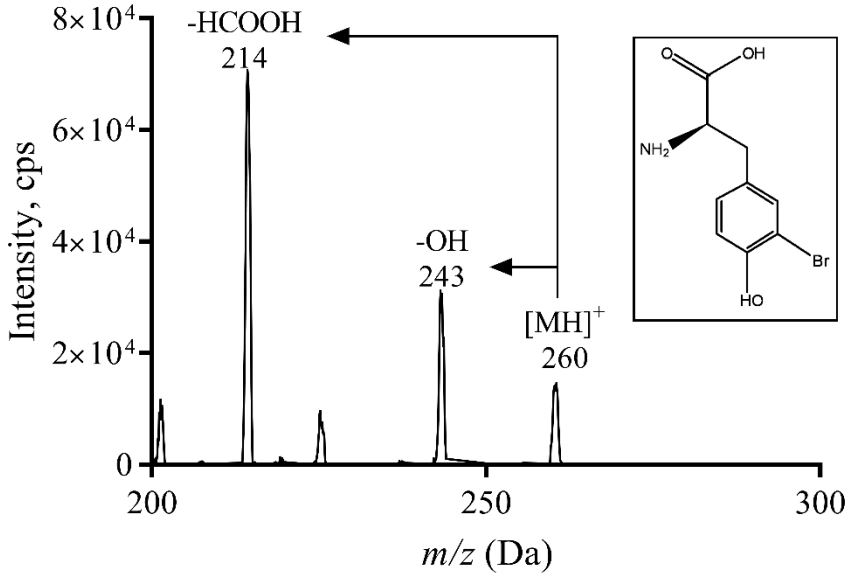


**Figure 32. The mass spectra and fragmentation patterns of Tyr and 3-Br-Tyr.** (a) Tyrosine (m/z 181) and (b) 3-bromotyrosine (m/z 260).In addition to parent ions $[MH]^+$, fragments and functional groups lost are shown. Structures of tyrosine and 3-bromotyrosine are shown in the insets.

a

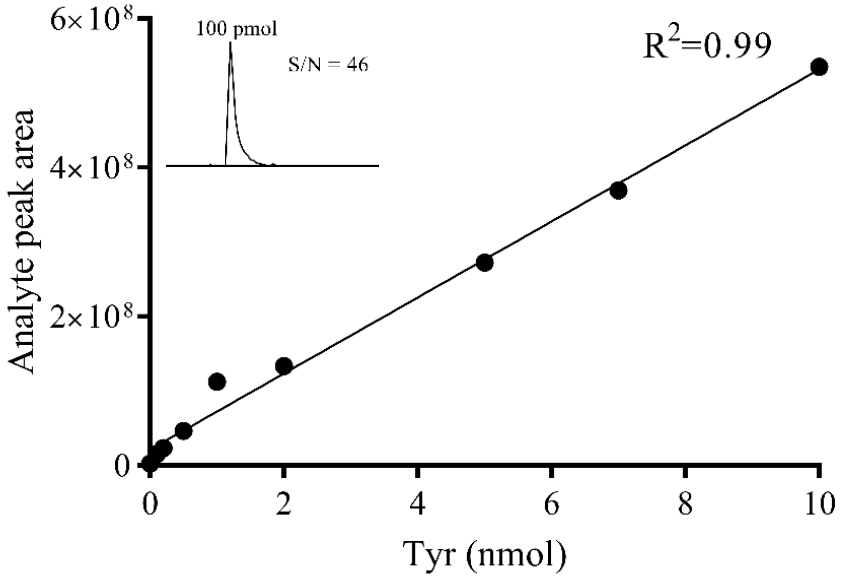


b

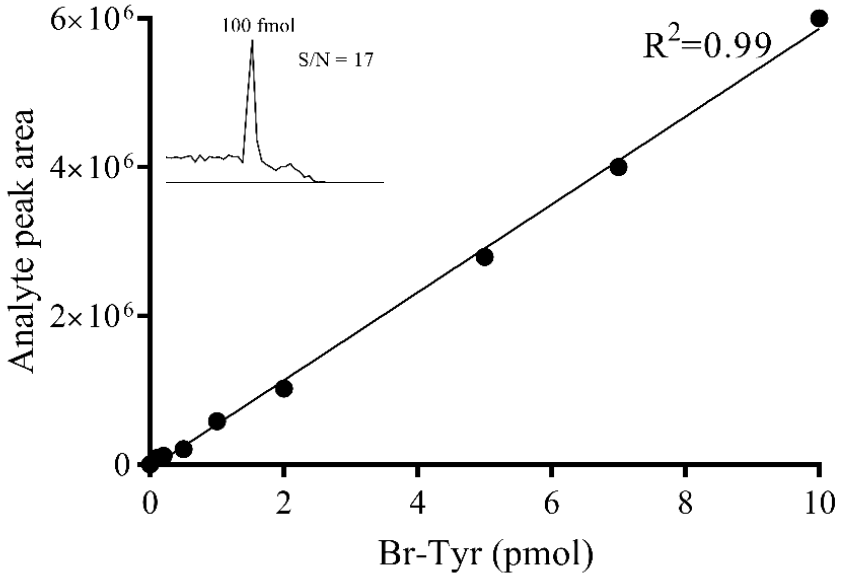


**Figure 33. Standard calibration curves for Tyr and 3-Br-Tyr**. (a) tyrosine in a range of 0.1-10 nmol and (b) 3-bromotyrosine in a range of 0.1-10 pmol. Insets show signal-to-noise ratios for 100 pmol for tyrosine and 100 fmol for 3-bromotyrosine.

### *2.2.18 Measuring 3-nitrotyrosine*

The method development for measurement of 3-nitrotyrosine is described in Chapter 5. Here I describe the final version of the optimised method. A stable isotope dilution LC/MS/MS method was used for the detection and quantification of 3-nitrotyrosine levels in proteins (198). Isotopically-labelled standards ($^{13}C_6$ tyrosine and $^{13}C_9$ 3-nitrotyrosine) were used. Chromatograms of 3-nitrotyrosine and $^{13}C_9$ 3-nitrotyrosine are shown in **Figure 34**. Information on tyrosine standards are described earlier in Section 2.2.17.

ECM samples were first hydrolysed to individual amino acids. Samples (50 µg) were placed in Kimble tubes with internal standards (6 nmol $^{13}C_6$ Tyr and 6 pmol $^{13}C_9$ 3-$NO_2$-Tyr) and dried in the SpeedVac. Then 100 µl of 6 M hydrochloric acid (HCl), supplemented with 1 % (w/v) phenol, was added to each tube and vortexed. The Kimble tubes were then placed into a capped vial, flushed with nitrogen gas four times and sealed under positive pressure. The vial was then placed in an oven inside a fume cupboard, and left at 110°C for 18 hours.

After hydrolysis, samples are left to cool down at room temperature before opening the vial. The Kimble tubes were removed from the vial, and the content was diluted by adding 500 µl $dH_2O$ with 0.1 % (v/v) TFA and vortexed. The hydrolysate was processed by SPE to remove the acid. Cartridges (Strata® C18-E (55 µm, 70 Å), 200 mg / 3 mL) were first conditioned with 5 ml methanol, followed by 2 ml $dH_2O$ with 0.1 % (v/v) TFA, without allowing cartridges to dry. Samples were then loaded onto cartridges, washed twice with 2 ml $dH_2O$ with 0.1 % (v/v) TFA. The analytes were eluted in 1.1 ml 30 % (v/v) methanol in 0.1 % (v/v) TFA, dried in the SpeedVac and reconstituted in 22 µl $dH_2O$ with 0.1 % (v/v) formic acid for analysis by HPLC-MS/MS.

The HPLC method, mobile phase, column and other settings are the same as described earlier in Section 2.2.17. The masses and transitions monitored for 3-nitrotyrosine are listed in **Table 15** and **Figure 35**. Standard calibration curves for 3-nitrotyrosine is shown in **Figure 36**.

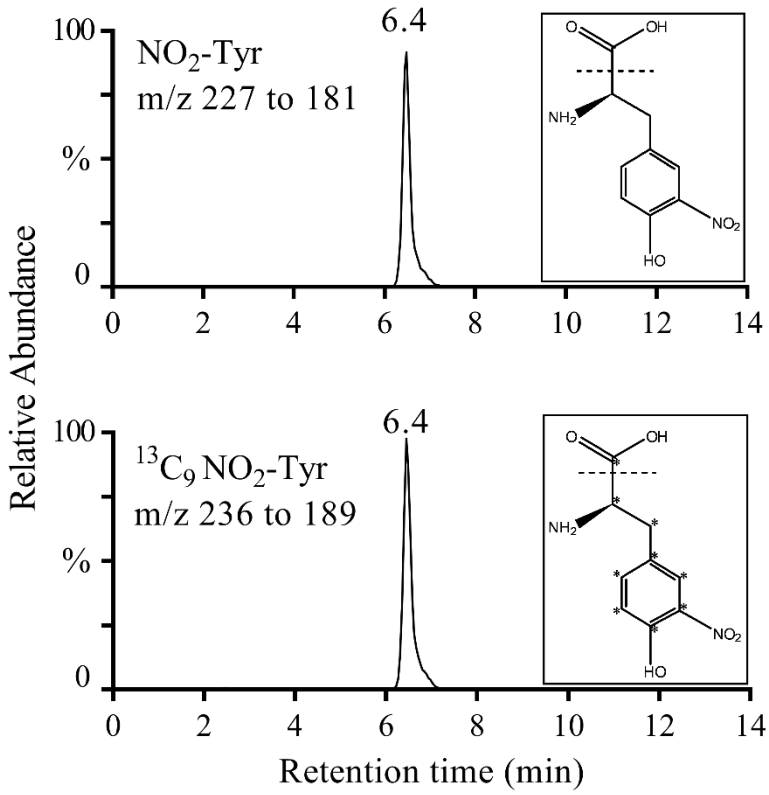


**Figure 34. Typical LC/MS/MS chromatograms for analysis of 3-$NO_2$-Tyr and isotopically-labelled $^{13}C_9$ 3-$NO_2$-Tyr**. Structures of 3-nitrotyrosine and its isotopically-labelled atoms (*) are shown in the insets.

**Table 15. Analysis of 3-$NO_2$-Tyr by MS**. Analytes and ions monitored for analysis of 3-$NO_2$-Tyr and isotopically-labelled 3-$NO_2$-Tyr.

| Analyte | Precursor ion (m/z) | Product ions (m/z) |
|---|---|---|
| $^{12}C$ $NO_2$-Tyr | 227 | 181, 210 |
| $^{13}C_6$ $NO_2$-Tyr | 233 | 187, 216 |
| $^{13}C_9$ $NO_2$-Tyr | 236 | 189, 219 |

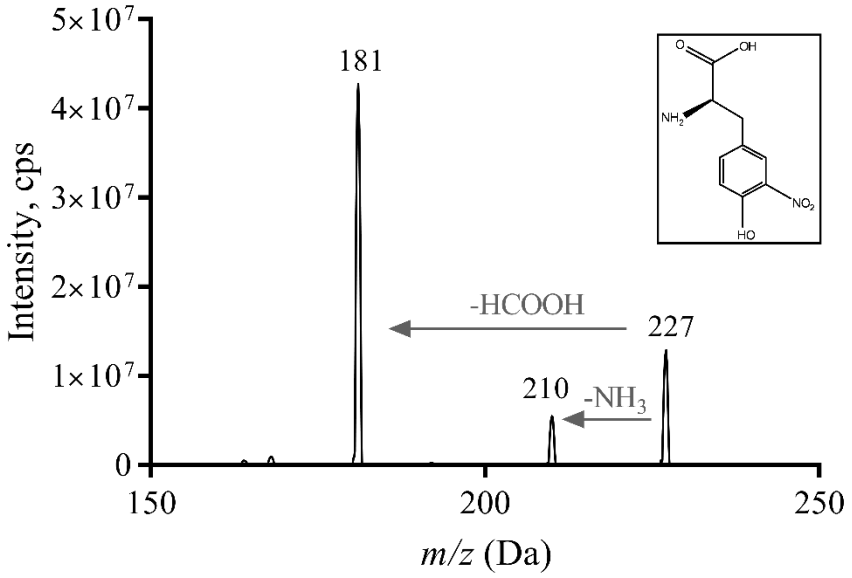


**Figure 35. The mass spectrum and fragmentation pattern of 3-$NO_2$-Tyr**. In addition to parent ions $(MH)^+$ (m/z 227), fragments and functional groups lost are shown. Structure 3-nitrotyrosine is shown in inset.

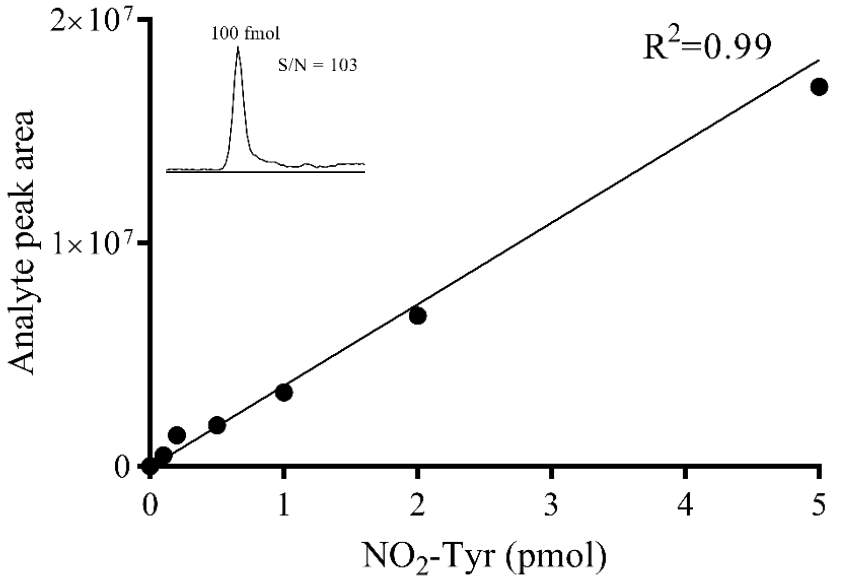


**Figure 36. Standard calibration curve for 3-$NO_2$-Tyr**. Range 0.1-5 pmol. Inset shows signal-to-noise ratios for 100 fmol 3-nitrotyrosine.

### *2.2.19 Statistical analysis*

Data are presented as means and standard errors of the mean, unless stated otherwise. Independent repeats stated in figure legends refer to biological repeats. Any technical repeats are averaged and counted as one biological repeat. Statistical significance was performed on data sets derived from three or more independent biological repeats and calculated by multiple comparison analysis of variance (ANOVA) or paired t-tests. A level of significance was set at $p<0.05$. The software Prism GraphPad was used for data analysis.

# Chapter 3 Enzymology of Peroxidasin in the ECM

The main findings in this chapter are published in: Bathish, B., *et al.*, *Characterisation of peroxidasin activity in isolated extracellular matrix and direct detection of hypobromous acid formation.* Arch Biochem Biophys, 2018. **646**: p. 120-127. (199)

## 3.1. Background

The physiological role of peroxidasin as the enzyme responsible for the sulfilimine cross link in collagen IV was revealed only recently (33). Peroxidasin catalyses the formation of the cross links between juxtaposed methionine and hydroxylysine at the non-collagenous domain (NCD) ends of collagen IV protomers. Peroxidasin oxidises bromide, and it is inferred that it produces HOBr, which is responsible for generating the cross link. The peculiar anabolic function of peroxidasin-produced HOBr poses a paradigm shift for the role of the otherwise destructive oxidant. The role of bromide in the collagen IV cross-linking reaction is the first essential function in mammals to be known of this trace element (35). The low physiological levels of bromide and the presence of other halides that are typical peroxidase substrates (140 mM $Cl^-$, 20-100 μM $Br^-$, 20-120 μM $SCN^-$, 0.1-0.5 μM $I^-$) raise questions about specificity and competition (14). Although there is compelling evidence that peroxidasin uses bromide to cross-link collagen IV, to date there has been no direct evidence that peroxidasin produces HOBr in the ECM. It is also not known whether peroxidasin releases HOBr into its surroundings or undergoes a concerted reaction with collagen IV in the ECM. In this chapter I explore some of the questions regarding peroxidasin substrate requirement, specificity and inhibition.

Peroxidasin is a highly-glycosylated homotrimer with multiple domains that are essential for protein-protein interactions in extracellular proteins. The intrinsic properties of peroxidasin make it difficult to purify or recombinantly express the protein for enzymatic studies. These technical difficulties prevent access to a pure

enzymatic system to probe the enzymology of a native full-length active form of peroxidasin.

As an alternative model system to the pure enzyme, the activity of peroxidasin can be investigated in the ECM. The mouse epithelial cell line, PFHR9 has been used in many studies that have characterised collagen IV cross-linking (33, 35, 49). These cells secrete ECM that contains associated peroxidasin. When they are grown for 6-8 days, an appreciable amount of ECM can be isolated after lysing the cells and then subsequently used to investigate the activity of peroxidasin within the matrix. When the cells are cultured in the presence of phloroglucinol (PHG), a reversible peroxidasin inhibitor (15), the secreted collagen IV is not cross-linked (33). Isolated uncross-linked ECM can then be treated with $H_2O_2$ and various peroxidase substrates and inhibitors, to investigate the modulation of peroxidasin enzymatic activity *in situ*. The peroxidasin-knockout PFHR9 cell line has been used in this study as a negative control. Cross-linking was analysed by isolating the NCD of collagen IV and resolving it by SDS-PAGE. Monomers and dimers were identified by Coomassie Blue staining and quantified by densitometry quantification.

## 3.2. Results

### *3.2.1 Identification of peroxidasin*

To confirm the presence of peroxidasin in the epithelial cells to be used as the experimental model, lysate and ECM isolated from PFHR9 cells were analysed by mass spectrometry and immunoblotting. The mass spectrometry method was developed by Dr. Louise Paton. The full method is outlined in Chapter 2. Two unique tryptic peptides were identified in the peroxidase domain of peroxidasin ($^{675}$AGEIFER$^{681}$ and $^{1101}$AFFSPFR$^{1107}$). The two peptides were used for identification of peroxidasin, and only the second peptide was used for semi-quantification in the intracellular extract and ECM of PFHR9 cells (**Figure 37**a).

The peptide $^{1101}$AFFSPFR$^{1107}$ was three-fold higher in the ECM than in the intracellular lysate. Neither of the peptides were detected in the peroxidasin-knockout PFHR9 cells.

For immunoblotting, lysate from PFHR9 cells and mouse epithelial fibroblast (MEF) cells were blotted and probed with anti peroxidasin antibody. In both cell lines, high molecular weight bands appeared to be consistent with being the 500 kDa trimeric peroxidasin (**Figure 37**b).

The mass spectrometry and immunoblotting data provide sufficient evidence that peroxidasin is present in the cell model system.

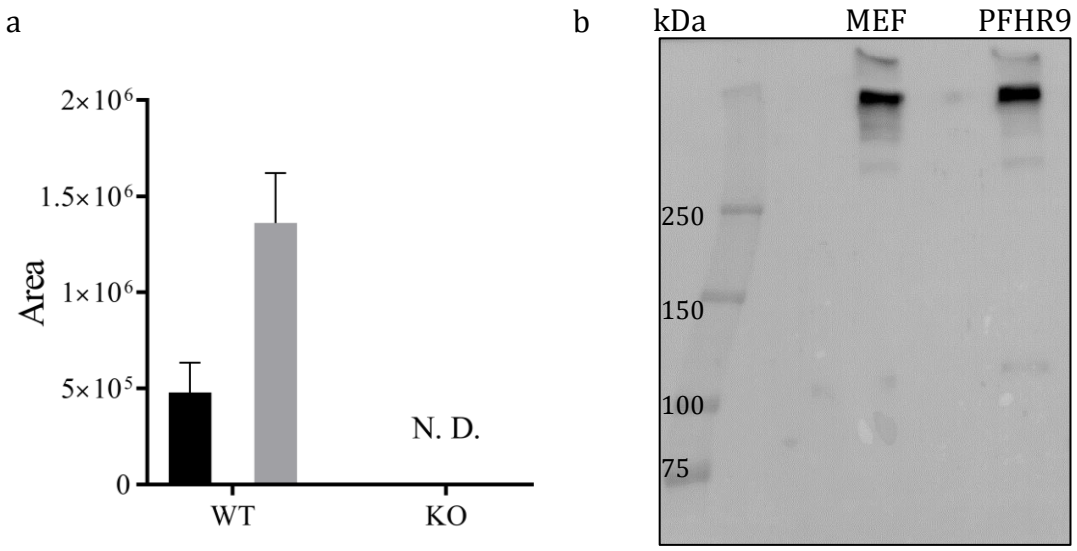


**Figure 37. Detection of peroxidasin in the cell system.** (a) The relative abundance of the peroxidasin tryptic peptide $^{1101}$AFFSPFR$^{1107}$ in 400 µg protein of intracellular extract (black bar) and extracellular matrix (grey bar) analysed by mass spectrometry (n=2 biological repeats). N.D., nothing detected (b) Lysate from mouse embryonic fibroblast (MEF) cells, and mouse epithelial cells (PFHR9) blotted under non-reducing conditions and probed for peroxidasin with anti-peroxidasin antibody.

### *3.2.2 Peroxidase activity in the isolated decellularised ECM*

The Amplex red assay was used to measure peroxidase activity in the isolated decellularised ECM to establish whether peroxidasin is in fact active in the ECM as a general peroxidase. Treatment of the isolated ECM with $H_2O_2$ resulted in the oxidation of Amplex red to fluorescent resorufin, and this activity was fully inhibited by PHG (peroxidasin inhibitor) and azide (general heme poison) (**Figure 38**). No peroxidase activity was detected in ECM isolated from peroxidasin-knockout cells. These results demonstrated that peroxidasin localised in the ECM was active, accessible and able to oxidise external substrates such as Amplex red. Notably, the fluorescence increase after 30 min with peroxidasin and 50 µM $H_2O_2$, corresponded to the response with less than 1 µM $H_2O_2$ when compared with $H_2O_2$ standard curve (not shown). This implies that only a small fraction of the $H_2O_2$ added to the ECM was consumed by peroxidase activity.

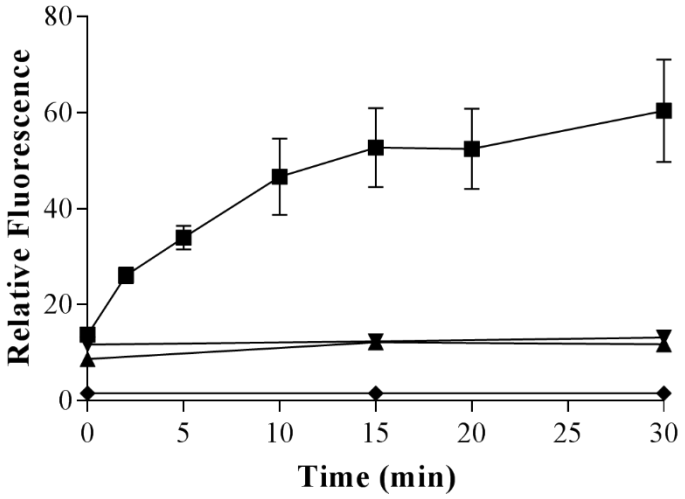


**Figure 38. Peroxidase activity in the isolated decellularised ECM**. Isolated ECM grown in the presence of PHG (200-250 µg per sample in 120 µl final volume of PBS) was incubated with 50 µM Amplex red + 50 µM $H_2O_2$ only (■), or + 50 µM PHG (▲), + 1 mM azide (▼), or 50 µM $H_2O_2$ + ECM isolated from peroxidasin-knockout cells (◆). The reaction was quenched by adding 1 mM azide and ECM was spun and 100 µl of the supernatant was transferred to 96 well plate to measure fluorescence (ex 544 nm/em 590 nm). In a standard curve of Amplex red, $H_2O_2$ and horseradish peroxidase, 0.5 µM $H_2O_2$ gives fluorescent signal of ~60 units. Values represent mean of 3 independent experiments ± SEM.

### *3.2.3 Detection of HOBr formation in the extracellular matrix*

The production of HOBr by peroxidasin was investigated by adding NADH to isolated decellularised ECM and analysing the reaction products. HOBr reacts rapidly with NADH (102), and adds across a double bond of the nicotinamide ring to produce bromohydrin isomers. Following NADH bromohydrin formation by mass spectrometry can provide definitive evidence for HOBr production, because bromine is incorporated into the products. Naturally occurring bromine occurs in equal proportions of two isotopes that differ by two mass units ($^{79}Br$ and $^{81}Br$), which give a distinctive MS pattern.

To establish the assay, oxidation of NADH by reagent HOBr was monitored by a LC/MS assay. Unreacted NADH (m/z 664) ran as a peak at 3.5 min (**Figure 39**a). After treatment with HOBr, two new peaks appeared at 4.5 and 6 min with the expected mass and isotopic distribution for HOBr addition (m/z 760.2 and 762.2). These are likely to be different bromohydrin isomers, depending on the form of addition across the double bond. The area of the major bromohydrin peak showed a linear response to low concentrations of HOBr (**Figure 39**b). When isolated decellularised ECM was incubated with NADH, $Br^-$ and $H_2O_2$, progressive bromohydrin formation over time was detected (**Figure 40**a). This increased with increasing bromide concentration up to 200 μM (**Figure 40**b). There was no difference between bromohydrin formation with 50 or 100 μM $H_2O_2$. As expected for a peroxidasin-dependent reaction, no bromohydrin formation was detected when the ECM was treated with PHG, or in ECM isolated from peroxidasin-knockout cells. Relating the ratio of bromohydrin to NADH peak areas measured with the ECM system to the HOBr standard curve (**Figure 39**b) gives a maximum of ~500 nM HOBr trapped by the NADH (**Figure 40**b). Thus HOBr was produced but the amount trapped corresponded to ~1% of the $H_2O_2$ added.

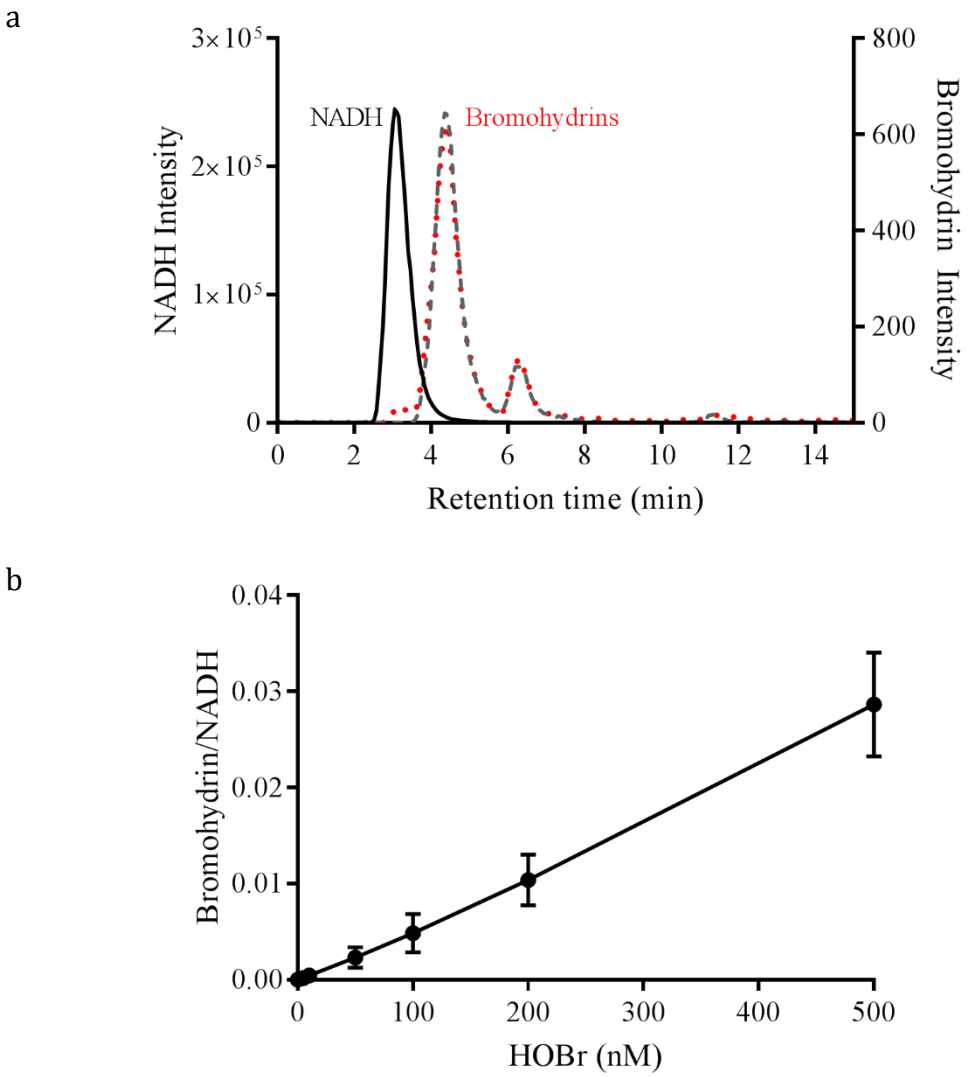


**Figure 39. Reaction of HOBr with NADH to form NADH bromohydrin.** (a) Chromatogram obtained in selective reaction mode for NADH (m/z 664.2 to 408.1, solid line) and the two bromine isotopes of bromohydrin (bromohydrin 1, m/z 760.2 to 680.2 in dashed line, bromohydrin 2, m/z 762.2 to 680.2, overlaid dotted line). (b) Standard curve of reacting NADH (200 μM) with reagent HOBr. Ratios were calculated from the bromohydrin peak areas and represent a combination of both isotopes. Values represent mean and standard error of ≥3 independent experiments.

a

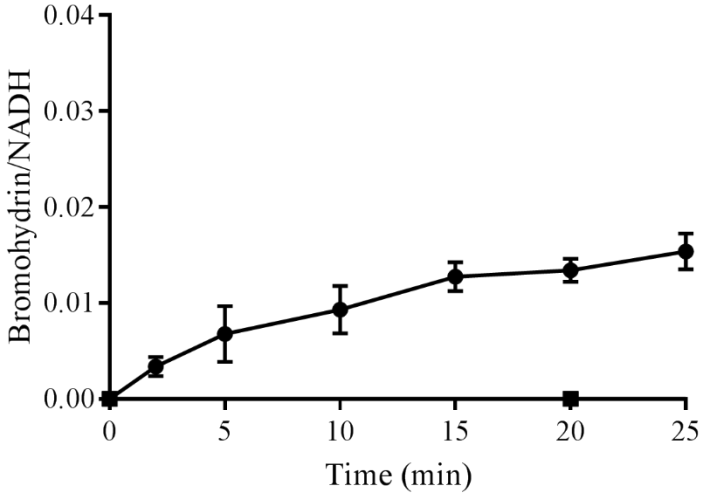


b

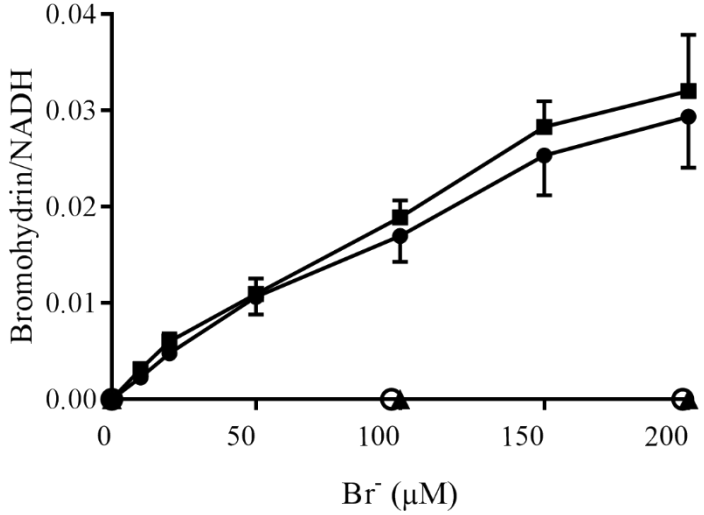


**Figure 40. Oxidation of NADH to bromohydrin by decellularised ECM.** (a) Ratio of bromohydrin to NADH peak areas when ~200 μg of isolated ECM from cells grown in the presence of PHG was incubated with 200 μM NADH, 50 μM $H_2O_2$ and 100 μM $Br^-$ at 37°C, and the reaction was quenched by adding 1 mM azide after the indicated times. (b) Ratio of bromohydrin to NADH peak areas after adding increasing concentrations of $Br^-$ plus 50 μM (●) or 100 μM $H_2O_2$ (■) to ECM and 200 μM NADH; or 100 μM $Br^-$ + 50 μM $H_2O_2$ with 50 μM PHG (○), or with ECM from peroxidasin-knockout cells (▲) for 15 min. Values represent mean of ≥3 independent experiments ± SEM.

The fluorescent probe R19-S reacts with hypochlorous and hypobromous acids to produce the fluorescent product R19 (195, 196). This probe was tested to determine whether it could be used to detect HOBr formation in isolated decellularised ECM. When the probe was mixed with reagent HOBr, it formed the fluorescent product (**Figure 41**a). As previously reported, the yield was lower with HOBr than with HOCl (196). When the probe was added to the isolated ECM with $Br^-$ and $H_2O_2$, no fluorescence was detected (data not shown). It is possible that the amount of HOBr produced in the ECM is very low and it reacts faster and more selectively with the ECM components than with the R19 probe. To test this hypothesis, reagent HOBr was mixed with the R19 probe in presence or absence of isolated ECM. In the presence of ECM, the fluorescence signal produced was negligible when compared to the signal produced when mixing the same amount of reagent HOBr with the R19 probe only (**Figure 41**b). Even when the R19-S probe was pre-incubated with reagent HOBr, the signal was reduced to a third after mixing with the ECM. Therefore, the probe was proven not suitable for this system.

In conclusion, the detection of peroxidasin-dependent oxidation of NADH to bromohydrin is evidence that HOBr is being released as a product of peroxidasin activity in the isolated decellularised ECM.

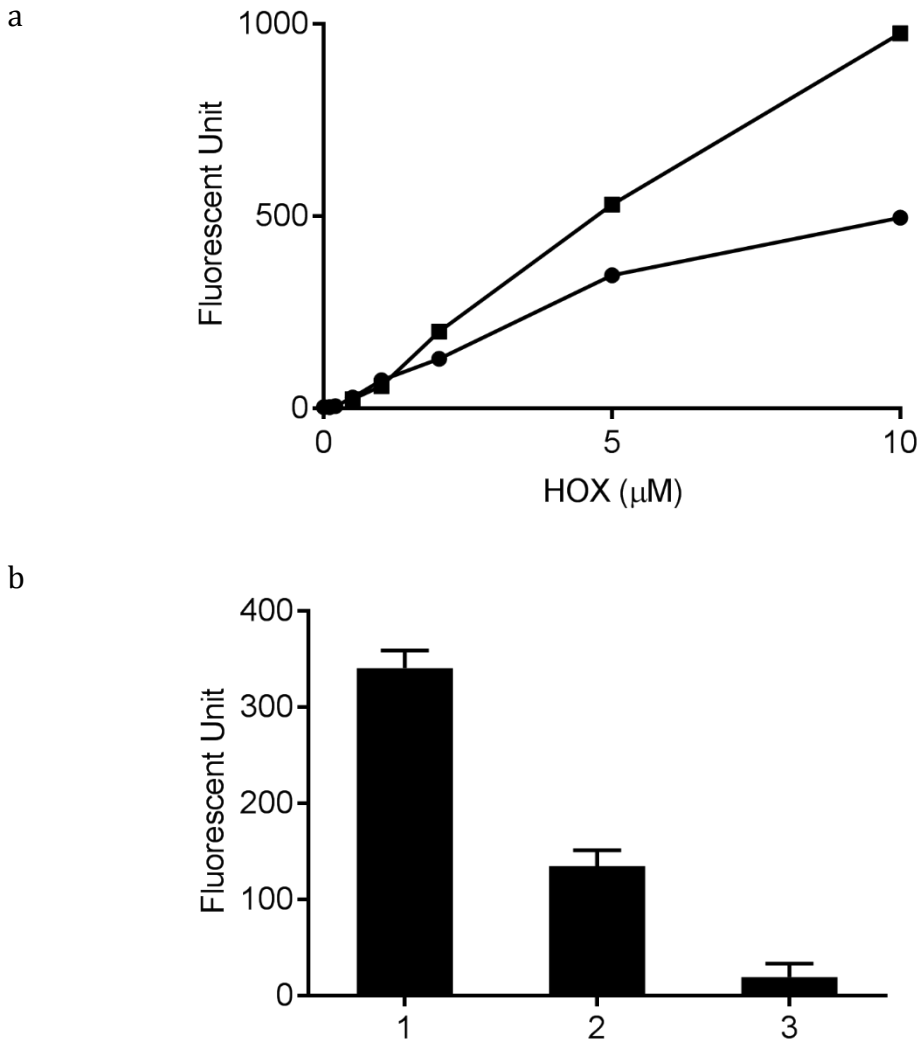


**Figure 41. Reaction of HOCl and HOBr with the probe R19-S.** (a) Titration of HOBr (●) or HOCl (■) with 50 μM R19-S probe and measuring fluorescence (ex 515 nm, em 550 nm). (b) Fluorescence signal when 5 μM HOBr was mixed with 50 μM R19-S probe only (bar 1), when HOBr was pre-incubated with the R19-S probe for 2 minutes before adding to ECM (bar 2), or when the probe was added to ECM first before adding reagent HOBr (bar 3). N=2 ± range.

### *3.2.4 Substrate requirement for collagen IV cross-linking*

Under normal cell culture conditions in growth medium, the non-collagenous domain (NCD) of collagen IV isolated from PFHR9 cells is ~70% cross-linked via one or two sulfilimine bonds to give dimers (designated D1 and D2) with different electrophoretic mobilities (**Figure 42**a and b, lane 1). When PHG, a reversible inhibitor of peroxidasin, was added to the cell culture medium, the proportion of dimer in the subsequently isolated ECM was decreased to ~15% (**Figure 42**a and b, lane 2). When the isolated decellularised uncross-linked ECM was treated with $H_2O_2$ and $Br^-$, the monomers were cross-linked (**Figure 42**a and b, lane 3). Collagen IV isolated from peroxidasin-knockout cells was not cross-linked (**Figure 42**a and b, lane 4). This uncross-linked ECM was used as a model system to investigate the cross-linking reaction by the embedded peroxidasin. When the uncross-linked ECM was treated with $Br^-$ and $H_2O_2$, the NCD cross link was progressively formed to a maximum of ~55% after 30-60 min (**Figure 43**). Cross-linking required both $Br^-$ and $H_2O_2$. It was near maximal with ~10 μM $H_2O_2$ regardless of the $Br^-$ concentration (**Figure 44**) and increased with $Br^-$ concentration up to at least 200 μM (**Figure 45**).

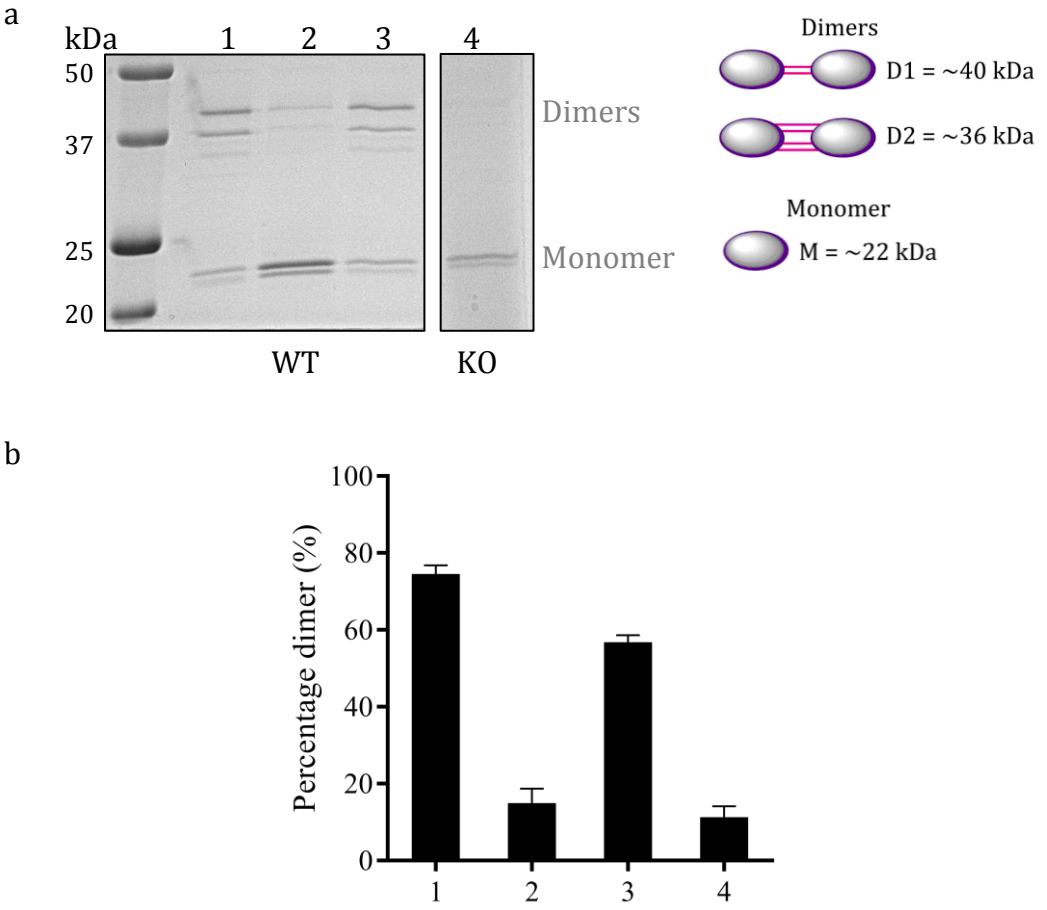


**Figure 42. Collagen IV cross-linking in cell culture or decellularised ECM.** (a) Coomassie-stained gel showing monomers and dimers of collagen IV NCD isolated from PFHR9 cells grown in the absence (lane 1) and presence (lane 2) of 50 μM PHG during deposition of ECM, or when grown in PHG then ECM was isolated and treated with 50 μM $H_2O_2$ and 100 μM $Br^-$ for 1 hour (lane 3). The left lane shows molecular weight markers. In a separate gel, NCD from peroxidasin-knockout cells (KO) treated with 50 μM $H_2O_2$ and 100 μM $Br^-$ for 30 minutes is shown. (b) Densitometry analysis of the gel bands. In all figures, the NCD (~5 μg per sample) was isolated by digestion with collagenase, purified, separated by SDS-PAGE and stained with Coomassie blue. Gel images are representative of ≥3 independent experiments. Percentage dimer was calculated by dividing the densitometry signal of the two dimer bands by the total signal of dimers and monomers within each lane $\frac{D1+(D2x2)}{D1+(D2x2)+M} \times 100$. Densitometry values represent mean of ≥3 independent experiments ± SEM.

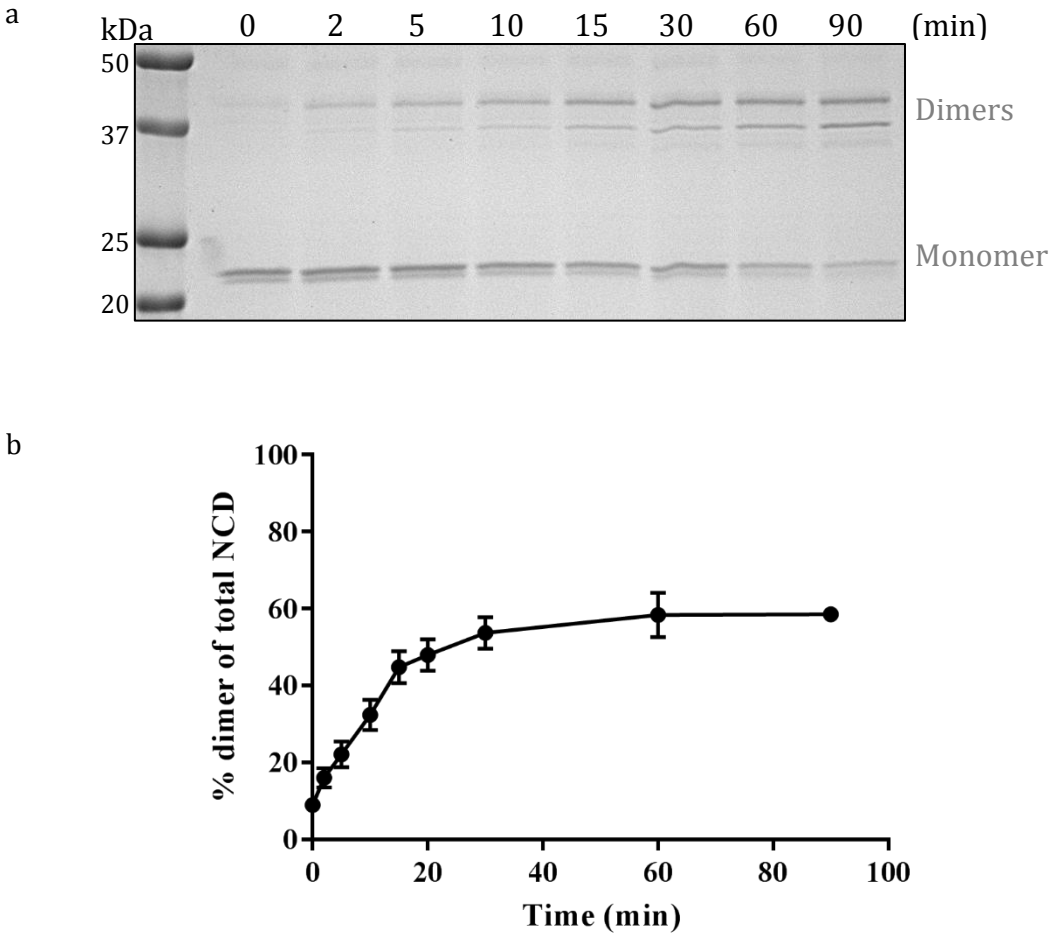


**Figure 43. Collagen IV cross-linking in decellularised ECM**. (a) Coomassie-stained gel showing monomers and dimers of collagen IV NCD isolated from PFHR9 cells grown in the presence of 50 μM PHG during deposition of ECM, then ECM was isolated and treated with 50 μM $H_2O_2$ and 100 μM $Br^-$ for 0-90 minutes at 37°C. The left lane shows molecular weight markers. (b) Densitometry analysis of the time course for dimer formation as detailed in (a). Percentage dimer was calculated as in **Figure 42**. Densitometry values represent mean of ≥3 independent experiments ± SEM.

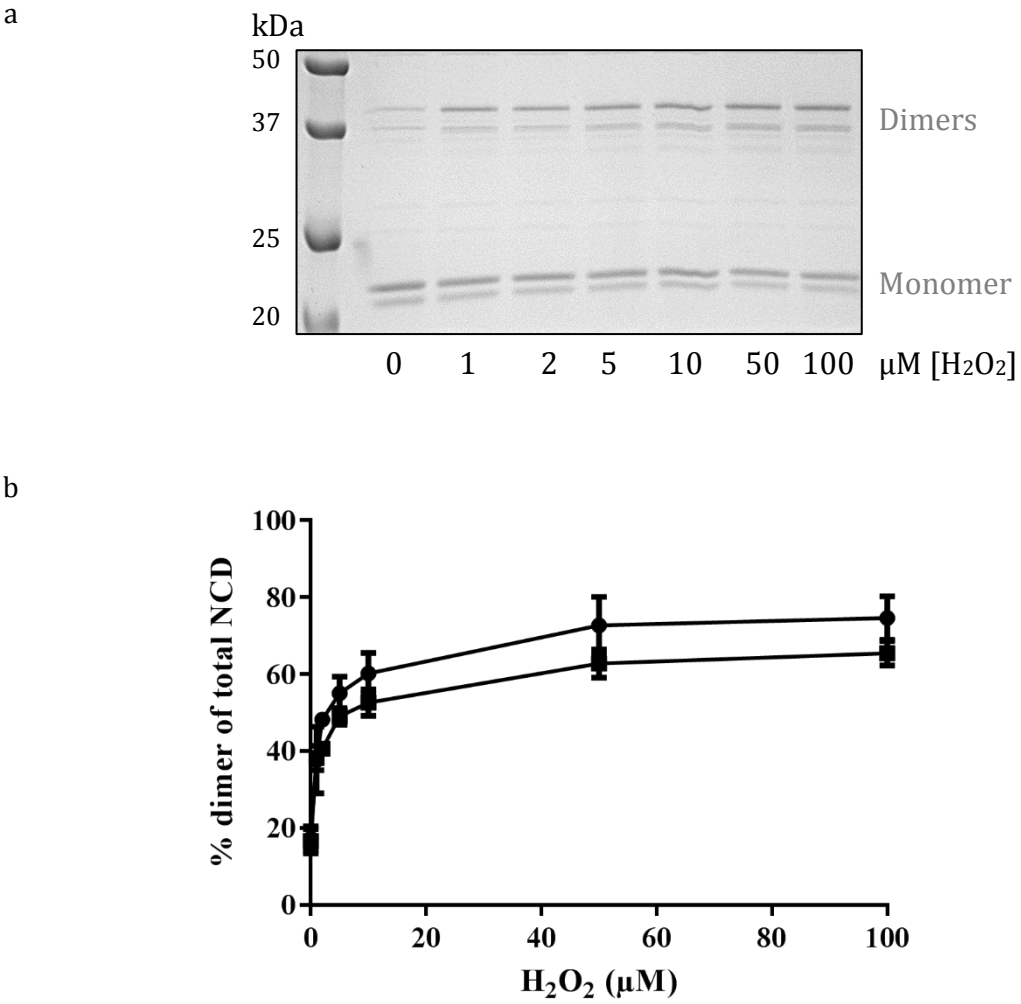


**Figure 44. The effect of $H_2O_2$ concentrations on the cross-linking**. (a) Commassie-stained gel showing dimer formation after treating uncross-linked ECM for 1 hr at 37°C in PBS with 50 μM $Br^-$ and increasing concentrations of $H_2O_2$. (b) Densitometry analysis of $H_2O_2$ dependence with 50 μM (■) and 100 μM $Br^-$ (●). Gel images are representative of ≥3 independent experiments. Percentage dimer was calculated as in **Figure 42**. Densitometry values represent mean of ≥3 independent experiments ± SEM.

a

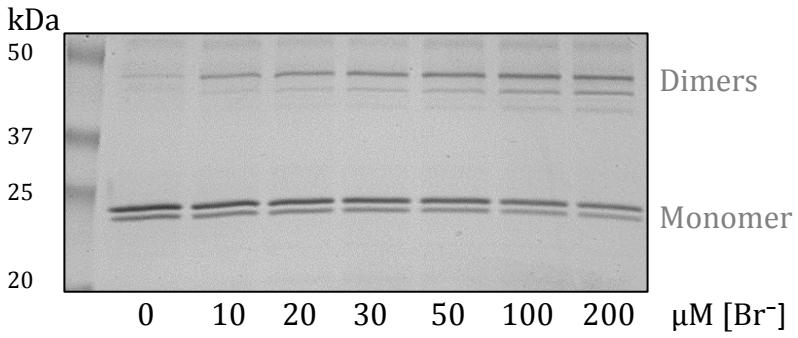


b

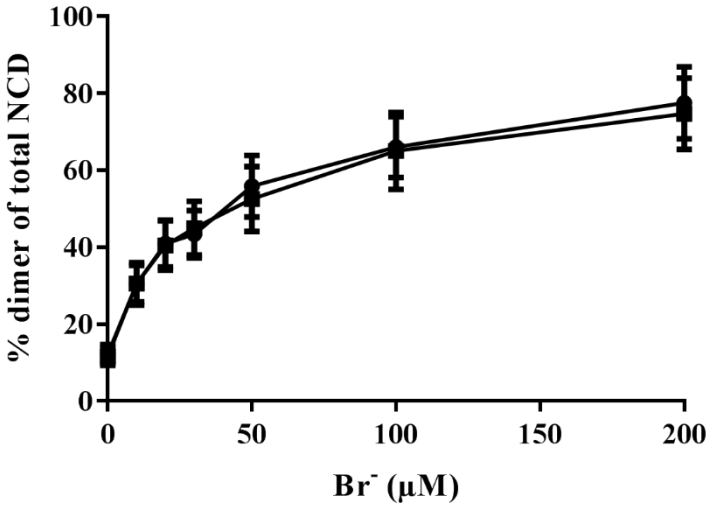


**Figure 45. The effect of bromide concentration on the cross-linking**. (a) Commassie-stained gel showing dimer formation after treating uncross-linked ECM for 1 hr at 37°C in PBS with 50 µM $H_2O_2$ and increasing concentrations of $Br^-$. (b) Densitometry analysis of $Br^-$ dependence with 50 µM (■) and 100 µM $H_2O_2$ (●). Gel images are representative of ≥3 independent experiments. Percentage dimer was calculated as in **Figure 42**. Densitometry values represent mean of ≥3 independent experiments ± SEM.

### *3.2.5 Consumption of hydrogen peroxide in the decellularised ECM*

Surprisingly high concentrations of $H_2O_2$ (~50 μM) were required for maximal dimer formation in the isolated decellularised ECM. Oxidation of Amplex red or NADH accounted for only a small fraction of the $H_2O_2$ added. To investigate the reason for this low stoichiometry, the consumption of $H_2O_2$ by the ECM was monitored using the ferrous oxidation-xylenol orange (FOX) assay. The majority of the $H_2O_2$ was consumed over 30 minutes irrespective of the absence or presence of bromide or PHG (**Figure 46**a). This time course mirrored the time courses for collagen IV cross-linking, Amplex red oxidation and NADH bromohydrin formation. Given that cross-linking only occurred when both $H_2O_2$ and $Br^-$ were added (**Figure 46**b), it appears that most of the $H_2O_2$ was consumed independently of these reactions. The $H_2O_2$ consumption was not due to peroxidasin, as it was just as rapid with ECM isolated from peroxidasin-knockout cells. However, consumption was inhibited by azide, indicating the involvement of a heme enzyme. With no other substrate present, I suspected catalase activity. Indeed I saw consumption of $H_2O_2$ in a standard catalase assay that measures loss of absorbance at 240 nm when ECM was added. The assay used 10 mM $H_2O_2$ and was accompanied by bubble formation as expected for $O_2$ evolution due to catalase action. However, I did not detect the presence of catalase in the isolated ECM by immunoblotting for catalase (**Figure 46**c). One possibility is that a small amount of intracellular catalase was released during cell lysis and bound to the ECM, although extra washing steps with high salt or urea did not decrease the activity. Regardless of the source of catalase activity, it clearly consumed most of the $H_2O_2$ added to the ECM, and this explains why the peroxidasin-dependent reactions occurred with apparently low efficiency.

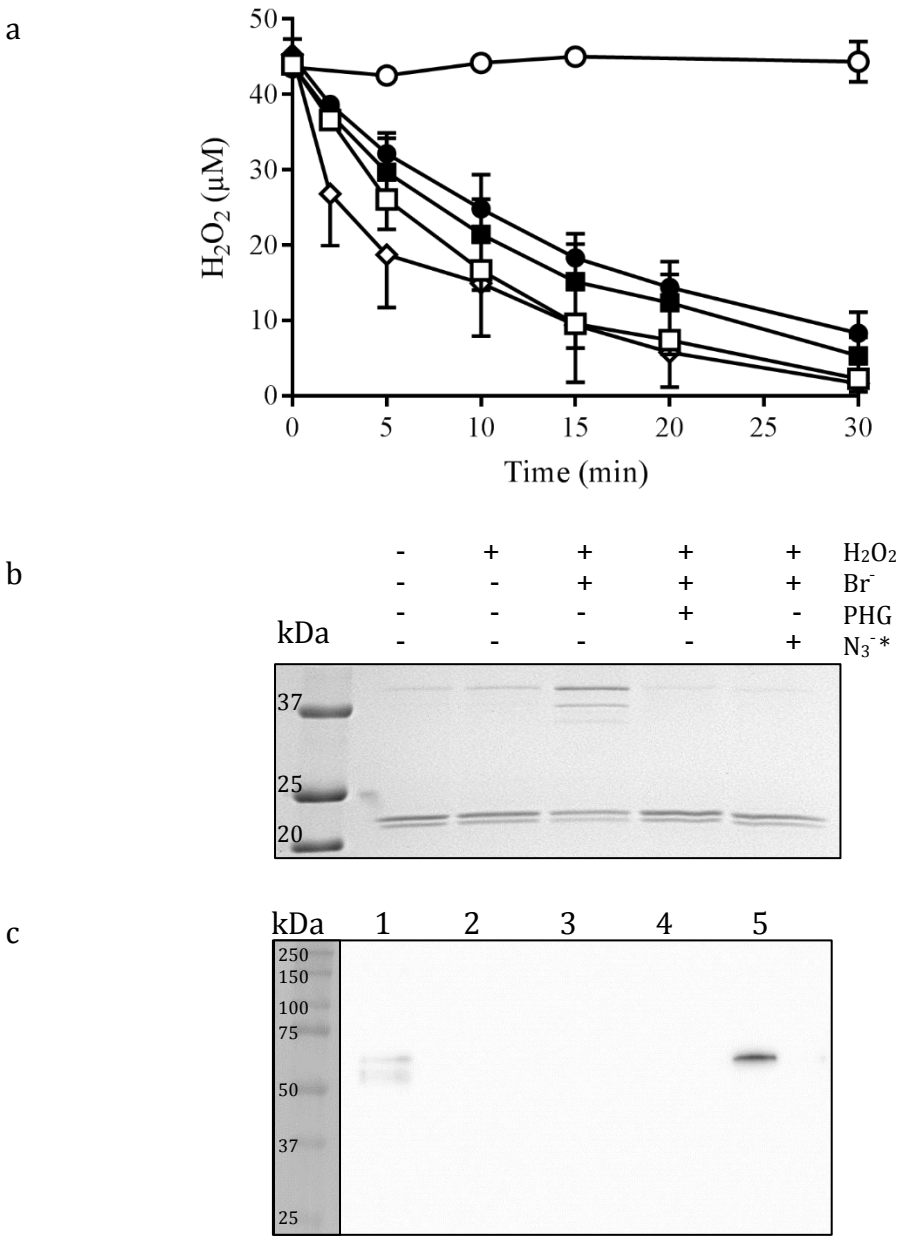


**Figure 46: Consumption of $H_2O_2$ by the decellularised ECM**. (a) ECM (~150-200 μg per sample in 120 μl final volume PBS) was incubated with 50 μM $H_2O_2$ alone (□), or 50 μM $H_2O_2$ with 100 μM $Br^-$ (■), 50 μM PHG (●), 1 mM azide (○), or 50 μM $H_2O_2$ + ECM isolated from peroxidasin-knockout cells (◇). The reaction was quenched with 1 mM azide ($N_3^-$) at each time point, and 50 μl of the supernatant was mixed with 950 μl FOX reagent. Absorbance was measured at 560 nm. Values represent mean of 3 independent experiments. For clarity, error bars are shown in one direction. (b) Gel showing dimers and monomer of NCD from collagen IV cross-linked in ECM isolated from cells grown in PHG, then treated as indicated with $H_2O_2$ and $Br^-$, PHG, or azide. (c) Immunoblot analysis of catalase (MW 60 kDa) using anti catalase antibody. Different samples analysed for the presence of catalase: 25 ng of pure bovine catalase as a positive control (lane 1), total cell lysate from PFHR9 cells (lane 2), intracellular extract (lane 3), isolated ECM (lane 4), lysate from red blood cells as a positive control (lane 5). Immunoblot image is representative of two independent blots.

### *3.2.6 Cross-linking collagen IV with taurine bromamine and HOBr*

Previous evidence points to collagen IV cross-linking being due to HOBr generated by peroxidasin. Bromamines, which are produced by the reaction of HOBr with amine groups, retain the oxidising capability of HOBr (200) and contribute to sulfilimine formation in Met- and Lys-containing small peptides (172). Based on these findings, cross-linking efficiency was compared between taurine bromamine, reagent HOBr and the enzymatic system with $Br^-$ plus $H_2O_2$. The cross link was formed with reagent HOBr and taurine bromamine, although less efficiently than with the enzymatic system ($Br^-$ + $H_2O_2$ + native ECM-bound peroxidasin) especially in forming dimer 2 (**Figure 47**a, b). As expected (35), negligible cross-linking was promoted by hypochlorous acid (**Figure 48**a, b).

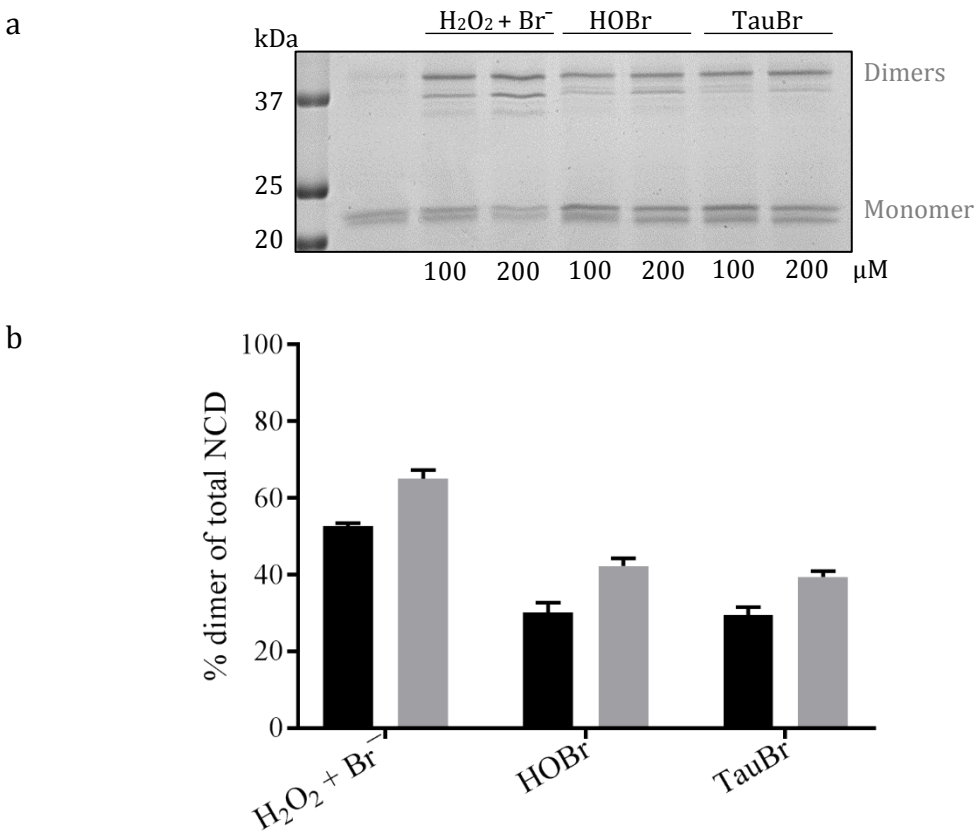


**Figure 47. Cross-linking collagen IV in decellularised ECM.** (a) Commassie-stained gel showing dimer formation after treating uncross-linked ECM for 1 hr at 37°C in PBS with $Br^- + H_2O_2$, reagent HOBr or taurine bromamine (TauBr) with the concentrations indicated below the gel in µM. (b) Densitometry analysis of dimer formation in conditions described in (a), 100 µM (black bars), 200 µM (grey bars) of the indicated substrates/reagents. Gel images are representative of ≥3 independent experiments. Percentage dimer was calculated as in **Figure 42**. Densitometry values represent mean of ≥3 independent experiments ± SEM.

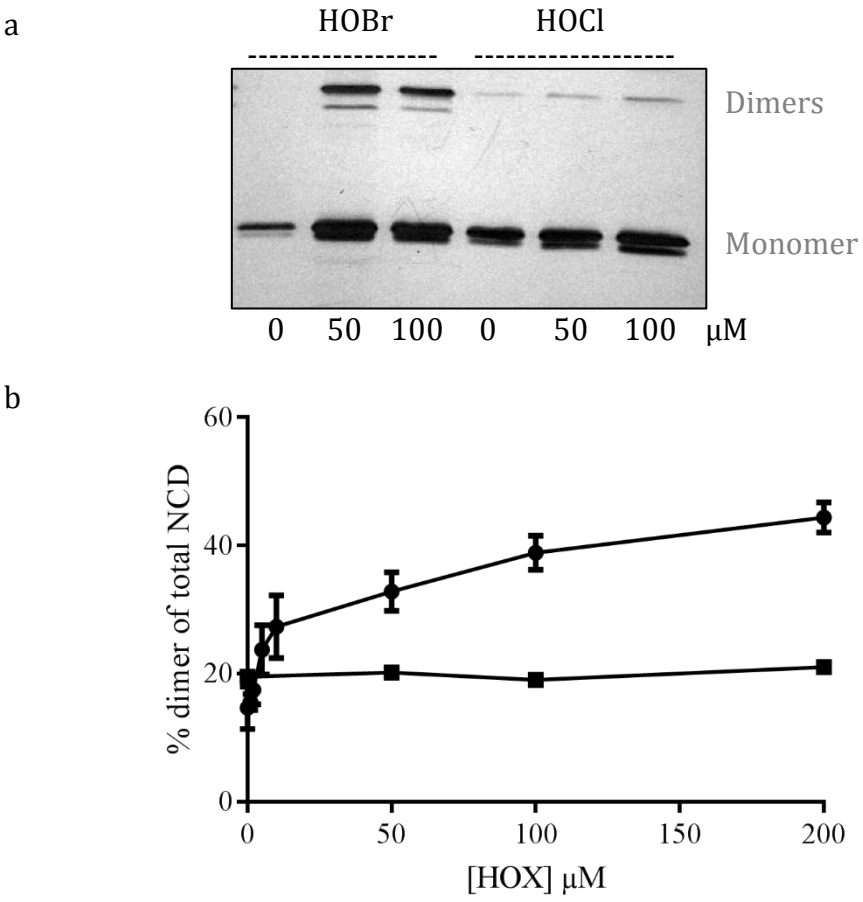


**Figure 48. Cross-linking collagen IV by hypohalous acids.** (a) Silver-stained gel showing dimer formation after treating uncross-linked ECM for 1 hr at 37°C in PBS with reagent HOBr or HOCl. (b) Densitometry analysis of dimer formation in correspondence to increasing concentrations of HOBr (●) or HOCl (■). Gel images are representative of ≥3 independent experiments. Percentage dimer was calculated as in Figure 42. Densitometry values represent mean of ≥3 independent experiments ± SEM.

### *3.2.7 Modulation of collagen IV cross-linking by endogenous substrates*

The halides chloride, bromide and iodide and the pseudohalide thiocyanate are physiological substrates (two electron donors) for heme peroxidases (201). The effects of these substrates on collagen IV cross-linking was tested in the isolated decellularised ECM. Chloride did not interfere with bromide, as all cross-linking reactions were carried out in 140 mM NaCl. Iodide and thiocyanate both inhibited dimer formation when added with $Br^-$ and $H_2O_2$ (**Figure 49**a, b). In each case, the concentration-dependence of inhibition was similar at 50 and 100 μM $Br^-$, with 200 μM iodide inhibiting dimerisation by ~30%, and 200 μM thiocyanate by ~50% (calculated as a proportion of the difference between maximum dimerisation of 70% and 10% dimers in the starting material). Thus iodide inhibited only at much higher than physiological concentrations, whereas inhibitory concentrations of thiocyanate were in the physiological range.

Urate and ascorbate are substrates for peroxidasin (one-electron donors) (47), as well as good oxidant scavengers. Low concentrations of urate inhibited dimerisation to a maximum of ~35% with an $IC_{50}$ of ~20 μM (**Figure 50**a). The extent of inhibition was similar at 50 and 100 μM bromide. Ascorbate had a minimal effect on cross-linking (**Figure 50**b).

a

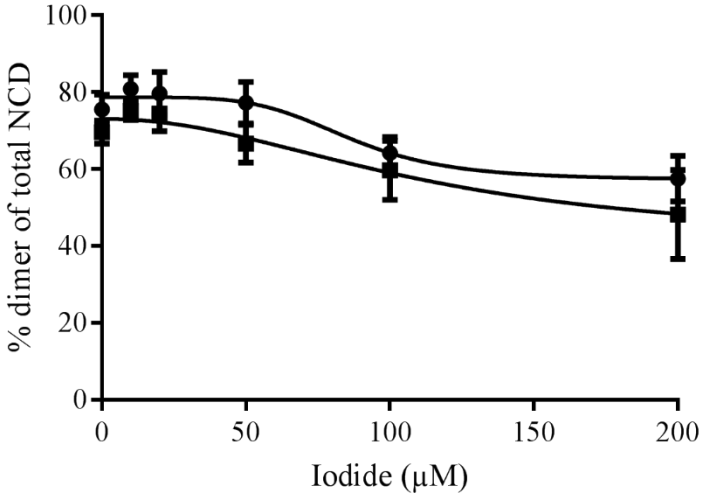


b

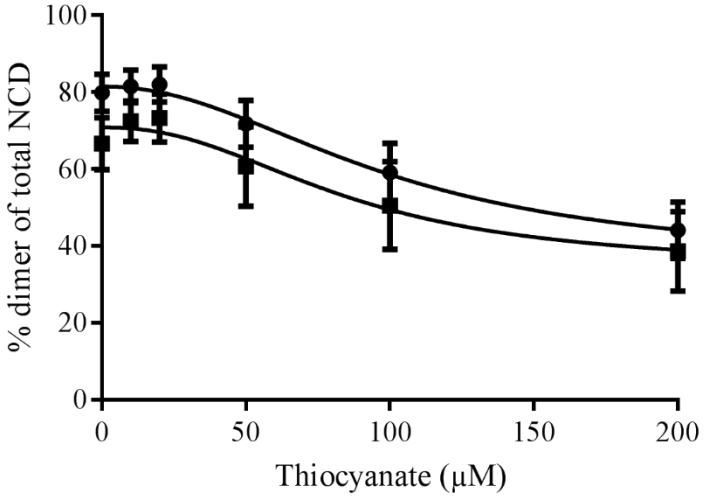


**Figure 49. The effects of iodide and thiocyanate on the cross-linking**. ECM isolated from epithelial cells grown with PHG was treated with (■ 50 μM or ● 100 μM) $Br^-$ + 50 μM $H_2O_2$ + the indicated concentrations of (a) iodide or (b) thiocyanate in PBS for 1 hour at 37°C. ECM digestion, purification of NCD and analysis of dimer as in Figure 42. Percentage dimer was calculated as in Figure 42. Densitometry values represent mean of ≥3 independent experiments ± SEM.

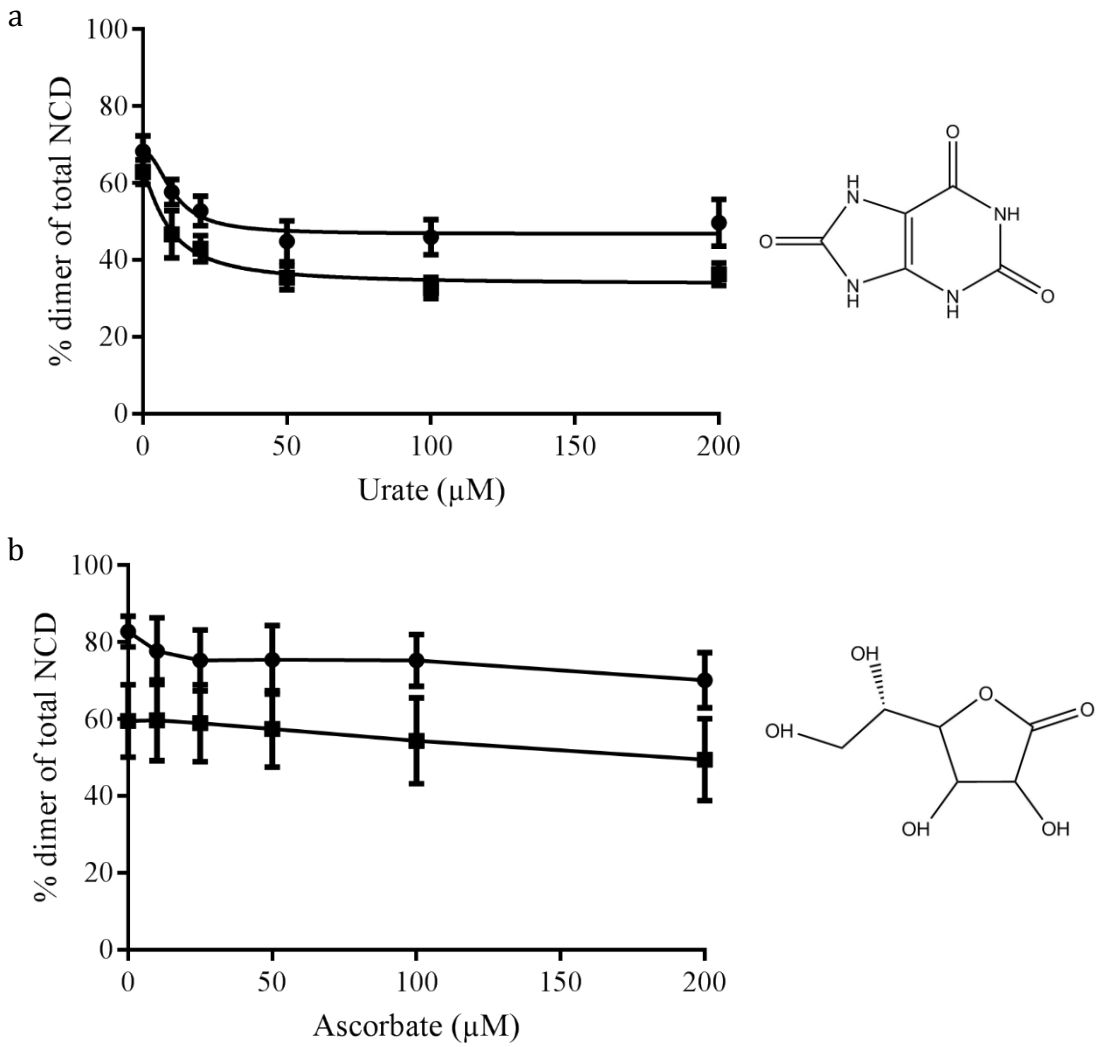


**Figure 50. The effects of urate and ascorbate on the cross-linking**. ECM isolated from epithelial cells grown with PHG was treated with (■ 50 μM or ● 100 μM) $Br^-$ + 50 μM $H_2O_2$ + the indicated concentrations of (a)urate or (b) ascorbate in PBS for 1 hour at 37°C. ECM digestion, purification of NCD, analysis of dimer as in Figure 42. Densitometry values represent mean of ≥3 independent experiments ± SEM. Structures of uric acid and ascorbic acid are shown next to their respective graphs.

The observed effects of the inhibitors could be due to them acting as competitive substrates for peroxidasin, as well as scavengers of HOBr being produced by peroxidasin. When comparing the effects on cross-linking with reagent HOBr versus the enzymatic system ($Br^- + H_2O_2$ + embedded peroxidasin), iodide, thiocyanate and urate all showed significant inhibition in the enzymatic system, indicating that they acted as substrates for peroxidasin (**Figure 51**). These scavengers had varied effects when added with reagent HOBr. Their inhibition of cross-linking is not statistically significant. However, a closer look at the effect of thiocyanate shows that it actually inhibited cross-linking almost to the starting point with phloroglucinol (10 % dimer). Experimental variation might have obscured an actual inhibition by thiocyanate when added with reagent HOBr. Ascorbate had no effect both when added with HOBr or in the enzymatic system.

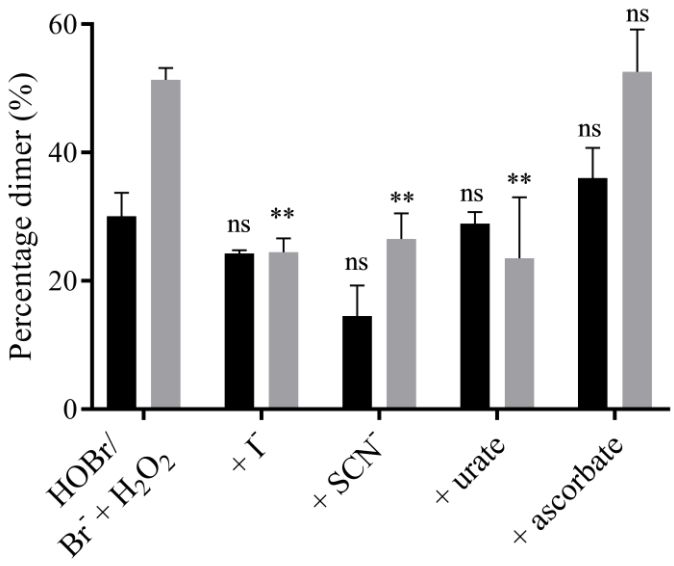


**Figure 51. The effects of peroxidase substrates and HOX scavengers on the cross-linking of collagen IV**. Densitometry analysis of dimer formation in uncross-linked isolated ECM by 100 µM reagent HOBr (black bars) or enzymatic system using 100 µM $Br^-$ and 100 µM $H_2O_2$ (grey bars), and comparing the effects of 100 µM iodide, thiocyanate, ascorbate and urate in both systems. N=2 ± range. ns, not significant, ** < 0.007, by multiple comparison 2-way ANOVA.

### *3.2.8 The effects of scavengers of HOBr on collagen IV cross-linking*

Methionine, reduced glutathione (GSH), thiodipropionic acid (TDPA) and NADH are all efficient scavengers of HOBr (structures shown in **Figure 52**). The rate constants of their reactions with HOBr are $4\times10^6$, $1\times10^7$ (*estimated*), $1.1\times10^6$, $4\times10^6$ $M^{-1}$ $s^{-1}$, respectively) (14, 102, 120). When present during the reaction of peroxidasin in the ECM with $Br^-$ and $H_2O_2$, all gave concentration-dependent inhibition of collagen IV dimerisation (**Figure 53**a, b). Thiodipropionic acid was the most effective, with almost complete inhibition at 5mM. Methionine, GSH and NADH had moderate effects on cross-linking.

I also compared the effect of TDPA in the cell culture system and decellularised ECM. TDPA had a stronger inhibitory effect in the isolated decellularised ECM system (**Figure 54**). This could be due to it reacting with other components in the growth medium, and being cell impermeable.

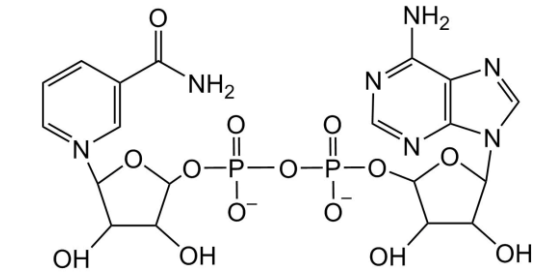

NADH

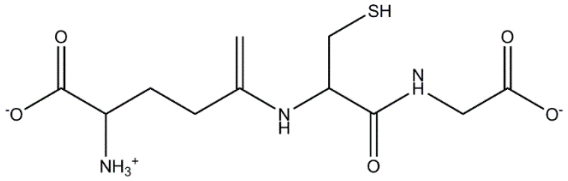

GSH

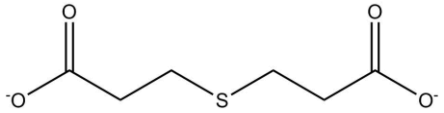

TDPA

**Figure 52. The chemical structures of NADH, GSH and TDPA.**

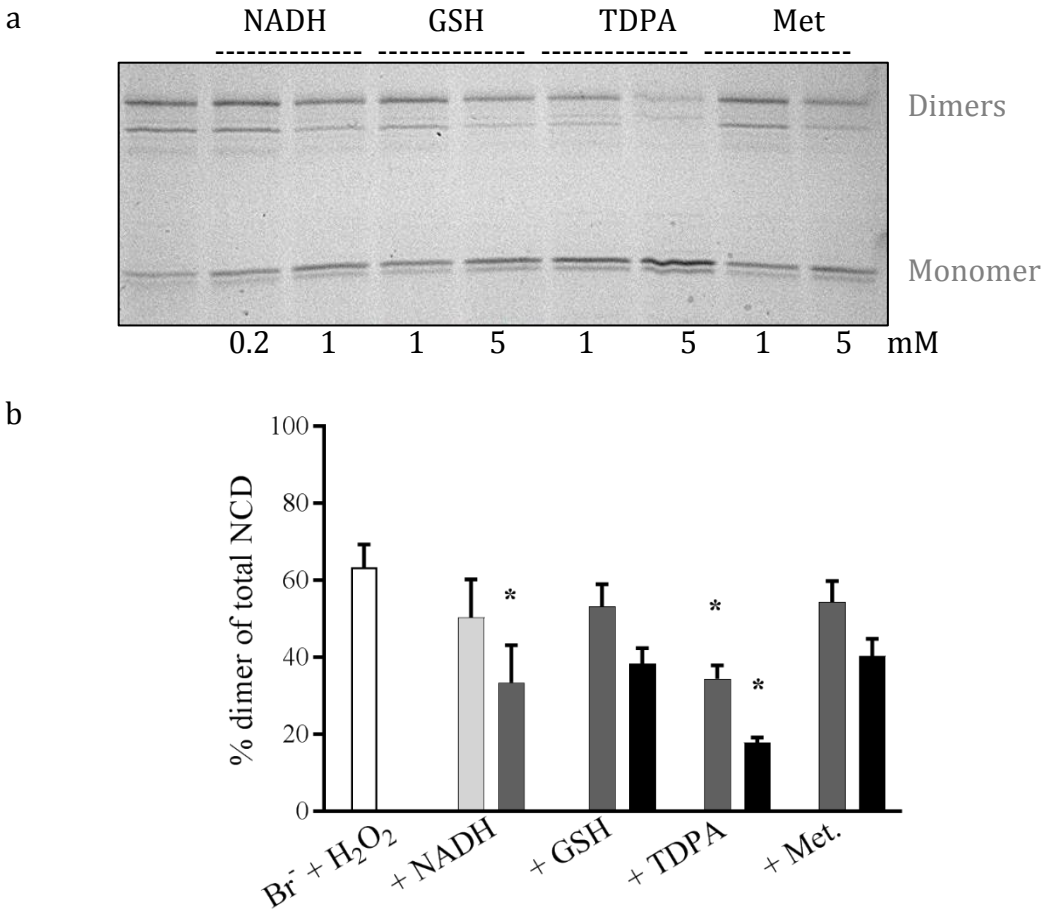


**Figure 53: The effects of scavengers of HOBr on the cross-linking of collagen IV.** (a) Commassie-stained gel showing dimer formation after treating uncross-linked ECM for 1 hr at 37°C in PBS with $Br^-$ + $H_2O_2$ in addition to different scavengers as labelled. (b) Densitometry analysis of dimer formation when treated only with 100 µM $Br^-$ + 50 µM $H_2O_2$ only (white bar), or in addition to NADH, GSH, methionine, or TDPA (0.2 mM in light grey bar, 1 mM in dark grey bars, 5 mM in black bars). ECM digestion, purification of NCD and analysis of dimer as in Figure 42. Values represent mean of ≥3 independent experiments ± SEM; * $p < 0.05$ by ANOVA analysis.

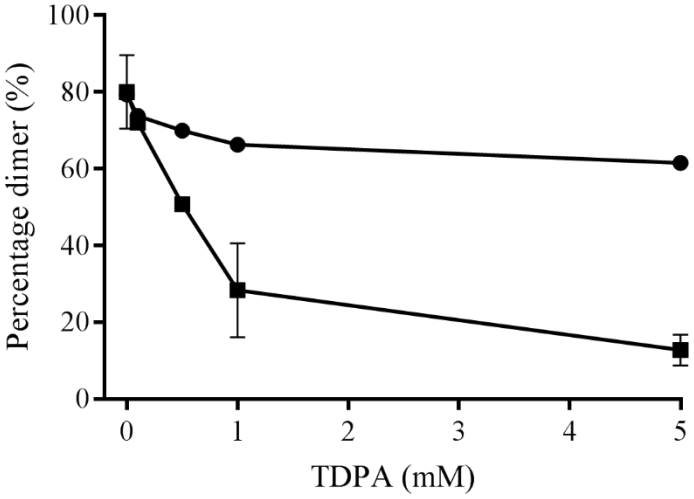


**Figure 54: The effect of TDPA on the cross-linking.** Comparing the effect of TDPA on dimer formation when added to cell culture medium during deposition of ECM (●) versus when added during the cross-linking reaction in the isolated uncross-linked ECM (■). ECM digestion, purification of NCD and analysis of dimer as in Figure 42. Values represent mean of ≥3 independent experiments ± SEM.

### *3.2.9 The effects of MPO inhibitors on collagen IV cross-linking*

Various compounds have been developed as inhibitors of myeloperoxidase in experimental systems or as potential therapeutic agents, and there are other drugs that show inhibitory activity against myeloperoxidase. The ability of some of these compounds to inhibit peroxidasin-catalysed cross-linking of collagen IV in isolated decellularised ECM was tested (**Figure 55**). 4-Aminobenzoic acid hydrazide gave 60% inhibition of dimer formation with ~10 μM. This is in the range that inhibits myeloperoxidase activity of stimulated neutrophils ($IC_{50}$ values of 2.2 and 15 μM; (202)). The 2-thioxanthine, TX1, was less potent at inhibiting peroxidasin ($IC_{50}$ ~20 μM) and is therefore much more specific for myeloperoxidase ($IC_{50}$ ~1μM with the purified enzyme or neutrophils, (203)). Acetaminophen (paracetamol), at concentrations in the therapeutic range (up to 150 μM) that inhibit neutrophil myeloperoxidase ($IC_{50}$ ~100 μM) (204) had little effect on the amount of dimer formed ($IC_{50}$ >1mM).

a

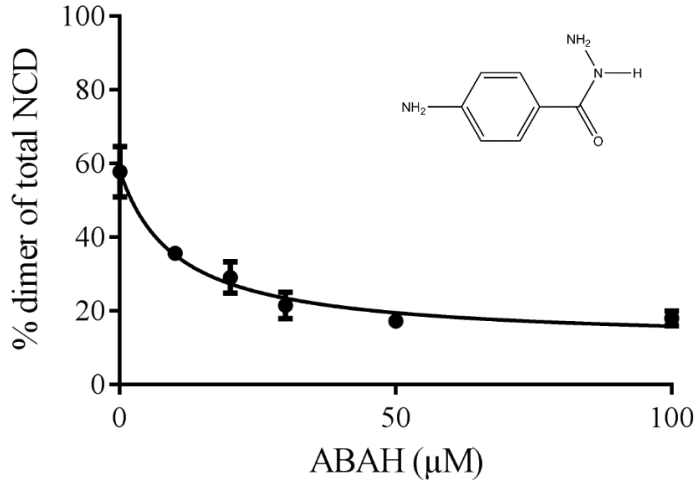


b

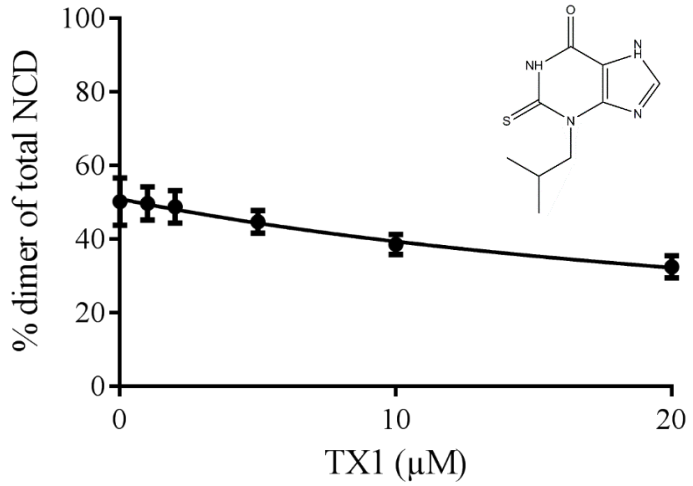


c

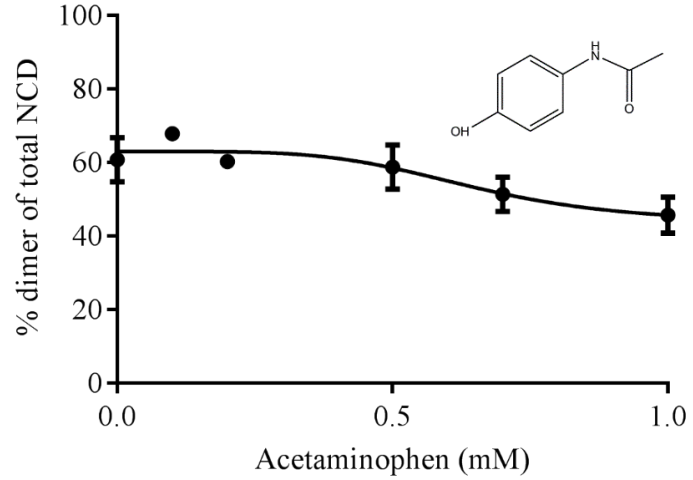


**Figure 55: The effects of inhibitors of myeloperoxidase on the cross-linking.** ECM from epithelial cells grown with PHG was treated with 100 μM $Br^-$, 50 μM $H_2O_2$ and the indicated concentrations of (a) ABAH, (b) TX1, and (c) acetaminophen, for 1 hour at 37°C in PBS. Chemical structures are shown next to each graph. ECM digestion, purification of NCD and analysis of dimer as in Figure 42. Values represent mean of ≥3 independent experiments ± SEM. Complete inhibition of the reaction would leave the 10% dimer already present in the untreated ECM.

## 3.3. Discussion

In this chapter I provided evidence that peroxidasin is present and active in the ECM as shown by mass spectrometry, western blotting, Amplex red assay and cross-linking of collagen IV. The isolated decellularised ECM proved to be a useful model to study the enzymology of peroxidasin *in situ*. The formation of dimer in the non-collagenous domain can be used to probe for the activity of peroxidasin both in the cell culture system and the isolated decellularised ECM system. I found that the cross-linking of collagen IV at the non-collagenous domain required the activity of peroxidasin, bromide and hydrogen peroxide, in agreement with the published findings (33).

Collagen IV protomers (triple helices) are large and require special secretion vesicles to the extracellular matrix (205). It is not known definitively whether the site of forming the sulfilimine cross link in the NCD of collagen IV is intracellular or extracellular. In this chapter, I showed that peroxidasin embedded in the isolated decellularised ECM was able to cross-link the uncross-linked collagen IV in the presence of $Br^-$ and $H_2O_2$. This indicates that cross-linking of collagen IV can occur extracellularly, which aligns with the findings that extracellular chloride concentrations are necessary for the oligomerization of collagen IV in an orientation that allows the NCD to be cross-linked (160). This finding does not rule out the possibility that any cross-linking also occurs intracellularly. Reagent HOBr and taurine bromamine were also able to generate the cross link, however less efficiently than the enzymatic system. The ability of a bromamine to promote the sulfilimine bond formation is consistent with published data that bromamines generate a sulfilimine link in peptides containing Met and Lys (172). It is possible that these secondary oxidants also play a role in cross-linking collagen IV.

The extent of cross-linking in the isolated decellularised ECM showed bromide dependency and approached its maximum at bromide concentrations within the physiological plasma range (20-100 μM) (206). Cross-linking collagen IV was the first essential biological function of bromide in mammals to be discovered (35). The

plasma concentration of bromide is maintained through diet and renal excretion. The effect of bromide deficiency in humans is yet to be studied.

Peroxidasin embedded in the isolated decellularised ECM showed peroxidase activity as shown by its ability to oxidise Amplex red. It also oxidised exogenous NADH to its bromohydrin, and this shows definitively that peroxidasin in the isolated decellularised ECM produces HOBr. Previous evidence showed that peroxidasin (purified from transfected HEK293 cells) was able to halogenate taurine to haloamines (33).

Cross link formation, Amplex red oxidation and NADH bromohydrin formation all followed a similar time course that reflected the rate of $H_2O_2$ consumption. This suggests they all depend on $H_2O_2$ / peroxidasin activity. Only a small fraction of the added $H_2O_2$ (~1 μM), however, was used by peroxidasin. The majority of the $H_2O_2$ was consumed by what appeared to be a heme enzyme with catalase-like activity. This enzyme was a complicating factor in studying the kinetics of peroxidasin *in situ*.

Calibration of the NADH assay against reagent HOBr indicated that peroxidasin in the ECM, plus 50 μM $H_2O_2$ generated approximately 250 nM HOBr in 15 minutes (**Figure 39**b, c). Over the same time, about 70 % of the $H_2O_2$ was consumed independently of peroxidasin (**Figure 46**a). Therefore, the HOBr trapped by NADH accounted for only 1% of the $H_2O_2$ consumed. As exogenous NADH inhibited cross-linking by about 20 % (0.2 mM NADH in **Figure 53**c), it is estimated that low micromolar HOBr generated by peroxidasin would be sufficient to give maximum cross-linking (~70 %). However, 50 μM reagent HOBr did not give maximal cross-linking, which implies that the enzymatic reaction is more selective for sulfilimine link formation. This might be due to peroxidasin being localised in the ECM or having an association with collagen IV which makes the reaction more targeted. It is noteworthy that efficiency of cross-linking by the enzymatic system is more remarkable when considering that catalase consumed most of the $H_2O_2$ added to the isolated ECM.

The effects of NADH, GSH, methionine and TDPA on dimer formation also suggest selectivity of HOBr reactions toward cross-linking collagen IV over scavengers. They all exhibited inefficient inhibitory effect; high micromolar to millimolar concentrations were required, even though the scavengers are at least as reactive with HOBr as the Met and Lys residues that form the sulfilimine bond (120). This may indicate localised reactions of HOBr to cross link collagen IV that are not accessible for other scavengers.

Iodide and thiocyanate are good substrates for peroxidases. In a study using a truncated recombinant form of peroxidasin, they were excellent two-electron donors. The rate constants of their reactions with compound I of the enzyme were 1.68 and $1.83 \times 10^7$ $M^{-1}$ $s^{-1}$ respectively (13). These rate constants are in fact higher than that for bromide ($5.6 \times 10^6$ $M^{-1}$ $s^{-1}$). However, none of these substrates promoted the cross-link. Rather, they acted as inhibitors in the presence of bromide, in line with previous evidence that iodide and thiocyanate inhibit the cross-linking reaction (33, 35). Iodide inhibited the cross link inefficiently ($IC_{50}$ > 200 μM), at concentration much higher than the physiological concentration (< 1 μM). Thiocyanate, however, inhibited the cross link at concentrations that fall within the physiological range (20-120 μM). Thiocyanate also reacts with HOBr at almost diffusion-controlled rate ($2.3 \times 10^9$), and its inhibitory effect can be due to scavenging some of the HOBr produced by peroxidasin. It is, however, surprising that thiocyanate does not lead to complete inhibition of the cross link, given that it is the best known substrate for peroxidasin and scavenger of HOBr. This again indicates high selectivity of the reaction of HOBr toward cross-linking collagen IV.

This inhibitory effect might have implications, especially in smokers who have elevated levels of thiocyanate (207). Indeed, smoking was shown to be associated with changes in the basement membrane (208), which may be due to the inhibitory effect observed in collagen IV.

Ascorbate had a minimal effect on the cross-linking of collagen IV in isolated ECM, even at 200 μM. This might have a physiological advantage, as plasma ascorbate

levels in healthy individuals are normally in the range 50-70 μM. Urate had a modest inhibitory effect on dimer formation ($IC_{50}$ ~20 μM), within the physiological range (200-400 μM, which can be higher in hyperuricemia) (209). Recently-submitted data from Obinger's group show that ascorbate and urate reduce compound I of hsPxd01-con4 to compound II in two one-electron reduction steps (rate constants for the reactions with compound I are 7.2 and $1.9 \times 10^4$ $M^{-1}$ $s^{-1}$, respectively) (47). The rate of reduction of compound II to the native enzyme is slower, which leads to accumulation of compound II and loss of the halogenation activity. It is not clear why urate showed inhibitory effect on the cross-linking while ascorbate did not. It might be related to accessibility to the active site of the enzyme (their chemical structures are shown in **Figure 50**).

The homology between peroxidasin and myeloperoxidase, and the interest in developing pharmacological inhibitors of myeloperoxidase motivated the investigation of how myeloperoxidase inhibitors affect peroxidasin and the sulfilimine cross-link. Acetaminophen is a moderate inhibitor of myeloperoxidases, while ABAH and TX1 are potent (203, 204, 210). In the isolated decellularised ECM system, only ABAH inhibited peroxidasin with comparable efficacy to inhibiting MPO. This would make it difficult to distinguish the two in a complex or *in vivo* system. However, TX1 was more specific for myeloperoxidase, and should not compromise its use for probing its pathophysiology.

In summary, in this chapter I have optimized the isolated decellularised ECM as an experimental model suitable for the study of peroxidasin *in situ*. The formation of the sulfilimine cross link in isolated collagen IV required both $H_2O_2$ and bromide, and was inhibited by iodide, thiocyanate and urate. Peroxidasin embedded in the ECM was active and able to oxidise external substrates. HOBr was formed and released in the ECM, as evident by oxidation of NADH to bromohydrin. It is not known whether the HOBr produced by peroxidasin reacts selectively with collagen IV to form the sulfilimine bond or extends to other endogenous targets in the ECM.

# Chapter 4 Peroxidasin-Catalysed Modifications of Proteins

## 4.1. Background

As shown in chapter 3, HOBr produced by peroxidasin in the ECM undergoes reactions that are not limited to the cross-linking of collagen IV. My focus in this chapter is to investigate the reactions of HOBr produced by peroxidasin with intracellular and extracellular protein targets.

Hypobromous acid reacts with proteins, lipids, carbohydrates, DNA and antioxidants (**Figure 13**) (120). Cysteine, methionine, tryptophan and histidine are the most reactive amino acids with HOBr, followed by lysine and tyrosine. HOBr reacts with methionine to produce methionine sulfoxide and dehydromethionine (114). The reaction of HOBr with tyrosine leads to the formation of 3-bromoytrosine and 3, 5-dibromotyrosine, which are stable and measurable biomarkers of HOBr-mediated damage (89, 132). HOBr reacts with amine groups to form bromamines, which retain some of the oxidising capabilities of HOBr and can undergo further reactions with other biological targets, including GSH, methionine and ascorbate (5).

Hypohalous acid-mediated damage to ECM alters the structure and function of proteins, which can cause them to aggregate and fragment. It can change proteolytic susceptibility, modulate molecular recognition and compromise ECM integrity (12, 211, 212). The ECM is particularly susceptible to oxidative damage due to limited extracellular antioxidant defence and its low turnover rate, which leads to accumulation of damage with age and disease (12). Oxidative damage to the ECM is implicated in many pathologies, including the development of atherosclerosis. Myeloperoxidase and eosinophil peroxidase have been implicated as the major culprits in exacerbating oxidative damage in inflammation (12, 129, 132, 185). The

role of peroxidasin as a generator of HOBr in the ECM has only been recognised recently. The extent and the physiological consequences of peroxidasin-mediated oxidation of biomolecules are not yet known. Increasing evidence is implicating peroxidasin in many diseases, including cardiovascular diseases and some cancers (56, 68, 70).

My aim in this chapter was to investigate whether peroxidasin leads to oxidative modifications of proteins. In particular, I studied oxidation of methionine and bromination of tyrosine residues on proteins. I also investigated the effects of other peroxidase substrates, namely thiocyanate, urate and nitrite in modulating these oxidative modifications in order to understand the specificity of the cross-linking reaction versus other reactions. Stable isotope dilution LC/MS/MS methods to measure methionine sulfoxide and 3-bromotyrosine were developed for application to ECM as detailed in Chapter 2.

## 4.2. Detection of protein modifications

### *4.2.1. Methionine sulfoxide in proteins*

The sulfilimine link in the non-collagenous domain forms between $Met^{93}$ and $Hyl^{211}$ residues on two opposing protomers of collagen IV. Depending on the isomer of collagen IV, there is one or two other methionine residues adjacent to the site of the cross link (168). Here I investigated whether the activity of peroxidasin leads to the oxidation of other methionine residues in the cell culture system.

Measuring methionine and its oxidised metabolites in proteins is inherently difficult due to its high susceptibility to oxidation during sample preparation. I encountered many technical challenges in developing a method to hydrolyse proteins and separate analytes by LC/MS/MS. After several months of optimisation, I was successful in measuring methionine sulfoxide with minimal artificial oxidation. To validate the method, ECM isolated from peroxidasin knock-out cells was treated with reagent HOBr then digested and analysed for methionine oxidation. The chromatogram in **Figure 56**a shows peaks of methionine and methionine sulfoxide. When the areas of the peaks were related to standard calibration curves of methionine and methionine sulfoxide, the percentage of oxidised methionine residues increased from 7% in the untreated ECM to 35 % after treatment with HOBr.

I then measured methionine oxidation in intracellular extracts and ECM isolated from epithelial cells grown in the presence or absence of bromide or phloroglucinol, or ECM isolated from peroxidasin knock-out cells. Samples were digested with pronase then analysed by LC/MS/MS for methionine and methionine sulfoxide. Isotopically labelled internal standards were used for normalisation and monitoring artificial oxidation. Approximately 6 % of methionine residues on proteins in the intracellular extract were oxidised to methionine sulfoxide (**Figure 56**b). Oxidation level was higher in the extracellular matrix, averaging at ~10 % of methionine residues on proteins. There was no significant difference between the

levels of methionine sulfoxide with bromide or phloroglucinol treatment, or in peroxidasin knock-out cells.

a

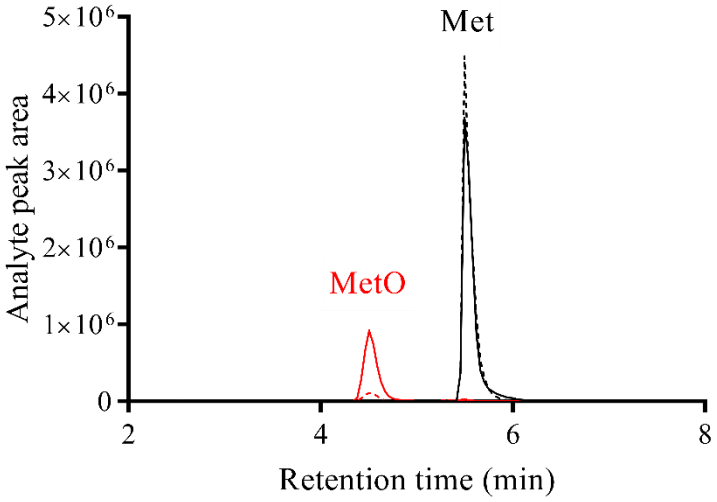


b

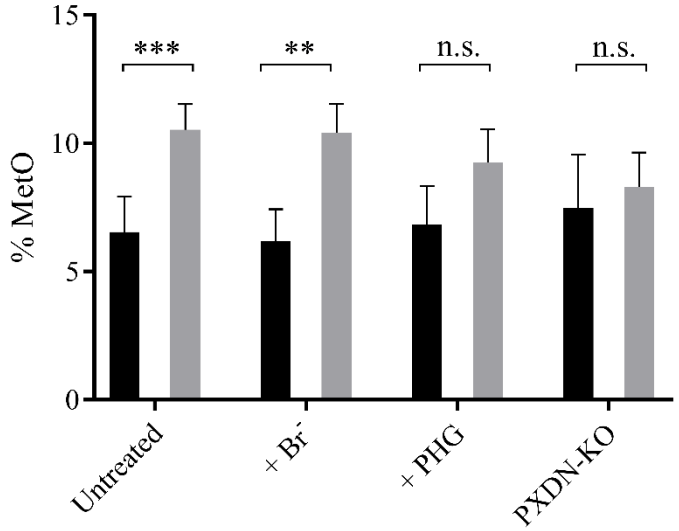


**Figure 56. Oxidation of methionine to methionine sulfoxide**. (a) Chromatogram obtained in multiple reaction monitoring mode for methionine (m/z 150 to 104, black lines) and methionine sulfoxide (m/z 166 to 74, red lines) in decellularised ECM isolated from peroxidasin knock-out epithelial cells untreated (dashed lines) or treated with 100 µM reagent HOBr (solid lines). (b) Levels of oxidised methionine residues on proteins in the intracellular extracts isolated by lysing cells in sodium deoxycholate as described in Section 2.2.2 (black bars), or in the isolated ECM (grey bars). Epithelial cells were grown either with culture medium only (untreated), or supplemented with 100 µM bromide or 50 µM phloroglucinol. Peroxidasin knock-out cells were grown in culture medium alone. Cells were lysed and the intracellular lysates were separated from the ECM. All samples were digested with pronase then analysed by LC/MS/MS as described in Chapter 2. Values are means of 4-5 independent experiments ± SEM. *** $p$=0.0003, ** $p$=0.008, n.s. not significant by two-tailed paired t test.

### *4.2.2. Peroxidasin leads to the formation of 3-bromotyrosine*

3-Bromotyrosine is one of the products of the reaction between tyrosine and HOBr. Here I investigated whether HOBr produced by peroxidasin reacts with tyrosine residues on proteins to form 3-bromotyrosine. Epithelial cells (WT or peroxidasin knock-out) were grown in culture for 6-8 days, with daily exchange of medium, in the presence or absence of the peroxidasin inhibitor phloroglucinol. Cells were lysed and ECM was isolated then hydrolysed to individual amino acids and analysed by LC/MS/MS (**Figure 57**). The same samples were also digested with collagenase and analysed by SDS-PAGE for dimer formation. The full method is described in Section 2.2.17.

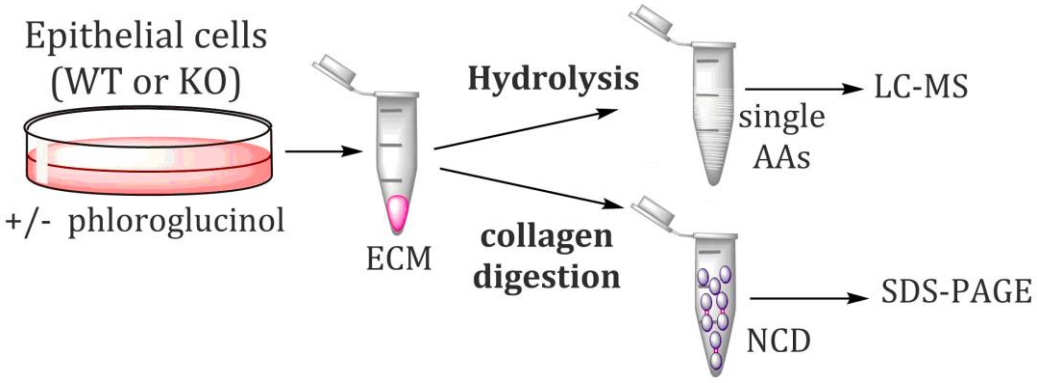


**Figure 57. Procedure schematic.** Epithelial cells (wild type or peroxidasin knock-out) were grown in the presence or absence of phloroglucinol. ECM was isolated and divided for processing and analysis by LC/MS/MS or SDS-PAGE.

3-Bromotyrosine was detected in the ECM isolated from WT epithelial cells. The chromatogram in **Figure 58** shows peaks for tyrosine and the two bromine isotopes of 3-bromotyrosine. Negligible amount of 3-bromotyrosine was detected in ECM isolated from peroxidasin knock-out cells.

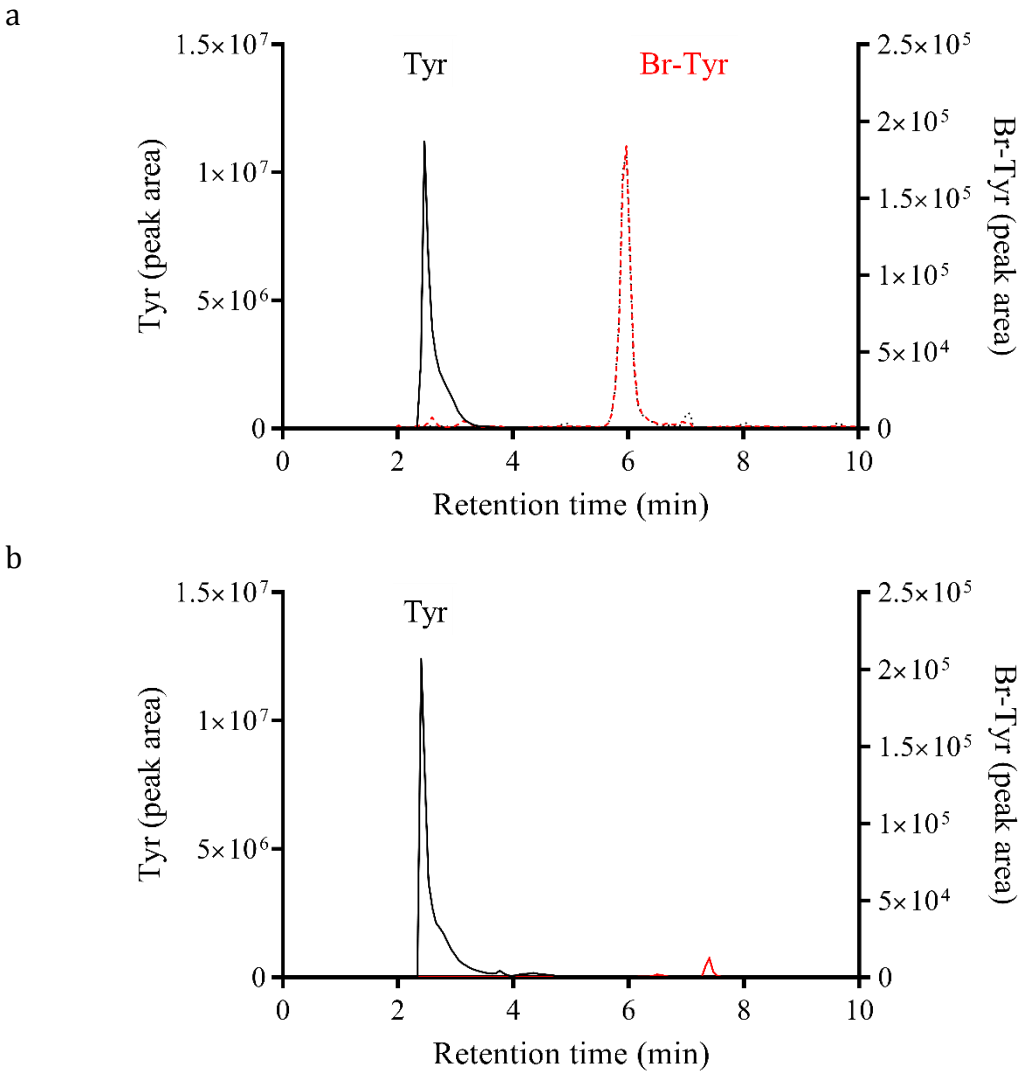


**Figure 58. Measuring 3- Br-Tyr in ECM**. Chromatograms obtained in multiple reaction monitoring mode for tyrosine (m/z 182 to 136, solid line) and two bromine isotopes of 3-bromotyrosine (BY1, m/z 260 to 214, red dashed line, and BY2, m/z 262 to 216, overlaid dotted black line) in ECM isolated from (a) wild type or (b) peroxidasin knock-out epithelial cells. ECM was hydrolysed with methane sulfonic acid then analysed by LC/MS/MS as described in Chapter 2. Chromatograms are representatives of 3-6 repeats.

The level of 3-bromotyrosine in ECM isolated from the WT cells was 1.13 mmol / mol tyrosine and decreased to 0.14 mmol / mol tyrosine when WT cells were grown in the presence of phloroglucinol. 3-Bromotyrosine level in ECM isolated from peroxidasin knock-out cells was 0.045 mmol / mol tyrosine (**Figure 59**a).

Collagen IV cross link was analysed in the same samples. As described earlier, isolated ECM samples were digested with collagenase, and NCD was analysed by SDS-PAGE, Coomassie staining and densitometry quantification. Dimer formation mirrored the trend of 3-bromotyrosine formation (**Figure 59**b). Consistent with the results shown in **Figure 42** in Chapter 3, when cells were grown in culture medium alone, dimer formation was approximately 75 % of the total NCD, which decreased to approximately 15 % when cells were grown in the presence of phloroglucinol or isolated from peroxidasin knock-out cells.

I also tested for the formation of 3-bromotyrosine in the decellularised ECM incubated with bromide and hydrogen peroxide. Within one hour, 3-bromotyrosine level increased from 0.14 to 0.93 mmol / mol tyrosine (**Figure 60**a). There was no significant increase in the level of 3-bromotyrosine when only $H_2O_2$ or $Br^-$ was added separately to ECM. A similar trend was observed in cross-linking collagen IV in the decellularised ECM (**Figure 60**b).

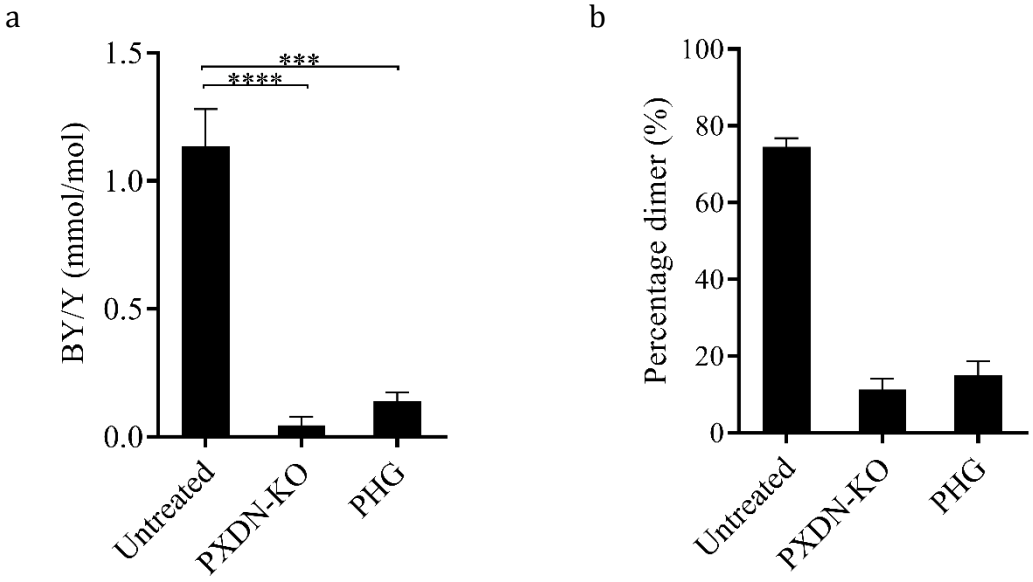


**Figure 59. Formation of 3- Br-Tyr and dimer in cell culture**. (a) 3-Bromotyrosine levels in ECM isolated from PFHR9 cells cultured for 6-8 days in the absence (Untreated) or presence of phloroglucinol (PHG), or isolated from peroxidasin knock-out PFHR9 cells (PXDN-KO). (b) Densitometry analysis of dimer formation in the NCD isolated from the same conditions described in (a). All ECM samples were hydrolysed with methane sulfonic acid then analysed by LC/MS/MS as described in Chapter 2. Values are mean of 3-8 independent experiments ± SEM. **** $p$ <0.0001, *** $p$<0.001 by multiple comparison ANOVA analysis. The NCD was isolated and analysed as described in **Figure 42**. Densitometry values represent mean of ≥3 independent experiments ±SEM.

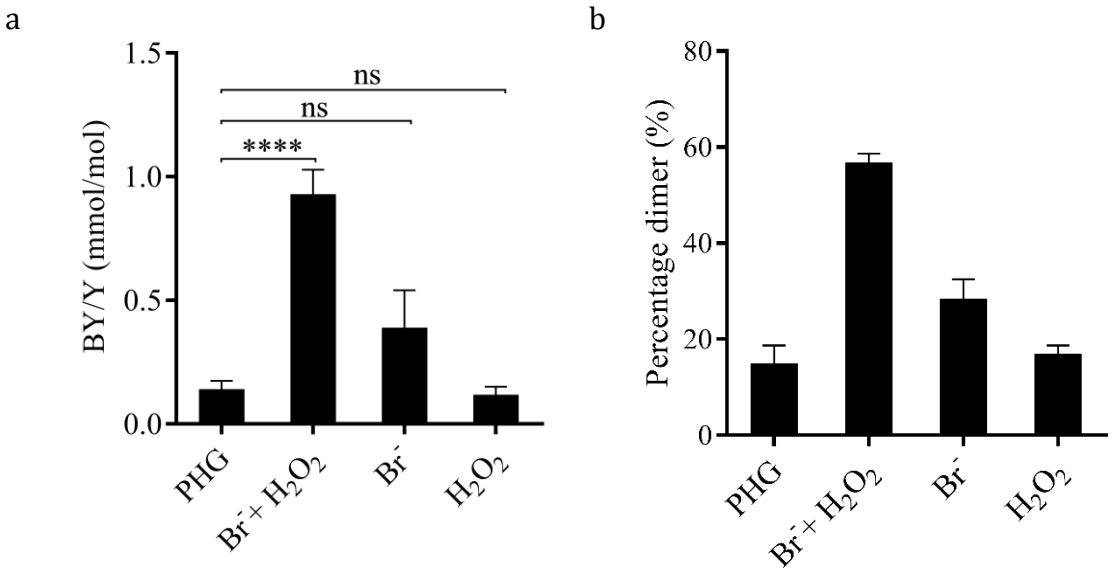


**Figure 60. Formation of 3- Br-Tyr and dimer in decellularised ECM**. (a) 3-Bromotyrosine levels in ECM from cells grown in the presence of PHG, then isolated and treated with 100 μM $Br^-$ and/or 50 μM $H_2O_2$ for 1 hour at 37°C. (b) Densitometry analysis of dimer formation in the NCD isolated from the same conditions described in (a). All ECM samples were hydrolysed with methane sulfonic acid then analysed by LC/MS/MS as described in Chapter 2. Values are mean of 3-8 independent experiments ± SEM. **** $p$ <0.0001, ns, not significant by multiple comparison ANOVA analysis. The NCD was isolated and analysed as described in **Figure 42**. Densitometry values represent mean of ≥3 independent experiments ±SEM.

### *4.2.3. The levels of 3-bromotyrosine increase with increasing bromide concentration*

To test the bromide requirement for the formation of 3-bromotyrosine during growth of cells, I cultured epithelial cells with daily supplementation of bromide. I then isolated the ECM and analysed it for 3-bromotyrosine as described earlier. It is worth noting that a trace amount of bromide is present in culture medium as contamination in sodium chloride, and was measured to be ~6 μM in 100 mM NaCl (35).

The levels of 3-bromotyrosine increased slightly with increasing bromide concentrations, and appeared to saturate above 50 μM bromide (**Figure 61a**). Analysis of dimer formation in the same samples showed that cross-linking was near maximal with the trace amounts of bromide present in the culture medium (**Figure 61**b).

The effect of bromide concentration was also tested in the decellularised ECM system. Uncross-linked ECM isolated from WT cells grown in the presence of phloroglucinol was decellularised and treated with hydrogen peroxide and increasing amounts of bromide for one hour. The levels of 3-bromotyrosine progressively increased from 0.1 to 1.4 mmol / mol tyrosine with 200 μM $Br^-$ (**Figure 62**a). Dimer formation in the same isolated ECM increased with increasing bromide levels and reached maximum at 100 μM $Br^-$ (**Figure 62**b).

The results shown in **Figure 59**b and **Figure 62**a combined demonstrate that peroxidasin can catalyse the formation of 3-bromotyrosine extracellularly in the decellularised ECM.

a

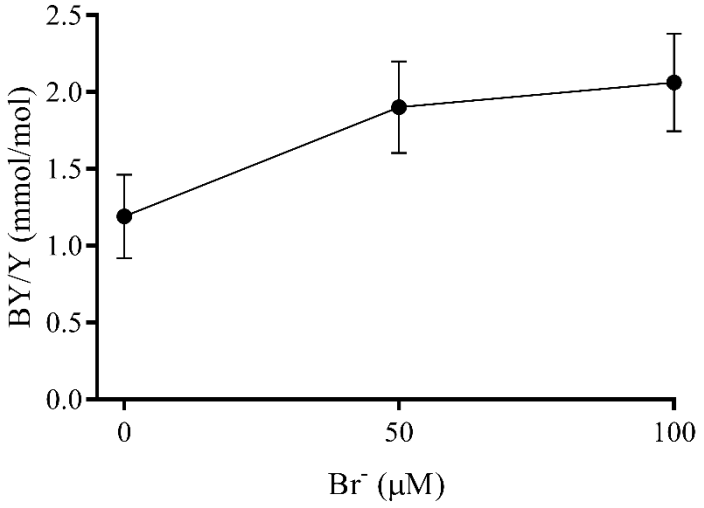


b

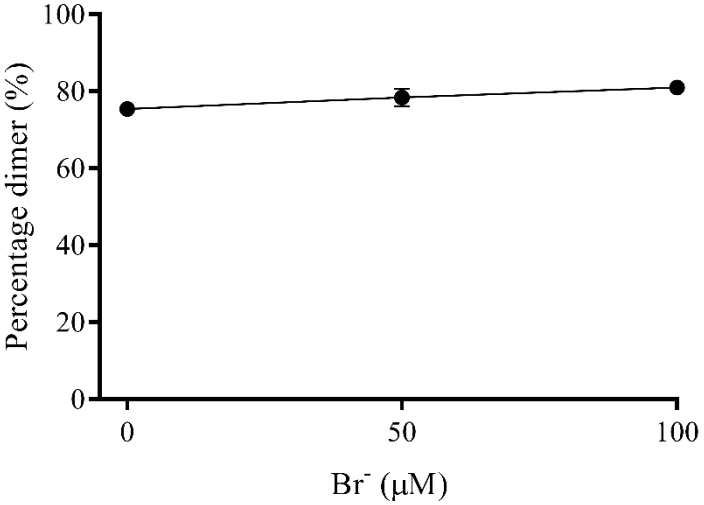


**Figure 61. The effect of bromide supplementation on the formation of 3-Br-Tyr and dimer in cell culture.** (a) 3-Bromotyrosine levels in ECM isolated from PFHR9 cells cultured for 6-8 days with daily supplementation of cell culture medium with the indicated concentrations of bromide. ECM samples were hydrolysed with methane sulfonic acid then analysed by LC/MS/MS as described in Chapter 2. Values are mean of 4 independent experiments ± SEM (b) Densitometry analysis of dimer formation in the same conditions described in (a). The NCD was isolated and analysed as described in **Figure 42**. Densitometry values represent mean of ≥3 independent experiments ± SEM.

a

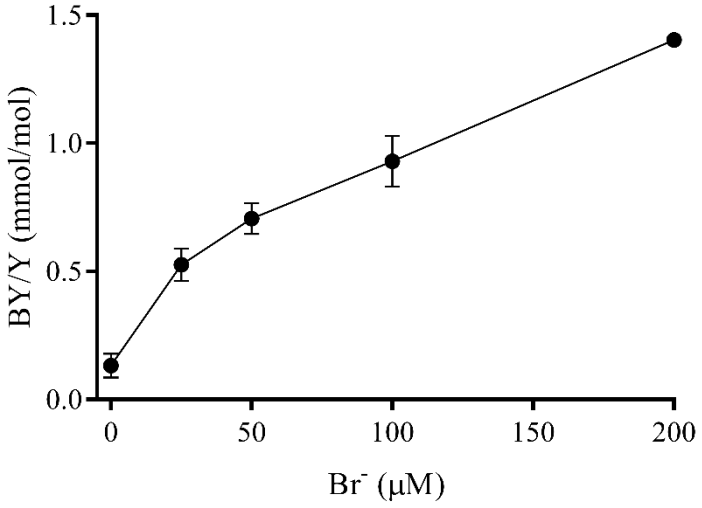


b

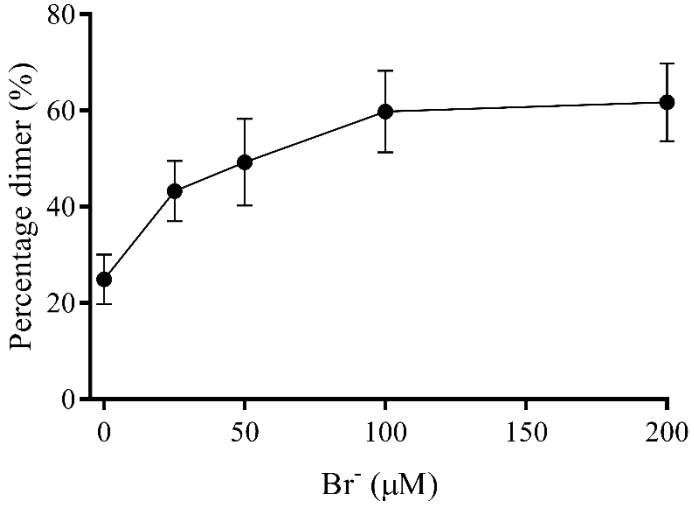


**Figure 62. The effect of bromide supplementation on the formation of 3- Br-Tyr and dimer in the isolated decellularised ECM.** (a) 3-Bromotyrosine levels in ECM from cells grown in the presence of PHG for 6-8 days, then isolated and treated with 50 μM $H_2O_2$ and the indicated concentrations of $Br^-$ for 1 hour at 37°C. ECM samples were hydrolysed with methane sulfonic acid then analysed by LC/MS/MS as described in Chapter 2. Values are mean of 3 independent experiments ± SEM (b) Densitometry analysis of dimer formation in the same conditions described in (a). The NCD was isolated and analysed as described in **Figure 42**. Densitometry values represent mean of 3 independent experiments ± SEM.

### *4.2.4. The levels of 3-bromotyrosine are higher in the ECM than in the intracellular extract*

It is unknown whether peroxidasin is active intracellularly or only upon secretion to the extracellular matrix. The formation of 3-bromotyrosine on proteins in the cell culture system can be used to track the activity of peroxidasin. To identify whether 3-bromotyrosine is present intracellularly as well as extracellularly, I separated extracts from epithelial cells into intracellular lysate and ECM, then digested the ECM with collagenase to separate the NCD. The different fractions were hydrolysed and analysed by LC/MS/MS.

The level of brominated tyrosine was very low in the intracellular fraction (0.13 mmol bromotyrosine/ mol tyrosine) (**Table 16**). It increased slightly with bromide supplementation and decreased with phloroglucinol treatment. The level of brominated tyrosine was significantly higher in the ECM than in the intracellular lysate (**Figure 63**). Furthermore, the NCD contained significantly higher levels of 3-bromotyrosine than the ECM.

**Table 16. The levels of 3-Br-Tyr in intracellular extract (ICE), extracellular matrix (ECM) and non-collagenous domain (NCD)**. Epithelial cells were grown in cell culture with medium alone (untreated), 100 μM bromide (+$Br^-$), 50 μM phloroglucinol (PHG). Peroxidasin knock-out cells (KO) were grown in cell culture medium alone. Values are means of 4-5 independent experiments ± SEM. ns, not significant, *, $p< 0.05$, ** $p<0.01$ by multiple comparison one-way ANOVA of each treatment to the untreated respective fraction.

| | **ICE** | **ECM** | **NCD** |
|---|---|---|---|
| Untreated | 0.13 ± 0.04 | 1.06 ±0.14 | 1.49 ±0.25 |
| + $Br^-$ | 0.18 ±0.06 $^{ns}$ | 1.43 ±0.22 $^{ns}$ | 1.93 ±0.41 $^{ns}$ |
| + PHG | 0.03 ±0.01 $^{ns}$ | 0.13 ±0.04 $^{**}$ | 0.29 ±0.08 $^{*}$ |
| KO | 0.07 ±0.03 $^{ns}$ | 0.05 ±0.02 $^{**}$ | 0.18 ±0.07 $^{*}$ |

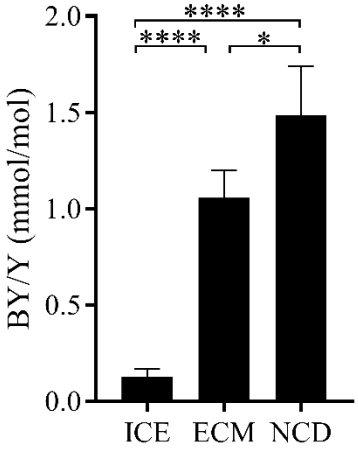


**Figure 63. Levels of 3- Br-Tyr in cellular lysate and ECM**. Levels of 3-bromotyrosine in intracellular extract (ICE), extracellular matrix (ECM) and non-collagenous domain (NCD) when cells were grown in cell culture for 6-8 days in culture medium alone. All samples were hydrolysed with methane sulfonic acid then analysed by LC/MS/MS as described in Chapter 2. Values are mean of 4-5 independent experiments ± SEM. * $p < 0.05$, **** $p < 0.0001$ by 2 way ANOVA analysis.

## 4.3. Modulation of protein modifications

### *4.3.1. Thiocyanate modulates the formation of 3-bromotyrosine*

As shown in Chapter 3, physiological levels of thiocyanate interfered with the cross-linking of collagen IV (Section 3.2.7). Here I investigated whether thiocyanate modulated the formation of 3-bromotyrosine as well. For comparison, I also looked at cross-linking of collagen IV within the same samples. The cross-linking results presented here are independent biological replicates of experiments reported earlier in chapter 3.

Here I used two experimental systems; a) adding thiocyanate to culture medium, and, b) adding thiocyanate to decellularised isolated ECM. In the cell culture system, increasing concentrations of thiocyanate (0 – 400 μM) were added to culture medium during cell growth, either alone or in combination with bromide (50 and 100 μM) to test for substrate competition.

The levels of 3-bromotyrosine in ECM isolated from epithelial cells decreased substantially with adding increasing concentrations of thiocyanate in the cell culture medium (**Figure 64**a). When no bromide was added, the maximum level of 3-bromotyrosine was 1.2 mmol / mol tyrosine, which decreased progressively with thiocyanate concentration to 0.3 mmol / mol tyrosine (inhibition by 78%). When 50 and 100 μM bromide were added to culture medium, the maximum levels of 3-bromotyrosine were 1.9 and 2.1 mmol / mol tyrosine, respectively, which decreased with adding thiocyanate to 0.36 and 0.41 mmol / mol tyrosine (inhibition by 81% for both bromide concentrations). The $IC_{50}$ increased with increasing bromide concentration (**Table 17**), which is indicative of competition between the two substrates.

Analysis of dimer formation in ECM isolated from the same conditions described above showed that thiocyanate in cell culture led to progressive but quite modest inhibition of the cross-linking of collagen IV (**Figure 64**b). Adding bromide also provided protection from the inhibitory effect of thiocyanate.

a

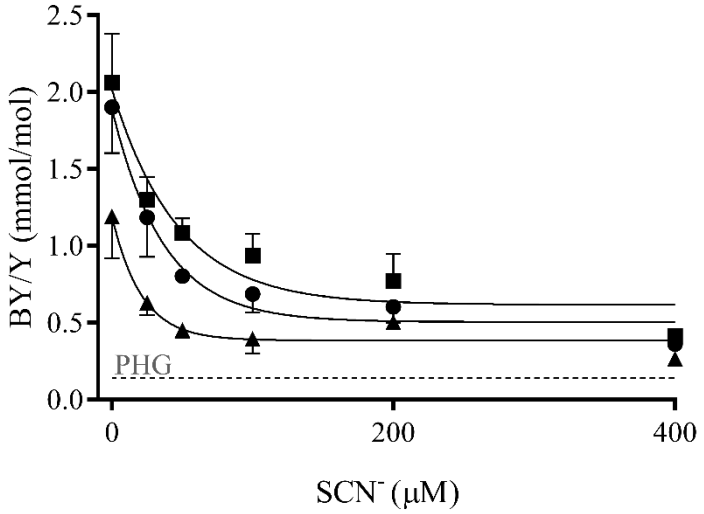


b

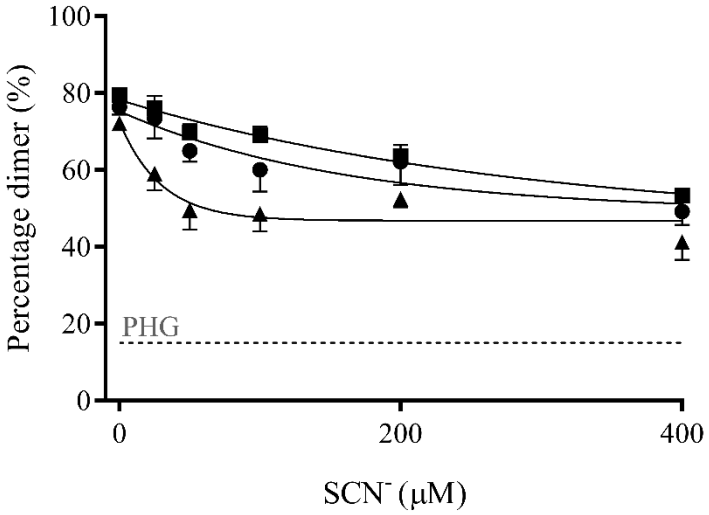


**Figure 64. The effects of thiocyanate on the formation of 3- Br-Tyr and dimer in cell culture.** (a) 3-Bromotyrosine levels in ECM isolated from PFHR9 cells cultured for 6-8 days with daily treatment of increasing concentrations of $SCN^-$ either without added $Br^-$ (▲), or with added 50 μM (●) or 100 μM $Br^-$ (■). Cells were lysed and ECM was isolated, hydrolysed with methane sulfonic acid then analysed by LC/MS/MS as described in Chapter 2. Values are mean of 3 independent experiments ± SEM. Curves are nonlinear fit. (b) Densitometry analysis of dimer formation in the same conditions described in (a). Densitometry values represent mean of 3 independent experiments ± SEM. The grey dashed lines in (a) and (b) represent inhibition by 50 μM phloroglucinol (PHG).

I also studied the effects of thiocyanate on 3-bromotyrosine and dimer formation in the decellularised isolated ECM system. Epithelial cells were grown in the presence of phloroglucinol for 6-8 days, the uncross-linked ECM was isolated and then treated with increasing concentrations of thiocyanate (0-400 μM), bromide (50 or 100 μM) and 50 μM hydrogen peroxide for one hour.

Similar to the results in the cell culture system, bromination of tyrosine residues in decellularised isolated ECM decreased with increasing concentration of thiocyanate (**Figure 65**a). Thiocyanate achieved near complete inhibition of 3-bromotyrosine formation in the isolated ECM. Increasing bromide concentration also led to an increase in $IC_{50}$ (**Table 17**). Note that in the cell culture system peroxidasin can be active without adding bromide to the growth medium, as it contains residual amounts of bromide in sodium chloride. In contrast, adding bromide to the decellularised system was necessary for the activity of peroxidasin. Therefore I only compared two concentrations of bromide (50 and 100 μM).

The maximal levels of 3-bromotyrosine and dimer formation were overall higher in the cell culture system than in the decellularised ECM system (**Table 17**, **Figure 64**a and **Figure 65**a). Thiocyanate was more effective in inhibiting 3-bromotyrosine formation than dimer formation both in the cell culture system and the decellularised system.

a

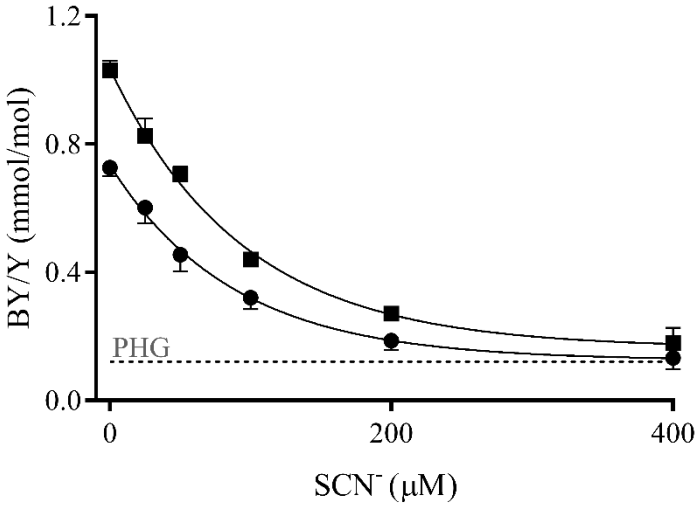


b

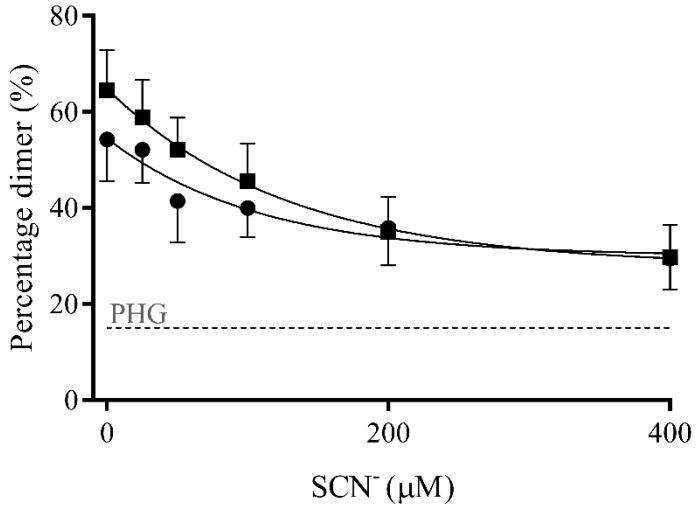


**Figure 65. The effect of thiocyanate on the formation of 3- Br-Tyr and dimer in decellularised ECM**. (a) 3-Bromotyrosine levels in ECM isolated from PFHR9 cells cultured for 6-8 days with daily treatment of 50 μM PHG. Isolated ECM was treated with 50 μM $H_2O_2$, $Br^-$ 50 μM (●) or 100 μM (■), and the indicated concentrations of $SCN^-$ for 1 hour at 37°C. ECM samples were hydrolysed with methane sulfonic acid then analysed by LC/MS/MS as described in Chapter 2. Values are mean of 3 independent experiments ± SEM. Curves are nonlinear fit. (b) Densitometry analysis of dimer formation in the same conditions described in (a). Densitometry values represent mean of 3 independent experiments ± SEM. The grey dashed lines in (a) and (b) represent inhibition by 50 μM phloroglucinol (PHG).

**Table 17. The formation of 3-Br-Tyr and its inhibition by thiocyanate.** Maximum (Max BY) and minimum (Min BY) levels of 3-bromotyrosine when treated with 400 μM thiocyanate. Values are average of 3 experiments ± SEM. $IC_{50}$ calculated by fitting exponential decay curves to data in Figure 64a and Figure 65a. *, *p* value < 0.05, ** < 0.01, *** < 0.001, comparing Min BY and Max BY of each column by two-tailed unpaired t test.

| | | $Br^-$ (μM) | | |
|---|---|---|---|---|
| | | Not added | 50 | 100 |
| **Cell culture system** | Max BY (mmol/ mol Y) | 1.2±0.27 | 1.9±0.3 | 2.1±0.32 |
| | Min BY (mmol/ mol Y) | 0.27±0.03* | 0.36±0.04** | 0.4±0.04** |
| | $IC_{50}$ (μM) | **14** | **25** | **32** |
| **Decellularised ECM system** | Max BY (mmol/ mol Y) | | 0.7±.03 | 1.0±0.03 |
| | Min BY (mmol/ mol Y) | | 0.13±0.04*** | 0.18±0.05*** |
| | $IC_{50}$ (μM) | | **61** | **65** |

### *4.3.2. Urate modulates the formation of 3-bromotyrosine*

As seen in Chapter 3, physiological levels of urate inhibited collagen IV cross-linking in the isolated decellularised ECM system. Here I investigated whether urate modulates the formation of 3-bromotyrosine in the cell culture system. The aim was to compare the ability of urate to compete as a substrate for peroxidasin and a scavenger of HOBr.

Increasing concentrations of urate (0 – 400 μM) were added to the cell culture medium alone or in combination with 100 μM bromide. ECM was then isolated and analysed for 3-bromotyrosine and dimer formation.

The levels of 3-bromotyrosine in the isolated ECM decreased slightly with increasing urate concentrations in culture medium (**Figure 66**a). When no bromide was added to the culture medium, the maximum level of 3-bromotyrosine was 1.2 mmol / mol tyrosine, which decreased progressively to 0.7 mmol / mol tyrosine (inhibition by 42 %). When 100 μM bromide was added to culture medium, the maximum level of 3-bromotyrosine was 1.7 mmol / mol tyrosine, which decreased to 1.3 mmol / mol tyrosine at 400 μM urate (inhibition by 24 %). The effect of adding urate to culture medium on dimer formation was minimal (**Figure 66**b).

Although fitting exponential decay curves to the data gives maximum inhibition and half inhibitory concentration ($IC_{50}$), these values are approximation as inhibition observed here is modest with large experimental variation. Adding bromide provided protection against inhibition of 3-bromotyrosine formation and increased the $IC_{50}$ from 77 to 195 μM urate (**Table 18**). Similar effect was observed on dimer formation (**Figure 66**b).

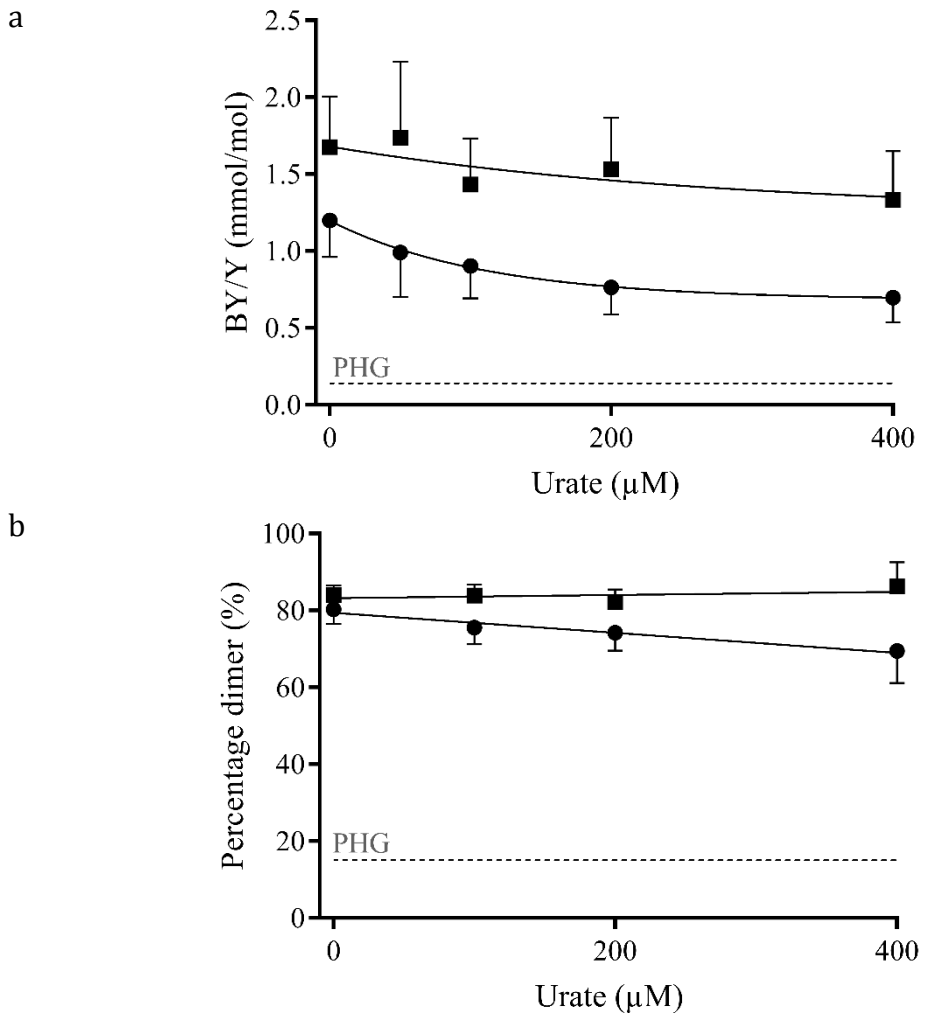


**Figure 66. The effect of urate on the formation of 3-Br-Tyr and dimer in cell culture**. (a) 3-Bromotyrosine levels in ECM isolated from PFHR9 cells cultured for 6-8 days with daily treatment of the indicated concentrations of urate to cell culture medium, either without (●), or with added 100 μM $Br^-$ (■). ECM samples were hydrolysed with methane sulfonic acid then analysed by LC/MS/MS as described in Chapter 2. Values are mean of 5 independent experiments ± SEM (b) Densitometry analysis of dimer formation in the same conditions described in (a). The NCD was isolated and analysed as described in **Figure 42**. Densitometry values represent mean of 6 independent experiments ± SEM. The grey dashed lines in (a) and (b) represent inhibition by 50 μM phloroglucinol (PHG).

**Table 18. The formation of 3-Br-Tyr and its inhibition by urate**. Maximum (Max BY) and minimum (Min BY) levels of 3-bromotyrosine when treated with 400 μM urate. Values are average of 5 experiments ± SEM. $IC_{50}$ calculated by fitting exponential decay curves to data in **Figure 66**a. ns, not significant difference between Min BY and Max BY by two-tailed unpaired t test.

| | Medium alone | + 100 μM $Br^-$ |
|---|---|---|
| Max BY (mmol/ mol Y) | 1.2±0.2 | 1.7±0.3 |
| Min BY (mmol/ mol Y) | 0.68±0.2 $^{ns}$ | 1.3±0.3 $^{ns}$ |
| $IC_{50}$ (μM) | **77** | **195** |

### *4.3.3. Nitrite modulates the formation of 3-bromotyrosine*

Nitrite is a peroxidase substrate and was shown recently to be a one-electron donor for hsPxd-con4, a truncated recombinant form of human peroxidasin (47). Therefore, I studied whether nitrite competes with bromide for peroxidasin in the ECM by looking at its effects on 3-bromotyrosine and dimer formation. Epithelial cells were cultured in media supplemented with sodium nitrite for 6 days. Cells were lysed and the ECM was isolated, washed thoroughly to remove any residual nitrite, hydrolysed and analysed by LC/MS/MS for 3-bromotyrosine and dimer formation.

Nitrite inhibited the formation of 3-bromotyrosine. The levels of 3-bromotyrosine decreased progressively with increasing concentrations of nitrite (42 % inhibition at 200 μM nitrite) (**Figure 67**a). In contrast, the effect on dimer formation was minimal (13 % reduction at 200 μM nitrite) (**Figure 67**b). These results indicate that nitrite can modulate the reactions of peroxidasin and HOBr in the ECM.

a

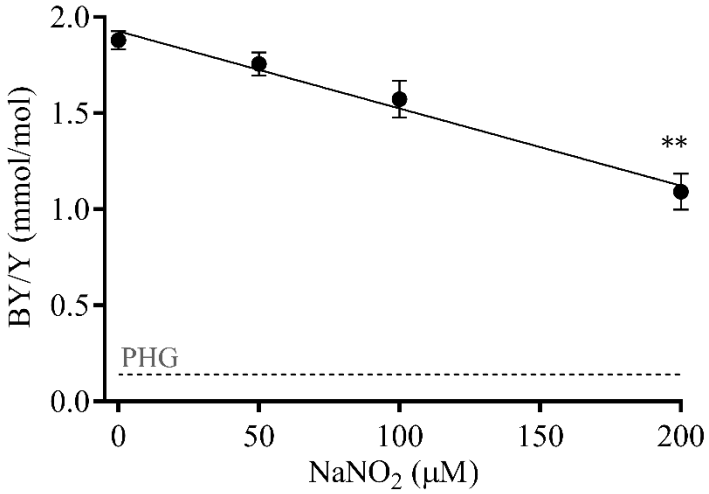


b

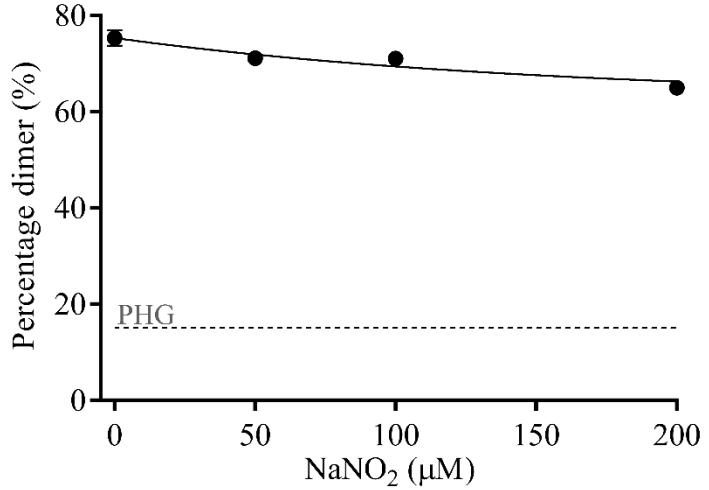


**Figure 67. The effects of nitrite on the formation of 3- Br-Tyr and dimer in cell culture**. (a) 3-Bromotyrosine levels in ECM isolated from PFHR9 cells cultured for 6 days with daily treatment of the indicated concentrations of sodium nitrite. ECM samples were hydrolysed with methane sulfonic acid then analysed by LC/MS/MS as described in Chapter 2. Values are mean of 3 independent experiments ± SEM. ** $p$= 0.0017 (Unpaired t test) (b) Densitometry analysis of dimer formation in the same conditions described in (a). The NCD was isolated and analysed as described in **Figure 42**. Densitometry values represent mean of 2 independent experiments. Range fell within symbol size. The grey dashed lines in (a) and (b) represent inhibition by 50 μM phloroglucinol (PHG).

## 4.4. Discussion

### *4.4.1. Protein modifications*

The main aim of this chapter was to investigate whether the activity of peroxidasin causes oxidative modifications of proteins in the ECM. Oxidation of methionine residues in proteins in the cell culture system did not show a response to modulation of peroxidasin activity (stimulation with bromide or inhibition with phloroglucinol). Methionine sulfoxide can be reduced to methionine by the methionine sulfoxide reductase system (116). Any reversible increase in the levels of methionine sulfoxide might be transient and not measured in this assay. Therefore, the contribution of HOBr produced by peroxidasin to the oxidation of methionine residues on proteins could not be ruled out. The two methionine residues adjacent to the site of the sulfilimine cross link were reported to be oxidised (33). It was not clear whether it was the result of an enzymatic or artefactual oxidation.

The analysis revealed that the levels of methionine sulfoxide were higher in the ECM than in the intracellular extracts. This might not be surprising, given that antioxidant defence systems are lower extracellularly than intracellularly (121), which might lead to accumulation of oxidised methionine residues in the ECM.

The detection of 3-bromotyrosine is an exciting novel finding. To the best of my knowledge, this is the first evidence that peroxidasin activity leads to the formation of 3-bromotyrosine on proteins during cell growth in culture. Inhibition or knocking down of peroxidasin resulted in significantly lower levels of 3-bromotyrosine.

The levels of 3-bromotyrosine increased with increasing bromide concentrations in cell culture and decellularised ECM. In comparison, maximal cross-linking of collagen IV was achieved with the trace amounts of bromide present in the culture medium and showed negligible increase with increasing bromide concentrations. This observation suggests that the reactions of HOBr produced by peroxidasin are specific for the cross-linking of collagen IV at low concentrations of bromide. Higher

concentrations (still within physiological range) lead to increased production of HOBr, which might result in increased reactions with other targets.

3-Bromotyrosine also formed in the isolated decellularised ECM when bromide and hydrogen peroxide were present, which confirms that peroxidasin is active and produces HOBr in the ECM. Higher concentrations of bromide were required in the isolated decellularised ECM to achieve equivalent levels of 3-bromotyrosine to that in cell culture. Similar results were observed in the effect of bromide concentrations on dimer formation. This might be due to different time scales of incubation; one hour in the isolated decellularised ECM versus 6-8 days in cell culture. Longer time of incubation might lead to accumulation of 3-bromotyrosine and dimer. Another possibility is that intact ECM may bind or concentrate bromide to a higher effective concentration than that of the medium. This compartmentalisation might be disrupted during the process of decellularisation and isolation of the ECM.

Although low levels of 3-bromotyrosine were detected in the intracellular extract, the levels were significantly higher in the ECM. This is not surprising given that peroxidasin is secreted to the ECM where it is presumed to catalyse the cross-linking of collagen IV. It is not certain whether the 3-bromotyrosine detected in the intracellular fraction is due to intracellular peroxidasin activity or contamination from solubilised ECM in the isolation process. The presence of peroxidasin was detected in the endoplasmic reticulum (22, 24). Cleavage of peroxidasin by proprotein convertase was shown to enhance its enzymatic activity, and is thought to occur extracellularly (27). This might be a regulatory mechanism to optimise cross-linking of collagen IV by peroxidasin extracellularly, while minimising oxidative damage intracellularly. Considering these observations, it is likely that intracellular 3-bromotyrosine is a residual contamination during the process of separation of intracellular lysate from the ECM.

The levels of 3-bromotyrosine were significantly higher in the isolated NCD than in the ECM. The NCD accounts for approximately 14 % of collagen IV (~230 amino acids of the total ~1600-1700 amino acids in collagen IV, with slight variation in

different isoforms). Collagen IV accounts for 50 % of the structural proteins in the basement membrane (**Figure 17** in Chapter 1), meaning that the NCD is approximately 7% of the total structural ECM proteins. Therefore, it is highly likely that bromination of tyrosine in the ECM is not restricted to the NCD.

The detection of 3-bromotyrosine provides evidence that HOBr produced by peroxidasin reacts with tyrosine residues on proteins. It suggests that the reactions of HOBr produced by peroxidasin are not limited to the sulfilimine link formation in collagen IV. It is noteworthy that the rate constants of the reactions of HOBr with some other amino acids are higher than with tyrosine (**Figure 13** in Chapter 1). However, 3-bromotyrosine is used as a relatively stable biomarker for the production of HOBr and an indication that other modifications of amino acids are likely to occur. It is possible that HOBr also reacts with other biomolecules, such as lipids and carbohydrate moieties in the ECM (94, 95).

3-Bromotyrosine is a biomarker of oxidative damage of tissues in various pathological conditions including asthma, sinonasal inflammation, cystic fibrosis, eosinophilic esophagitis and diabetes (132, 134, 213-216). It is elevated in bronchoalveolar lavage and urine obtained from asthmatic patients (139, 217) and used as a marker to assess their clinical responsiveness to pharmaceutical therapy (218). Brominated tyrosine can be metabolised by deamination and decarboxylation to form 4-hydroxyphenylacetic acid, and this urinary metabolite is also elevated in inflammation (219). Eosinophil peroxidase and myeloperoxidase secreted by activated phagocytes oxidise bromide and release potent brominating agents that cause tissue damage and oxidative modifications of proteins. While EPO and MPO are the main culprits known to date, the evidence I presented here demonstrates that peroxidasin also contributes to the formation of 3-bromotyrosine. It also opens the door to investigating the role of peroxidasin in catalysing oxidative modifications in inflammation and other pathological conditions.

### *4.4.2. Modulation of protein modifications*

Thiocyanate, urate and nitrite all inhibited the formation of 3-bromotyrosine to varying extents. The modulatory effect of thiocyanate on 3-bromotyrosine and dimer formation might be due to acting as a competitive substrate. This is supported by the kinetic data published recently which showed that thiocyanate reduces compound 1 of hsPxd-con4 faster than bromide (rate constants $1.83\times10^{7}$ and $5.6\times10^{6}$ $M^{-1}$ $s^{-1}$, respectively) (13). Thiocyanate is also a scavenger of HOBr. The reaction of HOBr with thiocyanate is much faster than that with tyrosine ($2.3\times10^{9}$ and $2.6\times10^{5}$ $M^{-1}$ $s^{-1}$, respectively) (14, 101), which can account for the inhibition of 3-bromotyrosine formation by thiocyanate. Relatively high concentrations of thiocyanate (400 μM) were required to achieve near maximal inhibition of 3-bromotyrosine formation (inhibition by 50 μM phloroglucinol is set as maximal inhibition). It is puzzling that thiocyanate does not lead to a complete loss of 3-bromotyrosine and dimer formation, given that it is the most efficient scavenger of HOBr reported to date. Based on the results presented in Chapter 3 and Chapter 4, it can be speculated that small amounts of targeted HOBr is sufficient for maximal collagen IV cross-linking. Inhibition of this targeted reaction remained moderate even at 400 μM thiocyanate. On the other hand, formation of 3-bromotyrosine requires higher concentrations of free HOBr, which can be scavenged by thiocyanate. These two models could explain the difference between the relatively efficient inhibition of 3-bromotyrosine formation by thiocyanate compared to its moderate inhibition of collagen IV cross-linking.

Adding a higher concentration of bromide protected against inhibition of 3-bromotyrosine and dimer formation, despite thiocyanate concentration being still higher than that of bromide (**Table 17**). These observations point to a competition between the two substrates. They also suggest a special affinity of peroxidasin for bromide and that selectivity is not determined solely by rate constants. The location and association of peroxidasin with the target protein might play a role in providing higher selectivity for bromide.

Comparing the effects of thiocyanate in two experimental systems revealed that inhibition of tyrosine bromination by thiocyanate was more effective (lower $IC_{50}$) in the cell culture system than in the decellularised isolated ECM (**Table 17**). This might be due to higher starting levels of 3-bromotyrosine in the cell culture system, which can be due to the difference in times of incubation, as explained earlier. It could also result from higher effective concentrations of bromide in the extracellular compartment in the cell culture system compared to the homogenous reaction mixture in the decellularised ECM system.

Interestingly, adding bromide to the decellularised ECM system was necessary for peroxidasin to catalyse collagen IV cross-linking or 3-bromotyrosine formation, despite the reaction being carried out in phosphate buffer saline which contains 140 mM sodium chloride. In contrast, adding bromide in the cell culture system was not necessary, as trace amount of bromide present as contamination in 110 mM sodium chloride in culture medium was sufficient for maximal cross-linking of collagen IV and formation of 3-bromotyrosine, as outlined in Sections 4.2.3 and 4.3.1. This again points to the possibility that the concentration of bromide might be higher in an intact ECM compartment in the cell culture system than in a homogenous reaction mixture in the decellularised ECM.

Urate showed poor inhibition of 3-bromotyrosine, especially when the culture medium was supplemented with 100 μM bromide. Urate acts as a one-electron donor for peroxidases, and was shown recently to be a substrate for hsPxd-con4 (47). The rate constant for the reduction of compound I of hsPxd-con4 by urate is lower than that for bromide ($7.2 \times 10^4$ and $5.6 \times 10^6$ $M^{-1}$ $s^{-1}$, respectively). Urate slows the reduction of compound II to the native enzyme, leading to accumulation of the compound II, which does not enter the halogenation cycle. This could account for the modest inhibition observed here.

Nitrite moderately inhibited the formation of 3-bromotyrosine by peroxidasin, and had a negligible effect on the cross-linking of collagen IV. Nitrite was recently shown to act as a one-electron donor for compound I of hsPxd-con4 (rate $1.9 \times 10^5$ $M^{-1}s^{-1}$)

(47). Nitrite also reacts with HOBr (rate constant $1.4 \times 10^4$ $M^{-1}$ $s^{-1}$) (220, 221) and that might contribute to its moderate inhibition of 3-bromotyrosine formation observed here.

Notably, thiocyanate, urate and nitrite all showed greater inhibitory effects on the generation of 3-bromotyrosine than on the formation of the sulfilimine link in collagen IV. This disparity indicates selectivity for the targeted reaction with collagen IV over the collateral reaction with tyrosine residues on proteins. It is also possible that the two reactions occur through different mechanisms; an enzyme-bound intermediate and freely-diffused HOBr. Kinetic studies using the native full length peroxidasin should reveal peroxidasin substrate preference and competition, and explain this observation. Access to a pure active native peroxidasin is currently limited due to technical challenges in expressing and purifying it. Peroxidasin is a large multi-domain highly-glycosylated homotrimer that requires heme insertion, modification and covalent linkage (26).

In summary, I presented here the first direct evidence that 3-bromotyrosine is a product of peroxidasin activity. With this finding, peroxidasin joins eosinophil peroxidase and myeloperoxidase as contributors to the formation of 3-bromotyrosine, a biomarker for oxidative modifications in a number of pathological situations. This is in line with a hypothesised role of peroxidasin in protein halogenation in experimental diabetes (187). There is a plethora of evidence that hypohalous acid-derived damage to ECM proteins alters the function of proteins and promotes diseases. Further investigation is needed to understand the contribution of peroxidasin, as a resident ECM protein, to the formation of specific biomarkers of oxidative damage in pathological situations.

# Chapter 5 Method Optimisation for the Analysis of 3-Nitrotyrosine

## 5.1 Background

Nitrite is a substrate for peroxidasin (47) and can modulate its bromination of tyrosine, as shown earlier in Chapter 4. With this observation, I asked the question whether peroxidasin activity leads to nitration of tyrosine residues on proteins. Peroxidases react with nitrite to produce nitrogen dioxide radicals ($^{\bullet}NO_2$). Peroxidases also react with tyrosine residues to produce tyrosyl radicals, which react with nitrogen dioxide radical to form 3-nitrotyrosine (**Figure 68**). The physiological levels of nitrotyrosine are generally very low, due to competing alternative reactions for nitrogen dioxide and tyrosyl radicals (142, 222). Nonetheless, nitration of tyrosine residues can profoundly alter protein structure and function, such as decrease in the pKa of the hydroxyl group on the phenol ring. The bulky nitro group can also add steric hindrance, lead to conformation changes and interfere with tyrosine phosphorylation (127). It is also an indicator of other potentially deleterious reactions of nitrogen dioxide. Nitrotyrosine has been detected in a variety of tissues and fluids including urine and plasma (122). It is used as a biomarker for oxidation, and is elevated in atherosclerotic lesions (126, 223). The baseline molar ratio of nitrotyrosine to tyrosine is estimated to be $1:10^6$ in proteins, although discrepancies in reported qualitative data on nitrotyrosine span several orders of magnitude (224).

Qualitative and quantitative analysis of nitrotyrosine is technically challenging. One of the key issues is artefactual nitration, due to ubiquity of nitrating agents and reactivity of the phenol group on tyrosine (224). Acid hydrolysis of proteins at high temperature leads to increased artefactual formation of nitrotyrosine.

My aim in this chapter was to develop a method to measure 3-nitrotyrosine and minimise these technical issues in order to investigate whether the activity of peroxidasin in the ECM leads to the generation of 3-nitrotyrosine on proteins.

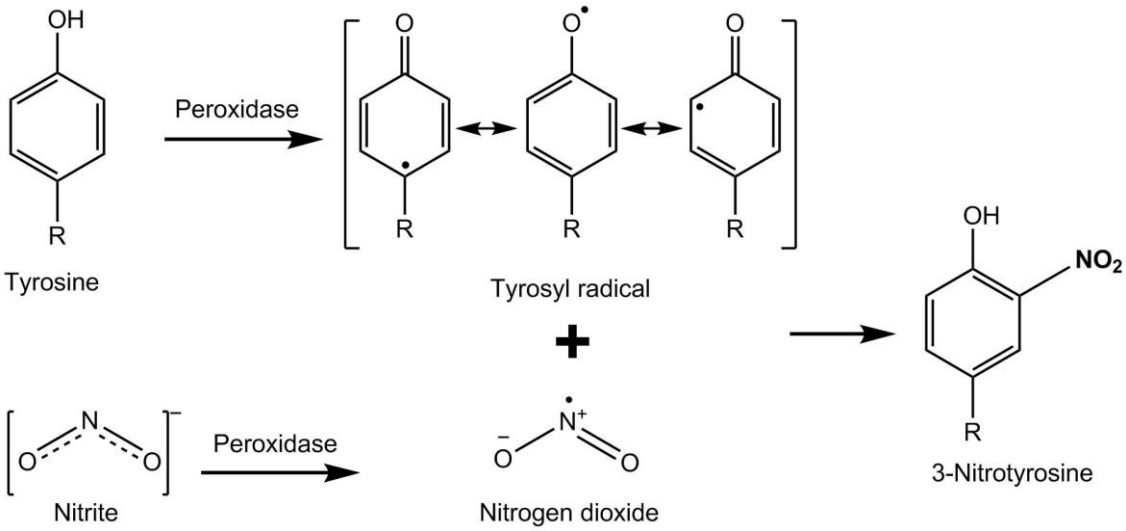


**Figure 68. Mechanism for the formation of 3-$NO_2$Tyr**. Peroxidases oxidise tyrosine to form tyrosyl radical and nitrite to form nitrogen dioxide. These two radicals react to form 3-nitrotryosine.

## 5.2 Results

### *5.2.1 Liquid chromatography and mass spectrometry*

I optimised the LC/MS/MS method using standards of tyrosine and 3-nitrotyrosine, and isotopically labelled internal standards ($^{13}C_6$ Tyr and $^{13}C_9$ 3-$NO_2$-Tyr) for normalisation and monitoring artefactual nitration (198). The chromatograms in **Figure 69** show the peaks for unlabelled and labelled tyrosine eluting around 2.5 ± 0.2 minutes, and unlabelled and labelled 3-nitrotyrosine eluting around 6.6 ± 0.2 minutes. The sensitivity of detection of 3-nitrotyrosine in the mass spectrometer is higher than that for tyrosine. This is an advantage as it is to be expected that 3-nitrotyrosine in the sample is only a small fraction of tyrosine. Therefore, the amounts used in the standard calibration curve are in in the nanomole range for tyrosine and picomole range for 3-nitrotyrosine. Artefactual nitration was monitored by measuring nitration of $^{13}C_6$ tyrosine to $^{13}C_6$ 3-nitrotyrosine.

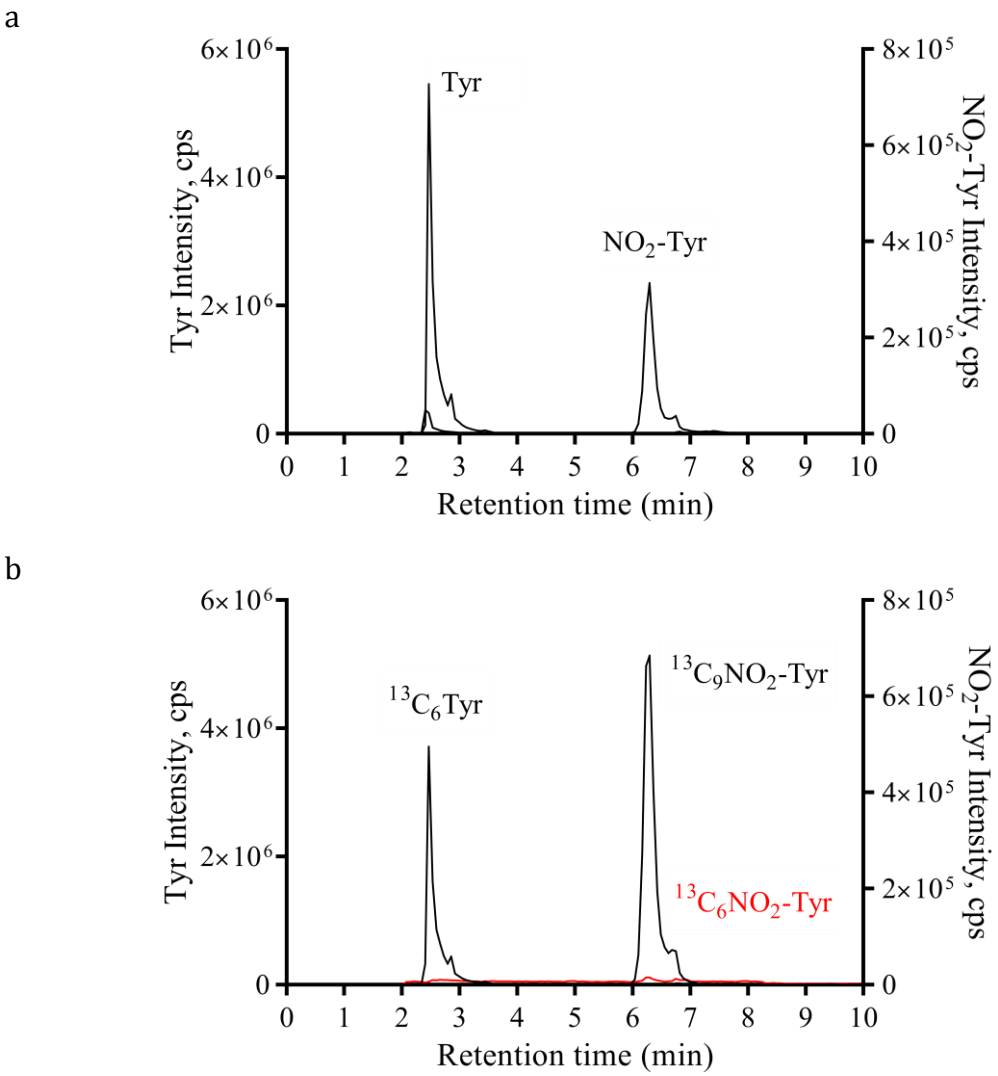


**Figure 69. Separation and detection of tyrosine and 3- $NO_2$Tyr by LC/MS/MS**. Chromatogram obtained in multiple reaction monitoring mode for (a) tyrosine (m/z 182 to 136, eluting at 2.5 minutes) and 3-nitrotyrosine (m/z 227 to 181, eluting at 6.6 minutes) and (b) isotopically-labeleled $^{13}C_6$ tyrosine (m/z 188 to 171), $^{13}C_9$ 3-nitrotyrosine (m/z 236 to 189) both eluting at the same times as their respective unlabelled counterparts in (a). The artefactual nitration was checked by monitoring conversion of $^{13}C_6$ tyrosine to $^{13}C_6$ 3-nitrotyrosine (m/z 233 to 216, red line).

### *5.2.2 Sample preparation for protein analysis*

After establishing the LC/MS/MS method, I tested the protein hydrolysis method on the isolated ECM. Briefly, ECM samples were hydrolysed with hydrochloric acid (HCl) supplemented with 1% phenol, and analytes were extracted by solid phase extraction (**Figure 70**). The full method is described in Chapter 2.

Analysis of samples revealed abnormally high levels of artefactual nitration (**Figure 71**a). This was only observed in samples but not in standards that were injected directly without prior processing, which indicated that artefactual nitration was occurring during sample preparation. Furthermore, I observed artefactual nitration when I mixed internal standards with HCl without heating. Testing different hypotheses to eliminate the source of nitration revealed that double deionized tap water contained a nitrating agent that reacted in HCl. I overcame this problem by using HPLC-grade bottled water, which minised artefactual nitration to the baseline observed in standards injected directly (**Figure 71**b).

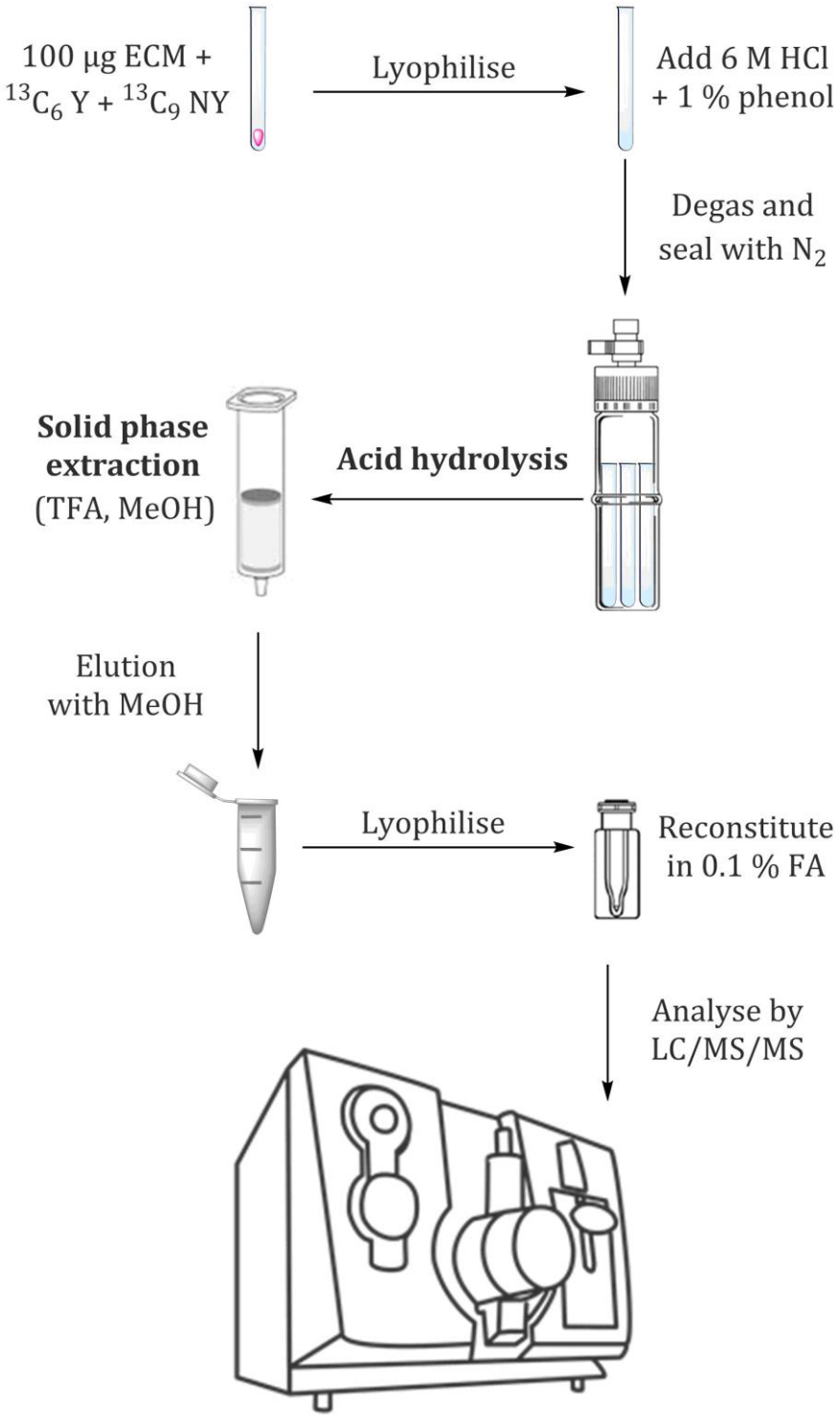


**Figure 70. Schematic diagram of sample preparation for analysis by LC/MS/MS**. Samples were mixed with internal standards, hydrolysed with HCl for 18 hours at 110°C then extracted by solid phase extraction using trifluoroacetic acid (TFA) and methanol (MeOH). The eluate was dried in the Speedvac then reconstituted in HPLC-grade $H_2O$ with 0.1 % formic acid (FA) and analysed by LC/MS/MS.

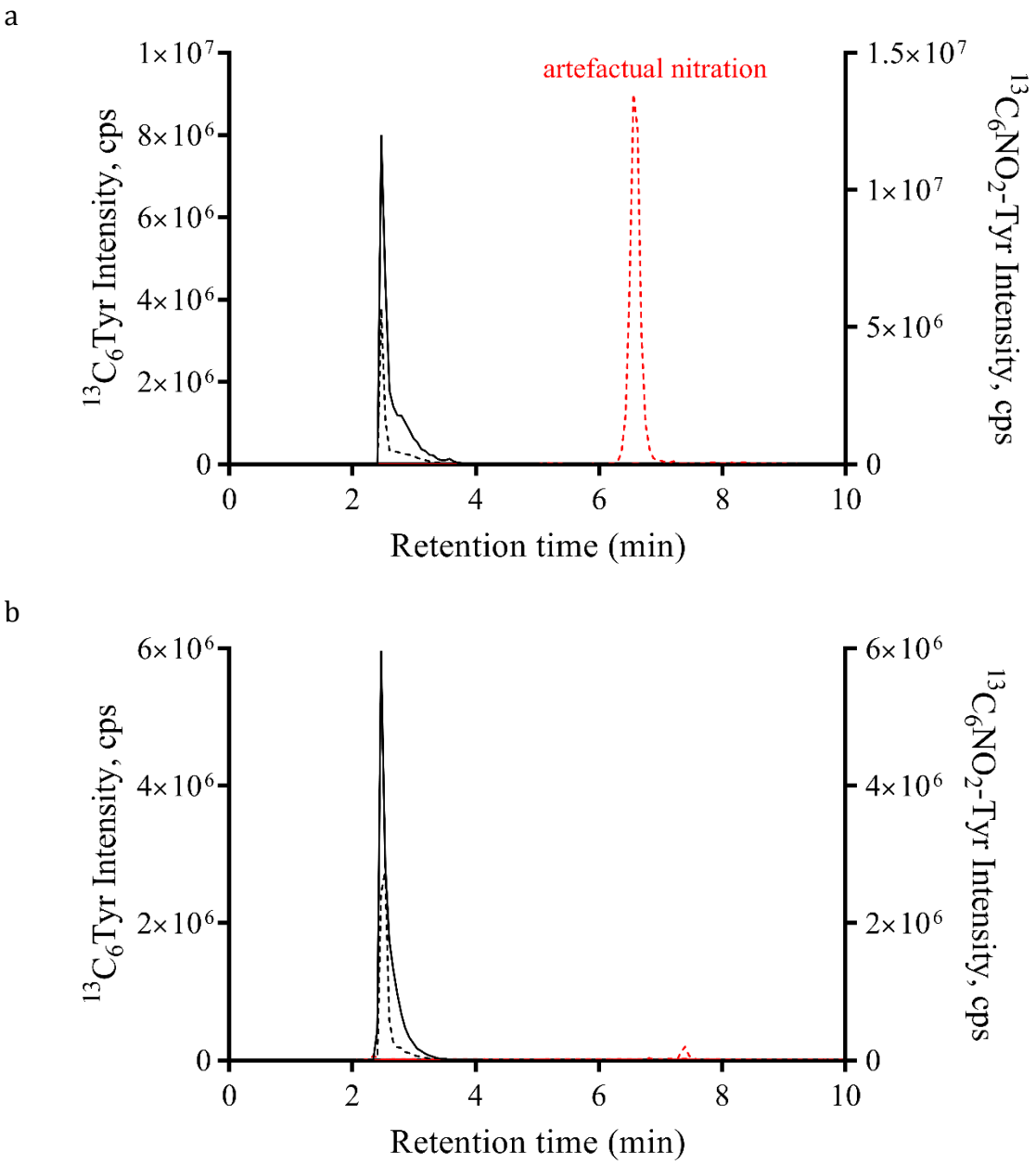


**Figure 71. Artefactual nitration during sample preparation**. Chromatograms obtained in multiple reaction monitoring for $^{13}C_6$ Tyr (black lines) and artefactual formation of $^{13}C_6$ $NO_2$-Tyr (red lines). In both chromatograms, 6 nmol of $^{13}C_6$ Tyr were injected directly (solid lines), or mixed with HCl then extracted with solid phase extraction, using (a) double deionized tap water or (b) HPLC-grade bottled water in all preparation steps.

After eliminating the main source of artefactual nitration, I proceeded to ECM sample processing using HPLC-grade $H_2O$ in all steps. The results revealed unusually high levels of 3-nitrotyrosine in ECM samples after hydrolysis and solid phase extraction. Puzzlingly, this was observed even in negative controls where I only added isotopically-labelled internal standards or only HCl immediately before solid phase extraction. To identify whether 3-nitrotyrosine is incidental to solid phase extraction, I tested different analytes separately (unlabelled and labelled tyrosine and 3-nitrotyrosine) before and after solid phase extraction. When each analyte was injected directly, 3-nitrotyrosine peak was detected only in the tube where it was added (**Figure 72**a). However, when the same analytes were processed by solid phase extraction first before injection, 3-nitrotyrosine peaks were detected in all other tubes, even the ones where no 3-nitrotyrosine was added, which indicated possible contamination with 3-nitrotyrosine during processing. To test this hypothesis, I analysed samplings of all the reagents used for acid hydrolysis and solid phase extraction. Indeed, the stock of TFA in standard use for washing steps during solid phase extraction was contaminated with 3-nitrotyrosine (**Figure 72**b). I overcame the contamination problem by using a fresh stock of TFA.

After troubleshooting and optimisation, I repeated the analysis of ECM samples. I encountered another issue with poor recovery of internal standards following hydrolysis and solid phase extraction, especially the isotopically labelled 3-nitrotyrosine. The chromatogram in **Figure 73** shows partial loss of both $^{13}C_6$ Tyr and $^{13}C_9$ $NO_2$-Tyr after brief mixing with HCl and solid phase extraction. When the analytes were heated at 110°C in HCl then processed by solid phase extraction, $^{13}C_9$ 3-$NO_2$-Tyr was completely lost. This poor recovery of $^{13}C_9$ 3-$NO_2$-Tyr after hydrolysis and solid phase extraction varied between samples (~ 0.1 - 10%), while recovery of $^{13}C_6$ Tyr was ~20 % on average. This was an issue because it indicated likely loss of 3-nitrotyrosine (the analyte of interest) in the samples as well. It also hindered normalisation to internal standards and relative quantification.

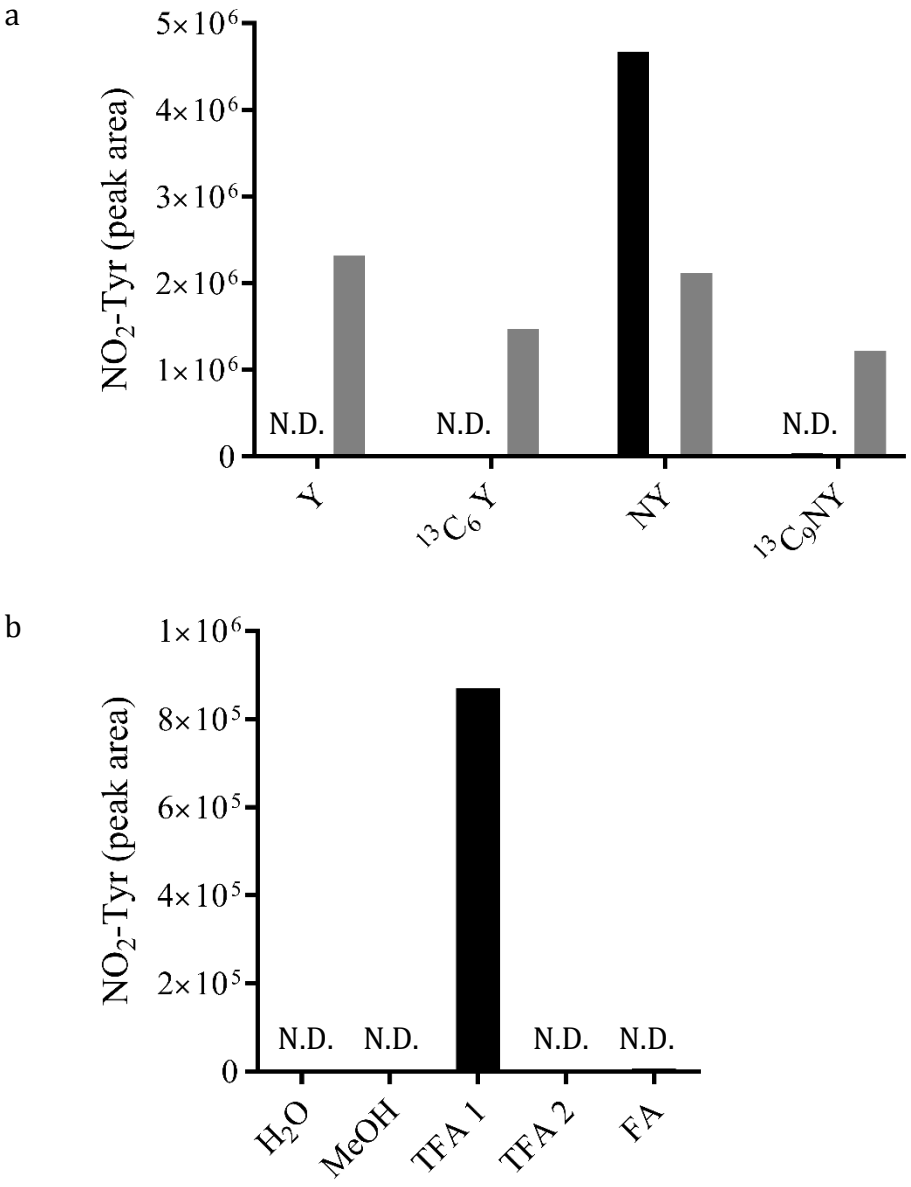


**Figure 72. Testing for the source of contamination with nitrotyrosine**. (a) The presence of 3-nitrotyrosine tested before and after solid phase extraction. Standards and internal standards; Tyrosine (Y, $^{13}C_6$ Y) and 3-nitrotyrosine (NY, $^{13}C_9$ NY) were either made in HPLC-grade $H_2O$ with 0.1% formic acid and each injected separately for LC/MS/MS analysis (black bars), or mixed with HCl, processed with solid phase extraction (which included washing with HPLC-grade $H_2O$ supplemented with 0.1% (v/v) TFA and elution with methanol), then lyophilised and reconstituted in HPLC-grade $H_2O$ with 0.1% FA and each injected separately into LC/MS/MS (grey bars). (b) 3-Nitrotyrosine peak areas in samplings from different reagents used in sample preparation; methanol (MeOH), two different stocks of trifluoroacetic acid (TFA) and formic acid (FA). N.D. nothing detected.

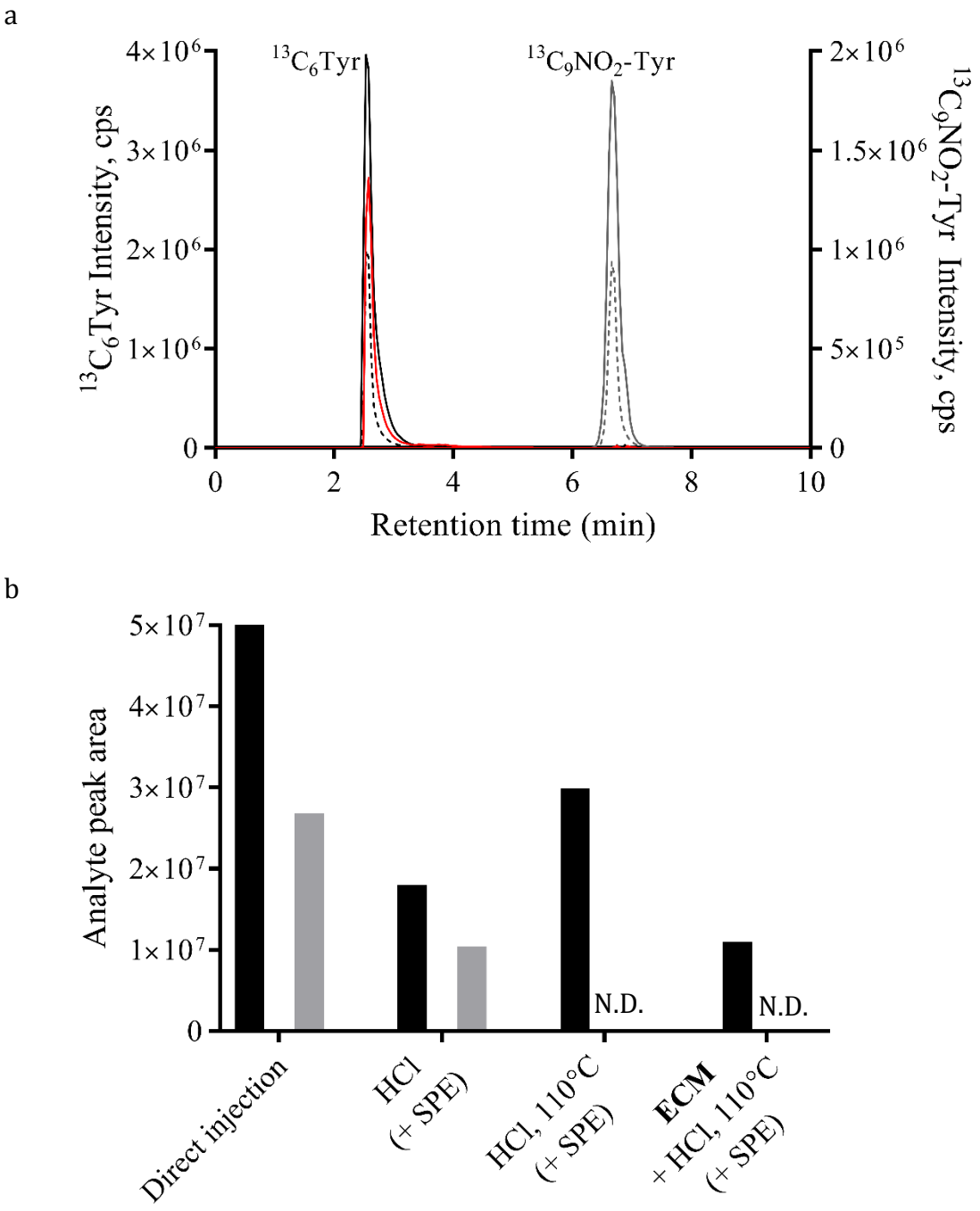


**Figure 73. Recovery of internal standards after sample preparation**. (a) Chromatogram for 6 nmol of $^{13}C_6$ Tyr (black lines) and 6 pmol of $^{13}C_9$ $NO_2$-Tyr (grey lines) when injected directly without processing (solid lines), or when mixed with HCl (without heating) and extracted with solid phase extraction (dashed lines), or when mixed with HCl and heated at 110°C for 18 hours then processed with solid phase extraction (red solid line). (b) Analyte peak areas for $^{13}C_6$ Tyr (black bars) and $^{13}C_9$ $NO_2$-Tyr (grey bars) with or without HCl, heating at 110°C, solid phase extraction (SPE) and when added to ECM sample.

### *5.2.3 Detection of 3-nitrotyrosine in the ECM*

Despite the numerous technical issues I encountered in optimising this method, I was determined to attempt to answer the question whether 3-nitrotyrosine is present in the ECM. Here, ECM samples isolated from epithelial cells (wild type and peroxidasin knock-out) were hydrolysed to individual amino acids and prepared for analysis as described earlier. I used HPLC-grade water in all steps to minimise artefactual nitration, and a fresh stock of TFA that was tested negative for contamination with 3-nitrotyrosine. To estimate the amounts of 3-nitrotyrosine in ECM samples, despite loss of internal standards during processing, I used analyte peak areas for the standard calibration curve without normalisation to internal standards (**Figure 74**). The isotopically-labelled analytes were used for identification and confirmation of elution times.

I was able to detect 3-nitrotyrosine in ECM isolated from wild type epithelial cells grown in culture medium supplemented with 200 μM nitrite (**Figure 75**a). The 3-nitrotyrosine peak eluted at 6.4 minutes, consistent with the transitions and elution times for 3-nitrotyrosine (m/z 227 to 181) and $^{13}C_9$ 3-nitrotyrosine (m/z 236 to 189) in standards (**Figure 69**). The peak area for 3-nitrotyrosine was $2.1 \times 10^5$, which is calculated to be 27 fmol on the standard calibration curve (**Figure 74**b). The peak area for tyrosine was $1.1 \times 10^8$, which is calculated to be 2 nmol on the standard calibration curve (**Figure 74**a). These values give a ratio of 13 μmol 3-nitrotyrosine/ mol tyrosine. This ratio is an estimation, as it does not account for losses of tyrosine and 3-nitrotyrosine. The level of 3-nitrotyrosine in ECM isolated from peroxidasin knock-out cells was below the limit of quantification (peak area $8.4 \times 10^3$) (**Figure 75**b).

a

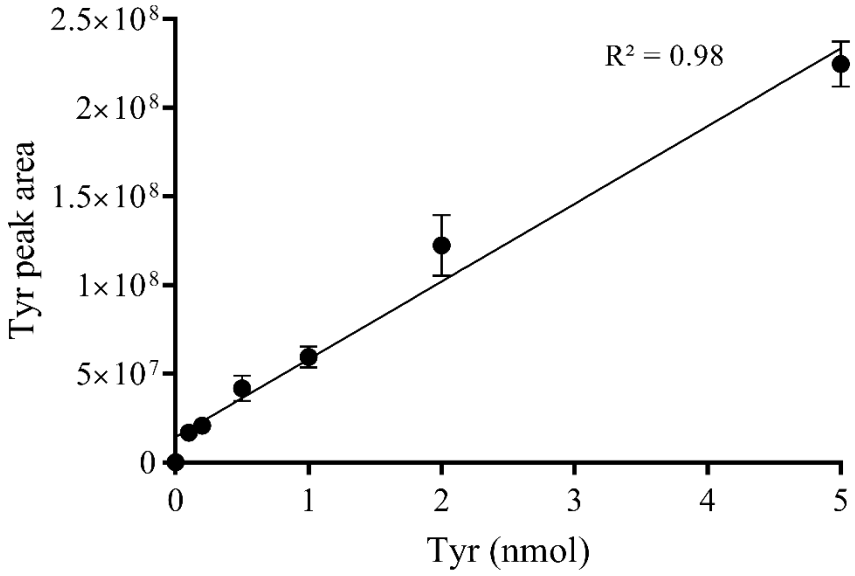


b

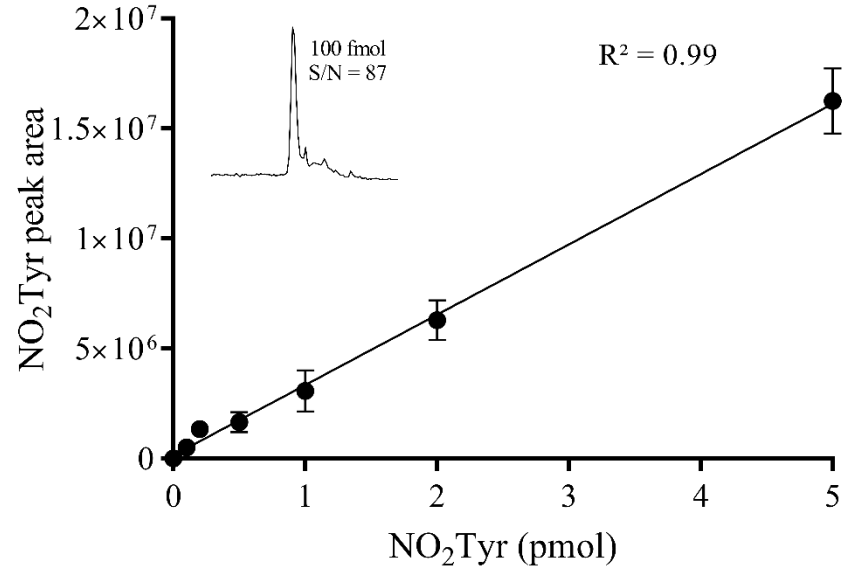


**Figure 74**. **Standard calibration curve for tyrosine and 3-$NO_2$Tyr**. Peak areas for standard dilutions of (a) tyrosine and (b) 3-nitrotyrosine injected directly into the liquid chromatography column without SPE. Inset shows signal-to-noise ratio for 100 fmol 3-nitrotyrosine. Values are average of three independent experiments ± SEM.

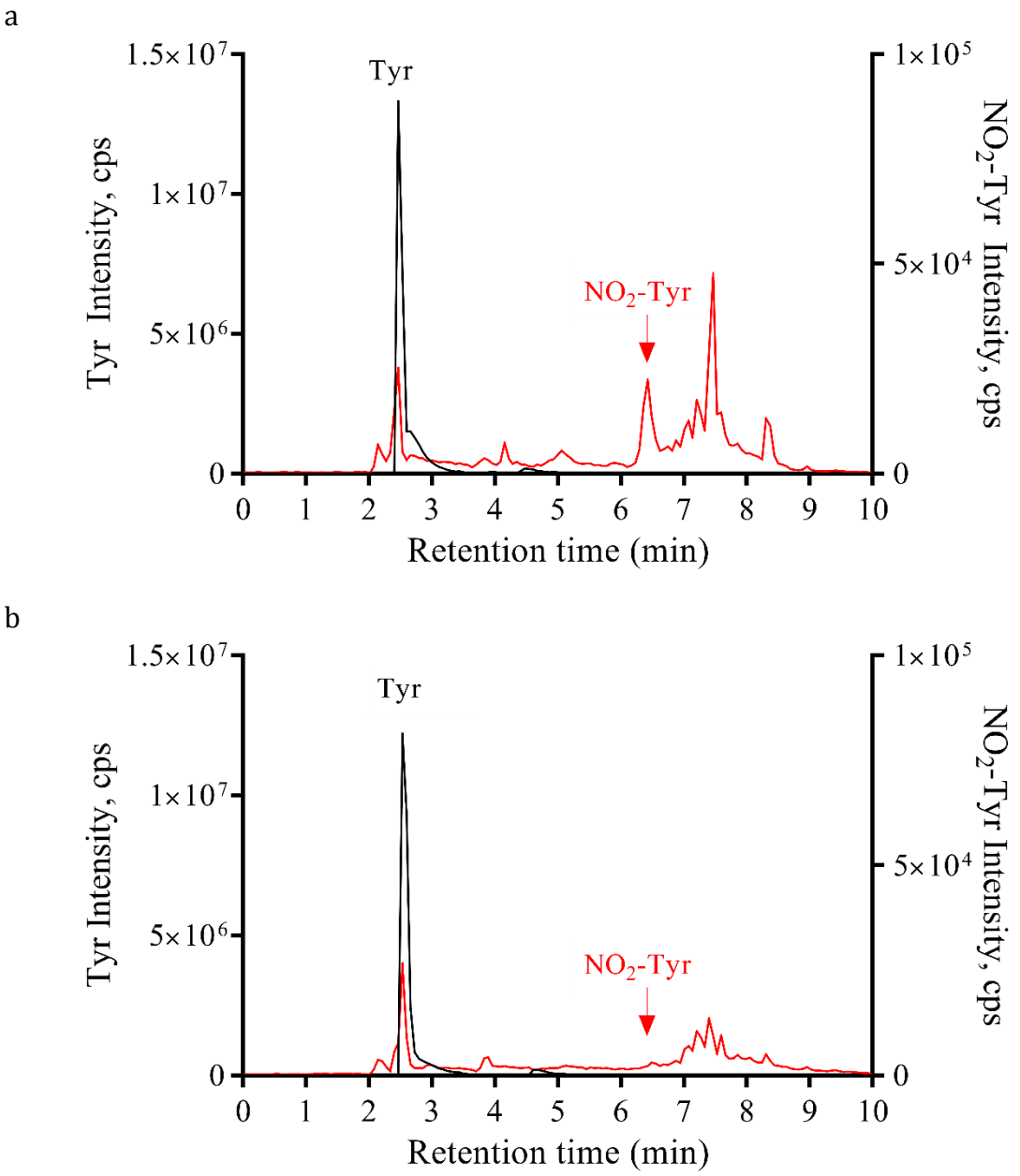


**Figure 75. 3-Nitrotyrosine in hydrolysed ECM.** Chromatograms obtained in multiple reaction monitoring mode for tyrosine (m/z 182 to 136, black lines) and 3-nitrotyrosine (m/z 227 to 181, red lines) in ECM from (a) wild type or (b) peroxidasin knock-out epithelial cells grown in culture medium supplemented with 200 μM $NaNO_2$. Samples were prepared by isolation and thorough washing of the ECM, hydrolysis with HCl, then processing by solid phase extraction and analysis by LC/MS/MS.

### *5.2.4 3-Nitrotyrosine increases with increasing nitrite concentration*

Here I investigated the effect of adding increasing concentrations of nitrite on the formation of 3-nitrotyrosine during cell growth. The isolated ECM was washed extensively to remove any nitrite before acid hydrolysis and analysis by LC/MS/MS for the presence of 3-nitrotyrosine. The preliminary results in **Figure 76**a indicate that the formation of 3-nitrotyrosine on proteins in the ECM increased with increasing concentrations of nitrite. Values in the graph are analyte peak areas that were not normalised due to low recovery or loss of isotopically labelled internal standards. The results presented here are from one experiment only. Although multiple independent biological experiments were conducted, several repeats of measurements did not yield usable data due to the technical challenges outlined earlier. I calculated the relative amounts of tyrosine and 3-nitrotyrosine in the samples using the standard calibration curve in **Figure 74** without normalisation to internal standards. Although absolute values are not reliable, the observed increase in 3-nitrotyrosine from 3 to 13 µmol / mol tyrosine is consistent with nitrite-dependent nitration in cell culture (**Figure 76**b).

Secondly, I investigated the formation of 3-nitrotyrosine when decellularised isolated ECM was treated with nitrite and hydrogen peroxide for one hour. The preliminary results in **Figure 77** (calculated using the standard calibration curve without normalisation to internal standards) show that 3-nitrotyrosine increased with increasing nitrite concentrations. When ECM isolated from peroxidasin knock-out cells was incubated with nitrite and hydrogen peroxide, the ratios were approximately 2 µmol 3-nitrotyrosine / mol tyrosine, and did not increase with increasing nitrite concentration (**Figure 77**).

While this is still work in progress, the pilot results presented here indicate that adding nitrite both during cell growth, or in decellularised ECM, led to formation of 3-nitrotyrosine in ECM from wild type epithelial cells, while ECM from peroxidasin knock-out cells did not show this response.

a

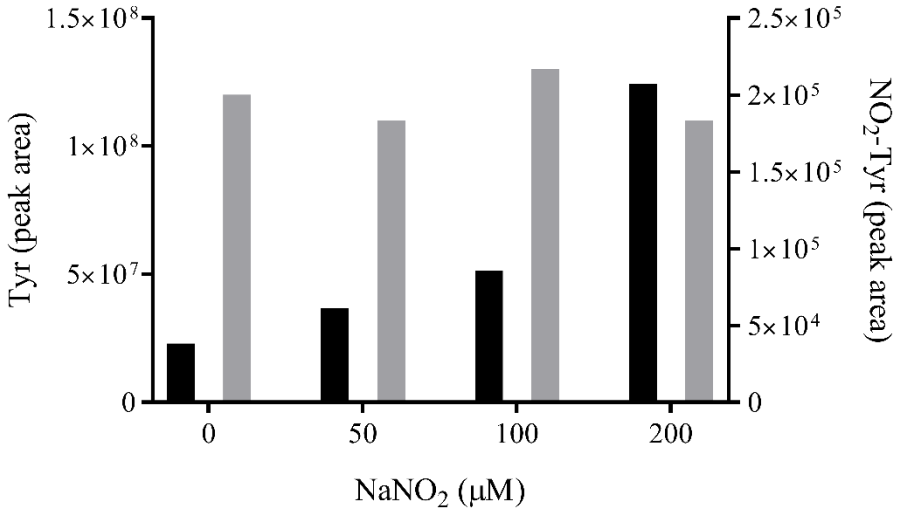


b

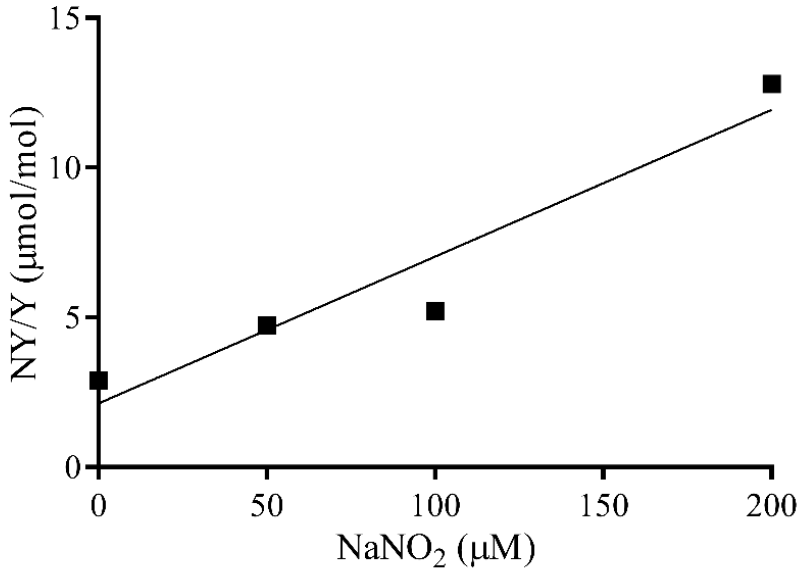


**Figure 76. Formation of 3-$NO_2$Tyr during cell growth**. Epithelial cells cultured for 6 days in media supplemented with the indicated concentrations of nitrite, then the ECM was isolated, hydrolysed and analysed for 3-nitrotyrosine by LC/MS/MS. (a) Peak areas of 3-nitrotyrosine (black bars) and tyrosine (grey bars). (b) Ratios of 3-nitrotyrosine to tyrosine when the peak areas were related to the standard calibration curve in **Figure 74** without normalisation to internal standards.

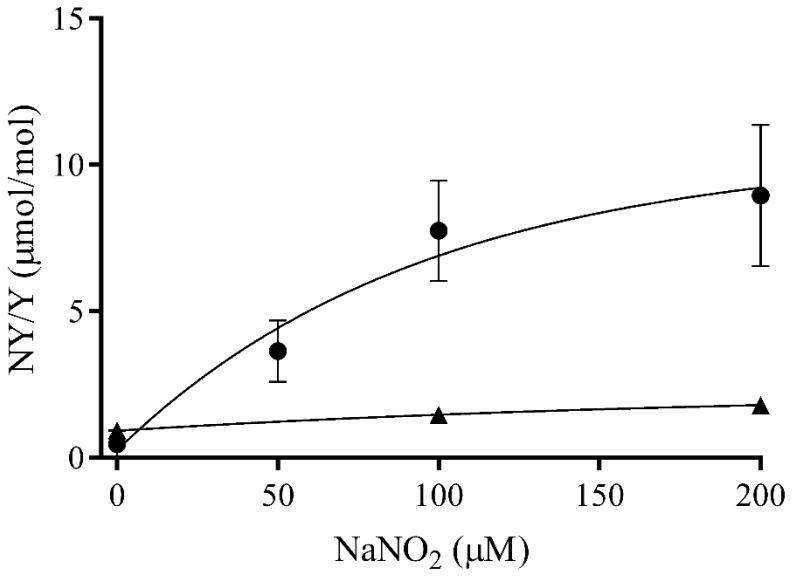


**Figure 77. 3-$NO_2$Tyr increased with increasing nitrite concentrations in decellularised ECM**. Ratios of 3-nitrotyrosine to tyrosine when the peak areas were related to the standard calibration curve in **Figure 74** without normalisation to internal standards. ECM was isolated from epithelial cells, wild type (●) or peroxidasin knock-out (▲), treated with 50 µM $H_2O_2$ and the indicated concentrations of $NaNO_2$ for 1 hour at 37°C, then washed extensively, hydrolysed with hydrochloric acid and analysed by LC/MS/MS. Values for WT are from two independent experiments ± range. Values for KO are from one experiment.

## 5.3 Discussion

In this chapter I outlined the technical challenges I faced in optimising and validating a method for the analysis of 3-nitrotyrosine in proteins in the ECM, some of which I was able to overcome while others still require further work. In summary, I optimised the method for liquid chromatography and tandem mass spectrometry. I improved the sample preparation method to eliminate the main sources of artefactual nitration and contamination with 3-nitrotyrosine. It is worth noting that artefactual nitration of tyrosine is a common methodological issue, especially in the presence of acid (in hydrolysis or chromatography mobile phase) (225).

Loss of the isotopically labelled 3-nitrotyrosine during sample processing continues to be an issue in this method. Mixing with HCl appeared to contribute to loss of the labelled 3-nitrotyrosine. It is also possible that using methanol to elute 3-nitrotyrosine in the final step of the solid phase extraction might lead to methylation of 3-nitrotyrosine during lyophilisation in the speed vacuum concentrator and contribute to the loss of 3-nitrotyrosine. Using acetonitrile for the elution step might improve recovery.

Pronase is an alternative way to digest ECM proteins to individual amino acids. However, I had limited success with this method. Further optimisation might improve digestion and minimise artefactual nitration. 3-Nitrotyrosine can also be detected by immunoblotting. There are two possible issues with using this method in this system: firstly, solubilising the ECM to be resolved by SDS-PAGE, and secondly, the low levels of 3-nitrotyrosine in this *in vitro* model might be below the level of detection by antibodies. However, it is worth trying this method to strengthen the evidence for 3-nitrotyrosine formation by peroxidasin.

The technical issues and limitations for reliable analysis of protein tyrosine nitration are well documented in the literature (127, 224, 225). The abundance of nitrating agents in the environment (air, water) which can contribute to artefactual nitration, particularly on acidification, coupled with the prevalence of tyrosine over

the extremely low levels of 3-nitrotyrosine in biological samples all make the task of accurate analysis of 3-nitrotyrosine levels exceedingly challenging.

Nonetheless, I detected low levels of 3-nitrotyrosine in the hydrolysed ECM. Preliminary evidence presented here indicate that peroxidasin activity leads to formation of 3-nitrotyrosine. This is in line with the observation in Chapter 4 that nitrite modulates formation of 3-bromotyrosine by peroxidasin, and with recently-submitted data that nitrite acts as a substrate for peroxidasin (47). Formation of 3-nitrotyrosine increased with increasing concentrations of nitrite during cell growth and in decellularised isolated ECM. The preliminary results from peroxidasin knock-out ECM suggest that formation of 3-nitrotyrosine is peroxidasin dependent. Further work is planned and underway to confirm these findings. Although the levels measured here can only be approximated and cannot be accurately quantified, they are in the same order of magnitude that is reported in some literature. For example, exposure of human fibronectin to peroxynitrite led to the formation of 3-nitrotyrosine (40 μmol/mol tyrosine) (226).

There are variety of pathways that lead to protein tyrosine nitration, including nitrating agents (e.g. peroxynitrite). Heme peroxidases (myeloperoxidase, eosinophil peroxidase and lactoperoxidase) are among the major sources of enzymatically derived nitration, especially in inflammation (119, 123, 227). The contribution of peroxidasin to protein nitration puts it among the enzymes that lead to oxidative damage, particularly in the ECM. Nitration can lead to altered protein structure and function, change in protein recognition, cell adhesion and proliferation (226, 228). 3-Nitrotyrosine is a biomarker for oxidative damage in inflammation. Antibodies against 3-nitrotyrosine were detected in patients with coronary artery disease, showing that oxidative modifications can be immunogenic (229). Nitration of tyrosine residues in α-synuclein is implicated in neurodegenerative diseases such as Alzheimer's and Parkinson's diseases (106). In this light, it is important to investigate the role of peroxidasin in protein tyrosine nitration in normal physiological processes and its contribution to abnormal pathological situations.

# Chapter 6 General Discussion

## 6.1. Summary of findings

The main aims of this research project were to investigate the activity and substrate specificity of peroxidasin in the ECM and to explore whether it mediates oxidative modifications of proteins other than cross-linking collagen IV. The graphical summary in **Figure 78** highlights the main findings.

In summary, I optimised a model system to study the activity of peroxidasin *in situ*, which demonstrated its requirement for hydrogen peroxide and bromide to catalyse the formation of the sulfilimine cross link in collagen IV. Physiological levels of bromide (<100 μM) were sufficient for maximal cross-linking. It is likely that very low levels of hydrogen peroxide are required (<1 μM), although its endogenous source remains elusive. Cross-linking collagen IV by peroxidasin in the decellularised ECM was more efficient than by adding reagent HOBr or taurine bromamine. The efficiency of peroxidasin in cross-linking collagen IV was especially apparent when considering the presence of a catalase that consumed most of the reagent hydrogen peroxide added to the decellularised ECM. Physiological levels of thiocyanate and urate modulated the formation of the sulfilimine cross link in collagen IV. One of the most exciting findings in this project was the detection of NADH bromohydrin, a fingerprint for the generation of HOBr by peroxidasin in the decellularised ECM.

During the course of this research project, I optimised methods to measure oxidative modifications of proteins by LC/MS/MS. Methionine sulfoxide was higher in the ECM than inside the cells, but did not show association with the activity of peroxidasin. On the other hand, 3-bromotyrosine was a product of peroxidasin activity. It increased with increasing bromide concentrations and did not form

when peroxidasin was inhibited by phloroglucinol or in peroxidasin knock-out cells. The levels of 3-bromotyrosine were higher in the non-collagenous domain than the ECM, which was higher than in the intracellular extract. Thiocyanate, urate and nitrite all modulated the formation of 3-bromotyrosine. Preliminary results showed that peroxidasin activity also led to the formation of 3-nitrotyrosine.

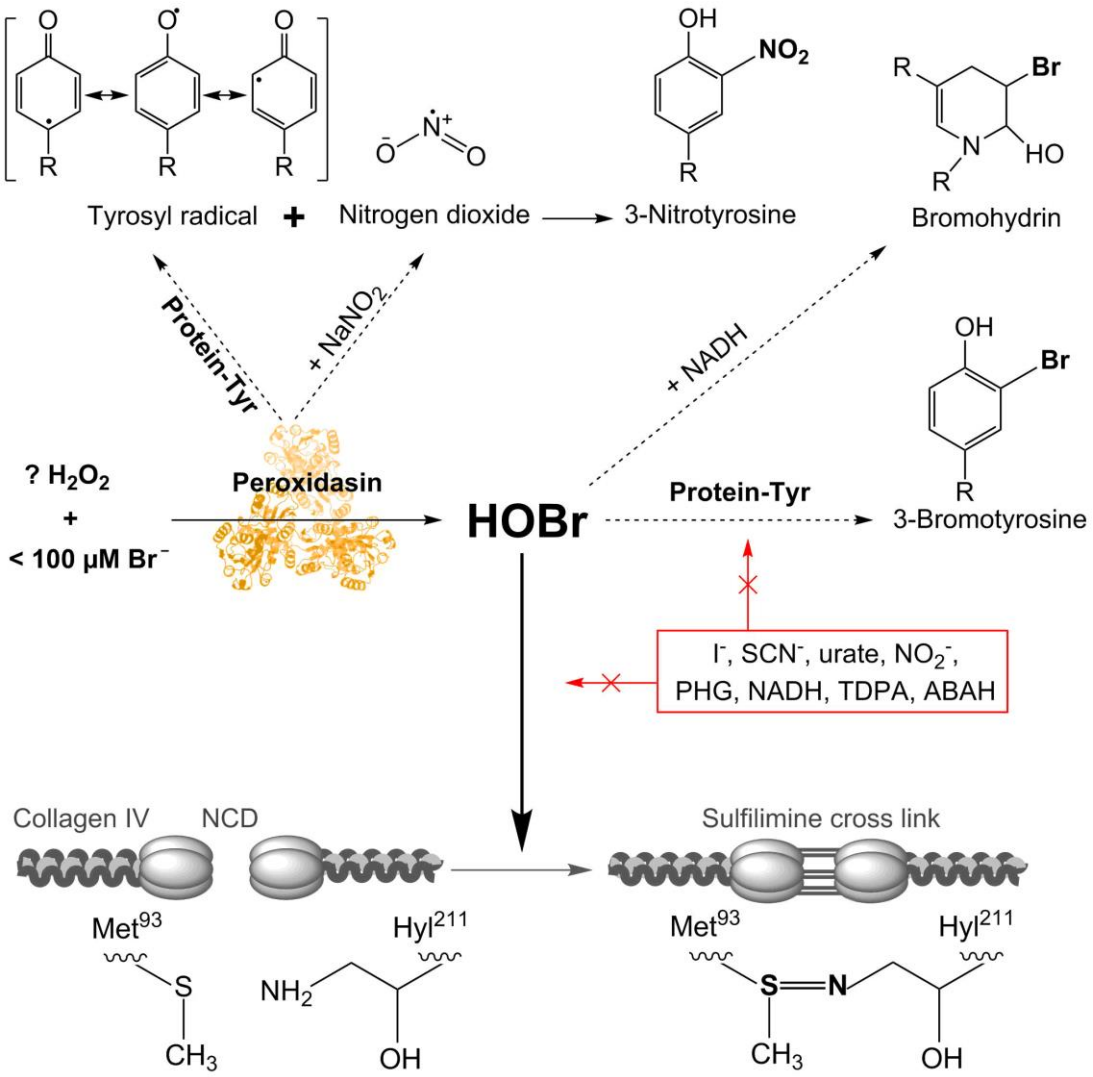


**Figure 78. Graphical summary of the main findings in this thesis**. Peroxidasin oxidises bromide to hypobromous acid, which facilitates the formation of the sulfilimine cross link in the NCD of collagen IV in the ECM. HOBr undergoes other reactions with endogenous tyrosine residues on proteins producing 3-bromotyrosine and exogenous NADH producing bromohydrin. Peroxidasin reacts with tyrosine residues and nitrite producing their respective radicals. Nitrogen dioxide can react with tyrosyl radical to produce 3-nitrotyrosine. Enclosed in the red frame are endogenous and exogenous substrates that modulate the activity of peroxidasin or the reactions of HOBr to varying extents. $I^-$, iodide, $SCN^-$, thiocyanate, $NO_2^-$, nitrite, PHG, phloroglucinol, NADH, nicotinamide adenine dinucleotide, TDPA, thiodipropionic acid, ABAH, 4-aminobenzoic acid hydrazide.

## 6.2. Significance and implications

The discovery of the sulfilimine bond that results from the deliberate enzymatically-catalysed oxidation of amino acids to cross link collagen IV (33) created a paradigm shift in the oxidative modifications by hypohalous acids. This case of constructive oxidative post-translational modification raises many curious questions about the enzymology of peroxidasin and its substrate specificity. Importantly, do peroxidasin activity and the production of HOBr lead to other, possibly damaging, oxidative modifications? Nelson *et al.* alluded to this conundrum in their seminal paper (15):

> "The concept of an extracellular peroxidase that is specifically attached to basement membranes opens up interesting new patho-physiological possibilities. Any metabolically hyperactive cell could secrete $H_20_2$ and would be damaged, or be at least marked by a change such as lipid peroxidation, upon encountering an externally anchored peroxidase. A marked cell would then be subject to detection by scavenger receptors (Krieger et al., 1992), phagocytic attack and removal. This could be important during development, as indicated by studies in Drosophila, mouse embryos (Pierce et al., 1991) and, if a human homolog of peroxidasin exists, in an early response against epithelia-derived neoplasms."

The results presented in this thesis answer some of these questions, and raise some more.

Firstly, peroxidasin reactions appear to be largely selective for, but not limited to, the cross-linking of collagen IV. The efficiency of the cross-linking reaction is higher when catalysed by the enzymatic system (bromide and hydrogen peroxide added to the decellularised ECM) than by the addition of reagent HOBr. This indicates selectivity of the reactions of HOBr with collagen IV conferred by peroxidasin, although the basis of this selectivity has not been demonstrated yet. It can be speculated that the selectivity arises from an association between peroxidasin and collagen IV or another protein in the ECM. It has been shown that the heme cavity of peroxidasin is not large enough to accommodate collagen IV for direct HOBr delivery (25, 26) and that peroxidasin does not form a stable complex with collagen

IV (28). This does not rule out a transient interaction between peroxidasin and collagen IV or a ternary complex with a third ECM protein. This interaction might trigger a conformational change that may activate peroxidasin or enhance selectivity of its reactions (26). The presence of the non-catalytic LRR and Ig domains might enable such interaction. This hypothesis is supported by the observation that eosinophil peroxidase was inefficient in cross-linking collagen IV even in a cell overlay assay which induced spatial proximity with the ECM (28). Although EPO contains the catalytic peroxidase domain and is able to generate HOBr, it lacks the Ig and LRR domains. It seems plausible to propose that the additional non-catalytic domains in peroxidasin facilitate an orientation to target HOBr release in proximity to the non-collagen domain of collagen IV.

Secondly, the enzymatic cross-linking of collagen IV proved resilient to competitive substrates of peroxidasin and scavengers of HOBr. Considering rate constants, thiocyanate is a better substrate for peroxidasin than bromide. The rate constant of the reaction of HOBr with thiocyanate is higher than that with methionine. Thiocyanate was more effective in inhibiting the formation of 3-bromotyrosine than the sulfilimine cross link. However, in both cases, inhibition was not as effective as predicted by rate constants of the reactions of thiocyanate with peroxidasin or with HOBr. Moreover, adding exogenous methionine (5 mM) to the decellularised ECM interfered only mildly with the cross-linking reaction. The mechanism of the formation of the sulfilimine cross link is hypothesised to involve bromination of methionine residue on collagen IV by HOBr. Given that methionine reacts with HOBr very rapidly, it is therefore perplexing that adding excess exogenous methionine does not scavenge all HOBr and completely stop the cross-linking reaction. All these observations suggest that there is more to the specificity of peroxidasin reactions than just the rate constants. They also clearly indicate a special affinity of peroxidasin for bromide, although the basis of this affinity is yet to be fully understood.

It is important to keep in mind that the studies which reported the rates of reactions of peroxidasin with various substrates used a recombinant monomeric form of peroxidasin that contains only the peroxidase and Ig domains, which are necessary

for its catalytic activity (13, 28, 47). This monomeric construct is active and provided extremely useful kinetic data on peroxidasin. However, as highlighted earlier, trimerisation and the presence of the other non-catalytic domains in peroxidasin might play a role in enhancing its affinity to bromide, or in altering the properties of the microenvironment to favour the cross-linking reaction with collagen IV.

Modulation of peroxidasin activity by physiological levels of thiocyanate could be advantageous. Hypothiocyanous acid (HOSCN) can be generated either through two-electron oxidation of thiocyanate by peroxidasin or by reaction with HOBr. HOSCN is less reactive than HOBr (1, 230), and its formation could be a way to protect from the harmful effects of HOBr. It might not be a coincidence that thiocyanate has a greater inhibitory effect on the formation of 3-bromotyrosine (presumably a collateral reaction) than the formation of the sulfilimine cross link. Likewise, urate can act as an antioxidant and mitigate HOBr-mediated damage without interfering with its physiological role in cross-linking collagen IV.

Thirdly, the detection of NADH bromohydrin shows that HOBr generated by peroxidasin in the decellularised ECM reacts with exogenous substrates. This indicates that HOBr produced by peroxidasin is released into the surroundings and its reactions are not limited to cross-linking collagen IV. Similarly, the detection of 3-bromotyrosine demonstrates that HOBr reacts with amino acid residues on proteins in the ECM. It is worth highlighting that 3-bromotyrosine is not the main product of the reactions of HOBr with amino acids, as it reacts faster with cysteine, methionine, tryptophan, histidine, lysine and terminal amines (120). However, due to its relative stability, 3-bromotyrosine is used as a biomarker to identify the presence of oxidative modifications of proteins by HOBr. It is difficult to estimate the amount of HOBr generated by peroxidasin in the ECM, because it is highly reactive and generates different reactive intermediates and products. However, the results indicate that small concentrations of HOBr (low micromolar) are sufficient for the cross-linking reaction. The reactions of HOBr appear to be specific for the cross-linking of collagen IV at low amounts of bromide and hydrogen peroxide. Excess HOBr can undergo reactions with other targets.

Finally, the novel finding that peroxidasin contributes to the formation of 3-bromotyrosine and 3-nitrotyrosine has many implications. It brings peroxidasin to the spotlight as a resident contributor to oxidative damage of proteins in the ECM, a ubiquitous tissue with poor antioxidant defence. It also confirms the inkling that Nelson and colleagues have mentioned and raises many new questions about the patho-physiological roles of peroxidasin. These oxidative modifications might be one of the mechanisms by which peroxidasin plays a role in pathological situations such as hypertension, diabetes and ischemia-reperfusion injury (56, 63, 64, 67, 187). In fact, evidence from a diabetic mouse model shows that halogenation of proteins in renal ECM impairs some protein functions and might be involved in diabetic glomerular injury (187). Peroxidasin might account for some of the oxidative damage to the ECM that is attributed to other heme peroxidases, such as myeloperoxidase and eosinophil peroxidase. Modifications of ECM proteins might be also one of the ways peroxidasin plays a role in cancer, especially when it is upregulated (17, 70, 73-75). Peroxidasin contributes to melanoma invasion, and silencing its gene blocks cellular invasion and adhesion (70). The mechanism is likely to involve epithelial mesenchymal transition (76, 78, 231). Being an extracellular protein, peroxidasin could also be a pharmaceutical target to impede tumour invasion.

## 6.3. Limitations and future work

Studying the activity of peroxidasin *in situ* as an alternative to the pure enzyme has advantages and disadvantages. It allows studying the enzyme in its native form and environment in the ECM and gives insight into the substrate specificity and modulation of the activity of peroxidasin. On the other hand, the ECM is a complex system that does not allow for pure kinetic studies of peroxidasin. For example, investigating peroxidasin requirement for hydrogen peroxide was complicated by the presence of a catalase in the ECM that appeared to consume most of the added hydrogen peroxide independently of peroxidasin. Studying substrate competition and inhibition was also complicated in this system, making it difficult to calculate kinetic parameters such as rate constants and the half maximal inhibitory

concentrations. Furthermore, this model system is labour intensive and low throughput. Despite its limitations, studying peroxidasin *in situ* is a useful and versatile model system. It also highlighted some differences from the enzymology of the truncated variant hsPxd01-con4.

One of the major challenges I encountered during this research project was setting up assays to quantify oxidative modifications in ECM proteins, particularly methionine sulfoxide and 3-nitrotyrosine. Many of the issues arise from the inherent chemical properties of these analytes and the artefactual oxidation and nitration. Work is underway to further optimise these assays.

Research on peroxidasin is ironically hindered by its own intrinsic characteristics. The biosynthesis of this large multi-domain trimeric enzyme requires heme insertion, modification and covalent attachment, in addition to glycosylation in the endoplasmic reticulum and Golgi before secretion and cleavage by proprotein convertase. Recombinant expression and purification of a native and active peroxidasin is an exceedingly challenging quest, as reported in the literature and in personal communications with researchers at international conferences. Furthermore, probing for peroxidasin with immunoblotting was a frustrating endeavour. I tested multiple commercially available and custom-made anti-peroxidasin antibodies, which showed low sensitivity, cross-reactivity or poor reproducibility. Research on peroxidasin would benefit from developing reliably specific and sensitive anti-peroxidasin antibodies that could be used in western blotting and immunohistochemistry. Access to a pure native and active peroxidasin would allow kinetic studies on its substrate preference, competition and inhibition. Solving the crystal structure of peroxidasin would help understanding the dynamism and mechanism of its activity.

Notwithstanding these challenges, the findings in this thesis provide insights into the activity of peroxidasin in the ECM, as outlined earlier, and stimulation for further investigation. Some of the specific questions that remain to be answered relate to the basis of the affinity of peroxidasin for bromide over other substrates,

such as thiocyanate. Elucidating the substrate preference and competition is essential for understanding the enzymology of peroxidasin. The source of hydrogen peroxide remains a mystery (49) and it would be interesting to pinpoint, as it is important for regulating the activity of peroxidasin.

Little is known about the mechanism by which phloroglucinol inhibits the activity of peroxidasin and the cross-linking of collagen IV. Phloroglucinol is an inhibitor of peroxidases (232) and has been used in many studies to inhibit the formation of the sulfilimine bond in collagen IV (15, 33). It has been shown to have a cytoprotective effect against oxidative stress (233) and myocardial ischaemia–reperfusion injury in *in vitro* studies (64, 234). Phlroglucinol is used pharmacologically as an antispasmodic drug for treatment of variety of diseases, including irritable bowel syndrome and urinary tract infection (235, 236). It would be interesting to perform kinetic studies on the reaction of phloroglucinol with peroxidasin and other heme peroxidases.

Future research can explore the interactive mechanism of peroxidasin and whether it binds to collagen IV or other ECM proteins to target HOBr release and limit nonspecific reactions. It will be interesting to investigate whether peroxidasin is active inside the cell or only upon secretion. Cleavage of peroxidasin by proprotein convertase was shown to occur primarily in the extracellular space (27). It also enhances the activity of peroxidasin, although the unprocessed enzyme is catalytically active. Current research conducted by my colleague Dr. Martina Paumann-Page shows that peroxidasin is constitutively secreted by melanoma cells to culture medium. It would be interesting to investigate the pattern of expression and functions in different developmental stages. Does peroxidasin serve functions other than cross-linking collagen IV, given that the ECM has a slow turnover rate? In this regard, future work can investigate the secretion of peroxidasin and its circulation in blood; how much and whether it is active. Work in our group is currently underway to optimise methods to address these questions.

The jury is still out on the reaction mechanism of sulfilimine bond formation between two juxtaposed methionine and hydroxylysine residues on opposing protomers of collagen IV. It is proposed that HOBr reacts with methionine to form a halosulfonium cation intermediate which is then attacked by the amine group of hydroxylysine to produce the sulfilimine bond (35). Alternatively, HOBr can react with hydroxylysine to form a bromamine intermediate which is then attacked by the sulfide of methionine. The rate constants of the reactions of HOBr with methionine and lysine are $4\times10^{6}$ and $4\times10^{5}$ $M^{-1}$ $s^{-1}$, respectively (120), which suggests that the first reaction is more kinetically favourable. On the other hand, bromamine led to the formation of intermolecular sulfilimine bond in peptides containing methionine and lysine, suggesting that bromamine can be the intermediate in forming the intermolecular cross link in collagen IV (172). Further research should elucidate the reaction mechanism.

Inhibition of collagen IV cross-linking by thiocyanate and iodide is interesting and warrants further investigation. Given that both thiocyanate and iodide are substrates for peroxidasin, it can be assumed that hypothiocyanous and hypoiodous acids are formed. However, the observed inhibitory effects of thiocyanate and iodide indicate that neither of their respective hypohalous acids promotes the sulfilimine cross link. This is interesting given that hypoiodous acid reacts with methionine to form dehydromethionine (114), which contains a sulfur-nitrogen bond analogous to that in the sulfilimine bond. Hypothiocyanous acid is unreactive with methionine (237). It may react with lysine to form an amino thiocyanate species that is not stable at physiological pH (238, 239). It would be interesting to test whether adding reagent hypoiodous acid and hypothiocyanous acid to monomeric collagen IV would generate the sulfilimine cross link. Future work should investigate the inhibition by these two substrates to shed more light on the chemical mechanism of the sulfilimine bond formation and the nature of the intermediates in this reaction.

Another area of fertile investigation is the physiological functions of peroxidasin, which are likely to extend beyond cross-linking collagen IV. Multiple lines of evidence point to its role in redox regulation (39, 77) and antimicrobial defence (37,

38). Peroxidasin is also proposed to play a role in wound healing by cross-linking tyrosine residues in the ECM (40).

There is exciting potential in taking *in vitro* findings to *in vivo* models. In this regard, it would be interesting to study how the activity of peroxidasin is affected by bromide deficiency in humans, which may occur in certain diseases or as a result of kidney dialysis (240, 241). High levels of thiocyanate in smokers (242, 243) can lead to functional bromide deficiency, which results in thiocyanate outcompeting bromide. There is evidence that links smoking to alteration in the structure of basement membranes (208). Whether this is related to peroxidasin and the cross-linking of collagen IV is yet to be explored.

Future research should focus on the role of peroxidasin in post-translational modifications of ECM proteins. It would be interesting to investigate the effect of peroxidasin-catalysed tyrosine bromination on the structure and function of the modified proteins. Mapping the specific sites of protein tyrosine bromination and nitration would also provide further insight into the specificity of these reactions and peroxidasin interaction with other proteins. Peroxidasin can also form dityrosine (15), and it would be interesting to investigate its formation in the ECM. Protein tyrosine cross-linking leads to protein aggregation which are hallmarks of neurodegenerative diseases such as Parkinson's and Alzheimer's diseases (244, 245). The role of peroxidasin in oxidative modifications is particularly interesting in pathological situations, such as diabetes and fibrosis, and in cancers where peroxidasin is upregulated.

Despite taking strides forward in the last few years, research on peroxidasin is still relatively in its infancy. Future work on the activity and regulation of peroxidasin will further our understanding of its roles in physiology and pathology.

# References


1. O'Brien PJ. Peroxidases. Chem Biol Interact. 2000;129(1-2):113-39.

2. Furtmuller PG, Zederbauer M, Jantschko W, Helm J, Bogner M, Jakopitsch C, et al. Active site structure and catalytic mechanisms of human peroxidases. Arch Biochem Biophys. 2006;445(2):199-213.

3. Kimura S, Ikeda-Saito M. Human myeloperoxidase and thyroid peroxidase, two enzymes with separate and distinct physiological functions, are evolutionarily related members of the same gene family. Proteins. 1988;3(2):113-20.

4. Raven EL, Dunford BH, Royal Society of Chemistry (Great Britain). Heme peroxidases. Cambridge: Royal Society of Chemistry; 2016. xxii, 366 pages p.

5. Davies MJ, Hawkins CL, Pattison DI, Rees MD. Mammalian heme peroxidases: from molecular mechanisms to health implications. Antioxid Redox Signal. 2008;10(7):1199-234.

6. Kettle AJ, Winterbourn CC. Myeloperoxidase: a key regulator of neutrophil oxidant production. Redox Rep. 1997;3(1):3-15.

7. Klebanoff SJ. A peroxidase-mediated antimicrobial system in leukocytes. J Clin Invest. 1967;46(6):1078.

8. Dogon IL, Amdur BH. Further characterization of an antibacterial factor in human parotid secretions, active against Lactobacillus casei. Arch Oral Biol. 1965;10(4):605-15.

9. Slowey RR, Eidelman S, Klebanoff SJ. Antibacterial activity of the purified peroxidase from human parotid saliva. J Bacteriol. 1968;96(3):575-9.

10. Carlson MG, Peterson CG, Venge P. Human eosinophil peroxidase: purification and characterization. J Immunol. 1985;134(3):1875-9.

11. Taurog A. Thyroid peroxidase and thyroxine biosynthesis. Recent progress in hormone research. 1970;26:189-247.

12. Rees MD, Kennett EC, Whitelock JM, Davies MJ. Oxidative damage to extracellular matrix and its role in human pathologies. Free Radic Biol Med. 2008;44(12):1973-2001.

13. Paumann-Page M, Katz RS, Bellei M, Schwartz I, Edenhofer E, Sevcnikar B, et al. Pre-steady-state Kinetics Reveal the Substrate Specificity and Mechanism of Halide Oxidation of Truncated Human Peroxidasin 1. J Biol Chem. 2017;292(11):4583-92.

14. Pattison DI, Davies MJ. Reactions of myeloperoxidase-derived oxidants with biological substrates: gaining chemical insight into human inflammatory diseases. Curr Med Chem. 2006;13(27):3271-90.

15. Nelson RE, Fessler LI, Takagi Y, Blumberg B, Keene DR, Olson PF, et al. Peroxidasin a novel enzyme-matrix protein of Drosophila development. EMBO J. 1994;13(15):3438-47.

16. Horikoshi N, Cong J, Kley N, Shenk T. Isolation of differentially expressed cDNAs from p53-dependent apoptotic cells: activation of the human homologue of the Drosophila peroxidasin gene. Biochem Biophys Res Commun 1999;261(3):864-9.

17. Mitchell MS, Kan-Mitchell J, Minev B, Edman C, Deans RJ. A novel melanoma gene (MG50) encoding the interleukin 1 receptor antagonist and six epitopes recognized by human cytolytic T lymphocytes. Cancer Res. 2000;60(22):6448-56.

18. Cheng G, Salerno JC, Cao Z, Pagano PJ, Lambeth JD. Identification and characterization of VPO1, a new animal heme-containing peroxidase. Free Radic Biol Med. 2008;45(12):1682-94.

19. Cheng G, Li H, Cao Z, Qiu X, McCormick S, Thannickal VJ, et al. Vascular peroxidase-1 is rapidly secreted, circulates in plasma, and supports dityrosine cross-linking reactions. Free Radic Biol Med. 2011;51(7):1445-53.

20. Peterfi Z, Toth ZE, Kovacs HA, Lazar E, Sum A, Donko A, et al. Peroxidasin-like protein: a novel peroxidase homologue in the human heart. Cardiovasc Res. 2014;101(3):393-9.

21. Soudi M, Zamocky M, Jakopitsch C, Furtmuller PG, Obinger C. Molecular Evolution, Structure, and Function of Peroxidasins. CHEMISTRY & BIODIVERSITY. 2012;9(9):1776-93.

22. Peterfi Z, Donko A, Orient A, Sum A, Prokai A, Molnar B, et al. Peroxidasin is secreted and incorporated into the extracellular matrix of myofibroblasts and fibrotic kidney. Am J Pathol. 2009;175(2):725-35.

23. Tindall AJ, Pownall ME, Morris ID, Isaacs HV. Xenopus tropicalis peroxidasin gene is expressed within the developing neural tube and pronephric kidney. Dev Dyn. 2005;232(2):377-84.

24. Lazar E, Peterfi Z, Sirokmany G, Kovacs HA, Klement E, Medzihradszky KF, et al. Structure-Function Analysis of Peroxidasin Provides Insight into the Mechanism of Collagen Iv Crosslinking. Free Radic Biol Med. 2015.

25. Soudi M, Paumann-Page M, Delporte C, Pirker KF, Bellei M, Edenhofer E, et al. Multidomain Human Peroxidasin 1 is a Highly Glycosylated and Stable Homotrimeric High-Spin Ferric Peroxidase. J Biol Chem. 2015.

26. Paumann-Page M, Tscheliessnig R, Sevcnikar B, Katz RS, Schwartz I, Hofbauer S, et al. Monomeric and homotrimeric solution structures of truncated human peroxidasin 1 variants. Biochim Biophys Acta Proteins Proteom. 2020;1868(1):140249.

27. Colon S, Bhave G. Proprotein Convertase Processing Enhances Peroxidasin Activity to Reinforce Collagen IV. J Biol Chem. 2016;291(46):24009-16.

28. Ero-Tolliver IA, Hudson BG, Bhave G. The Ancient Immunoglobulin Domains of Peroxidasin Are Required to Form Sulfilimine Cross-Links in Collagen IV. J Biol Chem. 2015.

29. Edenhofer E. Cloning expression and purification of human peroxidasin. Vienna: University of Natural Resources and Life Sciences; 2014.

30. LaFleur GJ, Jr., Horiuchi Y, Wessel GM. Sea urchin ovoperoxidase: oocyte-specific member of a heme-dependent peroxidase superfamily that functions in the block to polyspermy. Mech Dev. 1998;70(1-2):77-89.

31. Gotenstein JR, Swale RE, Fukuda T, Wu Z, Giurumescu CA, Goncharov A, et al. The C. elegans peroxidasin PXN-2 is essential for embryonic morphogenesis and inhibits adult axon regeneration. Development. 2010;137(21):3603-13.

32. Lee J, Bandyopadhyay J, Lee JI, Cho I, Park D, Cho JH. A Role for Peroxidasin PXN-1 in Aspects of C. elegans Development. Mol Cells. 2015;38(1):51-7.

33. Bhave G, Cummings CF, Vanacore RM, Kumagai-Cresse C, Ero-Tolliver IA, Rafi M, et al. Peroxidasin forms sulfilimine chemical bonds using hypohalous acids in tissue genesis. Nat Chem Biol. 2012;8(9):784-90.

34. Khan K, Rudkin A, Parry DA, Burdon KP, McKibbin M, Logan CV, et al. Homozygous mutations in PXDN cause congenital cataract, corneal opacity, and developmental glaucoma. Am J Hum Genet. 2011;89(3):464-73.

35. McCall AS, Cummings CF, Bhave G, Vanacore R, Page-McCaw A, Hudson BG. Bromine is an essential trace element for assembly of collagen IV scaffolds in tissue development and architecture. Cell. 2014;157(6):1380-92.

36. Garver LS, Xi Z, Dimopoulos G. Immunoglobulin superfamily members play an important role in the mosquito immune system. Dev Comp Immunol. 2008;32(5):519-31.

37. Li H, Cao Z, Moore DR, Jackson PL, Barnes S, Lambeth JD, et al. Microbicidal activity of vascular peroxidase 1 in human plasma via generation of hypochlorous acid. Infect Immun. 2012;80(7):2528-37.

38. Shi R, Cao Z, Li H, Graw J, Zhang G, Thannickal VJ, et al. Peroxidasin contributes to lung host defense by direct binding and killing of gram-negative bacteria. PLoS Pathog. 2018;14(5):e1007026.

39. Hanmer KL, Mavri-Damelin D. Peroxidasin is a novel target of the redox-sensitive transcription factor Nrf2. Gene. 2018;674:104-14.

40. Lévigne D, Modarressi A, Krause K, Pittet-Cuénod B. NADPH oxidase 4 deficiency leads to impaired wound repair and reduced dityrosine-crosslinking, but does not affect myofibroblast formation. Free Radical Biology and Medicine. 2016;96:374-84.

41. Medfai H, Khalil A, Rousseau A, Nuyens V, Paumann-Page M, Sevcnikar B, et al. Human peroxidasin 1 promotes angiogenesis through ERK1/2, Akt and FAK pathways. Cardiovasc Res. 2018.

42. Battistuzzi G, Bellei M, Zederbauer M, Furtmu P, Obinger C. Redox Thermodynamics of the Fe(III)/Fe(II) Couple of Human Myeloperoxidase in its High-Spin and Low-Spin Forms. Biochemistry 2006;45:12750-5.

43. Battistuzzi G, Bellei M, Vlasits J, Banerjee S, Furtmuller PG, Sola M, et al. Redox thermodynamics of lactoperoxidase and eosinophil peroxidase. Arch Biochem Biophys. 2010;494(1):72-7.

44. Furtmuller PG, Burner U, Obinger C. Reaction of myeloperoxidase compound I with chloride, bromide, iodide, and thiocyanate. Biochemistry. 1998;37(51):17923-30.

45. Li H, Cao Z, Zhang G, Thannickal VJ, Cheng G. Vascular peroxidase 1 catalyzes the formation of hypohalous acids: characterization of its substrate specificity and enzymatic properties. Free Radic Biol Med. 2012;53(10):1954-9.

46. Dypbukt JM, Bishop C, Brooks WM, Thong B, Eriksson H, Kettle AJ. A sensitive and selective assay for chloramine production by myeloperoxidase. Free Radic Biol Med. 2005;39(11):1468-77.

47. Sevcnikar B, Paumann-Page M, Hofbauer S, Pfanzagl V, Furtmüller P, Obinger C. Reaction of human peroxidasin 1 compound I and compound II with one-electron donors. Arch Biochem Biophys. 2020;Submitted.

48. Winterbourn CC. Biological Production, Detection, and Fate of Hydrogen Peroxide. Antioxid Redox Signal. 2018;29(6):541-51.

49. Sirokmany G, Kovacs HA, Lazar E, Konya K, Donko A, Enyedi B, et al. Peroxidasin-mediated crosslinking of collagen IV is independent of NADPH oxidases. Redox Biol. 2018;16:314-21.

50. Colon S, Page-McCaw P, Bhave G. Role of Hypohalous Acids in Basement Membrane Homeostasis. Antioxid Redox Signal. 2017;27(12):839-54.

51. Weiss SJ. Peroxidasin: tying the collagen-sulfilimine knot. Nat Chem Biol. 2012;8(9):740-1.

52. Yan X, Sabrautzki S, Horsch M, Fuchs H, Gailus-Durner V, Beckers J, et al. Peroxidasin is essential for eye development in the mouse. Hum Mol Genet. 2014;23(21):5597-614.

53. Choi A, Lao R, Ling-Fung Tang P, Wan E, Mayer W, Bardakjian T, et al. Novel mutations in PXDN cause microphthalmia and anterior segment dysgenesis. Eur J Hum Genet. 2015;23(3):337-41.

54. Yang Y, Xing Y, Liang C, Hu L, Xu F, Mei Q. An examination of the regulatory mechanism of Pxdn mutation-induced eye disorders using microarray analysis. Int J Mol Med. 2016;37(6):1449-56.

55. Bai YP, Hu CP, Yuan Q, Peng J, Shi RZ, Yang TL, et al. Role of VPO1, a newly identified heme-containing peroxidase, in ox-LDL induced endothelial cell apoptosis. Free Radic Biol Med. 2011;51(8):1492-500.

56. Ma QL, Zhang GG, Peng J. Vascular peroxidase 1: a novel enzyme in promoting oxidative stress in cardiovascular system. Trends Cardiovasc Med. 2013;23(5):179-83.

57. Peng H, Chen L, Huang X, Yang T, Yu Z, Cheng G, et al. Vascular peroxidase 1 up regulation by angiotensin II attenuates nitric oxide production through increasing asymmetrical dimethylarginine in HUVECs. J Am Soc Hypertens. 2016;10(9):741-51 e3.

58. Wang EL, Jia MM, Luo FM, Li T, Peng JJ, Luo XJ, et al. Coordination between NADPH oxidase and vascular peroxidase 1 promotes dysfunctions of endothelial progenitor cells in hypoxia-induced pulmonary hypertensive rats. Eur J Pharmacol. 2019;857:172459.

59. Liu Z, Xu Q, Yang Q, Cao J, Wu C, Peng H, et al. Vascular peroxidase 1 is a novel regulator of cardiac fibrosis after myocardial infarction. Redox Biol. 2019;22:101151.

60. You B, Liu Y, Chen J, Huang X, Peng H, Liu Z, et al. Vascular peroxidase 1 mediates hypoxia-induced pulmonary artery smooth muscle cell proliferation, apoptosis resistance and migration. Cardiovasc Res. 2018;114(1):188-99.

61. Yang Y, Shi R, Cao Z, Zhang G, Cheng G. VPO1 mediates oxidation of LDL and formation of foam cells. Oncotarget. 2016.

62. Yang Y, Cao Z, Tian L, Garvey WT, Cheng G. VPO1 mediates ApoE oxidation and impairs the clearance of plasma lipids. PLoS One. 2013;8(2):e57571.

63. Zhang YS, He L, Liu B, Li NS, Luo XJ, Hu CP, et al. A novel pathway of NADPH oxidase/vascular peroxidase 1 in mediating oxidative injury following ischemia-reperfusion. Basic Res Cardiol. 2012;107(3):266.

64. Li TT, Zhang YS, He L, Liu B, Shi RZ, Zhang GG, et al. Inhibition of vascular peroxidase alleviates cardiac dysfunction and apoptosis induced by ischemia-reperfusion. Can J Physiol Pharmacol. 2012;90(7):851-62.

65. Liu B LX, Yang ZB, Zhang JJ, Li TB, Zhang XJ, Ma QL, Zhang GG, Hu CP, Peng J. Inhibition of NOX VPO1 Pathway and Inflammatory Reaction by Trimethoxystilbene in Prevention of Cardiovascular Remodeling. J Cardiovasc Pharmacol. 2014;63(6):567-76. .

66. Shi R, Hu C, Yuan Q, Yang T, Peng J, Li Y, et al. Involvement of vascular peroxidase 1 in angiotensin II-induced vascular smooth muscle cell proliferation. Cardiovasc Res. 2011;91(1):27-36.

67. Yang L, Bai Y, Li N, Hu C, Peng J, Cheng G, et al. Vascular VPO1 expression is related to the endothelial dysfunction in spontaneously hypertensive rats. Biochem Biophys Res Commun. 2013;439(4):511-6.

68. Colon S, Luan H, Liu Y, Meyer C, Gewin L, Bhave G. Peroxidasin and eosinophil peroxidase, but not myeloperoxidase, contribute to renal fibrosis in the murine unilateral ureteral obstruction model. Am J Physiol Renal Physiol. 2019;316(2):F360-F71.

69. McCall AS, Bhave G, Pedchenko V, Hess J, Free M, Little DJ, et al. Inhibitory Anti-Peroxidasin Antibodies in Pulmonary-Renal Syndromes. J Am Soc Nephrol. 2018;29(11):2619-25.

70. Jayachandran A, Prithviraj P, Lo PH, Walkiewicz M, Anaka M, Woods BL, et al. Identifying and targeting determinants of melanoma cellular invasion. Oncotarget. 2016;7(27):41186-202.

71. Desmond JC, Raynaud S, Tung E, Hofmann WK, Haferlach T, Koeffler HP. Discovery of epigenetically silenced genes in acute myeloid leukemias. Leukemia. 2007;21(5):1026-34.

72. Castronovo V, Waltregny D, Kischel P, Roesli C, Elia G, Rybak JN, et al. A chemical proteomics approach for the identification of accessible antigens expressed in human kidney cancer. Mol Cell Proteomics. 2006;5(11):2083-91.

73. Liu Y, Carson-Walter EB, Cooper A, Winans BN, Johnson MD, Walter KA. Vascular gene expression patterns are conserved in primary and metastatic brain tumors. J Neurooncol. 2010;99(1):13-24.

74. Madden SL, Cook BP, Nacht M, Weber WD, Callahan MR, Jiang Y, et al. Vascular gene expression in nonneoplastic and malignant brain. Am J Pathol. 2004;165(2):601-8.

75. Hutchins JT, Deans RJ, Mitchell MS, Uchiyama C, Kan-Mitchell J. Novel gene sequences expressed by human melanoma cells identified by molecular subtraction. Cancer Res. 1991;51(5):1418-25.

76. Zheng YZ, Liang L. High expression of PXDN is associated with poor prognosis and promotes proliferation, invasion as well as migration in ovarian cancer. Ann Diagn Pathol. 2018;34:161-5.

77. Dougan J, Hawsawi O, Burton LJ, Edwards G, Jones K, Zou J, et al. Proteomics-Metabolomics Combined Approach Identifies Peroxidasin as a Protector against Metabolic and Oxidative Stress in Prostate Cancer. Int J Mol Sci. 2019;20(12).

78. Sitole BN, Mavri-Damelin D. Peroxidasin is regulated by the epithelial-mesenchymal transition master transcription factor Snai1. Gene. 2018.

79. Tauber S, Jais A, Jeitler M, Haider S, Husa J, Lindroos J, et al. Transcriptome analysis of human cancer reveals a functional role of heme oxygenase-1 in tumor cell adhesion. Mol Cancer. 2010;9:200.

80. Murphy MP. How mitochondria produce reactive oxygen species. Biochem J. 2009;417(1):1-13.

81. Winterbourn CC. Biological Chemistry of Reactive Oxygen Species. In: Chatgilialoglu CaS, A., editor. Encyclopedia of Radicals in Chemistry, Biology and Materials. 20122012.

82. Burdon RH. Superoxide and hydrogen peroxide in relation to mammalian cell proliferation. Free Radic Biol Med. 1995;18(4):775-94.

83. Winterbourn CC. Reconciling the chemistry and biology of reactive oxygen species. Nat Chem Biol. 2008;4(5):278-86.

84. Finkel T, Holbrook NJ. Oxidants, oxidative stress and the biology of ageing. Nature. 2000;408(6809):239-47.

85. McCord JM, Fridovich I. Superoxide dismutase. An enzymic function for erythrocuprein (hemocuprein). J Biol Chem. 1969;244(22):6049-55.

86. Murphy MP, Holmgren A, Larsson NG, Halliwell B, Chang CJ, Kalyanaraman B, et al. Unraveling the biological roles of reactive oxygen species. Cell Metab. 2011;13(4):361-6.

87. Pattison DI, Davies MJ, Hawkins CL. Reactions and reactivity of myeloperoxidase-derived oxidants: differential biological effects of hypochlorous and hypothiocyanous acids. Free Radic Res. 2012;46(8):975-95.

88. Clark RA, Klebanoff SJ. Myeloperoxidase--H2O2--halide system: cytotoxic effect on human blood leukocytes. Blood. 1977;50(1):65-70.

89. Wu W, Chen Y, d'Avignon A, Hazen SL. 3-Bromotyrosine and 3,5-Dibromotyrosine Are Major Products of Protein Oxidation by Eosinophil Peroxidase: Potential Markers for Eosinophil-Dependent Tissue Injury in Vivo. Biochem J. 1999;38:3538-48.

90. Winterbourn CC, Kettle AJ. Biomarkers of myeloperoxidase-derived hypochlorous acid. Free Radic Biol Med. 2000;29(5):403-9.

91. Senthilmohan R, Kettle AJ. Bromination and chlorination reactions of myeloperoxidase at physiological concentrations of bromide and chloride. Arch Biochem Biophys. 2006;445(2):235-44.

92. Winterbourn CC. Comparative reactivities of various biological compounds with myeloperoxidase-hydrogen peroxide-chloride, and similarity of the oxidant to hypochlorite. Biochim Biophys Acta. 1985;840(2):204-10.

93. Skaff O, Pattison DI, Davies MJ. Kinetics of hypobromous acid-mediated oxidation of lipid components and antioxidants. Chem Res Toxicol. 2007;20(12):1980-8.

94. Carr AC, Winterbourn CC, van den Berg JJ. Peroxidase-mediated bromination of unsaturated fatty acids to form bromohydrins. Arch Biochem Biophys. 1996;327(2):227-33.

95. Carr AC, van den Berg JJ, Winterbourn CC. Differential reactivities of hypochlorous and hypobromous acids with purified Escherichia coli phospholipid: formation of haloamines and halohydrins. Biochim Biophys Acta. 1998;1392(2-3):254-64.

96. Pantopoulos K, Schipper HM. Principles of free radical biomedicine. New York, NY: Nova Science Publishers. p. volumes.

97. Ximenes VF, Morgon NH, de Souza AR. Hypobromous acid, a powerful endogenous electrophile: Experimental and theoretical studies. J Inorg Biochem. 2015;146:61-8.

98. Zgliczynski JM, Stelmaszynska T, Domanski J, Ostrowski W. Chloramines as intermediates of oxidation reaction of amino acids by myeloperoxidase. Biochim Biophys Acta. 1971;235(3):419-24.

99. Thomas EL, Jefferson MM, Grisham MB. Myeloperoxidase-catalyzed incorporation of amines into proteins: role of hypochlorous acid and dichloramines. Biochemistry. 1982;21(24):6299-308.

100. Pattison DI, Davies MJ. Absolute Rate Constants for the Reaction of Hypochlorous Acid with Protein Side Chains and Peptide Bonds. Chem Res Toxicol. 2001;14:1453-64.

101. Nagy P, Beal JL, Ashby MT. Thiocyanate is an efficient endogenous scavenger of the phagocytic killing agent hypobromous acid. Chem Res Toxicol. 2006;19(4):587-93.

102. Prutz WA, Kissner R, Koppenol WH, Ruegger H. On the irreversible destruction of reduced nicotinamide nucleotides by hypohalous acids. ArchBiochemBiophys. 2000;380(1):181-91.

103. Morris JC. The Acid Ionization Constant of HOCl from 5 to 35°. The Journal of Physical Chemistry. 1966;70(12):3798-805.

104. Halliwell B, Gutteridge JMC. Free radicals in biology and medicine. Fifth edition. ed. Oxford, United Kingdom ;: Oxford University Press; 2015. xxxviii, 905 pages p.

105. Stamp LK, Khalilova I, Tarr JM, Senthilmohan R, Turner R, Haigh RC, et al. Myeloperoxidase and oxidative stress in rheumatoid arthritis. Rheumatology (Oxford). 2012;51(10):1796-803.

106. Chavarria C, Souza JM. Oxidation and nitration of alpha-synuclein and their implications in neurodegenerative diseases. Arch Biochem Biophys. 2013;533(1-2):25-32.

107. Green PS, Mendez AJ, Jacob JS, Crowley JR, Growdon W, Hyman BT, et al. Neuronal expression of myeloperoxidase is increased in Alzheimer's disease. J Neurochem. 2004;90(3):724-33.

108. Schoneich C. Methionine oxidation by reactive oxygen species: reaction mechanisms and relevance to Alzheimer's disease. Biochim Biophys Acta. 2005;1703(2):111-9.

109. Vissers MC, Winterbourn CC. Oxidative damage to fibronectin. II. The effect of H2O2 and the hydroxyl radical. Arch Biochem Biophys. 1991;285(2):357-64.

110. Vissers MC, Winterbourn CC. Oxidative damage to fibronectin. I. The effects of the neutrophil myeloperoxidase system and HOCl. Arch Biochem Biophys. 1991;285(1):53-9.

111. Vissers MC, Carr AC, Chapman AL. Comparison of human red cell lysis by hypochlorous and hypobromous acids: insights into the mechanism of lysis. Biochem J. 1998;330 ( Pt 1):131-8.

112. Lavine TF. An iodometric determination of methionine. J Biol Chem. 1943(161):281.

113. Vogt W. Oxidation of methionyl residues in proteins: tools, targets, and reversal. Free Radic Biol Med. 1995;18(1):93-105.

114. Peskin AV, Turner R, Maghzal GJ, Winterbourn CC, Kettle AJ. Oxidation of methionine to dehydromethionine by reactive halogen species generated by neutrophils. Biochemistry. 2009;48(42):10175-82.

115. Levine RL, Mosoni L, Berlett BS, Stadtman ER. Methionine residues as endogenous antioxidants in proteins. Proc Natl Acad Sci U S A. 1996;93(26):15036-40.

116. Brot N, Weissbach L, Werth J, Weissbach H. Enzymatic reduction of protein-bound methionine sulfoxide. Proc Natl Acad Sci U S A. 1981;78(4):2155-8.

117. Berlett BS, Stadtman ER. Protein oxidation in aging, disease, and oxidative stress. J Biol Chem. 1997;272(33):20313-6.

118. Stadtman ER, Berlett BS. Reactive oxygen-mediated protein oxidation in aging and disease. Chem Res Toxicol. 1997;10(5):485-94.

119. Houee-Levin C, Bobrowski K, Horakova L, Karademir B, Schoneich C, Davies MJ, et al. Exploring oxidative modifications of tyrosine: an update on mechanisms of formation, advances in analysis and biological consequences. Free Radic Res. 2015;49(4):347-73.

120. Pattison DI, Davies MJ. Kinetic Analysis of the Reactions of Hypobromous Acid with Protein Components. Biochemistry. 2004 43(16):4799-809.

121. Chuang CY, Degendorfer G, Davies MJ. Oxidation and modification of extracellular matrix and its role in disease. Free Radic Res. 2014;48(9):970-89.

122. Ischiropoulos H. Biological tyrosine nitration: a pathophysiological function of nitric oxide and reactive oxygen species. Arch Biochem Biophys. 1998;356(1):1-11.

123. van der Vliet A, Eiserich JP, Halliwell B, Cross CE. Formation of reactive nitrogen species during peroxidase-catalyzed oxidation of nitrite. A potential additional mechanism of nitric oxide-dependent toxicity. J Biol Chem. 1997;272(12):7617-25.

124. Brennan ML, Wu W, Fu X, Shen Z, Song W, Frost H, et al. A tale of two controversies: defining both the role of peroxidases in nitrotyrosine formation in vivo using eosinophil peroxidase and myeloperoxidase-deficient mice, and the nature of peroxidase-generated reactive nitrogen species. J Biol Chem. 2002;277(20):17415-27.

125. MacPherson JC, Comhair SA, Erzurum SC, Klein DF, Lipscomb MF, Kavuru MS, et al. Eosinophils are a major source of nitric oxide-derived oxidants in severe asthma: characterization of pathways available to eosinophils for generating reactive nitrogen species. J Immunol. 2001;166(9):5763-72.

126. Beckmann JS, Ye YZ, Anderson PG, Chen J, Accavitti MA, Tarpey MM, et al. Extensive nitration of protein tyrosines in human atherosclerosis detected by immunohistochemistry. Biol Chem Hoppe Seyler. 1994;375(2):81-8.

127. Radi R. Protein tyrosine nitration: biochemical mechanisms and structural basis of functional effects. Acc Chem Res. 2013;46(2):550-9.

128. Stadtman ER, Levine RL. Free radical-mediated oxidation of free amino acids and amino acid residues in proteins. Amino Acids. 2003;25(3-4):207-18.

129. Hazen SL, Heinecke JW. 3-Chlorotyrosine, a specific marker of myeloperoxidase-catalyzed oxidation, is markedly elevated in low density lipoprotein isolated from human atherosclerotic intima. J Clin Invest. 1997;99(9):2075-81.

130. Nybo T, Dieterich S, Gamon LF, Chuang CY, Hammer A, Hoefler G, et al. Chlorination and oxidation of the extracellular matrix protein laminin and basement membrane extracts by hypochlorous acid and myeloperoxidase. Redox Biol. 2019;20:496-513.

131. Kettle AJ, Chan T, Osberg I, Senthilmohan R, Chapman AL, Mocatta TJ, et al. Myeloperoxidase and protein oxidation in the airways of young children with cystic fibrosis. Am J Respir Crit Care Med. 2004;170(12):1317-23.

132. Aldridge RE, Chan T, van Dalen CJ, Senthilmohan R, Winn M, Venge P, et al. Eosinophil peroxidase produces hypobromous acid in the airways of stable asthmatics. Free Radic Biol Med. 2002;33(6):847-56.

133. Weiss SJ, Test ST, Eckmann CM, Roos D, Regiani S. Brominating oxidants generated by human eosinophils. Science. 1986;234(4773):200-3.

134. Thomson E, Brennan S, Senthilmohan R, Gangell CL, Chapman AL, Sly PD, et al. Identifying peroxidases and their oxidants in the early pathology of cystic fibrosis. Free Radic Biol Med. 2010;49(9):1354-60.

135. Kettle AJ, Turner R, Gangell CL, Harwood DT, Khalilova IS, Chapman AL, et al. Oxidation contributes to low glutathione in the airways of children with cystic fibrosis. Eur Respir J. 2014;44(1):122-9.

136. Magon NJ, Turner R, Gearry RB, Hampton MB, Sly PD, Kettle AJ. Oxidation of calprotectin by hypochlorous acid prevents chelation of essential metal ions and allows bacterial growth: Relevance to infections in cystic fibrosis. Free Radic Biol Med. 2015;86:133-44.

137. Dickerhof N, Pearson JF, Hoskin TS, Berry LJ, Turner R, Sly PD, et al. Oxidative stress in early cystic fibrosis lung disease is exacerbated by airway glutathione deficiency. Free Radic Biol Med. 2017;113:236-43.

138. Dickerhof N, Turner R, Khalilova I, Fantino E, Sly PD, Kettle AJ, et al. Oxidized glutathione and uric acid as biomarkers of early cystic fibrosis lung disease. J Cyst Fibros. 2017;16(2):214-21.

139. Wedes SH, Wu W, Comhair SA, McDowell KM, DiDonato JA, Erzurum SC, et al. Urinary bromotyrosine measures asthma control and predicts asthma exacerbations in children. J Pediatr. 2011;159(2):248-55 e1.

140. Shao B, Tang C, Sinha A, Mayer PS, Davenport GD, Brot N, et al. Humans with atherosclerosis have impaired ABCA1 cholesterol efflux and enhanced high-density lipoprotein oxidation by myeloperoxidase. Circ Res. 2014;114(11):1733-42.

141. Heinecke JW, Li W, Daehnke HL, 3rd, Goldstein JA. Dityrosine, a specific marker of oxidation, is synthesized by the myeloperoxidase-hydrogen peroxide system of human neutrophils and macrophages. J Biol Chem. 1993;268(6):4069-77.

142. Radi R. Nitric oxide, oxidants, and protein tyrosine nitration. Proc Natl Acad Sci U S A. 2004;101(12):4003-8.

143. Mecham RP. The extracellular matrix : an overview. Berlin ; New York: Springer Verlag; 2011. xiv, 425 p. p.

144. Hynes RO. The extracellular matrix: not just pretty fibrils. Science. 2009;326(5957):1216-9.

145. Mouw JK, Ou G, Weaver VM. Extracellular matrix assembly: a multiscale deconstruction. Nat Rev Mol Cell Biol. 2014;15(12):771-85.

146. Pickup MW, Mouw JK, Weaver VM. The extracellular matrix modulates the hallmarks of cancer. EMBO Rep. 2014;15(12):1243-53.

147. Lu P, Takai K, Weaver VM, Werb Z. Extracellular matrix degradation and remodeling in development and disease. Cold Spring Harb Perspect Biol. 2011;3(12).

148. Kalluri R. Basement membranes: structure, assembly and role in tumour angiogenesis. Nat Rev Cancer. 2003;3(6):422-33.

149. Khoshnoodi J, Pedchenko V, Hudson BG. Mammalian collagen IV. Microsc Res Tech. 2008;71(5):357-70.

150. Barber T, Esteban-Pretel G, Marin MP, Timoneda J. Vitamin a deficiency and alterations in the extracellular matrix. Nutrients. 2014;6(11):4984-5017.

151. Fidler AL, Darris CE, Chetyrkin SV, Pedchenko VK, Boudko SP, Brown KL, et al. Collagen IV and basement membrane at the evolutionary dawn of metazoan tissues. Elife. 2017;6.

152. Murray JC, Stingl G, Kleinman HK, Martin GR, Katz SI. Epidermal cells adhere preferentially to type IV (basement membrane) collagen. J Cell Biol. 1979;80(1):197-202.

153. Rubin K, Gullberg D, Borg TK, Obrink B. Hepatocyte adhesion to collagen. Isolation of membrane glycoproteins involved in adhesion to collagen. Exp Cell Res. 1986;164(1):127-38.

154. Kaido T, Yebra M, Cirulli V, Montgomery AM. Regulation of human beta-cell adhesion, motility, and insulin secretion by collagen IV and its receptor alpha1beta1. J Biol Chem. 2004;279(51):53762-9.

155. Robertson WE, Rose KL, Hudson BG, Vanacore RM. Supramolecular organization of the alpha121-alpha565 collagen IV network. J Biol Chem. 2014;289(37):25601-10.

156. Sundaramoorthy M, Meiyappan M, Todd P, Hudson BG. Crystal structure of NC1 domains. Structural basis for type IV collagen assembly in basement membranes. J Biol Chem. 2002;277(34):31142-53.

157. Basak T, Vega-Montoto L, Zimmerman LJ, Tabb DL, Hudson BG, Vanacore RM. Comprehensive Characterization of Glycosylation and Hydroxylation of Basement Membrane Collagen IV by High-Resolution Mass Spectrometry. J Proteome Res. 2016;15(1):245-58.

158. Ortega N, Werb Z. New functional roles for non-collagenous domains of basement membrane collagens. J Cell Sci. 2002;115(Pt 22):4201-14.

159. Chioran A, Duncan S, Catalano A, Brown TJ, Ringuette MJ. Collagen IV trafficking: The inside-out and beyond story. Dev Biol. 2017;431(2):124-33.

160. Cummings CF, Pedchenko V, Brown KL, Colon S, Rafi M, Jones-Paris C, et al. Extracellular chloride signals collagen IV network assembly during basement membrane formation. J Cell Biol. 2016;213(4):479-94.

161. Anazco C, Lopez-Jimenez AJ, Rafi M, Vega-Montoto L, Zhang MZ, Hudson BG, et al. Lysyl Oxidase-like-2 Cross-links Collagen IV of Glomerular Basement Membrane. J Biol Chem. 2016;291(50):25999-6012.

162. Hudson B, Tryggvason K, Sundaramoorthy M, Neilson EG. Alport's Syndrome, Goodpasture's Syndrome, and Type IV Collagen. N Engl J Med 2003;348(25):2543-56.

163. Siebold B, Deutzmann R, Kuhn K. The arrangement of intra- and intermolecular disulfide bonds in the carboxyterminal, non-collagenous aggregation and cross-linking domain of basement-membrane type IV collagen. Eur J Biochem. 1988;176(3):617-24.

164. Weber S, Dolz R, Timpl R, Fessler JH, Engel J. Reductive cleavage and reformation of the interchain and intrachain disulfide bonds in the globular hexameric domain NC1 involved in network assembly of basement membrane collagen (type IV). Eur J Biochem. 1988;175(2):229-36.

165. Than ME, Henrich S, Huber R, Ries A, Mann K, Kuhn K, et al. The 1.9-A crystal structure of the noncollagenous (NC1) domain of human placenta collagen IV shows stabilization via a novel type of covalent Met-Lys cross-link. Proc Natl Acad Sci U S A. 2002;99(10):6607-12.

166. Than ME, Bourenkov GP, Henrich S, Mann K, Bode W. The NC1 dimer of human placental basement membrane collagen IV: does a covalent crosslink exist? Biol Chem. 2005;386(8):759-66.

167. Vanacore RM, Friedman DB, Ham AJ, Sundaramoorthy M, Hudson BG. Identification of S-hydroxylysyl-methionine as the covalent cross-link of the noncollagenous (NC1) hexamer of the alpha1alpha1alpha2 collagen IV network: a role for the post-translational modification of lysine 211 to hydroxylysine 211 in hexamer assembly. J Biol Chem. 2005;280(32):29300-10.

168. Vanacore RM, Ham AJL, Voehler M, Sanders CR, Conrads TP, Veenstra TD, et al. A Sulfilimine Bond Identified in Collagen IV. Science. 2009;235:1230-4.

169. Bhave G, Colon S, Ferrell N. The sulfilimine cross-link of collagen IV contributes to kidney tubular basement membrane stiffness. Am J Physiol Renal Physiol. 2017;313(3):F596-F602.

170. Fidler AL, Vanacore RM, Chetyrkin SV, Pedchenko VK, Bhave G, Yin VP, et al. A unique covalent bond in basement membrane is a primordial innovation for tissue evolution. Proc Natl Acad Sci U S A. 2014;111(1):331-6.

171. Petkowski JJ, Bains W, Seager S. Natural Products Containing a Nitrogen-Sulfur Bond. J Nat Prod. 2018;81(2):423-46.

172. Ronsein GE, Winterbourn CC, Di Mascio P, Kettle AJ. Cross-linking methionine and amine residues with reactive halogen species. Free Radic Biol Med. 2014;70:278-87.

173. Vanacore RM, Ham AJ, Cartailler JP, Sundaramoorthy M, Todd P, Pedchenko V, et al. A role for collagen IV cross-links in conferring immune privilege to the Goodpasture autoantigen: structural basis for the crypticity of B cell epitopes. J Biol Chem. 2008;283(33):22737-48.

174. Boudko SP, Danylevych N, Hudson BG, Pedchenko VK. Basement membrane collagen IV: Isolation of functional domains. Methods Cell Biol. 2018;143:171-85.

175. Hudson BG. The molecular basis of Goodpasture and Alport syndromes: beacons for the discovery of the collagen IV family. J Am Soc Nephrol. 2004;15(10):2514-27.

176. Kashtan CE, Michael AF. Alport syndrome: from bedside to genome to bedside. Am J Kidney Dis. 1993;22(5):627-40.

177. Saus J, Wieslander J, Langeveld JP, Quinones S, Hudson BG. Identification of the Goodpasture antigen as the alpha 3(IV) chain of collagen IV. J Biol Chem. 1988;263(26):13374-80.

178. Chelberg MK, Tsilibary EC, Hauser AR, McCarthy JB. Type IV collagen-mediated melanoma cell adhesion and migration: involvement of multiple, distinct domains of the collagen molecule. Cancer Res. 1989;49(17):4796-802.

179. Abecassis J, Millon-Collard R, Klein-Soyer C, Nicora F, Fricker JP, Beretz A, et al. Adhesion of human breast cancer cell line MCF-7 to human vascular endothelial cells in culture. Enhancement by activated platelets. Int J Cancer. 1987;40(4):525-31.

180. Dedhar S, Saulnier R, Nagle R, Overall CM. Specific alterations in the expression of alpha 3 beta 1 and alpha 6 beta 4 integrins in highly invasive and metastatic variants of human prostate carcinoma cells selected by in vitro invasion through reconstituted basement membrane. Clin Exp Metastasis. 1993;11(5):391-400.

181. Iozzo RV, Gubbiotti MA. Extracellular matrix: The driving force of mammalian diseases. Matrix Biol. 2018;71-72:1-9.

182. Theocharis AD, Manou D, Karamanos NK. The extracellular matrix as a multitasking player in disease. FEBS J. 2019;286(15):2830-69.

183. Rockey DC, Bell PD, Hill JA. Fibrosis--A Common Pathway to Organ Injury and Failure. N Engl J Med. 2015;373(1):96.

184. Burlew BS, Weber KT. Cardiac fibrosis as a cause of diastolic dysfunction. Herz. 2002;27(2):92-8.

185. Nicholls SJ, Zheng L, Hazen SL. Formation of dysfunctional high-density lipoprotein by myeloperoxidase. Trends Cardiovasc Med. 2005;15(6):212-9.

186. Kubala L, Kolarova H, Vitecek J, Kremserova S, Klinke A, Lau D, et al. The potentiation of myeloperoxidase activity by the glycosaminoglycan-dependent binding of myeloperoxidase to proteins of the extracellular matrix. Biochim Biophys Acta. 2013;1830(10):4524-36.

187. Brown K, Darris C, Rose KL, Sanchez OA, Madu H, Avance J, et al. Hypohalous Acids Contribute to Renal Extracellular Matrix Damage in Experimental Diabetes. Diabetes. 2015;64:2242-53.

188. Wieslander J, Langeveld J, Butkowski R, Jodlowski M, Noelken M, Hudson BG. Physical and immunochemical studies of the globular domain of type IV collagen. Cryptic properties of the Goodpasture antigen. J Biol Chem. 1985;260(14):8564-70.

189. Langeveld JP, Wieslander J, Timoneda J, McKinney P, Butkowski RJ, Wisdom BJ, Jr., et al. Structural heterogeneity of the noncollagenous domain of basement membrane collagen. J Biol Chem. 1988;263:10481–8.

190. Laemmli UK. Cleavage of structural proteins during the assembly of the head of bacteriophage T4. Nature. 1970;227(5259):680-5.

191. Meyer TS, Lamberts BL. Use of coomassie brilliant blue R250 for the electrophoresis of microgram quantities of parotid saliva proteins on acrylamide-gel strips. Biochim Biophys Acta. 1965;107(1):144-5.

192. Towbin H, Staehelin T, Gordon J. Electrophoretic transfer of proteins from polyacrylamide gels to nitrocellulose sheets: procedure and some applications. Proc Natl Acad Sci U S A. 1979;76(9):4350-4.

193. Shevchenko A, Tomas H, Havli J, Olsen JV, Mann M. In-gel digestion for mass spectrometric characterization of proteins and proteomes. Nature Protocols. 2006;1(6):2856-60.

194. Wolff SP. Ferrous ion oxidation in presence of ferric ion indicator xylenol orange for measurement of hydroperoxides. Methods Enzymol. 1994;233:182-9.

195. Chen X, Lee KA, Ren X, Ryu JC, Kim G, Ryu JH, et al. Synthesis of a highly HOCl-selective fluorescent probe and its use for imaging HOCl in cells and organisms. Nat Protoc. 2016;11(7):1219-28.

196. Albrett AM, Ashby LV, Dickerhof N, Kettle AJ, Winterbourn CC. Heterogeneity of hypochlorous acid production in individual neutrophil phagosomes revealed by a rhodamine-based probe. J Biol Chem. 2018;293(40):15715-24.

197. Chen HJ, Chiu WL. Simultaneous detection and quantification of 3-nitrotyrosine and 3-bromotyrosine in human urine by stable isotope dilution liquid chromatography tandem mass spectrometry. Toxicol Lett. 2008;181(1):31-9.

198. Nicholls SJ, Shen Z, Fu X, Levison BS, Hazen SL. Quantification of 3-nitrotyrosine levels using a benchtop ion trap mass spectrometry method. Methods Enzymol. 2005;396:245-66.

199. Bathish B, Turner R, Paumann-Page M, Kettle AJ, Winterbourn CC. Characterisation of peroxidasin activity in isolated extracellular matrix and direct detection of hypobromous acid formation. Arch Biochem Biophys. 2018;646:120-7.

200. Thomas EL, Bozeman PM, Jefferson MM, King CC. Oxidation of bromide by the human leukocyte enzymes myeloperoxidase and eosinophil peroxidase. Formation of bromamines. J Biol Chem. 1995;270(7):2906-13.

201. Arnhold J, Monzani E, Furtmüller P, Zederbauer M, Casella L, Obinger C. Kinetics and Thermodynamics of Halide and Nitrite Oxidation by Mammalian Heme Peroxidases. European Journal of Inorganic Chemistry. 2006;2006(19):3801-11.

202. Kettle AJ, Gedye CA, Hampton MB, Winterbourn CC. Inhibition of myeloperoxidase by benzoic acid hydrazides. Biochemical Journal. 1995;308 ( Pt 2):559-63.

203. Tiden AK, Sjogren T, Svensson M, Bernlind A, Senthilmohan R, Auchere F, et al. 2-thioxanthines are mechanism-based inactivators of myeloperoxidase that block oxidative stress during inflammation. J Biol Chem. 2011;286(43):37578-89.

204. Koelsch M, Mallak R, Graham GG, Kajer T, Milligan MK, Nguyen LQ, et al. Acetaminophen (paracetamol) inhibits myeloperoxidase-catalyzed oxidant production and biological damage at therapeutically achievable concentrations. Biochemical Pharmacology. 2010;79(8):1156-64.

205. Stephens D. Collagen secretion explained. Nature. 2012;482.

206. Olszowy HA, Rossiter J, Hegarty J, Geoghegan P. Background levels of bromide in human blood. J Anal Toxicol. 1998;22(3):225-30.

207. Morgan PE, Pattison DI, Talib J, Summers FA, Harmer JA, Celermajer DS, et al. High plasma thiocyanate levels in smokers are a key determinant of thiol oxidation induced by myeloperoxidase. Free Radic Biol Med. 2011;51(9):1815-22.

208. Asmussen I. Fetal cardiovascular system as influenced by maternal smoking. Clin Cardiol. 1979;2(4):246-56.

209. Becker BF. Towards the physiological function of uric acid. Free Radic Biol Med. 1993;14(6):615-31.

210. Kettle AJ, Gedye CA, Winterbourn CC. Mechanism of inactivation of myeloperoxidase by 4-aminobenzoic acid hydrazide. Biochem J. 1997;321 ( Pt 2):503-8.

211. Vissers MCM, C. WC. The effect of oxidants on neutrophil-mediated degradation of glomerular basement membrane collagen. Biochemica et Biophysica Acta. 1986;889:277-86.

212. Vissers MC, Thomas C. Hypochlorous acid disrupts the adhesive properties of subendothelial matrix. Free Radic Biol Med. 1997;23(3):401-11.

213. Citardi MJ, Song W, Batra PS, Lanza DC, Hazen SL. Characterization of oxidative pathways in chronic rhinosinusitis and sinonasal polyposis. Am J Rhinol. 2006;20(3):353-9.

214. Cunnion KM, Willis LK, Minto HB, Burch TC, Werner AL, Shah TA, et al. Eosinophil Quantitated Urine Kinetic: A novel assay for assessment of eosinophilic esophagitis. Ann Allergy Asthma Immunol. 2016;116(5):435-9.

215. Sabir M, Tan YY, Aris A, Mani AR. The role of endogenous bromotyrosine in health and disease. Free Radic Res. 2019:1-361.

216. Kato Y, Dozaki N, Nakamura T, Kitamoto N, Yoshida A, Naito M, et al. Quantification of Modified Tyrosines in Healthy and Diabetic Human Urine using Liquid Chromatography/Tandem Mass Spectrometry. J Clin Biochem Nutr. 2009;44(1):67-78.

217. Wu W, Samoszuk MK, Comhair SA, Thomassen MJ, Farver CF, Dweik RA, et al. Eosinophils generate brominating oxidants in allergen-induced asthma. J Clin Invest. 2000;105(10):1455-63.

218. Cowan DC, Taylor DR, Peterson LE, Cowan JO, Palmay R, Williamson A, et al. Biomarker-based asthma phenotypes of corticosteroid response. J Allergy Clin Immunol. 2015;135(4):877-83 e1.

219. Mani AR, Moreno JC, Visser TJ, Moore KP. The metabolism and de-bromination of bromotyrosine in vivo. Free Radic Biol Med. 2016;90:243-51.

220. Lister MW, McLeod PE. The Rates of Some Reactions of Aqueous Hypobromous Acid and Hypobromite Ions. Canadian Journal of Chemistry. 1971;49(12):1987-92.

221. Lahoutifard N, Lagrange P, Lagrange J, Scott SL. Kinetics and Mechanism of Nitrite Oxidation by HOBr/BrO- in Atmospheric Water and Comparison with Oxidation by HOCl/ClO. The Journal of Physical Chemistry A. 2002;106(49):11891-6.

222. Bartesaghi S, Radi R. Fundamentals on the biochemistry of peroxynitrite and protein tyrosine nitration. Redox Biol. 2018;14:618-25.

223. Leeuwenburgh C, Hardy MM, Hazen SL, Wagner P, Oh-ishi S, Steinbrecher UP, et al. Reactive nitrogen intermediates promote low density lipoprotein oxidation in human atherosclerotic intima. J Biol Chem. 1997;272(3):1433-6.

224. Tsikas D. Analytical methods for 3-nitrotyrosine quantification in biological samples: the unique role of tandem mass spectrometry. Amino Acids. 2012;42(1):45-63.

225. Tsikas D, Duncan MW. Mass spectrometry and 3-nitrotyrosine: strategies, controversies, and our current perspective. Mass Spectrom Rev. 2014;33(4):237-76.

226. Degendorfer G, Chuang CY, Kawasaki H, Hammer A, Malle E, Yamakura F, et al. Peroxynitrite-mediated oxidation of plasma fibronectin. Free Radic Biol Med. 2016;97:602-15.

227. Baldus S, Eiserich JP, Brennan ML, Jackson RM, Alexander CB, Freeman BA. Spatial mapping of pulmonary and vascular nitrotyrosine reveals the pivotal role of myeloperoxidase as a catalyst for tyrosine nitration in inflammatory diseases. Free Radic Biol Med. 2002;33(7):1010.

228. Degendorfer G, Chuang CY, Mariotti M, Hammer A, Hoefler G, Hagglund P, et al. Exposure of tropoelastin to peroxynitrous acid gives high yields of nitrated tyrosine residues, di-tyrosine cross-links and altered protein structure and function. Free Radic Biol Med. 2018;115:219-31.

229. Thomson L, Tenopoulou M, Lightfoot R, Tsika E, Parastatidis I, Martinez M, et al. Immunoglobulins against tyrosine-nitrated epitopes in coronary artery disease. Circulation. 2012;126(20):2392-401.

230. Hawkins CL. The role of hypothiocyanous acid (HOSCN) in biological systems. Free Radic Res. 2009;43(12):1147-58.

231. Thiery JP, Acloque H, Huang RY, Nieto MA. Epithelial-mesenchymal transitions in development and disease. Cell. 2009;139(5):871-90.

232. Balls AK, Hale WS. On peroxidase. J Biol Chem. 1934;107:767-83.

233. Kang KA, Lee KH, Chae S, Zhang R, Jung MS, Ham YM, et al. Cytoprotective effect of phloroglucinol on oxidative stress induced cell damage via catalase activation. J Cell Biochem. 2006;97(3):609-20.

234. Li TT, Zhang YS, He L, Li NS, Peng J, Li YJ. Protective effect of phloroglucinol against myocardial ischaemia-reperfusion injury is related to inhibition of myeloperoxidase activity and inflammatory cell infiltration. Clin Exp Pharmacol Physiol. 2011;38(1):27-33.

235. Jafri W, Yakoob J, Hussain S, Jafri N, Islam M. Phloroglucinol in irritable bowel syndrome. J Pak Med Assoc. 2006;56(1):5-8.

236. He Y-Q, Zhang W-T, Shi C-H, Wang F-M, Tian X-J, Ma L-L. Phloroglucinol protects the urinary bladder via inhibition of oxidative stress and inflammation in a rat model of cyclophosphamide-induced interstitial cystitis. Chin Med J (Engl). 2015;128(7):956-62.

237. Nagy P, Jameson GNL, Winterbourn CC. Kinetics and Mechanisms of the Reaction of Hypothiocyanous Acid with 5-Thio-2-nitrobenzoic Acid and Reduced Glutathione. Chemical Research in Toxicology. 2009;22(11):1833-40.

238. Thomas EL. Lactoperoxidase-catalyzed oxidation of thiocyanate: equilibria between oxidized forms of thiocyanate. Biochemistry. 1981;20(11):3273-80.

239. Barrett TJ, Hawkins CL. Hypothiocyanous Acid: Benign or Deadly? Chemical Research in Toxicology. 2012;25(2):263-73.

240. Gallieni M, Brancaccio D, Cozzolino M, Sabbioni E. Trace elements in renal failure: are they clinically important? Nephrol Dial Transplant. 1996;11(7):1232-5.

241. Canavese C, De Costanzi E, Stratta P, Sabbioni E. A role for bromine deficiency in sleep disturbances of long-term dialysis patients. Am J Kidney Dis. 2006;48(6):1018-9; author reply 9.

242. Madiyal A, Ajila V, Babu SG, Hegde S, Kumari S, Madi M, et al. Status of thiocyanate levels in the serum and saliva of non-smokers, ex-smokers and smokers. Afr Health Sci. 2018;18(3):727-36.

243. Tsuge K, Kataoka M, Seto Y. Cyanide and Thiocyanate Levels in Blood and Saliva of Healthy Adult Volunteers. JOURNAL OF HEALTH SCIENCE. 2000;46(5):343-50.

244. Al-Hilaly YK, Biasetti L, Blakeman BJF, Pollack SJ, Zibaee S, Abdul-Sada A, et al. The involvement of dityrosine crosslinking in α-synuclein assembly and deposition in Lewy Bodies in Parkinson's disease. Scientific Reports. 2016;6(1):39171.

245. Al-Hilaly YK, Williams TL, Stewart-Parker M, Ford L, Skaria E, Cole M, et al. A central role for dityrosine crosslinking of Amyloid-β in Alzheimer's disease. Acta Neuropathol Commun. 2013;1:83-.